Vibrational Based Inspection of Civil Engineering Structures

Rytter, Anders

Publication date:
1993

Document Version
Publisher's PDF, also known as Version of record

INSTITUTTET FOR BYGNINGSTEKNIK
DEPT. OF BUILDING TECHNOLOGY AND STRUCTURAL ENGINEERING
AALBORG UNIVERSITETSCENTER • AUC • AALBORG • DANMARK

FRACTURE & DYNAMICS
PAPER NO. 44

Ph.D.-Thesis defended publicly at the University of Aalborg
April 20, 1993

A. RYTTER

VIBRATIONAL BASED INSPECTION OF CIVIL ENGINEERING STRUCTURES

MAY 1993

ISSN 0902-7513 R9314

The FRACTURE AND DYNAMICS papers are issued for early dissemination of research results from the Structural Fracture and Dynamics Group at the Department of Building Technology and Structural Engineering, University of Aalborg. These papers are generally submitted to scientific meetings, conferences or journals and should therefore not be widely distributed. Whenever possible reference should be given to the final publications (proceedings, journals, etc.) and not to the Fracture and Dynamics papers.

VIBRATIONAL BASED INSPECTION OF CIVIL ENGINEERING STRUCTURES

(Vibrationsbaseret inspektion af bærende konstruktioner)

Anders Rytter

Department of Building Technology and Structural Engineering
University of Aalborg
Sohngaardsholmsvej 57
DK-9000 Aalborg
&
Rambøll, Hannemann & Højlund A/S
Kjærulfsgade 2
DK-9400 Nørresundby

Denmark

APPENDIX

PREFACE

The present thesis *Vibrational Based Inspection of Civil Engineering Structures* has been made as a part of my Ph.D. study programme from November 1988 to February 1993 at the Department of Building Technology and Structural Engineering, University of Aalborg, Denmark.

The thesis has been written in relation to two different research projects. Firstly, an offshore test programme, *Integrated Experimental/Numerical Analysis of the Dynamic behavior of Offshore Structures*, which was performed at the Department of Building Technology and Structural Engineering at the University of Aalborg from 1988 to 1991. Secondly, a research project, *In-Field Vibration Based Inspection of Civil Engineering Structures*, which has been performed as a pilot project by the Consulting Engineers Rambøll, Hannemann and Højlund in cooperation with the Department of Building Technology and Structural Engineering at the University of Aalborg since the beginning of 1992. Both projects have been supported by the Danish Technical Research Council. Further, the first mentioned project was supported by the Danish Energy Agency. Their financial support is gratefully acknowledged.

I would like to thank my supervisors Lars Pilegaard Hansen, Associate Professor, Ph.D., and Rune Brincker, Assistant Professor, Ph.D., from the Department of Building Technology and Structural Engineering, University of Aalborg for their guidance, patience and not at least technical and moral support during the years.

Further, a great thank is given to Poul Henning Kirkegaard, Assistant Professor, Ph.D., Department of Building Technology and Structural Engineering, University of Aalborg for a good and inspirational cooperation during my study.

The figures in the thesis have been prepared by draughtsman Mrs. Norma Hornung from the University of Aalborg and draughtsman Mrs. Birgitte Albrechtsen from Rambøll, Hannemann & Højlund. The proof-reading has been performed by senior secretary Mrs. Kirsten Aakjær from University of Aalborg. Their carefully performed work is greatly appreciated.

Thanks are also given to the staff in laboratory, led by engineering assistant Mr. Henning Andersen, for help during the performance of the experimental tests.

The economic and moral support given by my employer, Rambøll, Hannemann & Højlund, is gratefully appreciated.

Finally, I would like to thank my son and wife for their great patience during my Ph.D. study.

Aalborg
February 1993

Anders Rytter

CHAPTER 1
INTRODUCTION

The accumulation of damage in a structure will cause a change in the dynamic characteristics of the structure.

The basic idea in **V**ibration **B**ased **I**nspection (abbreviated **VBI**) is to measure these dynamic characteristics during the lifetime of the structure and use them as a basis for identification of structural damage. A complete VBI-programme for a civil engineering structure includes the application of methods from many different engineering disciplines.

The main purpose of this thesis has been to establish a basic knowledge to the different activities included in a complete VBI-programme and to describe the interaction between these activities. This has been accomplished by a survey of literature and by development of different approaches for solving some of the problems which occur during the performance of a VBI-programme. The developed methods and some of the methods proposed in the literature have been implemented and tested on simulated as well as experimental data. The results from test examples presented in this thesis and the literature have been used to illustrate different important factors and to set up rules for choice of these factors. Thus, the thesis might be used as an introductory handbook for people who want to design a VBI-programme for a certain civil engineering structure.

1.1 BACKGROUND AND MOTIVES

The fact that defects like e.g. cracks and cavities causes changes in the dynamic characteristics of an item has in fact been used for safety inspection and control of production ever since the first pottery was produced. The item is struck by a finger or a hammer and the inspector can then by listening to the sound tell whether the item is intact or has a defect. This form of testing is also well known by everybody who have

been travelling by train and seen the man with the long-handled small hammer striking the wheels. The method is also widespread in the casting industry.

The method has been improved a great deal together with the development of the electronics industry. For instance, the human ear has been replaced by a microphone (see e.g. Spain et al. [64.1] and Curtis et al. [80.3]).

VBI has also been widely used for many years in connection with rotating machinery to detect damage in the form of e.g. unbalance and a broken ball in a ball-bearing. In fact this kind of error can be revealed by an experienced inspector by means of a screwdriver. However, during the last twenty years the screwdriver has been replaced by more advanced equipment as e.g accelerometers and frequency analysers to perform a continuous inspection and obtain a more exact damage detection.

A common feature in the above-mentioned examples of fields of application is that they concern items from batch productions. However, civil engineering structures are often one of a kind. Therefore, normally no experience about the performance of VBI on a certain structure is known at the birth of the structure. This is probably one of the reasons why vibration based inspection for civil engineering structures are still in their infancy although they have been used for probably thousands of years in other subject fields. Further, the performance of dynamic measurements on civil engineering structures was very limited and primitive until the early seventies because of poor test and analysis equipment.

The application of modern technology in the design of civil engineering structures has lead to an enormous increase in the performance of systematic inspection and maintenance of civil engineering structures during the last one or two decades. Further, it has become profitable to perform inspection and repair of old structures instead of demolition and replacement. The aim of these activities is to detect deteriorations at a stage early enough to guarantee adequate safety and low costs of reconstruction.

This increase in need for and extent of systematic inspection has resulted in

- development of new non-destructive inspection methods
- improvement of the existing non-destructive inspection methods
- development of methods for optimal inspection strategies

Therefore, VBI of civil engineering has been given more and more attention during the last 20 years. For instance, VBI-methods have been widely used for inspection of

bridges, piles and offshore platforms (see section 3.2). These structures have in common that they are covered by water or soil and are large and expensive structures.

The reasons for the great attention given to VBI are several. For instance, the applicability does not depend on the building material in use, which means that VBI e.g. can be used for non-metallic structures and composite structures. The fact that damage can be detected at unmeasured points is another great advantage of VBI. Further, the availability of small, high-power portable computers and data acquisition systems has made it feasible to contemplate vibration measurements at remote sites in a routine way and at a relatively low cost.

The growing interest for VBI can be seen in the number of papers on the subject presented at the International Modal Analysis Conference (in brief IMAC) during the last four years, see table 1.1.

	No. of papers on VBI
IMAC 8, 1990	2
IMAC 9, 1991	6
IMAC 10, 1992	12
IMAC 11, 1993	17

Table 1.1 Number of papers on VBI presented at IMAC, 1990-1993.

Many different schemes/methods for damage detection have been given during the last twenty to thirty years. However, the words "damage detection" have been used at random. This implies that the results from the different methods are quite different. For clarity the following four categories will used in this thesis.

Level 1 The method gives a qualitative indication that damage might be present in the structure. (DETECTION)

Level 2 The method gives information about the probable location of the damage too. (LOCALIZATION)

Level 3 The method gives information about the size of the damage. (ASSESSMENT)

Level 4 The method gives information about the actual safety of the structure given a certain damage state. (CONSEQUENCE)

1.2 READER'S GUIDE

The questions given below are often brought up, when the talk is about vibration based inspection. The aim of chapters 2 to 8 is to give some answers to these questions. Thus, the thesis should be applicable as a guidance for people who want to use VBI. The chapter(-s) of relevance is/are indicated after each question :

- Why choose VBI instead of other non-destructive inspection methods (NDI-methods) ? (see chapter 2)
- How can the rate and extent of the VBI be determined in a proper manner ? (see chapter 2)
- Which activities shall be included in a VBI-programme ? (see chapter 3)
- Has VBI ever been used on real structures ? (see chapter 3)
- Is it possible to establish an adequate mathematical model of the damage ? (see chapter 4)
- Which dynamic characteristics can be used as damage indicators ? (see chapter 5)
- Is it possible to distinguish between effects produced by damage and those brought about as a result of changes in e.g. non-structural components and the environmental conditions ? (see chapter 6)
- How sensitive are the different indicators to damage and which shall be used in a given situation ? (see chapter 6)
- How many sensors shall be used and where shall they be placed to get the most optimally information at the lowest cost ? (see chapter 6)

- Can the dynamic characteristics be identified with the required accuracy ? (see chapter 6)

- How can the obtained information be used to update the design model ? (see chapter 7)

- How can the identified dynamic characteristics be used to detect and locate damage ? (see chapter 8)

A thesis on vibration based inspection involves theoretical as well as practical considerations. The practical experiences referred to in this thesis are related to

- References

- Laboratory experiments with six hollow section cantilevers of 2 m (Experimental case no. 1)

- Full-scale experiments with a lattice mast of 20 m (Experimental case no. 2)

The experimental cases are described in section 1.3.

References are given as NAME [YEAR.NUMBER], where NAME is the name of the first and the second author, if any, YEAR is the year of printing and NUMBER is a successive number in that particular year.

Figures, tables, etc. are numbered as follows CHAPTER.NUMBER, where CHAPTER is the number of the actual chapter and NUMBER is a successive number in that chapter.

1.3 THE EXPERIMENTAL CASES

Short presentations of the structures used and the performed measurements/analyses performed in the two experimental cases are given in the present section.

1.3.1 Experimental Case No. 1

The experimental tests were performed on six different hollow section cantilevers made of steel. In the remaining part of this thesis the six beams will be referred to as B1, B2, B3, B4, B5 and B6 respectively.

The aim of the tests was to obtain experimental estimates for the modal parameters for different size and location of a true fatigue crack.

In many tests concerning the same problem saw cuts have been used to emulate fatigue cracks (see e.g. Wendtland [72.1] and Ju and Mimovich [88.13]). However, these kinds of tests will often lead to a false picture of the relationship between the crack length and the changes in the modal parameters. This is due to the fact that the changes in the modal parameters depend on the width of the crack/cut too (see e.g. Cawley and Ray [88.3]). Further, the non-linear effects due to opening and closing of a fatigue crack will be missed in tests, where saw cuts are used to emulate fatigue cracks. Therefore, small narrow laser cuts (width $\approx$ 0.15 mm) have been used to initiate the fatigue cracks in the six test beams (see figure 1.1).

The profile of fatigue cracks will often be irregular, which means that it some times can be difficult to get a reliable measure of the crack depth/length during fatigue tests. To avoid this the wall thickness of the six test beams has been chosen as 2 mm. Thereby it should be possible to measure the crack length at the outside of the profiles.

The crack lengths given in this thesis are referred to the centre line of the profile. The crack lengths on each side of the centre line have been measured and reported (see figure 1.1) to avoid misunderstandings in cases with skew crack growth ($a_l \neq a_r$). The latter occurred to more or less extent for all six test beams.

The cracks in beams B1-B3 and B4-B6 were initiated at z = 1.0 m and z = 0.1 m, respectively. The fatigue cracks were initiated and developed by attaching a sinus-varying load to the beams by means of a shaker at z = 0.24m. The frequency of the sinus was either the actual first or second bending natural frequency. The use of the second natural frequency gave a fast crack growth. However, the tests showed that the use of this frequency increased the risk for skew crack growth and fatigue cracks in the weld at the fixture considerably.

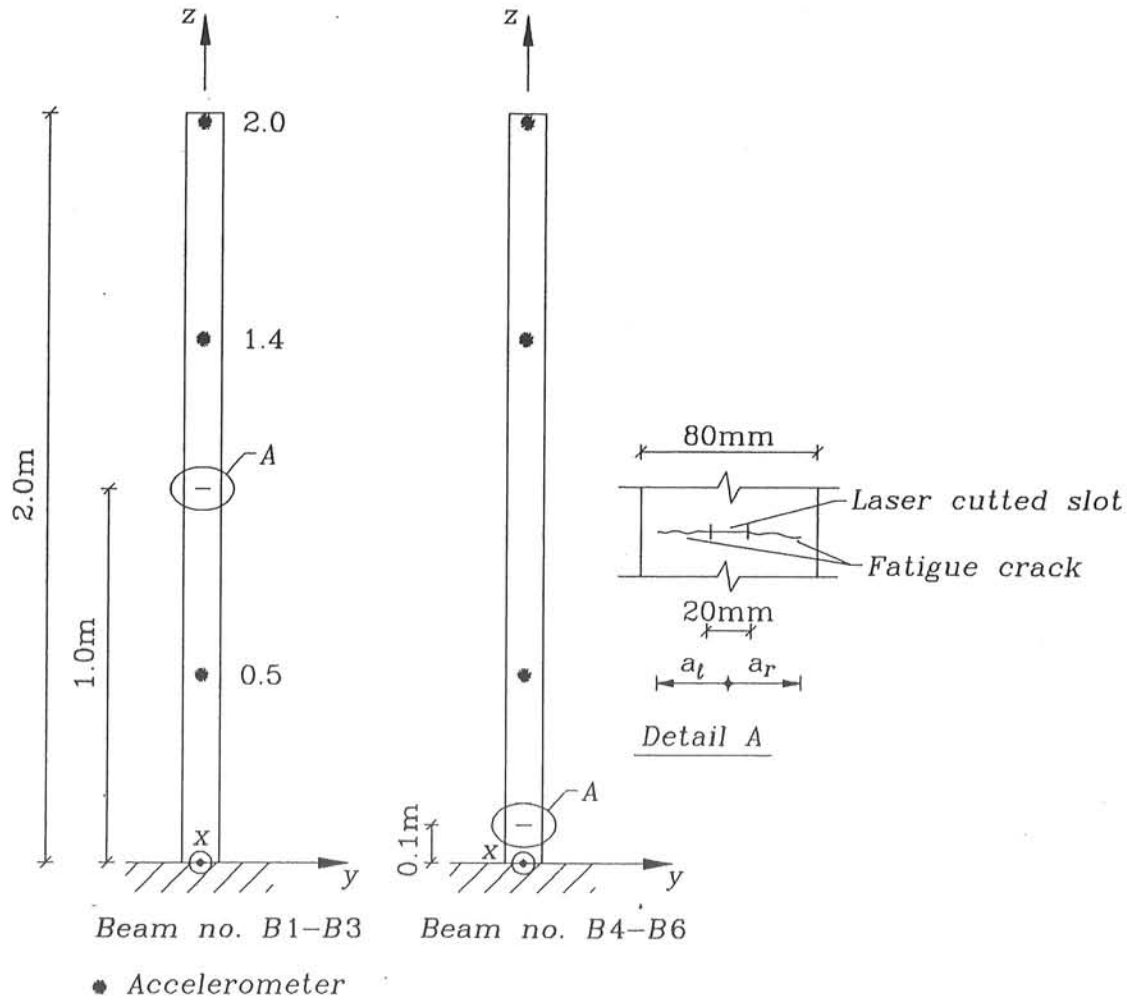

Figure 1.1 Crack and accelerometer locations.

A serie of 6-10 free decay tests was performed for a number of crack lengths. The test serie for the different crack length was denoted *A*, *B*, *C* ..., where *A* correspond to a = 0m and *B* correspond to a = 0.02m. Further each measurement in a test serie was given a serial number. Thus, i.e. *B4_L3* is the third measuremnt in test serie *L* for bema B3.

The tests on beams B1 and B2 were interrupted due to fatigue cracks in the fixture weld. Therefore, a reinforcement arrangement was mounted during the fatigue of beams B3, B5 and B6. The fatigue of beam B4 was performed at the first natural frequency without reinforcement. No unwanted fatigue cracks were initiated in this beam.

The test beams were removed from their fixture in between test A (a = 0 m) and test B (a = 0.02 m) for practical reasons. However, this has caused an increase in the

natural frequencies from test A to B even though damage was introduced. Therefore, the test B series have been taken as virgin state measurements in some of the analysis performed in this thesis.

Estimates for the modal parameters were obtained through curve fit on free decays and experimental modal analysis.

Figure 1.2 Symbols used in figures showing results from experimental case no. 1.

For further informations see Rytter et al. [92.7].

1.3.2 Experimental Case No. 2

A steel mast with a height of 20.0 m has been used as test object in the experimental case no. 2. Originally the mast was constructed as one of the legs in portal high tension pole.

The mast has a 0.9x0.9 m cross-section in its full height.

The eight lower diagonals were cut and provided with a bolted joint (see figure 1.4). Damage was introduced in the structure by removing one or more splice plates in these bolted joints.

The modal parameters have been estimated by means of ARMA models used on wind induced response.

For further informations see Rytter and Kirkegaard [93.1].

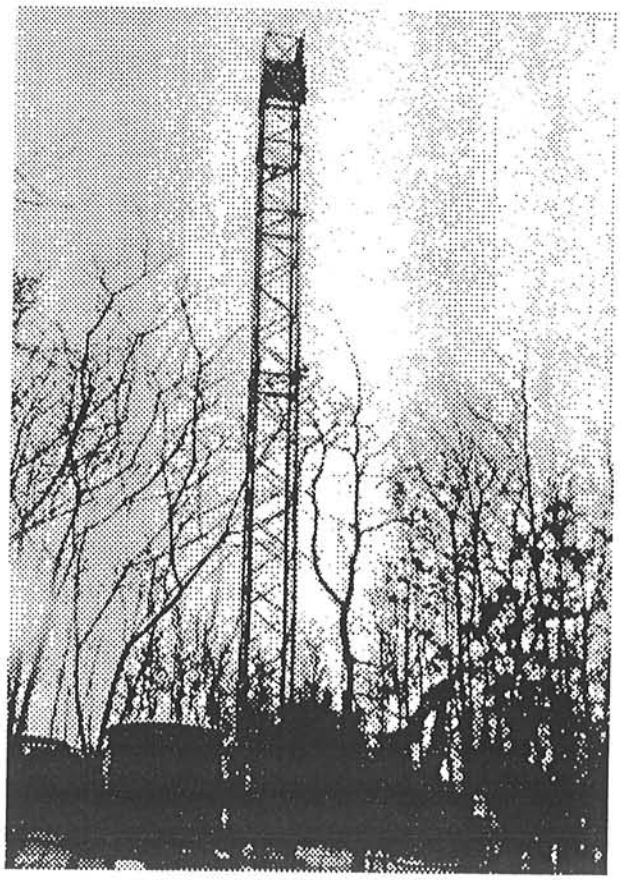

Figure 1.3 Mast.

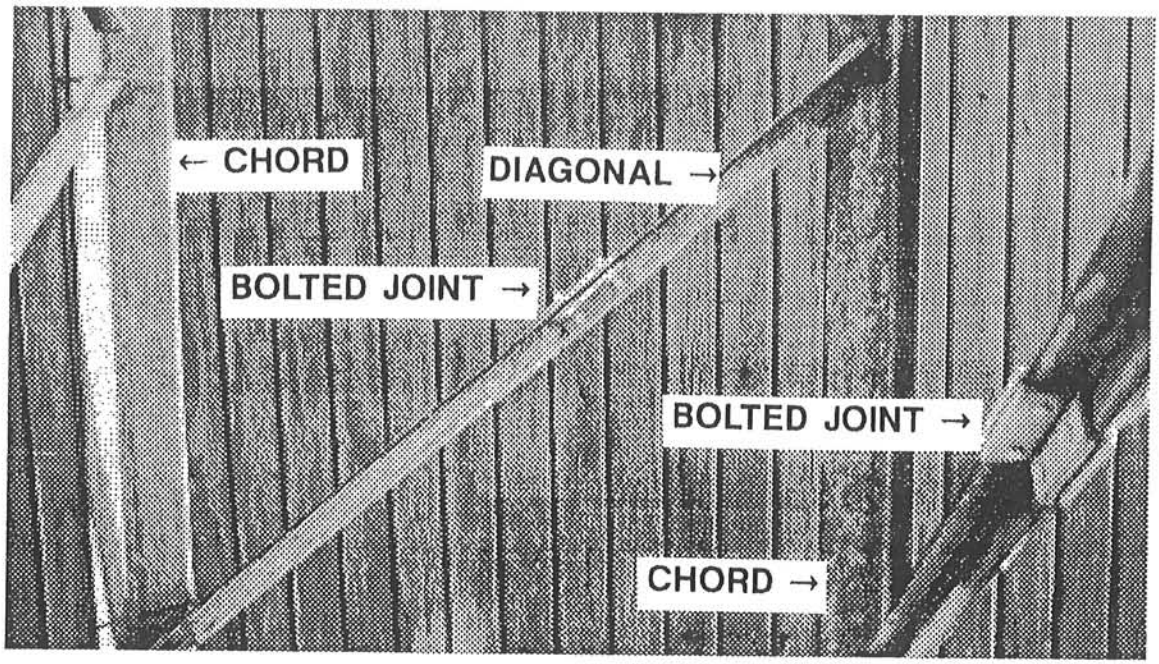

Figure 1.4 Bolted joints in diagonal members.

CHAPTER 2
INSPECTION OF STRUCTURES IN GENERAL

The performance of systematic inspection and maintenance of civil engineering structures has increased enormously during the last decades. The aim of these activities is to detect deteriorations at an early stage to guarantee adequate safety and low costs of repair. This increase is due to a combination of several factors.

The application of modern technology like e.g. high strength materials and refined analysis techniques has led to more optimal design of new structures during the last one or two decades. However, these optimized structures can be very vulnerable to failure in just a single structural member. Therefore, it is very important to detect damage like e.g. cracks as early as possible. Furthermore, the optimized structures are often more dynamically sensitive than their predecessors. In the offshore business for instance the use of optimal design techniques combined with structures being placed in deeper and deeper water has caused the eigenfrequencies of the structures to move downwards into the energy rich part of the wave spectrum. This means that there is a higher risk of fatigue damage.

There is a great number of old structures such as railroad bridges erected at the turn of this century, which are still in service. During the last ten years it has become profitable to perform inspection and repair instead of demolition and replacement. Furthermore, the amount of damage in these old bridges has increased due to the ravages of time combined with an increase in traffic loads and traffic intensity.

The risk of some kind of non-momentary damage in both kinds of structures is very high but also very difficult to estimate. The latter is primary due to the fact that the stochastic nature of the environmental loads and the service loads together with the uncertainties in the models for strength reduction due to ageing phenomena make it impossible to

perform a reliable calculation of the state of damage at any time in the lifetime of the structure.

The use and the reliability of inspection methods for crack detection have therefore become an even more important factor in the safety evaluation of civil engineering structures. During the past 2-3 decades various scientists have therefore put considerable efforts into the development of new, more reliable and less time consuming detection methods in order to minimize the costs of crack detection in civil engineering structures. The methods are either based upon on-line measurements or periodical measurements. The first category seems to be the most reliable, but, on the other hand, it is clearly the most expensive of the two. Many scientists have therefore concentrated their work on the development of reliable methods for making the decisions on the extent and the time interval between the periodical inspections.

The first section of this chapter contains a presentation of different methods used for the decision making on the extent and the time interval between the periodical inspections. A short survey of the most common used non-destructive inspection methods in use for inspection of steel and concrete civil engineering structures is given in section 2.2. The last section contains a summary and a conclusion.

2.1 RATE AND EXTENT OF INSPECTION

Periodical inspections of civil engineering structures will typically be performed in accordance with the flow-chart shown in figure 2.1. This scheme is for instance widely used as a basis for operation and maintenance of offshore platforms and bridges.

The rate and extent of the periodical inspections have traditionally been determined by experienced structural engineers. The decision is primarily based upon professional experience and some information about the utility ratios obtained in the design phase and the results of previous inspections. For instance the inspection rate for tubular joints in offshore platforms placed in the Danish sector of the North Sea was until the mid eighties solely based upon the utility ratio obtained in a Palmgren-Miner fatigue analysis at the design stage and the placing of the tubular joint with respect to the water level.

The time for the next inspection was determined in a similarly simple way in connection with the performance of a visual inspection of all concrete bridges belonging to The Danish State Railways (DSB). The bridges were graded on scale from 0 to 5. The

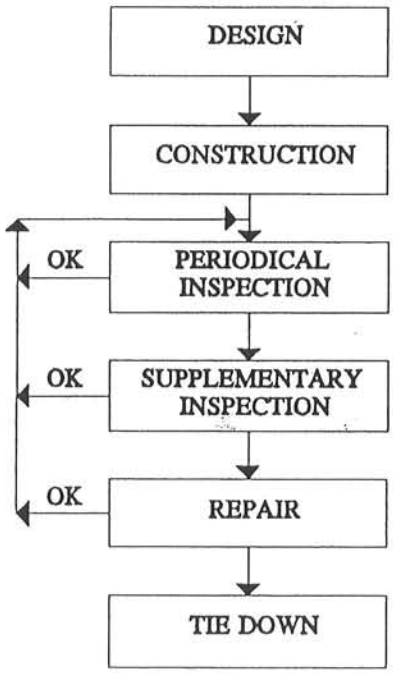

Figure 2.1. Typical life cyclus for civil engineering structures.

decision about the time for the next inspection was then based upon the criteria given in table 2.1, which was made by structural engineers with great experience in inspection of concrete bridges.

Character	Action	Next inspection
0	Negligible damage	8 years later
1	No repair	6 years later
2	Repair any suitable time	4 years later
3	Repair as soon as possible	2 years later
4	Repair immediately	Variable[1)]
5	Alarm	Variable[1)]

1) The time depends upon the performed repair

Table 2.1 Example of a primitive scheme for determination of inspection rate ([80.7]).

The high degree of simplicity in the procedure used in the two examples mentioned above is clearly introduced to prevent that the inspection rate will depend on the engineer performing the inspection.

Clearly, the main disadvantages in this traditional procedure are that the knowledge is limited to a few people and that in many cases the decision will be subjective.

The growing interest among building owners, etc. for periodical inspection has caused an increase in the performance of research in the field of optimum strategies for the rate and extent of inspection of civil engineering structures.

The most promising approaches for solving the problem have, from the authors point of view, been those, which are based upon pattern recognition (see e.g. Ishizuka et al. [83.1]) and probability based optimization (see e.g. Madsen and Sørensen [90.1] and Sommer et al. [91.1]).

Madsen and Sørensen [90.1] show how a probability-based optimization of fatigue design, inspection and maintenance can be used as a powerful tool in connection with the preparation of inspection plans. An optimized inspection plan is determined at the design stage, at the installation stage and after each inspection by minimizing the total expected cost for the remaining lifetime of the structure. The minimization is performed with respect to four optimization variables: inspection number, inspection times, inspection quality and member thickness.

The reliability of the obtained safety factor is of course very dependent on how good the data obtained during the inspection are or, in other words, the applicability and effeciency of the applied inspection methods. The most typically used inspection methods are described in the next section.

2.2 INSPECTION TECHNIQUES

The above-mentioned increase of interest for systematic inspection and maintenance of civil engineering structures has of course led to a similar increase in the work performed to develop and improve inspection methods.

The main efforts have been given to the development and improvement of the non-destructive inspection methods (abbreviated NDI-methods), since it is rather seldom that destructive inspection methods can be used in civil engineering.

The use of various material,types of structure, etc. have led to many different methods, which are more or less applicable to general use. Further, the generally usable methods

also have some kind of limitation, which makes them excellent for revealing one kind of damage and useless for revealing others. Therefore, the primary choice of inspection method should always be based upon a preceding thorough analysis of the structure, and the inspection plan should be critically evaluated throughout the inspection period. The final inspection plan will often include more than one inspection method.

The aim of this section is to give a short description of the most commonly used NDI-methods for the inspection of civil engineering structures. The presentation is primarily based on the book by Bøving et al. [87.1].

2.2.1 Visual Inspection

Visual inspection is without any doubt the oldest and the most commonly used inspection method in civil engineering and it will probably never be abandoned. Visual inspection is usually defined as an inspection, where the supervisor makes use of one or more of the human senses like e.g. eye sight, hearing and taste. These senses will normally be supplemented by some kind of simple auxiliary equipment like e.g. a hammer and a magnifying glass. Cavities and debonding/cracking in concrete structures can for instance be found by means of a hammer. The magnifying glass can for example be used to reveal small cracks in both steel and concrete structures.

The quality of a visual inspection is primarily dependent on the experience and the imagination of the supervisor supplemented with as-built drawings plus photographs, reports, etc. from any previous inspections. This means that the development in the area of visual inspection is mainly concentrated on the training of the supervisor through the performance of inspections.

The documentation from a visual inspection is normally a written report supplemented with photographs, sketches, etc. if necessary.

Visual inspection is often used to give a general view of the structure and to tell whether some more advanced inspection method or repair is needed in some part of the structure. The supervisor will typically be using a standard damage nomenclature in the report, which should prevent ambiguities in the description of the damages.

Such a standard damage nomenclature is e.g. used in connection with the inspection of bridges belonging to The Danish Road Authorities (VD) and The Danish Railroad Authorities (DSB) (see [80.7]). These bridges are periodically subjected to so-called

"General inspections", which exclusively consist of a visual inspection. If the "General inspection" reveals some problems, then a "Special inspection" is performed. This "Special inspection" includes a more detailed visual inspection supplemented with different forms of more advanced inspection methods, like e.g. ultrasonic (see section 2.2.4).

A visual inspection can only reveal defects at or close to accessible surfaces. This means that the method cannot stand alone, but has to be supplemented with other inspection methods.

2.2.2 Vibration Based Inspection and Monitoring

The presentation of vibration inspection and monitoring methods given in this section is very short and general. Chapters 3 to 8 contain a more detailed description of methods applicable to inspection of civil engineering structures. The emphasis is therefore here put on the disadvantages and advantages of the method in connection with the other inspection methods presented in this chapter.

The fundamental idea in vibration inspection and monitoring is to get information about the soundness of a structure from its dynamic response to either artificial or in service loads. The method is relatively new in connection with civil engineering structures but it has been widely used for inspection of machinery through many years.

The response of the structure will typically be measured by means of accelerometers and/or strain gauges. A local defect somewhere in a structure will in principle lead to a change in the overall dynamic characteristics of the structure. This means that the sensors can be placed anywhere in the structure and away from the defect, which of course makes the method very attractive. However, this form of global measurement is only applicable to detection of defects of a certain magnitude, since small defects will have no significant influence on the overall dynamic parameters. The detection of small damage quantities must therefore be based on local measurement. The distinction between global and local measurement is after all just a question of words, since the diagnostic methods are the same for the two.

Various methods (see chapter 8) exist for the interpretation of the measurements, but they are not fully developed yet. This means that vibration inspection and monitoring at the moment have to be supplemented with other inspection methods to get a total view of the soundness of the structure. The method only requires a limited amount of cleaning and is independent of the structural material. Further, the method is cheap and quick.

2.2.3 Acoustic Emission

The basic idea in acoustic emission is to measure those elastic waves, which are produced when a material undergoes a change of state. This change can for instance be yielding, crack initiation, crack growth and metallurgy changes.

Acoustic emission normally takes place in the most commonly used structural material like e.g. steel, wood and concrete, when the stresses exceed the previous stresses. This means that acoustic emission can only detect defects which arise during the measurement. Acoustic emission is therefore very suitable for continuous monitoring.

The acoustic emission is measured by means of transducers placed at the surface of the material. Measurement of arrival time in at least three transducers is necessary to detect the location of the defect.

Acoustic emission cannot be used to estimate the size of the defect. When dealing with steel structures the sensors can be mounted away from the area to be examined, which makes the method very attractive for inspection of complex structures like e.g. offshore jacket structures. The maximum distance between the sensors especially depends on the type of material and the level of background noise from machinery, etc. The latter may cause major problems, since the acoustic emission signals are normally very weak. Acoustic emission has become more and more widely used for inspection of offshore structures (see e.g. Chinn [90.3] and Sommer et al. [90.4]).

2.2.4 Ultrasonic

The basic idea in the ultrasonic testing technique is to introduce an ultrasonic (frequency greater than 20 kHz) into the test item by means of a transmitter (see figure 2.2) and to measure the echoes of the ultrasonic by means of a receiver. The velocity of the ultrasonic is a property of the material, which means that the received echo can be used to detect discontinuities and flaws within the item.

A large number of different ultrasonic testing techniques exist (see e.g. Bøving et al. [87.1] and Sommer et al. [90.4]), which first of all differ from each other in the number, the location and the construction of the receiver and transmitters.

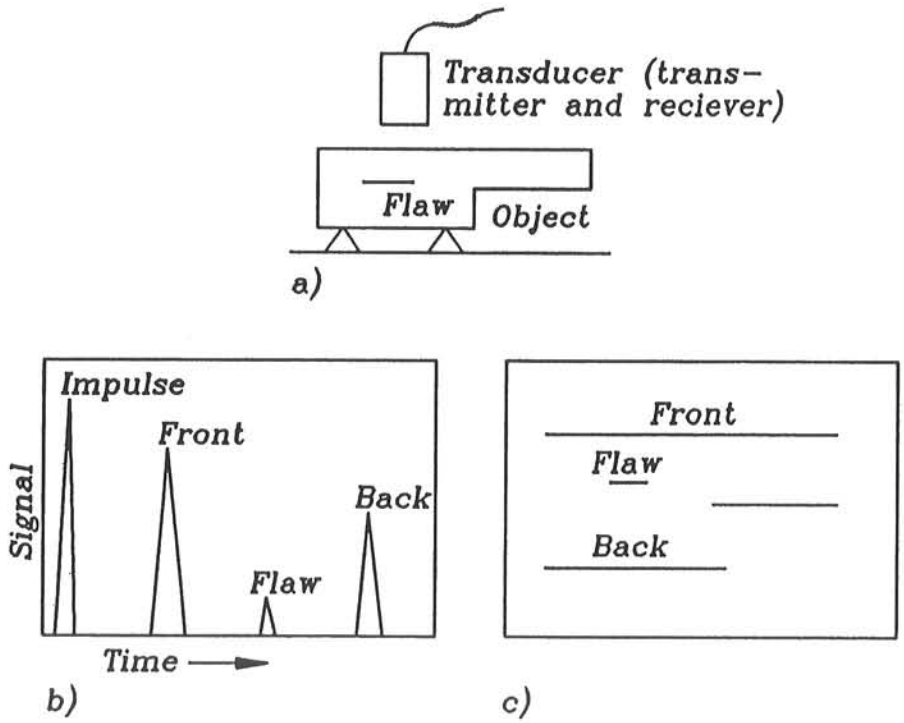

Figure 2.2 Ultrasonic test in principle.

Ultrasonic is widely used for the detection of defects in welds and lamination in steel items. The surface of the item has to be clean in the test area. However, ultrasonic is at the moment only reliable and practicable for local use close to a defect. It will therefore be very time-consuming and expensive to perform an overall inspection solely based on ultrasonic. For that reason ultrasonic cannot stand alone, but can only be used as a supplement to other inspection methods.

2.2.5 Magnetic Particle Inspection

The magnetic particle inspection method is suitable for detection of surface defects like e.g. fatigue cracks in ferromagnetic materials. The method works in principal as follows. A magnetic field of an appropriate power is supplied to the test item. The magnetic field is then made visible by means of magnetic particles. The defects, if any, will cause disturbances in the magnetic field and will thereby be detected.

Defects parallel or almost parallel will not be detected, which means that it is necessary to magnetize the item in two mutually perpendicular directions to get a full picture of the

extent of the defects. This can sometimes be troublesome due the geometry of the item, etc.

The magnetic particle inspection method is according to Sommer et al. [90.4] applicable to inspection below water.

The surface of the item has to be clean in the area of testing.

A magnetic particle inspection can only reveal a defect at or close to accessible surfaces. This means that the method cannot stand alone, but has to be supplemented with other inspection methods.

2.2.6 Radiography

A radiographic inspection is based on the property of X-rays and gamma rays to penetrate through solids and to blacken a film.

The amount of radiation which gets through the item depends among other things on the thickness of the item. This means that flaws, cavities, etc. inside the item will appear as dark spots on the film.

Radiographic inspection can be used for inspection of all kinds of material and needs no cleaning of the surfaces.

However, the method requires that both sides of the item are accessible, which reduces the area of application considerably. Further, it will be too time-consuming and expensive to perform an overall inspection based upon radiography. Thus radiographic inspection can never stand alone, but it has to be supplemented by other inspection techniques.

2.2.7 Eddy Current

The basic idea in the eddy current testing method is to produce an eddy current in the test item by means of an alternating current in a coil held close to the surface of the item. The alternating current in the coil raises a magnetic field called the primary field,

which produces the eddy current in the item (see figure 2.3). The latter raises a secondary magnetic field reverse to the primary field. A surface defect will cause a change in the eddy current and thereby also in the secondary field. The latter will then raise a change in the primary field, which gives a change in the current in the coil. This change in current is measured by means of an ammeter and used to detect the surface defects.

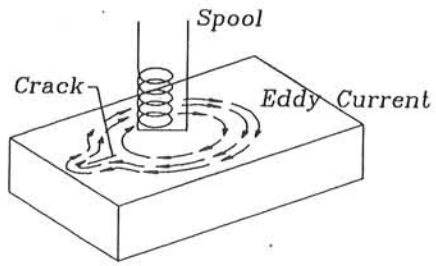

Figure 2.3. Principle in eddy current.

The eddy current is very attractive because it needs no cleaning of and contact to the surface of the item. The method is thus very quick, but its area of application is limited to inspection of small test areas on metallic items. It will be too time-consuming and expensive to perform an overall inspection based upon eddy current. Thus, eddy current inspection can never stand alone, but it has to be supplemented by other inspection techniques.

2.3 CONCLUSION

The performed literature study has shown that at the moment there is a high activity in the area of developing of methods for decision-making on the rate and extent of inspection.

The probability-based optimization of fatigue design, inspection and maintenance method presented by Madsen and Sørensen [90.1] is the most promising approach to solve the problem. However, the reliability and quality of the inspection methods is the weak link in all the methods.

A review of the most commonly used NDI-methods (see section 2.2) has revealed that none of these methods have so far been developed to such an extent yet that they can be used to perform a quick and still reliable inspection of a civil engineering structure, see table 2.2.

	1	2	3	4	5	6	7	8	9
Visual inspection	+	(+)	-	-	(+)	-	+	+	(+)
Vibration inspection	+	+	-	-	+	(+)	+	+	(+)
Acoustic emission	+	+	-	-	+	(+)	+	+	-
Ultrasonic	-	-	+	-	+	-	+	+	+
Magnetic particle	-	-	+	-	-	-	+	+	(+)
Radiography	-	(+)	+	-	+	-	-	+	+
Eddy current	-	(+)	+	-	-	-	+	+	(+)

1 : Usable for global inspection
2 : No cleaning required
3 : Not sensible to measurement noise
4 : Stand alone
5 : Detection of internal defects
6 : Detection of defects far away from the sensors
7 : Defects in areas with one surface accessible
8 : Defects in areas with two surfaces accessible
9 : Estimation of the size and location of the defect

Table 2.2 Advantages and disadvantages of NDI-methods.

A (+) in the table indicates that the method is only partially applicable to the actual purpose. Magnetic particle for instance only give the length of a crack but leave the depth unknown.

It shall be noticed that the nine groups used in table 2.2 are very general, which means that the type of material, structure, etc. has not been taken into account. However, the table clearly shows that a complete inspection of a given structure has to be based upon a combination of two or more inspection methods. The three first-mentioned inspection methods will typically be used to point out the areas, where the four latter methods shall be used.

Vibration monitoring and acoustic emission are the two most promising methods of the nine methods included in table 2.2. Since it is reasonable to believe, that they can be developed to cover all nine areas to a high degree, the remaining part of this thesis concerns the state-of-art of vibration monitoring and the possibilities for development.

The latter is especially concentrated on the area of estimation of the size and location of the defect.

CHAPTER 3
VIBRATION BASED INSPECTION

The aim of this chapter is to give a short general description of the different topics included in a complete VBI-programme and a review of examples on VBI. The chapter is divided in to two sections. A short "step by step"-description of a VBI-programme is given in section 3.1. Section 3.2 contains a review of papers dealing with the use of VBI on real structures.

3.1 VBI, STEP BY STEP

A vibration based monitoring programme might follow the flow-chart shown in figure 3.1. This flow-chart is a detailed version of the flow-chart in figure 2.1.

The design and planning of the measuring programme shall be performed parallel with the traditional structural design. Following this procedure it is possible to incorporate fixing points for accelerometers, etc. as natural parts of the structure and thereby minimize the risk of damage in the structure at these points. The fatigue crack which lead to the failure of the offshore platform Alexander Kielland was for instance initiated during the installation of a hydrophone support after the construction was finished (see Moan [85.2]).

The planning and design of the measuring program, which primarily is based on the results from the sensitivity analysis, can be performed in more or less sophisticated ways. The accelerometers have mainly been placed by intuition. Mathematical methods, which are based on different requirements for optimal information, have just recently been developed (see e.g. Kirkegaard et al. [90.7]). Section 6.4 contains a short presentation of some of the methods applicable to the design of a measuring programme.

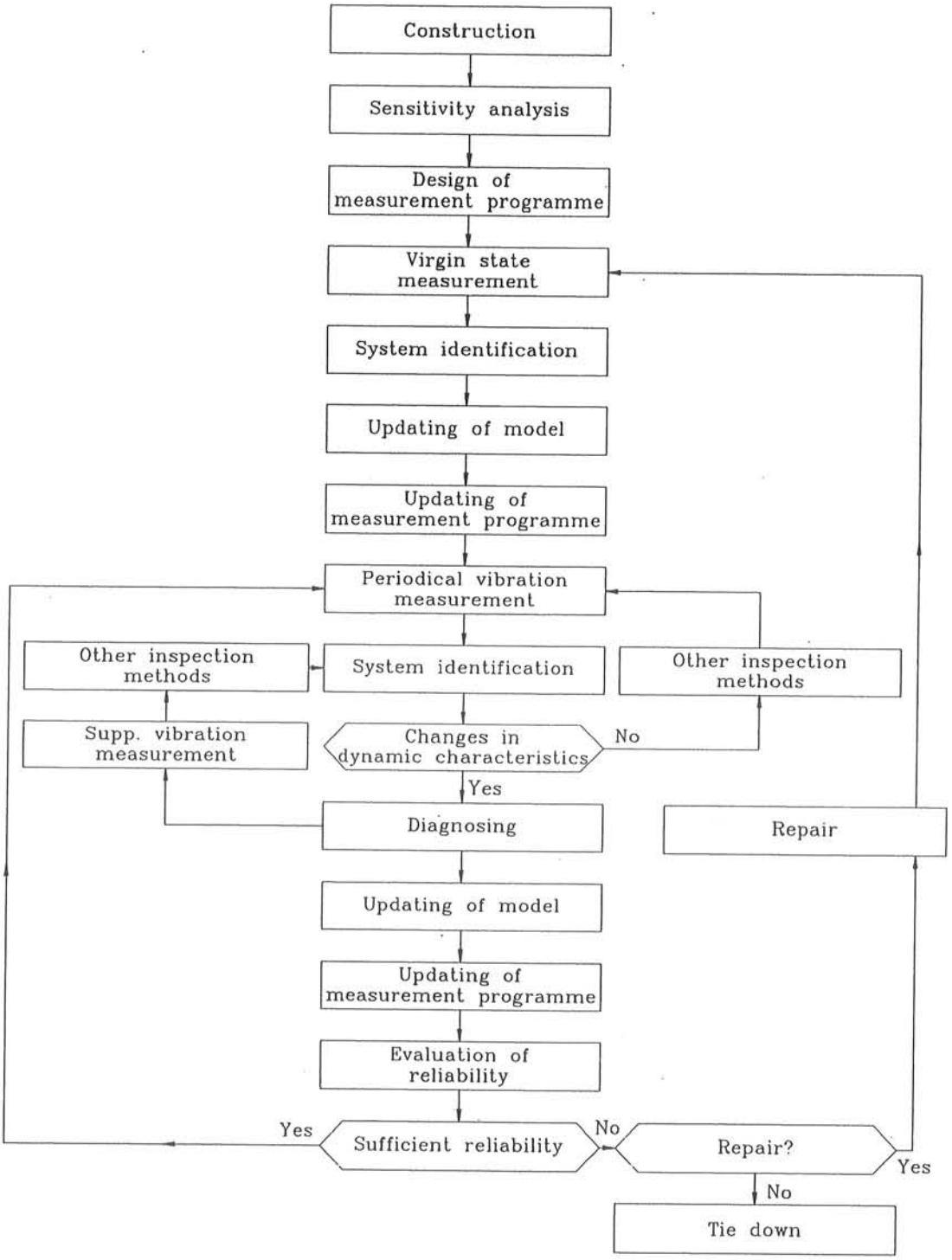

Figure 3.1. Flow-chart for a VBI-programme (Rytter et al. [91.12]).

VBI can in principle be used on all kinds of structures, whether they are designed for dynamic loads or not. A dynamic model has to be developed during the sensitivity analysis, if the latter is relevant.

The dynamic models used in the traditional design are often conservative, which means that they do not necessarily describe all relevant dynamic characteristics very well. For

instance it is only necessary to have a good estimate for the basic natural frequency of a chimney to perform a gust design in accordance with the Danish codes (see DS410 [82.3]). However, good estimates might be required for other natural frequencies as well, if a VBI-programme has to be applied to the chimney. This means that a modification of a dynamic model used in the design is often needed before it can be used in a VBI-programme.

The aim of the sensitivity analysis is to reveal which of the damage indicators (see chapter 5) are applicable to detect damage in the hot spots of the structure. It is important to take all potential not damage depending variation of the structural properties into account during the sensitivity analysis. The marine growth on offshore structures causes for instance a decrease in the natural frequencies of the structures. Further details about the performance of sensitivity analysis are given in section 6.2.

The results from the sensitivity analysis can sometimes be used to establish confidence intervals for the relevant dynamic characteristics (see figure 3.2), which can be used for decision making after each periodical measurement.

The virgin state measurements, which must be performed immediately after the ending

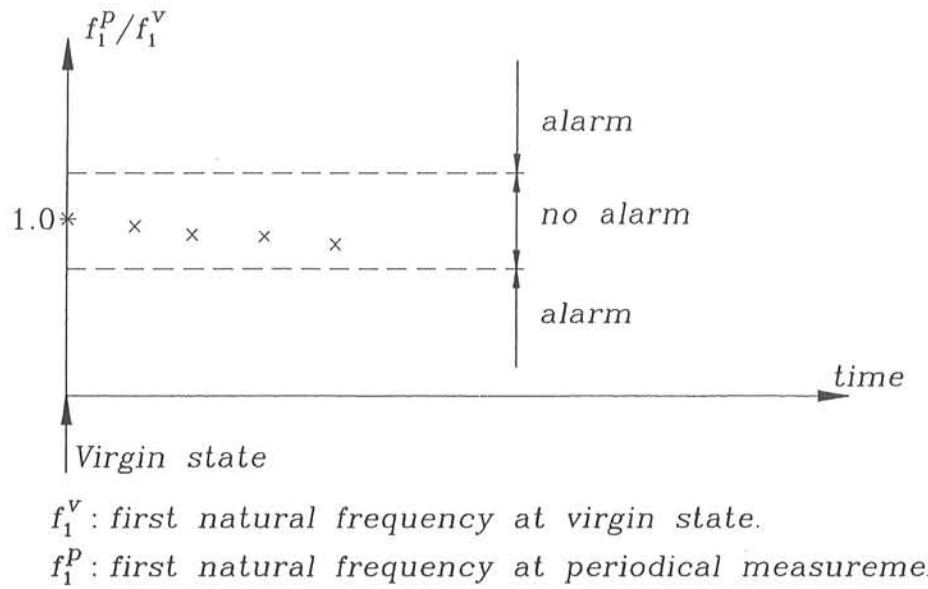

Figure 3.2. Example of decision making graph.

of the construction work, are the most important and comprehensive in the whole VBI-

programme. The results from these measurements are used as reference values after each periodical measurement through the life of the structure. This implies that all dynamic quantities, which are potential to be used as a damage indicator during the lifetime of the structure, have to be measured/identified at the virgin state measurement session.

The virgin state values for the dynamic characteristics are used for calibration of the mathematical model (typically a finite element model) to ensure that the model describes the real structure in the best possible way.

The calibration of FEM's is commonly performed by convergence analysis, where the number of elements is increased until convergence is obtained for the natural frequencies of relevance. However, an increase in the number of elements leads to more time-consuming and expensive computer runs. This is clearly undesirable, since the FEM has to be used after each of the subsequent periodical measurements. Further, a full agreement between the modal parameter of the model obtained through convergence and the experimental values will seldom be reached due to uncertainties in the distribution of mass and stiffness. More advanced methods are described in chapter 7.

Thus, the virgin state measurement is fundamental in a VBI-programme. However, this measurement will often be missing for old structures, which makes a VBI of such structures a little more complicated. One way of solving the problem is to perform a detailed visual inspection of the structure in connection with the first session of dynamic measurement and by including damage mechanism's during the "virgin state updating of model". The problems concerning missing a real virgin state measurement is dicussed further in chapter 7.

The dynamic characteristics of the structure are estimated by means of system identification methods during or after the virgin state measurements and the periodical measurement. A large number of system identification methods is available (see e.g Jensen [90.8]). The different methods used in this thesis in connection with the experimental cases (see section 1.3) are outlined in section 6.3.

Each periodical measurement and system identification session leads to new estimates for the dynamic characteristics of the structure. The VBI-programme remains unchanged, if these estimates are not significantly different from the estimates obtained during the virgin state measurement or earlier performed periodical measurements. The decision whether a change is significant or not is among other things based on decision making graphs like the one shown in figure 3.2.

A diagnosis of the state of damage has to be given if there have been significant changes in the dynamic characteristics. This diagnostic problem can in general be written as shown in equation (3.1)

$$\boldsymbol{D} = F(\boldsymbol{R}) \tag{3.1}$$

$\boldsymbol{D}$ is a damage vector, which for instance contains informations about the size and location of a crack. The vector $\boldsymbol{R}$ contains information about the actual damage indicators (see chapter 5). Thus, the main task in the development of a damage diagnostic scheme based upon results from vibration measurements is to develop an expression for the function $F(\boldsymbol{R})$, which gives an unambiguous $\boldsymbol{D}$ for a given $\boldsymbol{R}$.

A crack in a structure is defined by its size and location, thus $\boldsymbol{D}$ contains four elements for each crack. It is therefore obvious that $\boldsymbol{R}$ should contain at least four elements for each crack to be revealed. However, the required number of elements in $\boldsymbol{R}$ will in many cases be increased for symmetry reasons. The size of $\boldsymbol{D}$ is of course unknown in a practical problem and can in principle be infinite, whereas the number of elements in $\boldsymbol{R}$ will normally be limited by the measurement system in use. Furthermore, the elements in $\boldsymbol{R}$ will be defective due to different factors such as the signal-to-noise ratio and the length of the records.

The problem becomes even more complicated, when the dynamic characteristics are influenced by non-damage depending time-varying factors such as for instance changes in the mass. One way to tackle this problem is to incorporate these factors in $\boldsymbol{D}$.

The above-mentioned problems mean that a measured vector $\tilde{\boldsymbol{R}}$ in many cases will give multiple solutions to equation (3.1). In such cases $\tilde{\boldsymbol{R}}$ and the multiple solutions must be considered as outcomes of stochastic variables. The solution which has the highest conditional probability will be taken as the actual solution.

To reduce the size of the problem it can be preferable to supply the measurements with results from other inspection methods (e.g. a visual inspection). These results should then be incorporated in the analysis in a reasonable way.

In many practical situations the function $F(\boldsymbol{R})$ has been found indirectly by means of the results from sensitivity analysis, etc. where equation (3.2) has been solved either analytically or by numerical analysis (see e.g. Gudmundson [82.4], Wendtland [72.1] or Stubbs and Osegueda [85.3]). An approximate expression for $F(\boldsymbol{R})$ can then be found.

$$R=F^{-1}(D) \tag{3.2}$$

The applicability of the function $F(R)$ obtained in this way is clearly depending on how well the analytical models used in the sensitivity analysis fits with the real structure. Especially it is of major importance to have good reliable models for the change in stiffness and damping due to cracking (see chapter 4). Furthermore, it will be of major importance if the function $F(R)$ can be calibrated through some tests, where the size and location of the crack are well-defined.

Different methods of solving the problem given in equation (3.1) are presented and evaluated in chapter 8.

The reliability of the structure should be recalculated, when the diagnostic session is finished. If the structure is safe enough, a new periodical vibration measurement is performed later. The safety evaluation may show that a repair is required and possible, which means that the structure will be changed more or less. Therefore, a new virgin state measurement is required immediately after the repair work is finished. It will be of great interest to use the structure for calibration of the diagnostic functions, if a tie down of the structure is the only possible solution.

3.2 EXAMPLES OF VBI IN CIVIL ENGINEERING

The use of VBI in civil engineering has increased considerably during the last two decades.

Due to economical considerations the method has primarily been developed for use on large and expensive structures, such as bridges and offshore platforms. VBI has been widely used in connection with inspection of offshore platforms, because damage in the foundation and the structure below water level can be detected through vibration measurements at top site. The fact that VBI can be used to detect damage in inaccessible areas of a structure has made it profitable to use the methods in testing of piles.

Examples of VBI used in connection with inspection of offshore platforms, bridges and piles are given in the remaining part of this section. The presentation is not a complete state-of-the-art.

3.2.1 Offshore Platforms

The majority of the development of methods for structural integrity monitoring through dynamic measurements has concentrated on offshore platforms since the middle of the seventies. The methods have been used as an economically advantageous supplement to the traditional underwater inspection by divers. The latter has become increasingly difficult and costly as offshore developments move into deeper waters involving hostile oceanographic and seismic environments.

Vandiver [75.1] concludes that successive measurements of natural frequencies under certain conditions can be used to detect damage of significant subsurface members in an offshore pile supported steel space frame with bracing. The conclusion is based on results from field measurement and computer simulation on an offshore jacket.

The problem with high sensitivity to changes in masses has been tackled with success by some scientists (see e.g. Sunder [85.1]) by using the fundamental mode shapes instead of natural frequencies as damage indicators.

Begg et al. [76.1] (see also Loland and Dodds [76.2]) realized during a research project concerning three steel platforms in the North Sea that above water level measurements of the overall dynamic response can only reveal complete member severance or pile failure. A damage of that character may in many cases lead to secondary failure in some of the other structural members. Therefore the expense for underwater repair work will be limited if the damage can be detected at an earlier stage. Begg et al. [76.1] suggest this problem to be solved by the performance of local measurements on the single members.

The conclusions made by Begg et al. [76.1] are confirmed by Kenley and Dodds [80.1] in their paper concerning the results from field measurements on the West Sole WE platform. The platform was deliberately and progressively damaged prior to removal by cutting members. Measurements of the dynamic response to ambient sea loading were made before and after each cut by means of accelerometers. The tests included global as well as local measurements.

3.2.2 Bridges

A VBI-method for the safety inspection of large prestressed bridges has been under development at the Technical University of Graz and BFVA of Vienna since 1981 (see Flesch [90.2]). This method is one of the most well documented and well tested VBI-method seen by the author during a comprehensive review of papers, etc. dealing with methods for structural integrity monitoring through dynamic measurements. The development has taken place in connection with the performance of safety inspection of several bridges in Austria (see e.g. Flesch and Kernbichler [88.4] and Kernbichler and Flesch [84.3]) and has not been finished yet.

The basic idea in the method is to detect damage in the bridge by fitting a finite element model to some measured modal parameter. Powerful tools for the performance of this fitting and for the system identification are according to Flesch [90.2] the areas with the largest number of unsolved problems. Among other things which make the method attractive it is worth mentioning that the bridges can be open for traffic during the tests and that the method to some extent takes account of the environmental conditions like e.g. temperature.

According to Thronton and Alexander [87.2], Baldwin et al. have performed a successful detection of structural degradation of a three span continuous composite bridge by use of a mechanical impedance and change-in-stiffness technique. The bridge was field tested under fatigue loading. During the fatigue loading the bridge was inspected periodically by eight different inspection methods, including visual inspection, ultrasonic, radiographic, acoustic emission and dynamic techniques.

Nishimura et al. [88.1] have been using what they call "Percussive Test for Structure Response" (PTRS) to test the integrity of some railway bridge piers and their foundations. The tests are solely based on natural frequencies, which are obtained through FFT-analysis of response time series from impact tests (see figure 3.3A). Impact tests have been chosen in favour of tests based on forced vibration, because they are less time-consuming and cheaper. The actual strength of the soil and the pier is determined through a trial and error method.

A similar method has been successfully used by Thronton and Alexander [87.2] in field resonant frequency measurements on eight concrete piers.

The PTRS-method has been used before, during and after the performance of reinforcement works on the Kamikawa bridge (see figure 3.3). The footings of the bridge piers

were excavated to their underside, which corresponds to a severe deterioration of the foundation. The two basic natural frequencies were reduced by 0.5 Hz from 5.5 Hz and 6.5 Hz to 5.0 Hz and 6.0 Hz, respectively. Nishimura et al. [88.1] have found similar results for an another bridge. The measured reductions in natural frequencies seem to be rather low compared with the extent of "deterioration".

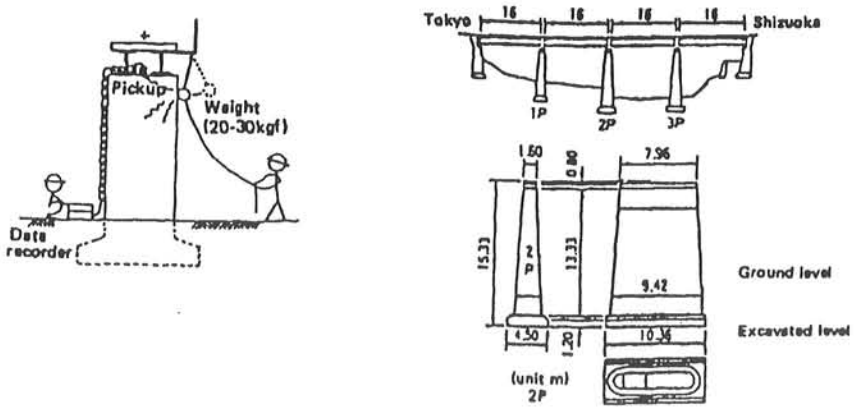

Figure 3.3 A) Loading procedure in PTRS. B) Sideview and plan of Kamikawa bridge (Nishimura et al [88.1]).

Turner and Pretlove [84.1] have investigated the possibility for using both natural frequencies and damping characteristics as damage indicators for different kinds of bridges. Their results from field measurements on a concrete footbridge show (see table 3.1) that only the natural frequencies are useful for damage detection, because the damping is too susceptible to environmental-induced changes.

Turner and Pretlove [84.1] have further found that these natural frequencies can be obtained by analysis of the bridge response to traffic. However, they recommend the use of artificial excitation, when the bridge is highly damped and/or has little traffic passing. The conclusion of the performed work is: *It has been shown that an appropriate analysis of the traffic-induced response of both beam-like and arched bridges can in most cases be used as an indication of structural changes*. Turner and Pretlove [84.1] point out that the potential confusion due to environmental effects is an area, where further study is urgent.

The latter is confirmed by comparing the results in table 3.1 with the results obtained by Askegaard and Mossing [88.2] (see figure 3.4).

Date	Test Method	Fund. Hz	2nd Hz	3rd Hz	Log. Dec (Fund)	Condition (°C)
07/10/81	Impulse	7.29	32.15	61.55	0.08	22, sunny
02/12/81	Impulse	7.29	32.15	61.50	0.11	7, rain
03/03/82	Impulse	7.29	32.20	61.60	0.07	-1, dry
02/08/82	Impulse	7.28	32.15	61.55	0.10	19, rain
16/11/82	Impulse	7.28	32.20	61.55	0.09	5, damp
15/03/83	Exciter	7.284	32.181	61.550	0.06	3, dry
20/07/83	Exciter	7.284	32.180	61.550	0.10	26, drought

Table 3.1 Natural Frequencies of University Footbridge (Turner and Pretlove [84.1]).

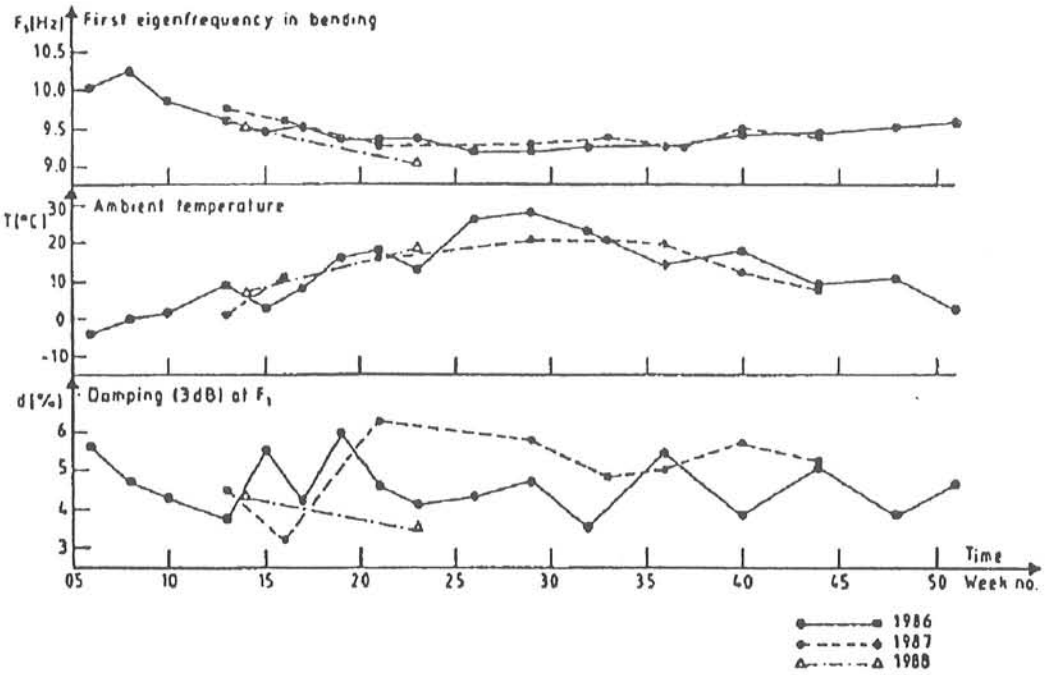

Figure 3.4 Changes in relative frequency, damping and temperature for a RC-footbridge (Askegaard and Mossing [88.2]).

The results in table 3.1 show no changes in natural frequencies due to changes in ambient temperature, while the results shown in figure 3.4 show a relatively large variation due to changes in ambient temperature. However, the variation seems to be identical from year to year. The damping values show no similar systematic variations and can therefore not be used as damage indicators. Askegaard and Mossing conclude that the measurement of natural frequencies in a certain week year after year can be used

to give an idea of the overall development of long-term deterioration and cracking in RC structures.

Mazurek and DeWolf [90.13] have developed an automated monitoring system for bridges based on the ambient vibration method. The natural frequencies, mode shapes and damping ratios are determined from auto- and cross-spectra measured, when the bridge is loaded with ambient loads. The development is due to some cases, where major cracks developed in a bridge over a few days.

The reliability of the results from a VBI-session is highly dependent on modelling of the damage and the system identification methods in use. Therefore it is clearly preferable to perform some calibration tests on the structure, when it contains with well defined damages.

This kind of calibration has e.g. been used by Biswas et al. [90.5] on a two span composite highway bridge, by Kernbichler and Flesch [84.3] on a three span prestressed concrete bridge of 244 m and by Ågårdh ([90.6] and [91.4]) on two concrete bridges. Biswas et al. [90.5] introduced damage by removing bolts from a bolted splice in the lower flange of one of the steel girders. Kernbichler and Flesch [84.3] used cutting of tendons to introduce damage. Ågårdh [90.6] introduces successive damage in the two bridges by statical overloading in four different steps. After each step the dynamic characteristics of the bridge were estimated by means of the SMS/STAR-modal analysis programme. Clearly the damage used by Ågårdh is the most realistic.

3.3.1 Piles

Vibration tests of piles are used for two different purposes, namely to determine the load-carrying capacity and to detect damages introduced during the pile driving or the in situ casting. The two purposes are closely related to each other and they are in some cases based upon the same measurements.

The determination of the load-carrying capacity of a pile is normally (see e.g. Lilley et al. [82.1], Davis et al. [74.1] and Goble et al. [80.2]) based upon measurements of the driving force and the velocity at the top of the pile, see figure 3.5. The measurements are performed during the last period of the actual pile driving at sites with sand and after some days at sites with clay, etc.

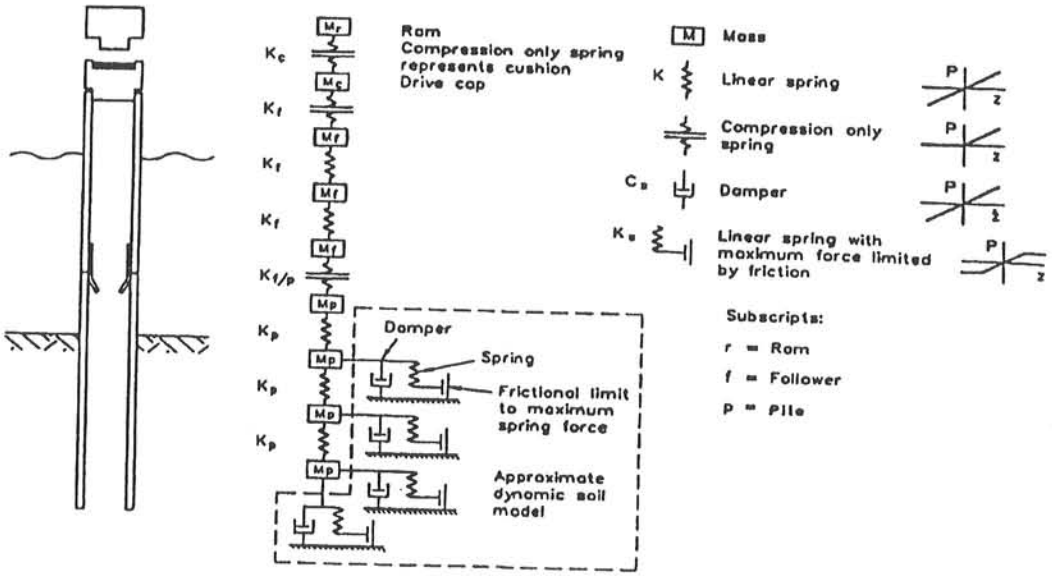

Figure 3.5 Pile testing in principle.

The load-carrying capacity of the pile and the soil properties along the pile are then determined by fitting similar curves obtained from numerical analysis of the spring-dashpot model in figure 3.5 to the measured curves.

This way of determining the load-carrying capacity is clearly much cheaper, less time consuming and more flexible than the traditional static loading tests. These things make the method very attractive. The unveiling of defects in piles immediately subsequent to the pile driving, or in situ casting, is of great economic importance.

The design of a pile group foundation is normally based upon a plastic limit state solution, which makes the total load-carrying capacity of the pile group very sensitive to missing load-carrying capacity in one or more single piles.

The main part of the load of a pile is very often concentrated at the lower end of the pile. This means that a broken pile will have a load-carrying capacity, which is much lower than the that of an intact pile. One or more broken piles in a group of piles may also cause unfortunate settlements in the structure and thereby perhaps give raise to damages in the building. Repair or reinforcement of a complete building due to a broken pile will be much more expensive than the cost of driving or casting of extra piles in the piloting phase.

Due the facts mentioned above the non-destructive testing of piles is very attractive from an economic point of view and has been used by several people.

Davis et al. [74.1] for instance present the results from vibration tests of more than 500 in situ cast concrete piles in France and Great Britain. The piles were loaded by a sinusoidal force at the top by means of a vibrator. The frequency was varied from 20 to 1000 Hz, while the amplitude of the force was fixed. A velocity transducer was mounted and used to monitor the vertical velocity of the pile head. Figure 3.6a shows the theoretical appearance of the mechanical admittance plotted against the frequency. The mechanical admittance is defined as the absolute value of the ratio between the maximum vertical velocity V_o of the pile head and the maximum vertical force F_o applied to the pile head. The length of the pile is determined from the distance between the peaks, as shown in figure 3.6a. A defect is revealed if this length differs from the theoretical length. Figure 3.6b shows the response curve from a pile with a theoretical length of 15 m, which apparently has a defect about 4.0 to 4.5 m below the upper end. This defect was certified by coring of the pile.

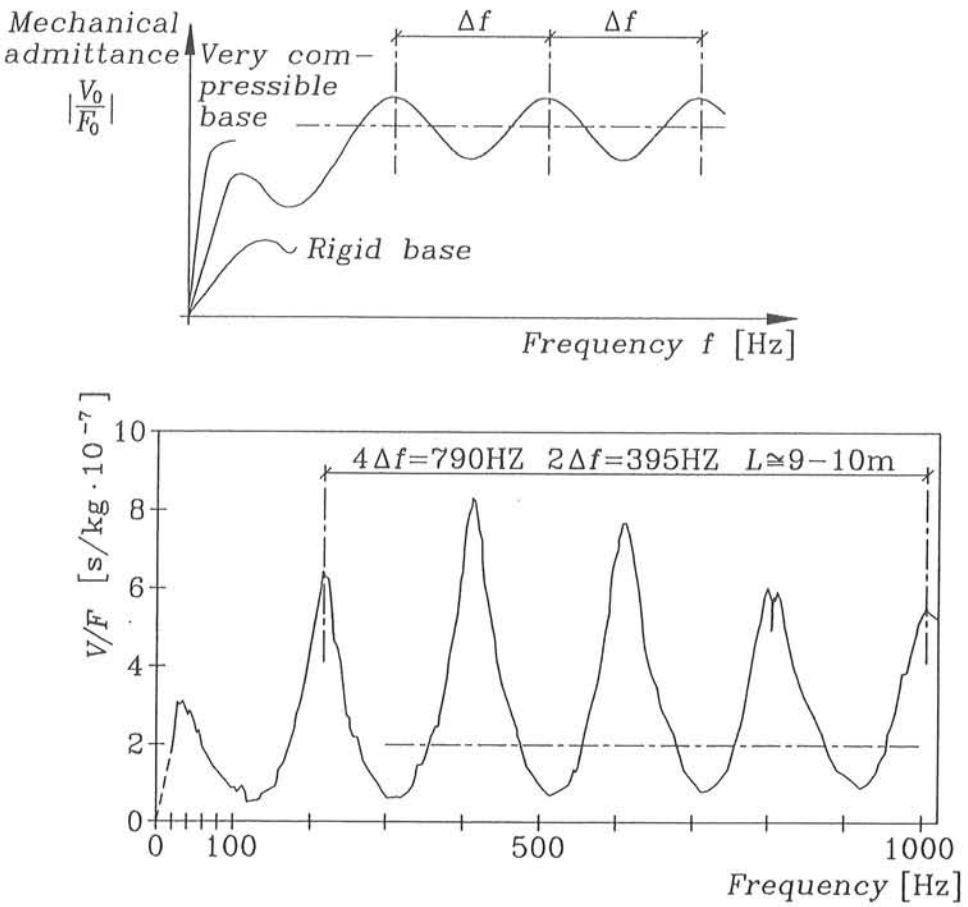

Figure 3.6 Upper : Theoretical response curve for a cylindrical pile, Lower : Response curve for a cylindrical pile of 15 m (Davis and Dunn [74.1]).

The above clearly demonstrates that there is a possibility to get an economic benefit by performing vibration tests on piles.

3.3 CONCLUSION

The step by step description in section 3.1 revealed that a complete VBI-programme includes the use of many different advanced engineering disciplines. These disciplines will be treated in the remaining part of this thesis.

The performed review has shown that the use of dynamic measurement for structural integrity monitoring of civil engineering structures is an area, which has been given much attention during the last decade. However, it will require a lot of research work before the methods are fully developed.

VBI has been widely used on piles and is almost fully developed to these kinds of structures. This is primarily because piles are relatively simple structures and that there is a large number of almost identical piles. Further, the fact that VBI is cheaper than other NDI-methods for piles has also stimulated a quick development.

Many investigators have performed calibration tests on either models or real structures, which contained a well defined state of damage. The results from these tests have primary led to a solution of equation (3.2) for that particular type of structure. Only a limited number of investigators have used their results to calibrate a model of damage and/or to obtain the functional $F(R)$ in equation (3.1). However, the performed tests are of course very significant in the further development of the VBI-methods.

The performed tests have primarily been focused on the use of natural frequencies as damage indicators, because it is quite easy to measure these. However, the use of mode shapes has been given more and more attention. A common feature of the test is that the investigators only use one of the two. Diagnostic methods which includes both parameters as damage indicators are presented in chapter 8.

The results from the calibration tests have shown that small local damages only lead to relatively small changes in the global dynamic characteristics. This means that such damages can only be detected through a local test (see e.g. Kenley & Dodds [80.1] and Crohas & Lepert [82.2]). Often the changes in e.g. natural frequencies will be comparable to for instance changes in the ambient climate (see e.g. table 3.1). This fact

leads to a demand for high accuracy and reliability of the system identification methods in use.

The choice of excitation is a topic, which has been subject to much attention in many of the performed calibration tests. The use of vibration originating from ambient sources such as traffic and wind is preferable from a practical point of view, because the structure can continue its normal operation during performance of the tests. However, the use of ambient vibration may give problems in the form of e.g. missing energy at important frequency. Mazurek and DeWolf [90.13] point out, that ambient vibration is the only source of vibration, which can reasonably be used in an automatic VBI-programme. The choice of excitation will be treated further in section 6.3.

The possibility of revealing damage in a hidden structural component like e.g. foundation is clearly a feature which make VBI very attractive in comparison with other NDI-methods. Furhter, as a by-product, the VBI gives an extended knowledge about the dynamic behaviour of structures, which can be used in the design phase of subsequent projects. However, the gain can be limited due to the one-of-a-kind problem in civil engineering.

The performed review has shown that VBI has been used in many cases and it is a serious alternative to other NDI-methods. However, the method is still in its infancy. It is unrealistic to believe that the method ever will be developed to a "stand alone" method.

CHAPTER 4
MODELLING OF A CRACKED BEAM

The introduction of a crack in a beam will cause a local change in stiffness and damping capacity. The local change in stiffness will lead to a change of the natural frequencies of the structure and changes in the derivatives of the mode shapes at the crack position. The stiffness will normally decrease when a crack is introduced. This means that the natural frequencies will either decrease or remain unchanged (see figure 4.1).

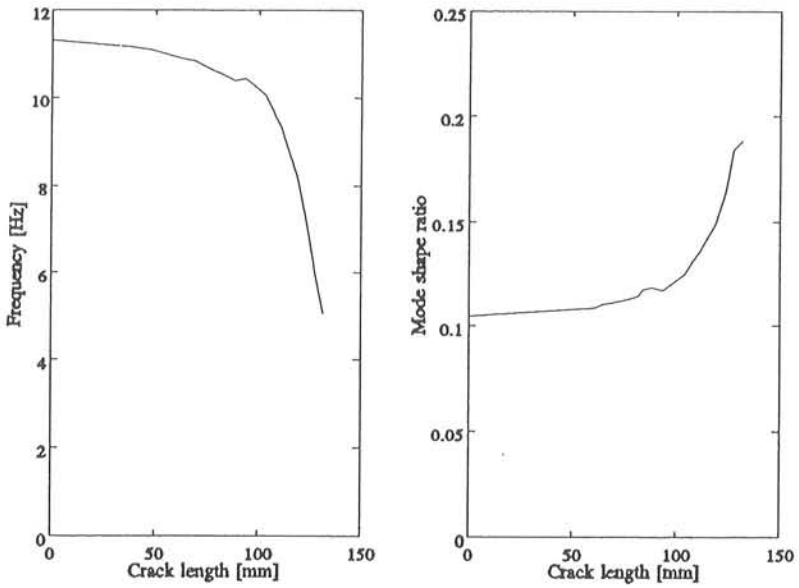

Figure 4.1 Results from experimental case 1, beam 4 (Rytter et al. [92.7]).

The basic idea in VBI is to measure these dynamic characteristics throughout the lifetime of the structure and use them as a basis for detection of the position and magnitude of cracks, if any. However a successful detection of cracks through measuring of the dynamic characteristics is very dependent on exact modelling of the crack depending changes in stiffness and damping.

The change in stiffness due to a crack has been investigated by many researchers, whereas methods to calculate the change in damping due to cracking are very limited. A review of different models for the change in stiffness of linear elastic beams is given in section 4.1. Section 4.2 contains a summary of published models of damping due to cracking.

4.1 STIFFNESS

This section contains a presentation and an evaluation of the most commonly used models for a cracked beam in bending modes.

4.1.1 Short Beam Element

In this model the presence of a crack is taken into account by introducing a short beam element with a reduced bending stiffness at the position of the crack (see figure 4.2). The modelling of the beam in the neighbourhood of the crack is solely based on traditional beam theory.

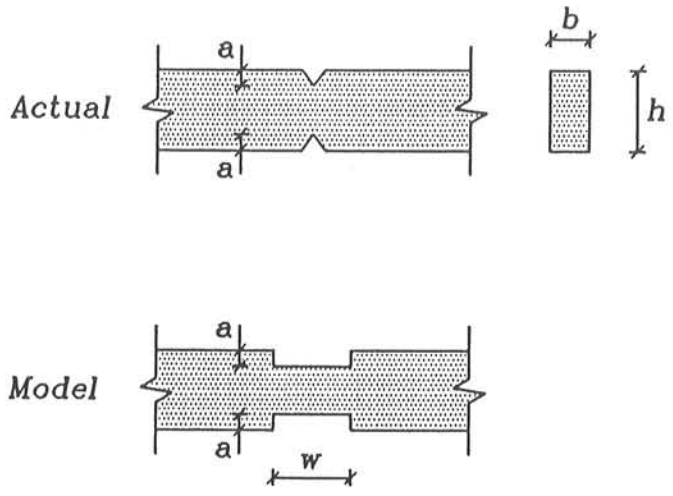

Figure 4.2. Short beam element model.

This way of modelling a cracked beam was probably the most commonly used model until the mid seventies, where the fracture mechanical model (see section 4.1.3) became the most preferred model.

The main reason for the widespread use of the model is that it is easy and quick to use in connection with both analytical solutions (see e.g. Joshi and Madhusudhan [91.5]) and traditional FE-programme. A further feature of the model is that no details of the geometry of the cracked zone are required (see e.g. Yuen [85.7]).

Notches and cracks in a beam will cause irregularities in the stress distribution and local deformations in the vicinity of the notch/crack. Part of the beam will in fact be inefficient due to the changes in the stress distribution. The main disadvantage of the short beam element model is that it does not take account of this ineffective material and the local deformations.

This lack of the model has been known for many years, but a general solution to the problem has never been given. The most commonly suggested solution is the introduction of an equivalent width w of the slot/crack (see figure 4.2). For instance this solution has been suggested by Kirsmer [44.1], Thomson [49.1] and Petroski [81.1].

Kirsmer [44.1] obtained a relationship between the changes in the first natural frequency of a simply supported beam and an equivalent slot width through energy considerations. Kirsmer used experimental data to calibrate his expression with respect to the equivalent width of the slot. He found that an equivalent width equal to five times the actual width of the slot gave reasonable agreement between analytical and experimental data.

In 1949 Thomson (see Thomson [49.1]) developed a procedure for the determination of the vibrational characteristics of slender bars with discontinuities in stiffness due to a narrow slot or crack. Thomson developed his model from a method given by Hetényi [37.1] for a statically loaded beam. The basic idea is to determine the deflection of the slotted/cracked beam by considering the beam to be uniform with a pair of moments M' applied at the slot/crack position (see figure 4.3). However it was pointed out by Thomson, that the procedure would only be applicable, if an equivalent slot accounting for the inefficient material adjacent to the slot was determined through experiments.

Petroski [81.1] used results from tests with a three point bending specimen and fracture mechanics theory to calculate an equivalent width of the slot/crack to be used in the model developed by Thomson. Petroski found that the equivalent width W_{eq} of the slot in this special case should be taken as

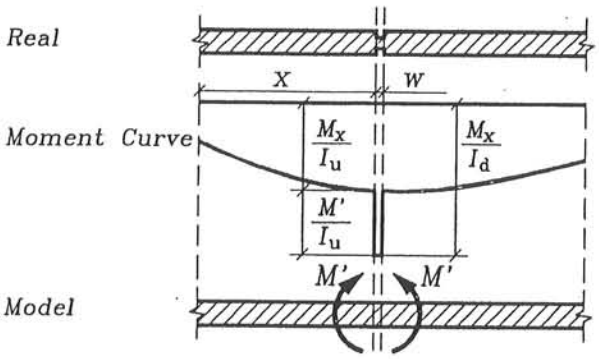

Figure 4.3 Thomson's model (Thomson [49.1]).

$$W_{eq} = \frac{PL^2V(l)}{16M}$$

where

$$l=\frac{a}{h} \qquad (4.1)$$

$$V(l) = (5.58-19.57l+36.82l^2-34.94l^3+12.77l^4)(\frac{l}{1-l})^2$$

where P is the point load, L is the beam length, M is the bending moment, a is the crack length and h is the beam height.

However, it is unlikely to believe, that such a relatively simple relationship can be used in general. For instance the results in example 4.1 (see figure 4.6) show a variation in the required equivalent crack width as the crack length is increased.

Example 4.1

The aim of this example is to

- demonstrate the practical use of the short beam element
- compare the results with results obtained from beam B3 in experimental case no. 1
- evaluate the usefulness of the model in connection with level 2 and 3 methods

An FE-model of test beam B3 (see figure 4.4) has been established. The model consists of 13 linear beam elements. 3 lumped masses of 0.1 kg were included to take into account the presence of the accelerometers during the tests.

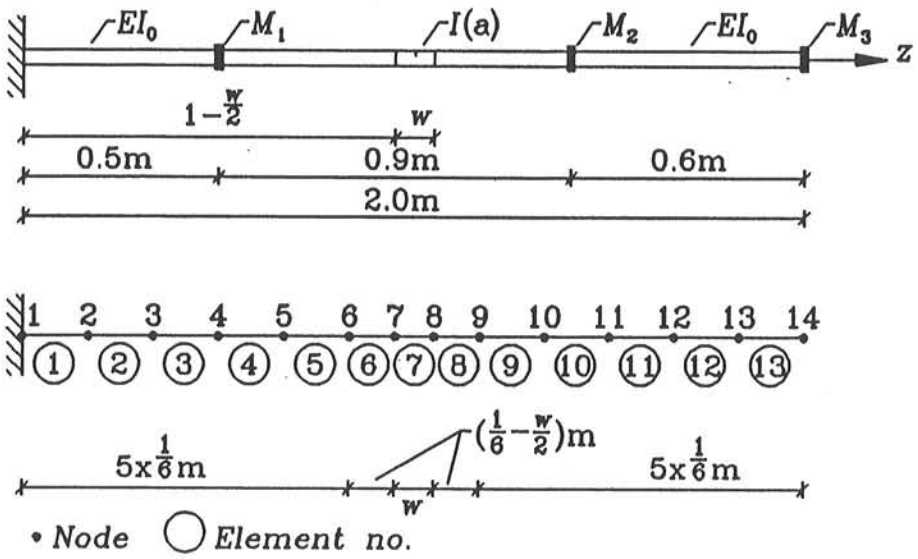

Figure 4.4 FE-model of beam B3.

The crack was located in element no. 7 and assumed to be symmetric with respect to the z-axis. The moment of inertia I as function of the crack length is shown in figure 4.5.

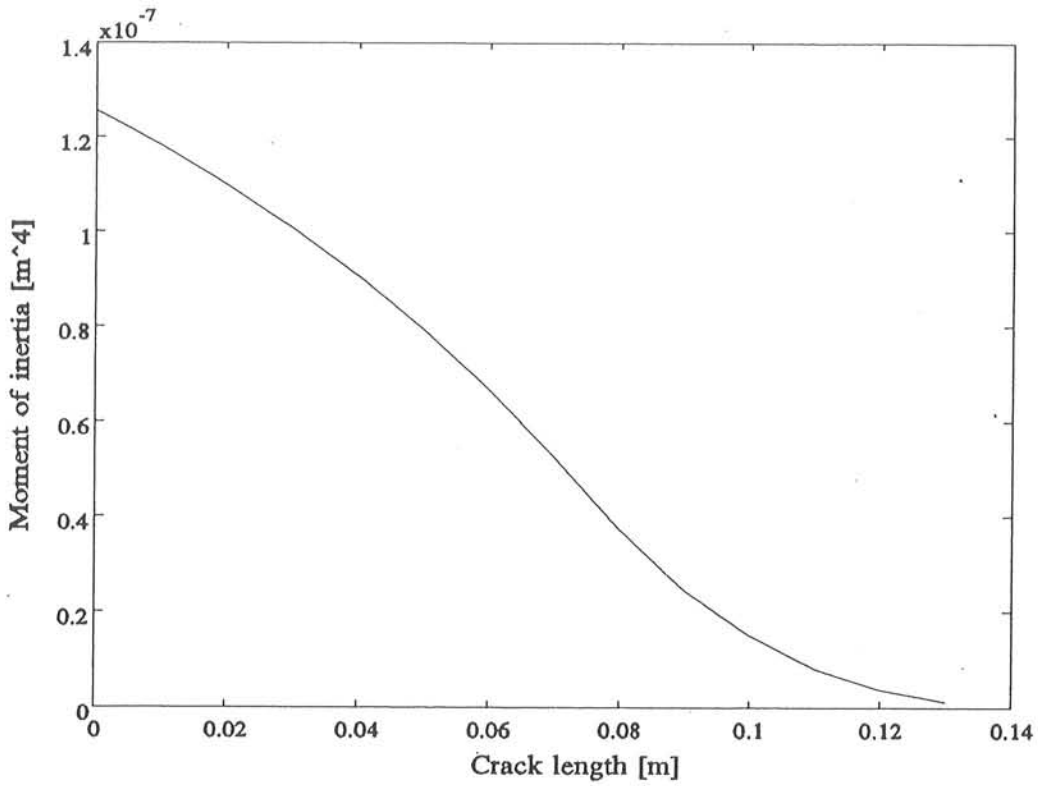

Figure 4.5 Variation of moment of inertia with crack length

The first natural frequency was calculated for all possible combinations of the following values of the crack length $a \in$ [0;0.1;0.2;0.3;0.4;0.5;0.6;0.7;0.8;0.9;0.1;0.11;0.12;0.13] m and element length $L_7 \in$ [0.03;0.05;0.07] m. The results are shown in figure 4.6 together with the experimental data for beam B3.

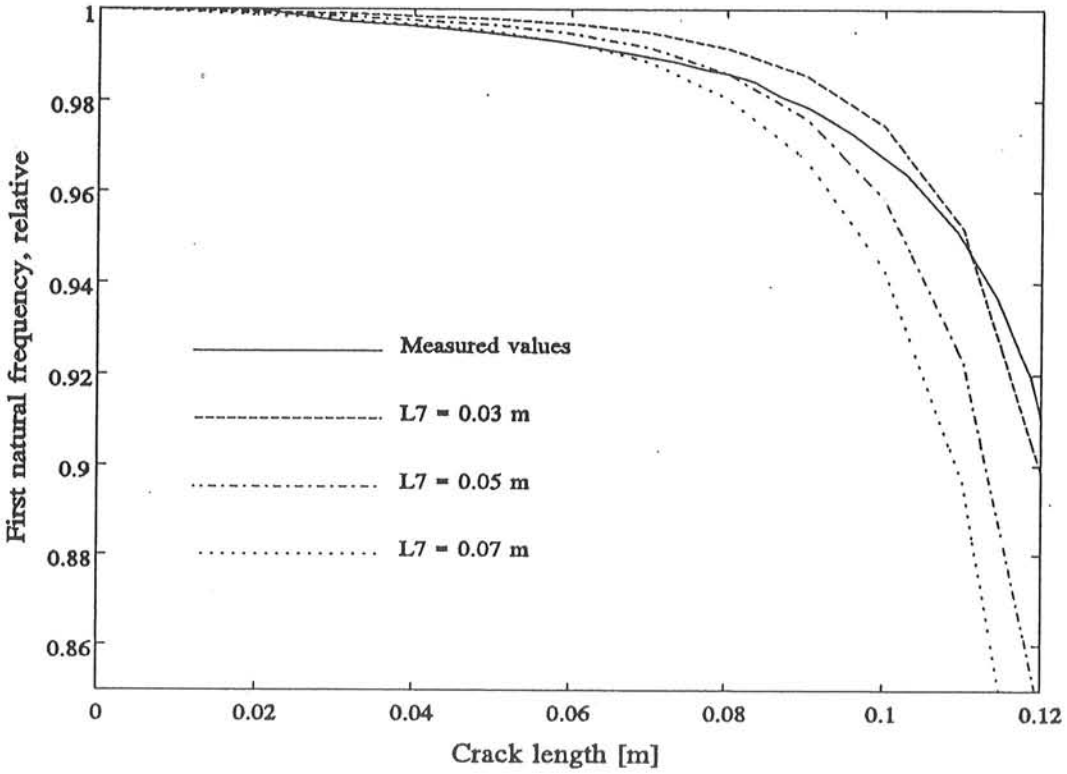

Figure 4.6 First natural frequency, B3.

It can be seen from figure 4.6 that the curve from the experimental tests does not coincide with any of the curves determined through FE-calculations. This means that it is impossible to define a simple equivalent crack width like e.g. the one found by Kirsmer [44.1]. Therefore, it can be concluded that the model is practicable in level 2 methods but not in level 3 methods.

From the above it can be concluded that the model is rather primitive and cannot be expected to give answers correct to several decimals. However, it can provide fundamental insight and give order of magnitude results that are often sufficient for some engineering purposes. Thus the model is not applicable to detection of fatigue cracks.

However, the model has in many cases been successfully calibrated/verified through laboratory tests on beams containing saw cuts (see e.g. Wendtland [72.1]). Wendtland concludes that the model fails for small width of the slot. In that case Wendtland recommend the use of a rotational bending spring (see section 4.1.3). Wendtland [72.1] derives an expression for the stiffness of such a rotational spring through ordinary beam theory. The stiffness depends on the width and depth of the slot/crack. Wendtland verifies the usability of the model by comparison of data from analytical and experimental test on cantilevers containing narrow saw cuts. However, Wendtland points out that the model leads to an underestimation of the decrease in natural frequencies in cases with a relatively large depth of the crack, because it does not take into account the areas of inactive material in the zone close to the crack opening.

In connection with VBI the model will only be applicable to level 1 and 2 methods.

4.1.2 Smeared model

This model is mainly used in connection with FE-analysis. The basic idea is to retain the original configuration of nodes and elements. The presence of a crack is then simply taken into account by reducing the bending stiffness of the element, which in principle contains the crack.

Thus the model is even more simple and rough than the short beam element presented in section 4.1.1. Variations in natural frequencies with respect to the size of damage calculated by means of the model will have poor accuracy and will typically be overestimated (see figure 4.7).

Therefore, the model has primarily been used in connection with sensitivity studies of the modal parameter of a damaged structure. For instance the model has been used for this purpose by Yuen [85.7] in his study of a damaged cantilever.

Example 4.2

The aim of this example is to

- demonstrate the practical use of the smeared model
- compare the results with results obtained from beam B3 in experimental case no. 1

An FE-model of test beam B3 (see figure 4.4) has been used. The model consists of 13 linear beam elements. 3 lumped masses of 0.1 kg were included to take into account the presence of the accelerometers during the tests.

The crack in beam B3 is located at z = 1.0 m, which is equal to the location of node no. 7. Therefore, both element 6 and 7 have been considered as possible damage sites in the performed analysis. The moment of inertia has been reduced successive for I_o to $0.1I_o$ in steps of $0.1I_o$, where I_o is the moment of inertia of the undamaged profile. The results are shown in figure 4.7 together with the experimental data for beam B3.

It can be seen from figure 4.7 that the use of the smeared model as expected lead to an overestimation of the decrease in the natural frequency due the introduction of a crack.

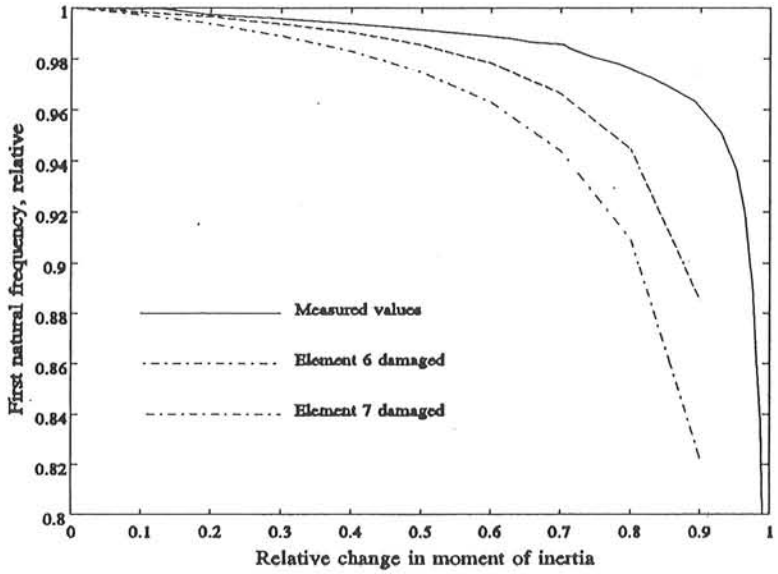

Figure 4.7 First natural frequency, B3.

In connection with VBI the model will only be applicable to level 2 methods to a limited extent, because the use of the model will give a relatively large area as the damage location instead of a certain spot. However, the method can be used as a basis for evaluation of new level 2 methods. For instance, this possible field of application has been utilized by Pandey et al. [91.9].

The model can be used in connection with level 2 methods based on results from global measurements on complex structures like e.g. the tower in experimental case no. 2. In this case potentially damaged elements are identified. The exact location of the crack can then be found in a subsequent local measurement on these elements.

4.1.3 Fracture Mechanical Model

The basic idea of this model is to model the crack zone of a beam by means of a local flexibility matrix found from fracture mechanics.

The fundamental principle in the determination of this flexibility matrix will be summarized in the following for a prismatic beam (see figure 4.8). However, in principle the model can be used for all kinds of cross-sections.

The additional displacement u_i along the force P_i is in accordance to Castigliano's theorem (see e.g. Timoshenko and Goodier [82.8]) related to the strain energy Φ due

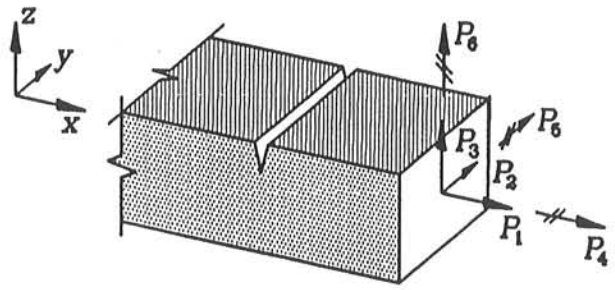

Figure 4.8 Prismatic beam.

to a crack by

$$u_i = \frac{\partial \Phi}{\partial P_i} \tag{4.2}$$

The strain energy Φ due to a crack is given as

$$\Phi = \int_0^{A_c} \frac{\partial \Phi}{\partial A} dA = \int_0^{A_c} J dA \tag{4.3}$$

where J is the strain energy release rate (see e.g. Hellan [85.5]) and A_c is the crack surface. The flexibility influence coefficient α_{ij} will be

$$\alpha_{ij} = \frac{\partial \dot{u}_i}{\partial P_j} = \frac{\partial^2}{\partial P_j \partial P_i} \int_0^{A_c} J dA \tag{4.4}$$

Thus the flexibility matrix will be a 6x6 matrix if all the degrees of freedom are taken into account.

The relation between J and the stress intensity factors for linear elasticity is given by (see e.g. Hellan [85.5])

$$J = \frac{\beta}{E} K_I^2 + \frac{\beta}{E} K_{II}^2 + \frac{1+\nu}{E} K_{III}^2, \qquad \beta = \begin{cases} 1 & for\, plane\, stress \\ 1-\nu^2 & for\, plane\, strain \end{cases} \tag{4.5}$$

where ν is Poisson's ratio, E is the modulus of elasticity and K_I, K_{II} and K_{III} are the stress intensity factors for modes I, II and III respectively.

This means that the local flexibility caused by a crack can be calculated by

$$\alpha_{ij} = \frac{1}{E}\int_0^{A_c} \frac{\partial^2}{\partial P_i \partial P_j}\left[\beta K_I^2 + \beta K_{II}^2 + (1+\nu) K_{III}^2\right] dA \qquad (4.6)$$

if K_I, K_{II} and K_{III} are known.

The effect of the ineffective material discussed in section 4.1.1 is inherent in the expression for the stress intensity factors and thereby in the local flexibility matrix. Thus a high level of accuracy can be expected when using this model. The level of accuracy depends on reliable expressions for the stress intensity factors (see example 4.3) and a detailed description of the geometry of the cracked zone.

Expressions for the stress intensity factors for different cross-sections can be found in standard handbooks like e.g. Tada et al. [73.1]. However, an expression for K_I for a crack in a rectangular box profile like the one used in experimental case no. 1 cannot be found in any of the standard handbooks. This problem has been solved by means of the following three methods (see appendix A)

a) Adjustment and piecing together known expressions

b) FEM analysis

c) Calibration based on experimental data

The three expressions have been evaluated by comparison of the variation of the first natural frequency of beams B3 and B4 with crack length (see figure 4.9).
The curves in figure 4.9 do not point out clearly the expression to be preferred. However, it is better to overestimate than underestimate crack lengths in connection with VBI. Therefore, the expression found through calibration (expression 3) will be used in subsequent part of this thesis. Thus K_I will be calculated as

$$K_I = \sigma_o \sqrt{\pi a}\,(0.90 + 1.72(\frac{a}{b+h}) - 11.42(\frac{a}{b+h})^3 + 140.17(\frac{a}{b+h})^5) \qquad (4.7)$$

The model presented above has probably been the most widely used model through the past 2-3 decades. In connection with VBI the model is applicable to level 1-3 methods (see e.g. Rytter et al. [91.8] and chapter 8).

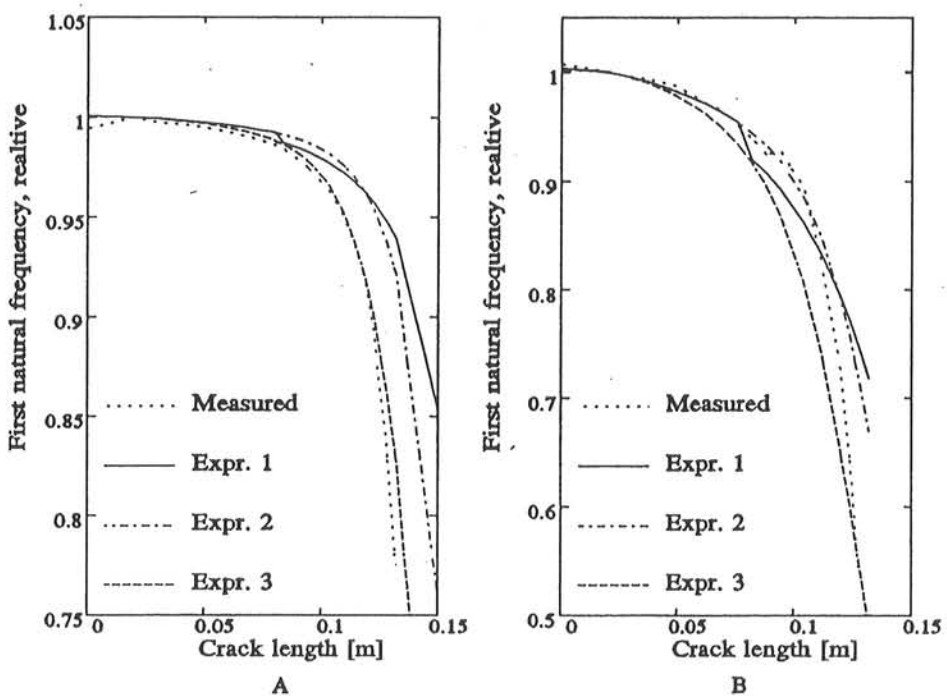

Figure 4.9 Comparison of the measured and the calculated variations in the first natural frequency, A) Beam B3 and B) Beam 4 (See appendix A).

Irwin [60.1] was probably the first person to relate the local flexibility of a cracked beam to the stress intensity factor. Initially the model was primarily used to study the effect of the local flexibility of a cracked column upon its buckling load (see e.g. Liebowitz et al. [67.1] and Okamura et al. [69.1]).

Okamura et al. [72.2] found the local flexibility for axial load and bending in rectangular beam separately. They studied the variation of the first natural frequency of a free-free beam as a function of the crack length.

Ju et al. [82.5] considered a beam in pure bending and used the results in connection with damage detection. Ju et al. [82.5] are mentioned as originators of the model in several papers (see e.g. Haisty and Springer [88.10]) in spite of the fact that Okamura et al. [72.2] presented the model in dynamic analysis approximately ten years earlier.

A common feature of the above-mentioned papers and many other papers is that only a limit number of members (typically diagonal elements) of the flexibility matrix were included.

Dimarogonas and Paipetis [83.6] established a 5x5 flexibility matrix to model the vicinity of a crack. The model did not include torsion. Later Papadopoulos and Dimarogonas [87.10] completed the matrix by adding torsion and obtained a full 6x6 flexibility matrix.

Gudmundson [83.7] presented a complete flexibility matrix for the cracked zone of a beam at the same time as Dimarogonas and Paipetis [83.6]. Gudmundson reports on results from experimental verifications. However, disagreements between predicted and actual frequencies for beams containing fatigue cracks were observed. Gudmundson gives the crack closure effect (see section 4.1.5) as the primary reason for these disagreements.

Example 4.3

The fracture mechanical model has been used by several authors in their investigations of cracked beams. A beam with rectangular cross-section has been one of the most preferred test subjects. This is probably because expressions for K_I can be found in standard handbooks for stress intensity factors. However, the expression used for K_I varies from paper to paper. The aim of this example is to study the effect of these inconsistencies on the variation in the first natural frequency of a cantilever with a rectangular cross section (see figure 4.10).

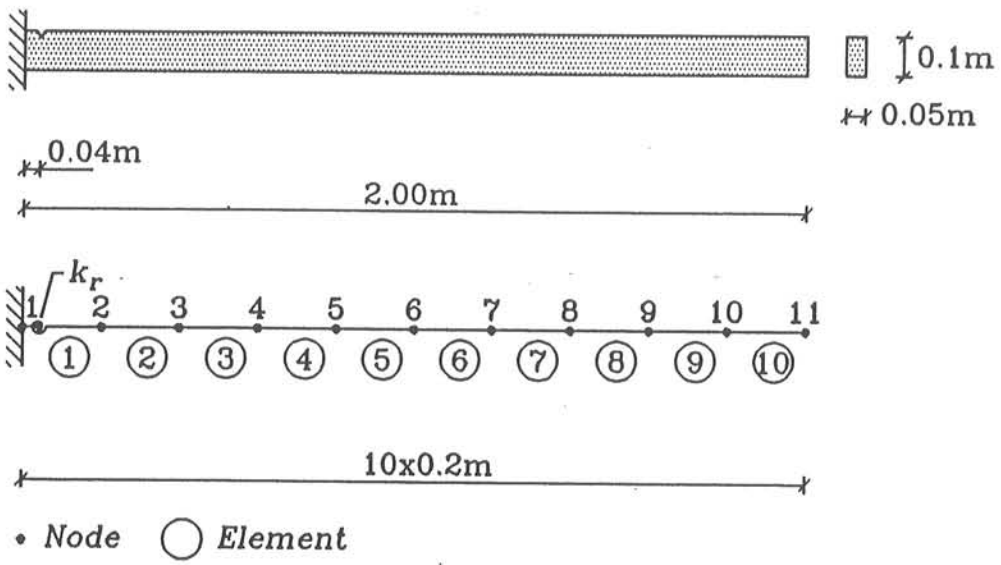

Figure 4.10 Definition of crack location.

Normally the stress intensity factor K_I is written as

$$K_I = \sigma_o \sqrt{(\pi a)} f(\frac{a}{h}) \tag{4.8}$$

where σ_o is a characteristic stress value of the undamaged beam, a is the crack length and h is the beam height. It is the function $f(\frac{a}{h})$, which varies in the different papers.

Tada et al. [73.1] give the following two expressions

$$f(\frac{a}{h}) = 1.122 - 1.4(\frac{a}{h}) + 7.33(\frac{a}{h})^2 - 13.08(\frac{a}{h})^3 + 14(\frac{a}{h})^4 \ , \quad for \ \frac{a}{h} < 0.6 \tag{4.9}$$

$$f(\frac{a}{h}) = \sqrt{\frac{\tan\zeta}{\zeta}} \frac{0.923 + 0.199(1-\sin\zeta)^4}{\cos\zeta}, \quad for \ all \ \frac{a}{h}, \quad where \quad \zeta = \frac{\pi a}{2h} \tag{4.10}$$

Gudmundson [82.4] uses this expression for small values of $\frac{a}{h}$

$$f(\frac{a}{h}) = 1.12, \quad for \ \frac{a}{h} < 1 \tag{4.11}$$

Ostachowicz and Krawczuk [91.13] use

$$f(\frac{a}{h}) = 1.13 - 1.374(\frac{a}{h}) + 5.749(\frac{a}{h})^2 - 4.464(\frac{a}{h})^3 \ , \quad for \ \frac{a}{h} < 0.5 \tag{4.12}$$

Hellan [85.5] gives

$$f(\frac{a}{h}) = 1.12 - 1.39(\frac{a}{h}) + 7.3(\frac{a}{h})^2 - 13(\frac{a}{h})^3 + 14(\frac{a}{h})^4 \ , \quad for \ \frac{a}{h} < 0.7 \tag{4.13}$$

The five different expressions for $f(\frac{a}{h})$ have been calculated for the beam shown in figure 4.10. The results are shown in figure 4.11.

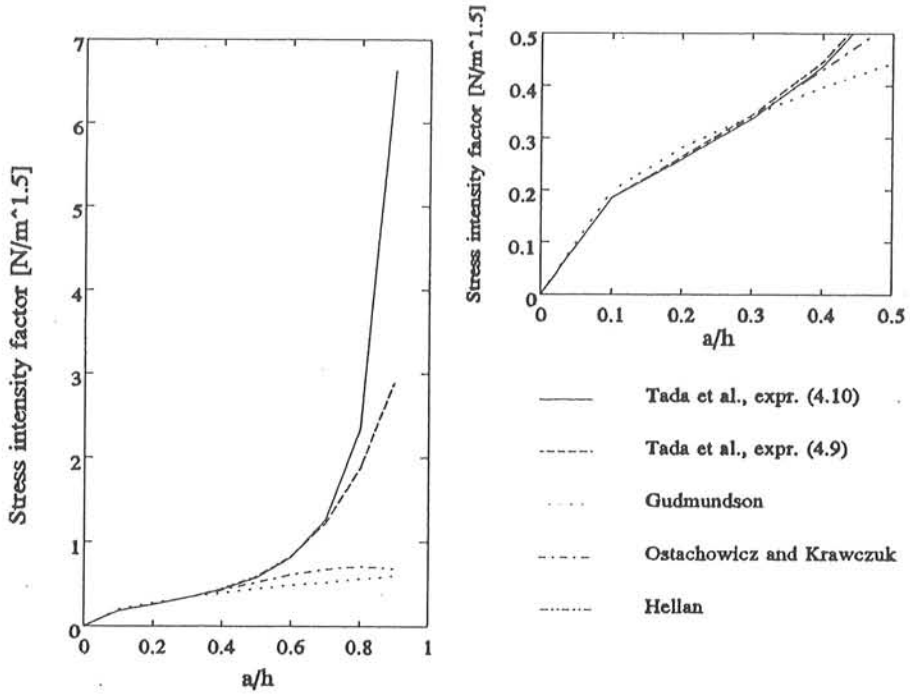

Figure 4.11 Variation of stress intensity factors with crack-height ratio.

The graphs in figure 4.11 show only small differences between the five expressions for $\frac{a}{h} < 0.3$. The maximum difference is 2-3 % for the simple expression given in (4.11). Further, it can be seen, that the upper bound for the expression in (4.12) is rather 0.4 than 0.5, if the expression in (4.10) is used as reference. As expected, the small variations in the polynomium coefficients in (4.9) and (4.13) do not cause any difference of importance between the shape of the two curves.

To investigate the influence of the difference between the expressions for K_I the first natural frequency has been calculated for the prismatic beam shown in figure 4.10. The results are shown in figure 4.12.

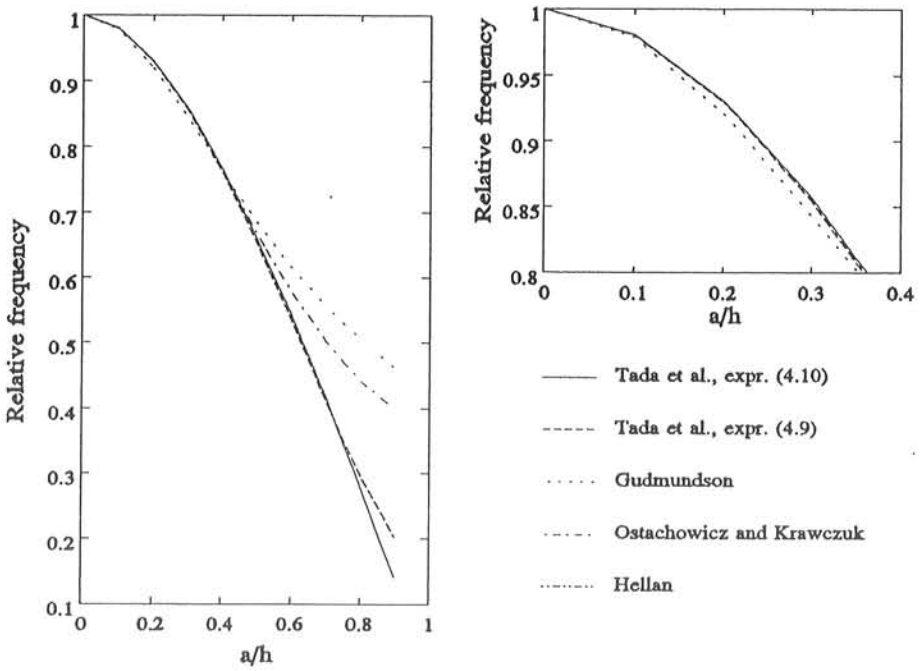

Figure 4.12 Variation of the first natural frequency with crack-height ratio.

The graphs in figure 4.12 show very small differences between the five curves for $\frac{a}{h} < 0.4$. Therefore, it will be preferable to use the expression in equation (4.11) for small cracks, because this simplifies the integral in (4.6) considerably. Further, it can be seen that in fact the upper validity bound of (4.12) is 0.5, if (4.10) is taken as reference.

The fracture mechanical model can easily be included in a finite element. For instance this has been done by Haisty and Springer [88.10], Gounaris and Dimarogonas [88.11] and Ostachowicz and Krawczuk [92.6]. Only the diagonal elements of the local flexibility matrix are included in the FE presented by Haisty and Springer [88.10], whereas Gounaris and Dimarogonas [88.11] and Ostachowicz and Krawczuk [92.6] included the complete 6x6 local flexibility matrix.

A finite beam element containing a crack has been established in connection with the preparation of the present thesis. This model includes only the diagonal element of the local flexibility matrix that concerns bending about the y-axis (see figure 4.8).

4.1.4 Advanced FE-Models

The use of plate finite elements gives the opportunity for a more detailed and exact modelling of the area around a crack in a beam. The uncertainties of the modal parameter will of course decrease, when the FE-model is refined.

The number of degrees of freedom increases considerable by the introduction of plate elements instead of beam elements. This increase causes a considerable increase in the use of CPU in connection with e.g. the solution of eigenvalue problems (see figure 4.13).

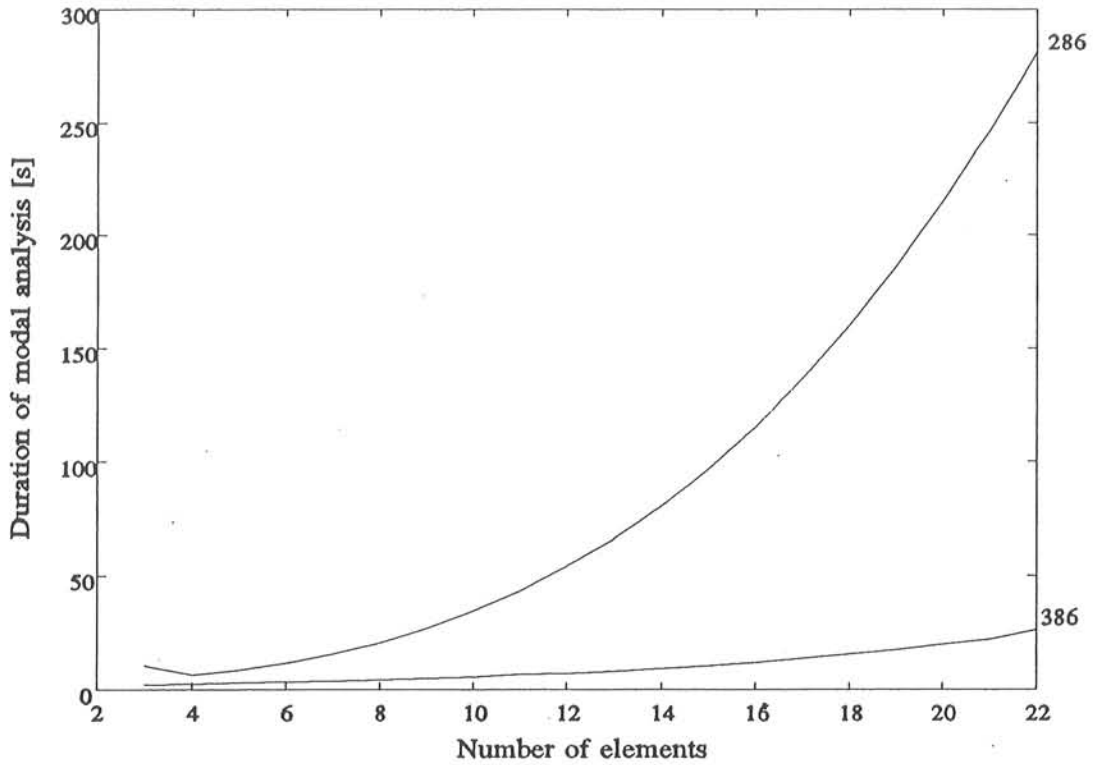

Figure 4.13 Time of calculation as a function of the number of degrees of freedom.

The number of degrees of freedom might be reduced by using a combination of plate and beam elements as suggested in Sato [83.5]. Sato [83.5] uses an FEM-mesh to model local discontinuity and combines it with the transfer matrix method TMM (see e.g.

Thomson [81.3]). However, the TMM-part can easily be replaced by FE-beam elements. Sato evaluated his method by comparing the variation of the first natural frequency due to changes in the dimensions of the slot found through calculations and tests on a free-free beam. Further he used simple beam theory (see section 4.1.1) to demonstrate the effectiveness of his method. The results are shown in figure 4.14. The effectiveness of the Sato-model is obvious from the good agreement between calculated data and the experimental data. Further, it can be seen that the simple beam theory fails for small values of the ratio between the slot width and the beam height. This is because the extent of the ineffective material (see section 4.1.1) and the width of the slot are of the same order of magnitude.

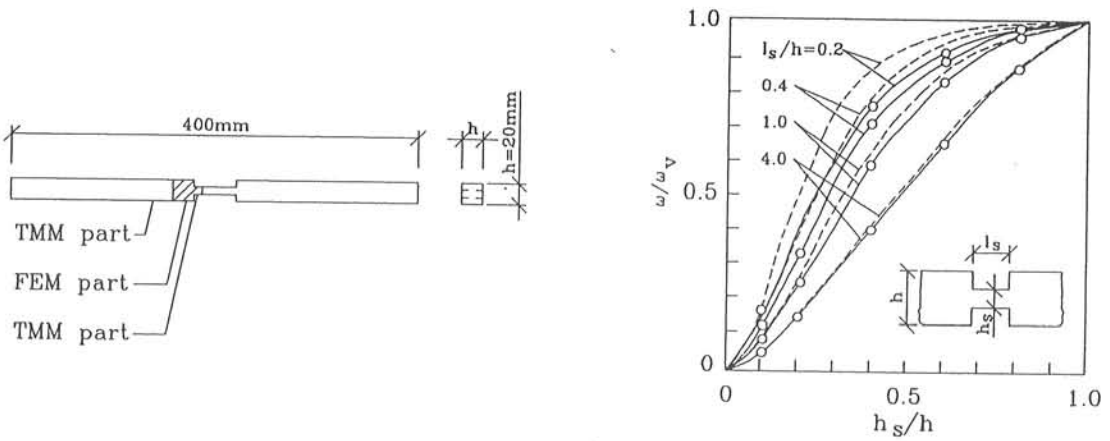

Figure 4.14 Variation of the first natural frequency with slot dimensions, Sato's theory ————, simple beam theory ---- and ○ experiment (Sato [83.5]).

The modelling of the area around a crack in a beam can be performed in a more or less sophisticated way. Two of the more sophisticated models of a cracked beam are presented in Shen and Pierre [90.17] and Ostachowicz and Krawczuk [90.16], respectively.

Shen and Pierre [90.17] use three different types of elements in connection with the validation of results from their theory for calculation of the natural modes of Bernoulli-Euler beams with symmetric cracks (see figure 4.15). The area around the crack has been modelled by means of either an eight-node quadrilateral element or a six-point triangular element, where the mid-side nodes near the crack tip are moved to the quarterside position. The remaining part of the beam was modelled by means of ordinary quadrilateral eight-node elements.

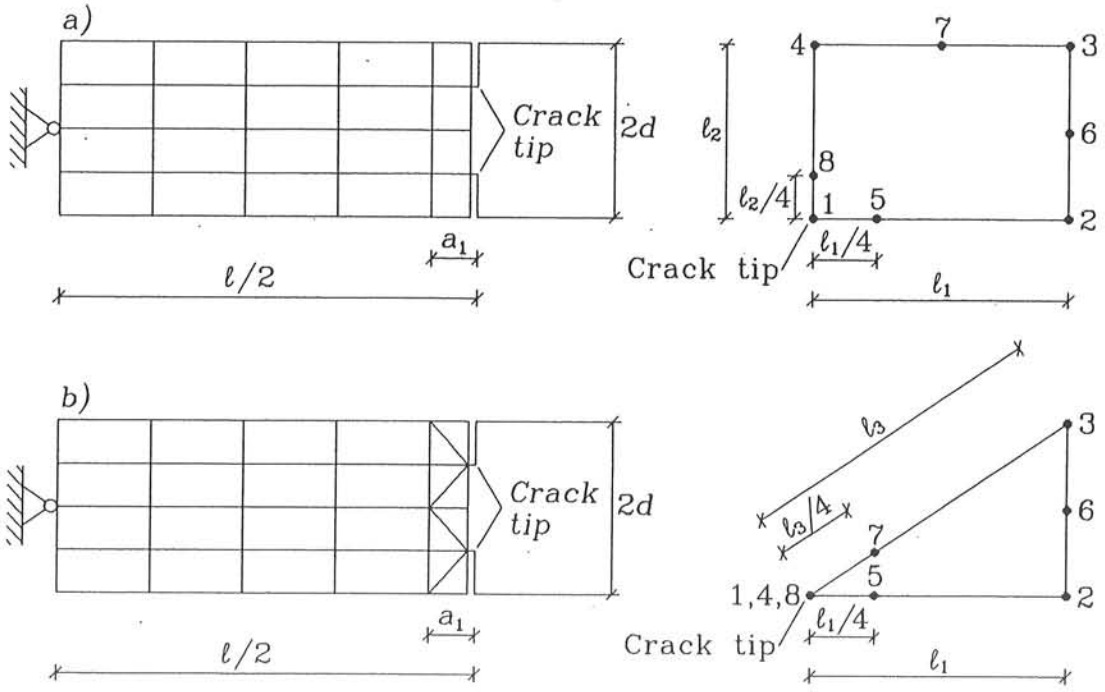

Figure 4.15 Example of a detailed finite element model of a cracked beam (Shen and Pierre [90.17]).

Ostachowicz and Krawczuk [90.16] use a so-called point finite element (PFE) to model the local flexibility due to a crack. The PFE allows for modelling of the non-linear behaviour in the crack due to a regular opening and closing of the crack (see figure 4.16).

The rest of the beam is modelled by triangular finite elements having two degrees of freedom at each node.

The relatively long computer time compared with the accuracy of the data (e.g. natural frequencies) obtained from experimental tests causes limited use of the advanced FE-models in connection with VBI.

Therefore, the advanced FE-models are mainly used in connection with calibration of expressions for stress intensity factors and in simulation studies as a basis for the evaluation of new level 2-4 methods.

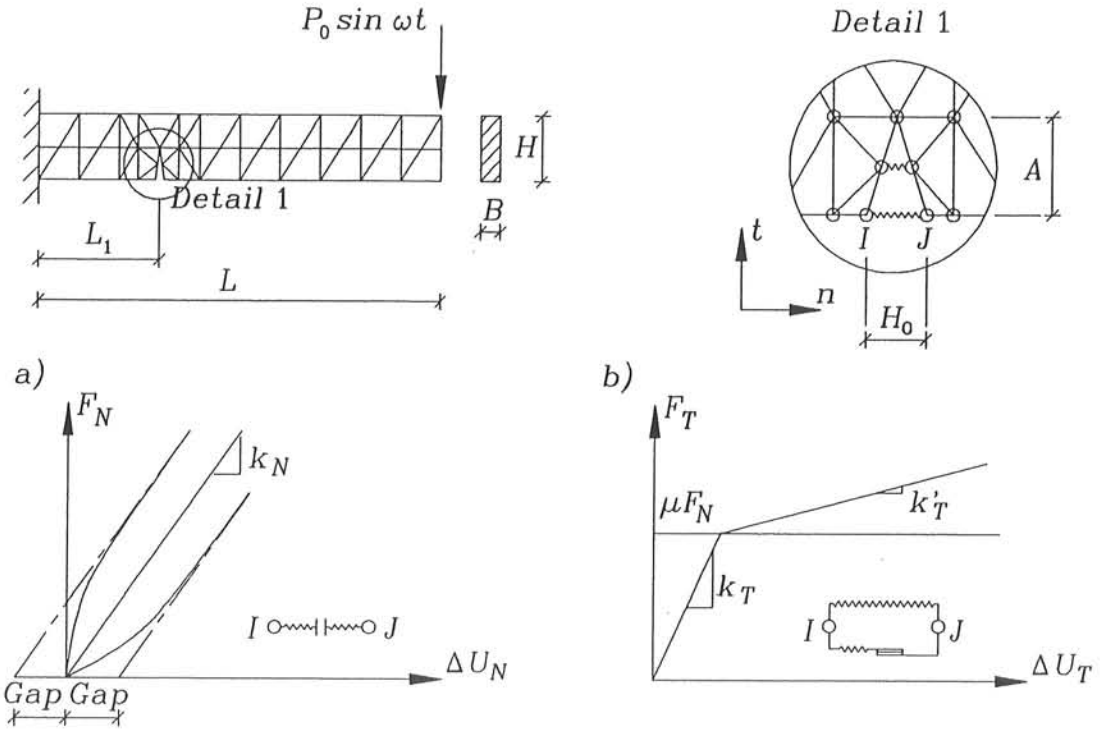

Figure 4.16 Example of a detailed finite element model of a cracked beam. a) Load-displacement curve of the PFE for axial loads, b) Load-displacement curve of the PFE for shear loads (Ostachowicz and Krawczuk [90.16]).

4.1.5 Non-Linearities

A crack in a beam will in many cases in turn be open and closed depending on the sign and magnitude of the internal forces (e.g bending moments) at the crack position. This implies that the stiffness of the beam becomes non-linear.

Further, in the growth of a crack, plastic deformations are introduced in the vicinity of the crack tip. These deformations result in residual stresses in the beam attempting to close the crack. Thus for small vibrational amplitudes, the crack will not open, and the beam will act as an uncracked beam. For longer cracks, also as a result of the residual stresses, a small part of the crack is open. This partially opened crack is, for small

vibrational amplitudes, equivalent to a beam with a shorter crack. This phenomenon is known as crack closure.

Clark et al. [87.7] have studied the effect of crack closure on the reliability of different NDT predictions of crack size. They used four point bending specimens and measured the crack opening by means of a clip gauge. Figure 4.17 shows a crack opening/closing displacement versus applied load. The figure shows that the crack closure effect should be given great attention.

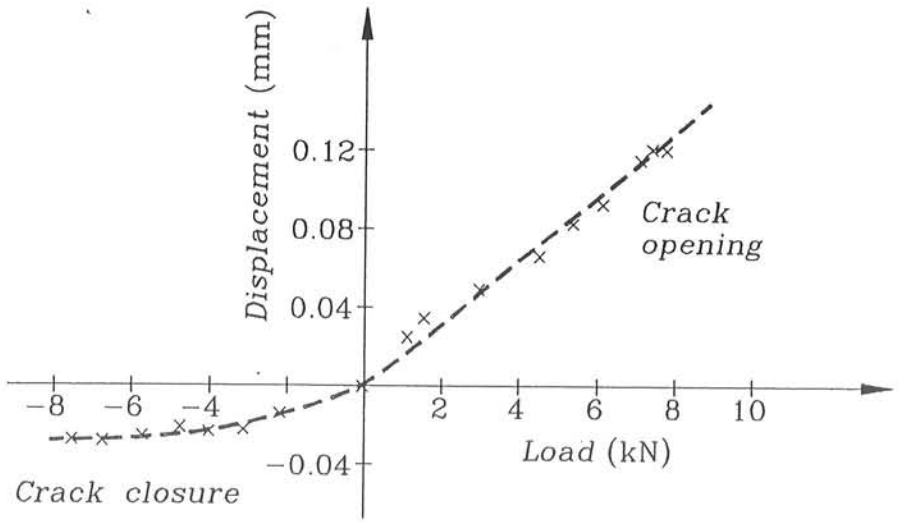

Figure 4.17 Crack opening/closening displacement versus load (Clark et al [87.7]).

Gudmundson [83.7] reports on an inconsistency between analytical and experimental data and explains it by the crack closure effect.

Field investigations performed by Abdundur and Duchêne [90.19] on a concrete bridge show (see figure 4.18) that the rotation of the cracked section and the crack gap is linear with 3 level changes.

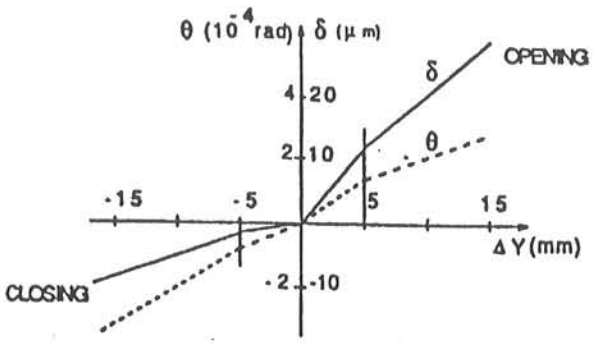

Figure 4.18 Gap δ and rotation θ of a cracked section due to level change $\pm \Delta y$ at an end support (Abundur and Duchêne [90.19])

A non-linear rotational spring (see figure 4.19) is a commonly used model (see e.g. Friswell and Penny [92.3] and Dimarogonas and Paipetis [83.6]) to take this non-linearity into account. Wang et al. [87.13] use an approximate linear model to tackle the problem.

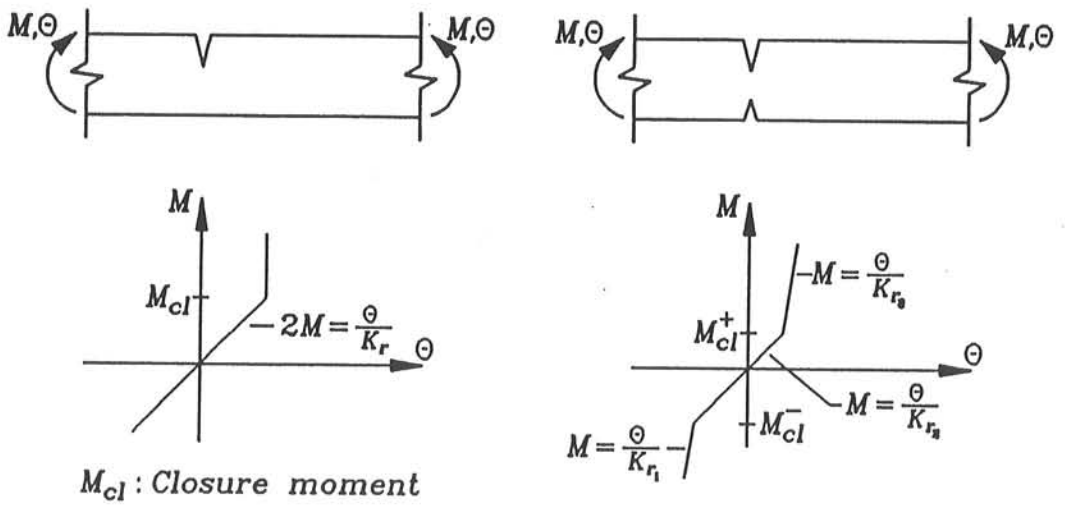

Figure 4.19 Nonlinear crack models (Rytter et al. [91.12]).

Ostachowicz and Krawczuk [90.16] use a so-called point finite element (PFE) to model the non-linear behaviour in a crack (see section 4.1.4).

4.1.6 Summary

A lot of different models for a cracked beam have been presented and used through the last fifty years.

A short beam element with a reduced bending stiffness (see section 4.1.1) was the preferred model until the mid seventies, where the fracture mechanical model was introduced (see section 4.1.3). The latter model is rather simple to use and gives agreements with real cracks.

However, the choice of model depends on the purpose of the investigations. For instance the smeared model (see section 4.1.2), which is the most rough model of those presented, has often been used in connection with sensitivity studies.

The applicability of the different models in connection with VBI are summarized in table 4.1.

Model	Level			
	1	2	3	4
Short beam element	+	+		
Smeared	+	(+)		
Fracture Mechanical	+	+	+	(+)
Advanced FEM	+	+	+	(+)

Table 4.1 Applicability of beam models in connection with VBI.

The reliability of the results from a VBI-session depends on how well the applied model describes the cracked zone. However, the advanced FEM, which gives the most detailed description, will cause a considerable increase in the use of CPU. Further, it will be pointless to use such an FEM instead of e.g. the fracture mechanical model to obtain better estimates for natural frequencies, if the correction is comparable to the uncertainties of the estimated natural frequencies from the tests.

Thus the fracture mechanical model will often be the optimal model with respect to accuracy and duration of the computer calculations. Still the applications of this model require reasonable expressions for the stress intensity factors of relevance. These expressions might be found in standard handbooks, by use of detailed FEM or by calibration through experimental tests (see appendix A). The latter is to prefer, because the influence of local conditions will be included (see eg. Chandros and Dimarogonas [80.4]).

The local flexibility at a real fatigue cracks may be non linear (see section 4.1.5). Therefore, it is very important to perform the calibrations on beams containing fatigue cracks.

Cawley and Ray [88.3] have compared the effect of slots and fatigue cracks and conclude "*Unfortunately, the changes produced increase with the width, so if it is found that a slot of a particular depth can reliably be found in nondestructive test, it does not follow that a crack of the same depth will be found*".

Nevertheless, saw cuts have been used in several tests to calibrate/verify models for cracked beams (see e.g. Wendtland [72.1] and Gomes and Silva [90.12]). Gomes and Silva [90.12] conclude that the saw cuts are excellent to make out for fatigue cracks during tests.

On the basis of the above it has been decided to use the fracture mechanical model in the subsequent studies of experimental case no. 1. The stress intensity factor K_I has been taken as given in equation (4.7).

4.2 DAMPING

A yield zone will be extended from the crack tip, when a cracked beam is loaded (see figure 4.20). The dimensions of this yield zone depend on the crack length a, the yield stress f_y and the actual stress level σ_o (see e.g. Hellan [85.5]).

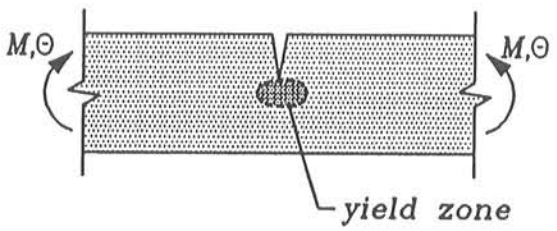

Figure 4.20 Yield zone at a crack tip (Rytter et al. [91.12]).

Energy will be dissipated in the yield zone during a load cycle, which implies an increase in the damping capacity of the structure. This fact has been supported by the results from experimental case no. 1 (see figure 4.21).

Therefore, changes in damping ratios are potential as damage indicator. However, the applicability of the damping in level 2-4 methods requires derivation of a sufficiently good mathematical model.

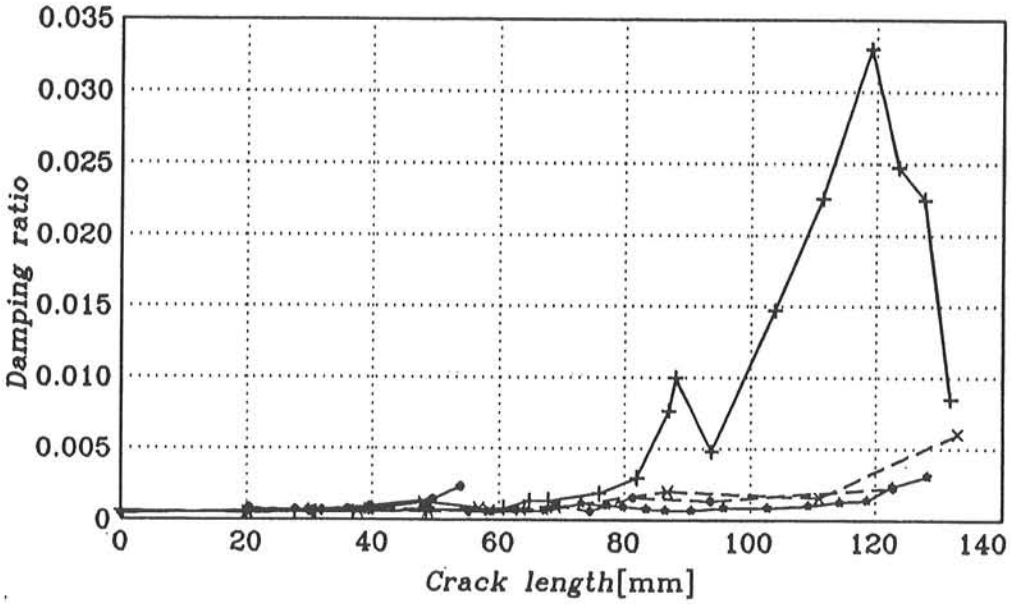

Figure 4.21 First modal damping ratio of beam B1-B6 (see section 1.3.1 for a list of symbols).

The dependence between the dimensions of the yield zone and the actual stress level indicates that the damping of a cracked beam depends on the amplitude of the vibrations. The relationship is confirmed by the results from the experimental case no. 1 (see figure 4.22).

Figure 4.22 shows the log-value of the peaks in two free decays against the peak number. A straight line indicates no dependence between damping and amplitude. Thus the damping for the beam during test J clearly depends on the amplitude. The degree of dependence decrease with decreasing amplitude.

Further, the results from experimental case no. 1 have shown, that the damping depends on the load history too. A sinusoidal load at the first natural frequency f_1 was used to develop the crack in B4. This has caused larger amplitudes and thereby a higher stress level and extent of the yield zone than in B3, B5 and B6, which were fatigued at f_2. Therefore, the increase in damping of B4 was considerably larger than the increase in damping of the other three beams (see figure 4.21).

Similar results have been found by Adams [72.3] (see figure 4.23), who also found a certain degree of dependence between the damping and the treatment of steel. Further, Adam [72.3] reports on temperature sensitivity of the damping of copper.

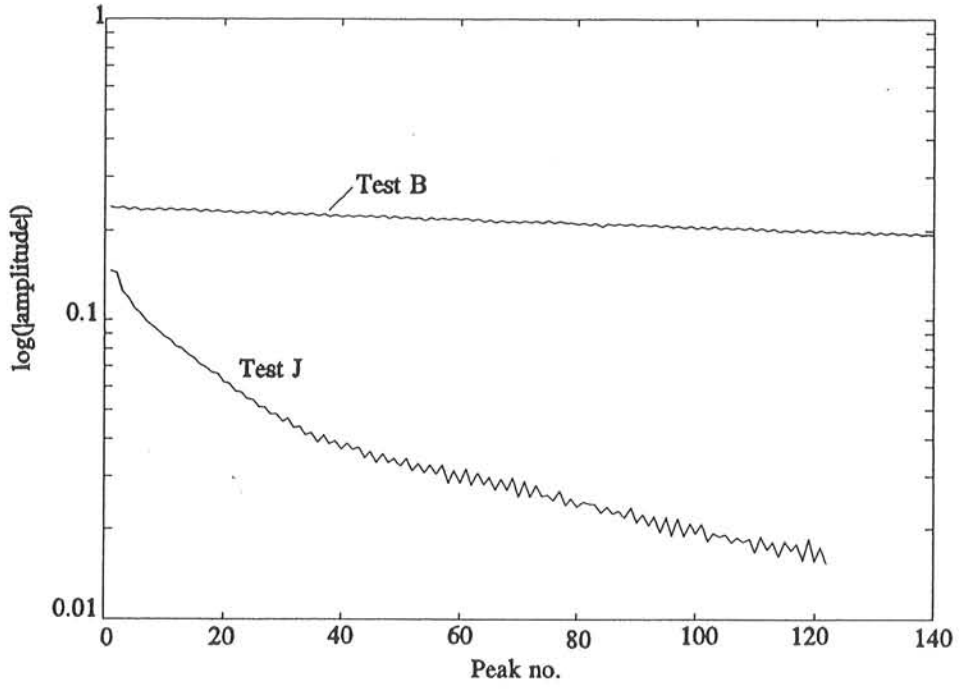

Figure 4.22 Log(peak) versus peak no.

The above clearly demonstrates that the damping is sensitive to several more parameters than for instance the stiffness. Therefore, it will be very difficult (impossible ?) to derive a general mathematical model for the damping in cracked beam.

Maybe a model can be established for the crack dependence in structures subjected to well-defined loads, temperatures, etc. like e.g. machines. For instance, Hochrein and Yeager [78.1] use the following simple linear relationship between the damping capacity $\Delta W/W$ and the number of load cycles N_{cycles}

$$\frac{\Delta W}{W} = aN_{cycle} + b \qquad (4.14)$$

The constants a and b have to be determined by tests.

However, it will not be feasible to use such a simple model when dealing with civil engineering structures like e.g. bridges (see e.g. table 3.1) and offshore structures.

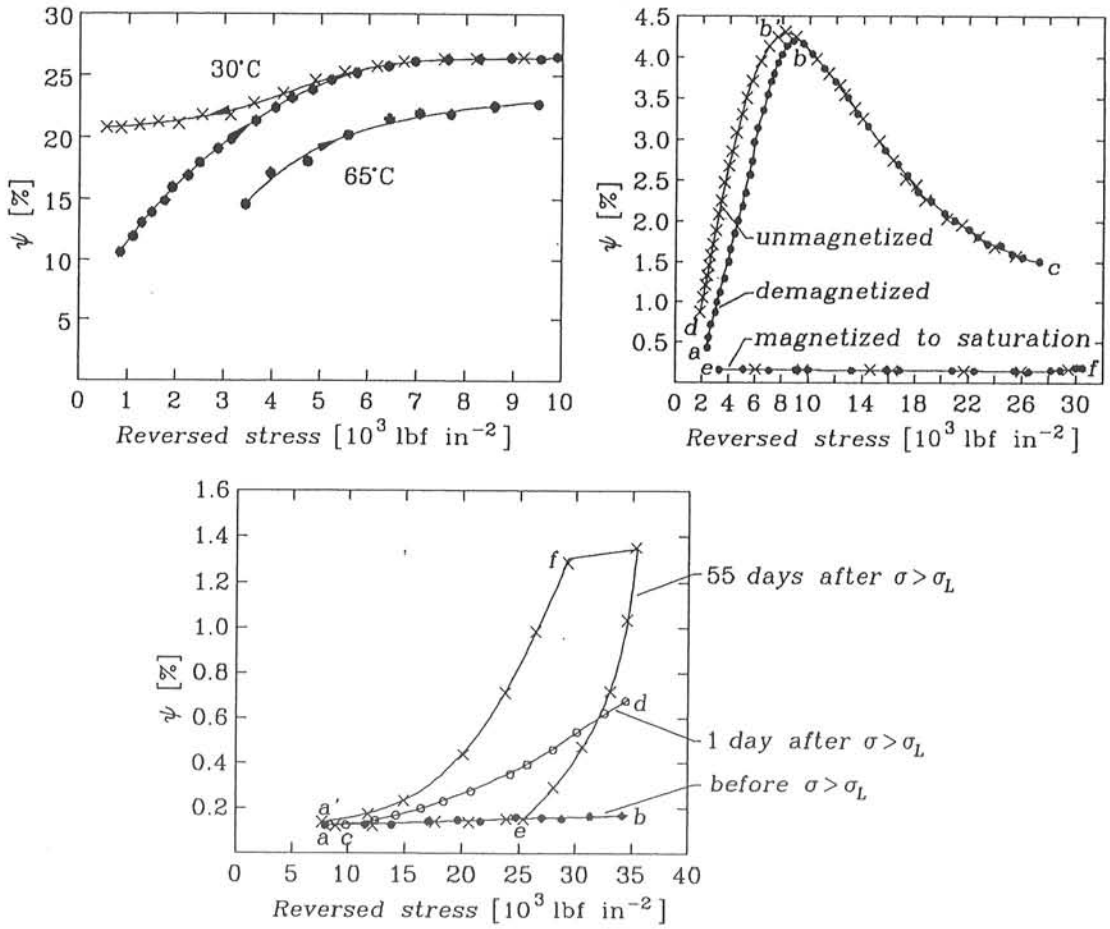

Figure 4.23 Damping versus stress. a) Effect of temperature, b) Effect of magnetizing, c) Effect of stress history (Adams [72.3]).

4.3 CONCLUSION

Five more or less different models for the stiffness of a cracked beam have been presented and evaluated in section 4.1.

The applicability of these five models in connection with VBI is summarized in table 4.1. The performed evaluation showed that the fracture mechanical model can be expected to be the optimal model with respect to accuracy and duration of calculation in most cases. This model will be used in the remaining part of this thesis in connection with experimental case no. 1.

Further, the evaluation showed that great care should be taken with respect to non-linearities and that it is preferable to perform calibration tests.

A qualitative check of influence of the factors on the damping of a cracked beam revealed that the damping is more sensitive to factors like e.g stress history than the stiffness. Therefore, no mathematical model for the change in damping due to a crack has been given.

CHAPTER 5
DAMAGE INDICATORS

The basic idea in VBI (see chapter 3) is to use the changes in the dynamic behaviour of a structure due to damage as a basis for an identification of this damage. The dynamical behaviour of a structure can be characterized by numerous single-valued parameters (e.g. natural frequencies) and plots (e.g. autospectral density functions). These parameters and plots will be referred to as *DAMAGE INDICATORS* (DI), when their sensibility to damage is used in connection with VBI. Thus a DI is defined as : *A dynamic quantity, which can be used to identify the existence of damage in a structure.*

The use of a DI gives primarily a qualitative indication of the existence of damage. However some of the DIs will in some cases give rough estimates for the locations of the damage, which is identical with a primitive level 2 method.

The aim of the present chapter is to introduce the different DIs, which have been used in connection with the experimental cases. The single DIs will be presented separately although they are very correlated and often will be used in combination in level 2 and 3 methods. The experimental cases concern steel structures. However, the DIs can be used on other kinds of structures as well, e.g. concrete structures.

5.1 NATURAL FREQUENCIES

Changes in natural frequencies may be called the classical DIs, if any. They are without any doubt the most used DI both formerly and nowadays.

The main reason for the great popularity is, that natural frequencies are rather easy to determine with a relatively high level of accuracy. In fact, one sensor placed on a structure and connected to a frequency analyzer gives estimates for several natural

frequencies. Further, natural frequencies are sensible to all kind of damage both local and global damage.

This sensibility to global damage can easily be seen from the following formula for the natural frequencies of linear beams with constant cross-section and material properties

$$f_i = \frac{\beta_i}{2\pi L^2}\sqrt{\frac{EI}{\mu}} \tag{5.1}$$

where β_i is a constant depending on boundary conditions and mode no., L is the beam length, μ is the mass per unit length, I is the moment of inertia and E is the modulus of elasticity. For instance a global damage like corrosion of steel will lead to a change in both I and μ and thereby in f_i.

The sensitivity against a local damage like e.g. a crack has been clearly demonstrated through the results from experimental case no. 1 (see figure 5.1).

The natural frequencies depend on the square root of the stiffness change, which is the reason why some people reject them as DI in the favour of other potential DIs (see e.g. Sunder and Ting [85.1]).

Fox [92.4] and Alampalli et al. [92.1] conclude that natural frequencies are reasonable as DIs, but they are insufficient to locate the damage when used alone. This is not always true (see e.g. section 8.8).

Another disadvantage is that any change in the non-structural mass (e.g. the mass of the top site on an offshore platform) will be reflected in the natural frequencies. Therefore, it is important to record all such changes and take them into account if natural frequencies are used in level 2 and 3 methods.

Normally, the natural frequencies which change due to the occurrence of damage have been in focus. However, a natural frequency which does not decrease when the other one does is very valuable as damage indicator, because this indicates that damage is placed in a zero-point for the curvature of that mode shape. For instance, this happened in the experimental test with beam B3 (see figure 5.1). In this case the third natural frequency remained unchanged during the test, while the other observed natural frequencies decreased. Thus the possible location of the crack are reduced to three narrow areas on the beam around the points where the curvature of the third mode shape is zero.

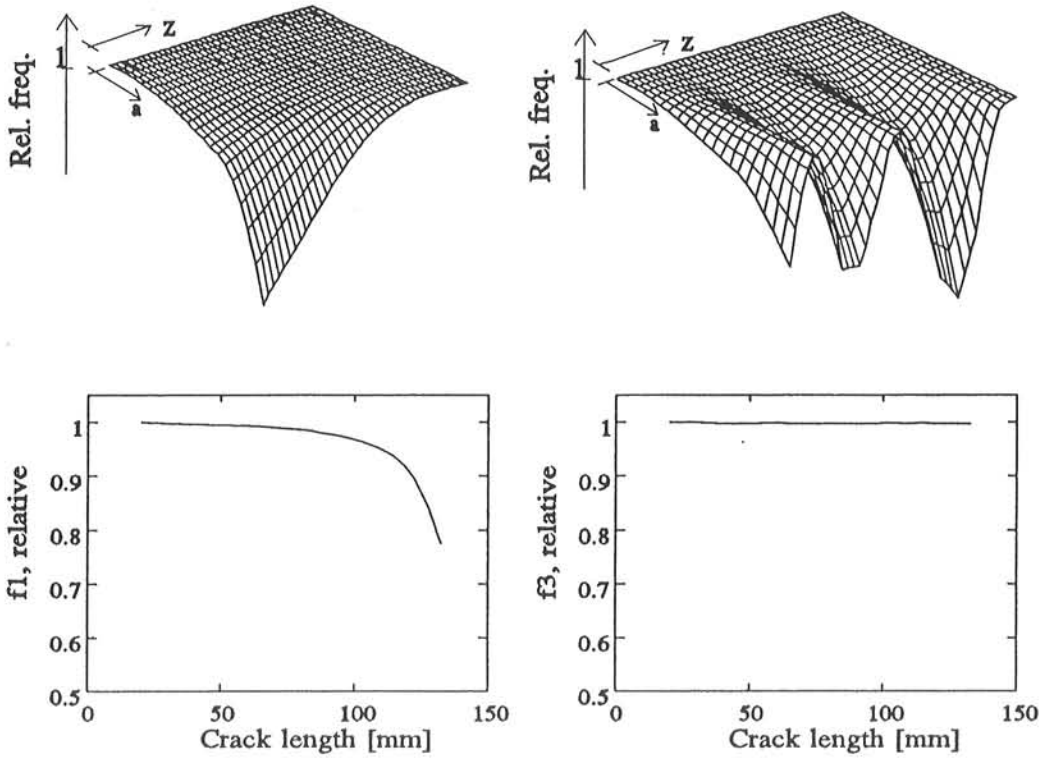

Figure 5.1 Upper : Variation of the first and third natural frequencies with crack position z and crack length a, Lower : Test results from beam B3.

Traditionally the introduction of damage is related to a decrease in stiffness and thereby in the natural frequencies. However, Maguire [90.14] reports on increase in natural frequencies when damage is introduced in some prestressed concrete beams. These increases are due to the fact that the modulus of elasticity of the concrete increases as the prestressing decrease. However, a decrease must occur, when a certain degree of damage of the prestressing is introduced. This means at worst that the damage will not be revealed if the second measurement is made at this damage state. Thus frequent measurement of the natural frequencies of prestressed concrete structures with a high risk of developing damage must be recommended.

The crack closure effect (see section 4.1.5) is another, which can make the use of natural frequencies as DI unreliable. If crack closure occurs in a fatigue crack in the structure then the measured decrease in natural frequencies will be lower than if the crack was open all the time. Thus, the use of these changes in natural frequencies in level 2 and 3 methods based on linear elasticity will lead to underestimation of the crack. Of course this uncertainty can be included in the same way as errors due to measurement noise, etc. However, the best result will always be obtained if non-linearities are revealed.

For instance this can simply be done by checking whether the natural frequency depends on the amplitude of the vibration or not. Figure 5.2 shows the amplitude dependence of

the zero upcrossing frequency during a free decay of beam B6 for test B (a_{tot} = 0.02 m) and test J (a_{tot} = 0.132 m). The figures reveal that the beam has become non-linear as the crack has grown from 0.02 m to 0.132 m. However, apparently the degree of non-linearity decreases as the amplitude of the vibration decreases (increasing cycle no.).

The estimated frequencies shown in figure 5.2 have been found through curve fits on time series of 600 point and a sampling frequency of 317 Hz at the start of the free decays. Approximately this corresponds to 22 and 10 cycles in test B and J, respectively.

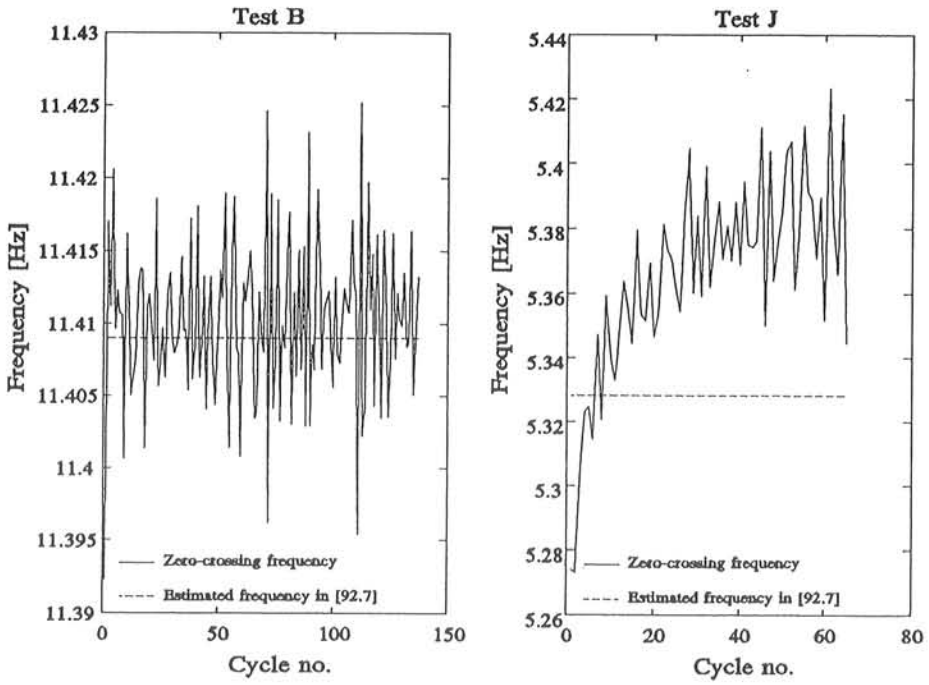

Figure 5.2 Test results from beam B6, test B and J.

The decrease in stiffness and increase in damping due to the introduction of a crack in a steel beam will both lead to decrease in the damped natural frequencies. This means that natural frequencies read from the screen on a frequency analyzer will lead to an overestimation of the damage. This problem occurs also when damage detection is based on graphical comparison of spectra or FRF (see e.g. Biswas et al. [90.5]).

5.2 MODE SHAPES

A local damage will cause a change in the derivatives of the mode shapes at the position of the damage. This facts have resulted in an increase in the application of changes in

mode shapes as DIs up through the eighties as the accuracy and fastness of the experimental equipment were increased.

Sunder and Ting [85.1] use the stiffness dependence to recommend the flexibility monitoring based on mode shapes to be used instead of natural frequencies in connection with the performance of damage detection on offshore platforms.

Estimates of the natural frequencies can, as mentioned in section 5.1, be obtained from measurement of the vibration in only one point on the structure. However, to get estimates for the mode shape one has to perform a measurement at each of the points, where estimates are wanted. Thus, the duration of a measurement session will increase considerably if a detailed mode shape shall be estimated. This is probably the main disadvantage in using mode shapes as DI.

The deflection, rotation and curvature of the first mode shape of beam B5 are shown in figure 5.3 as functions of the crack length. An FE-model consisting of 20 element of equal length has been used in the numerical calculations.

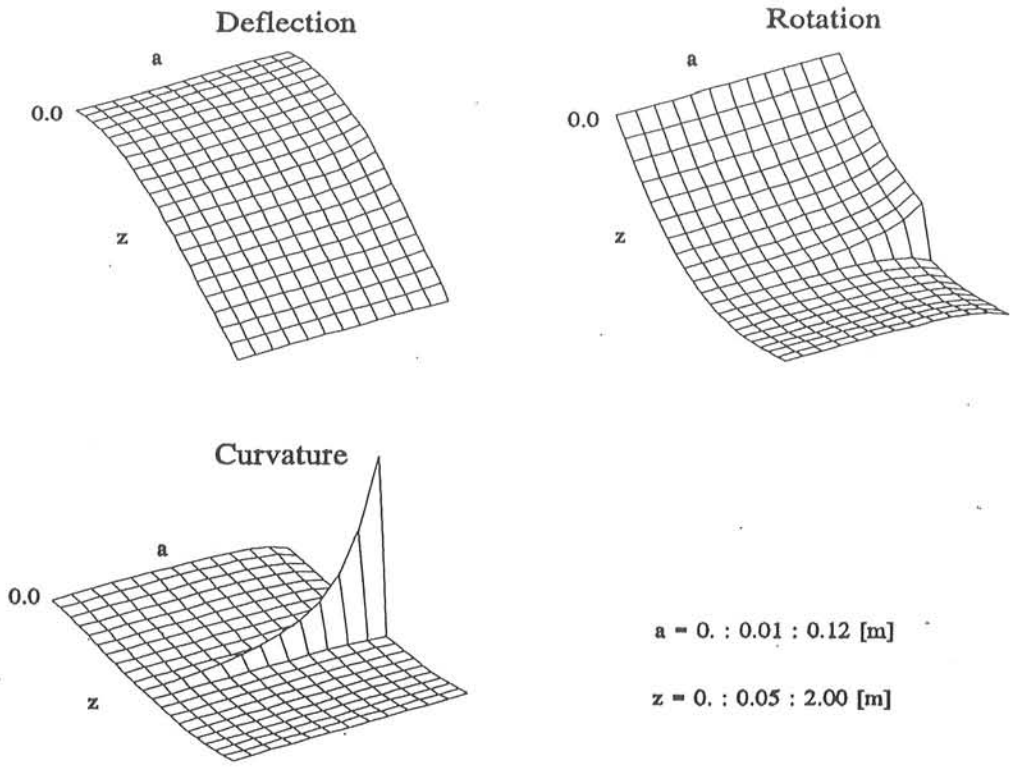

Figure 5.3 Mode shape of mode 1 for beam B5.

From figure 5.3 it can be seen, that the rotation and the curvature are much more sensitive than the displacement mode shape. Therefore, these two functions have been suggested to be used as DI in different papers (see e.g. Yuen [85.7], Ostachowicz and

Krawczuk [90.16], Pandey et al. [91.9] and Gounaris and Dimarogonas [88.11]). However, these functions are even more complicated to measure than the displacement mode shapes, which means that their applicability as DI are poor. This has also been realized by Gounaris and Dimarogonas [88.11].

The local bending stiffness of the beam at the crack will decrease towards zero as the crack grows. For instance, this means that the upper part of a cantilever will move as a rigid body connected to the lower part by a hinge as shown in figure 5.4 for mode shape. Thus, the ratio between estimates for the mode shape coordinates in two measurement points (briefly the mode shape ratio) will change as the crack grows. Three accelerometers were mounted on the beams in experimental case no. 1 at 0.5 m, 1.4 and 2.0 m from the fixture, respectively. The mode shape ratio between the upper measurement point and the two lower measurement points are shown in figure 5.5 a and b, respectively. Figure 5.5 clearly shows that the measured curves move against the boundary values, which are shown in figure 5.4.

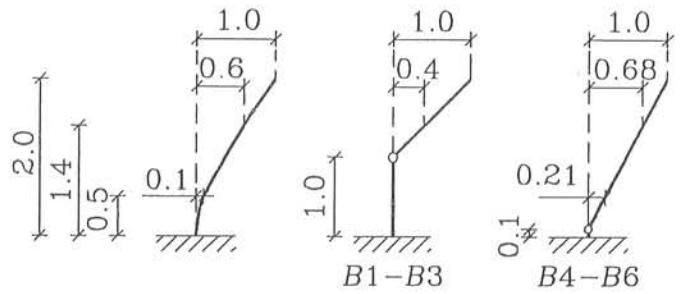

Figure 5.4 Deflection of beams, mode 1. (Rytter et al. [92.7]).

The ratio between the oscillation in two different measurement points during a free decay of a lightly damped structure will approximately be equal to the ratio between the coordinates of mode 1 at these two points. Thus, by plotting the rough signals from the two measurement point against each other in a Cartesian coordinate system during a free decay a straight line should be obtained. The slope of this is equal to the mode shape ratio. A change in stiffness might then be revealed by a change in slope. Further, the plot will only be a straight line if the structure is linear. For instance the existence of crack closure (see section 4.1.5) will cause a broken line (see figure 5.6). This means that such plots can be used as DI to reveal damage causing both linear and non-linear effects.

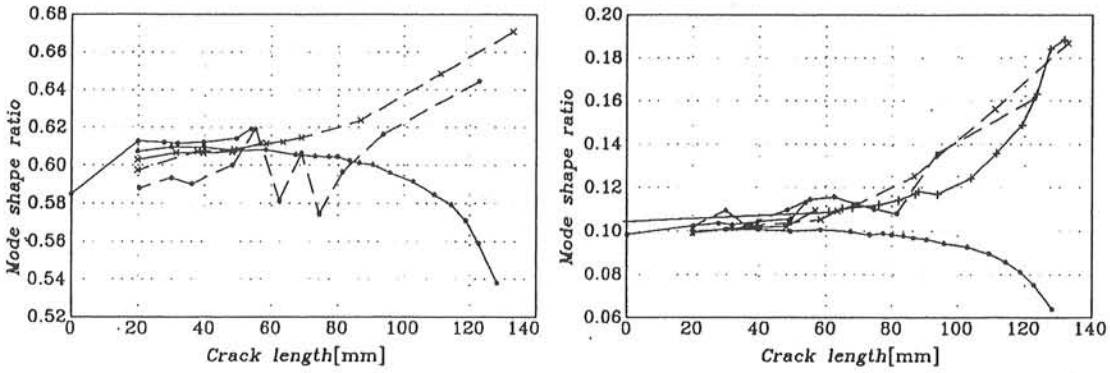

Figure 5.5 Mode shape ratios for test beams. A) Between the upper measurement point and the middle measurement point, B) Between the upper measurement point and the lower measurement point . The symbols are explained in section 1.3.1.

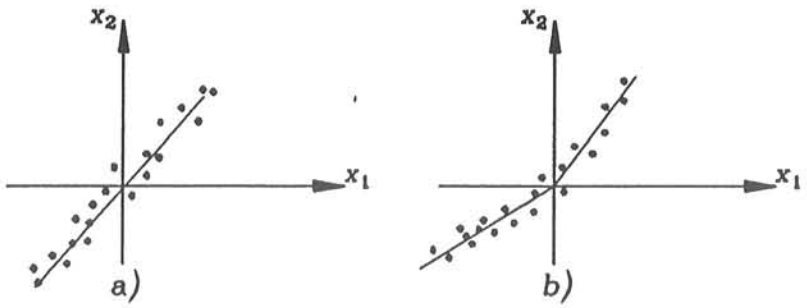

Figure 5.6 Mode shape ratio plots.

The modal assurance criterion (MAC) introduced by Allemang and Brown in 1982 (see Allemang and Brown [82.7]) has been used as DI in different papers (see e.g. Alampalli et al. [92.1], Biswas et al. [90.5]). The MAC-value between two eigenvectors ϕ_i and ϕ_j is defined by

$$MAC(\phi_i,\phi_j) = \frac{|\phi_i^T \phi_j|^2}{\phi_i^T \phi_i \; \phi_j^T \phi_j} \qquad (5.2)$$

The MAC-values express the correlation between two sets of estimates for the same mode shape. A value equal to 1 indicates a full correlation.

Several other similar single-number parameters based on mode shapes have been suggested an alternative to or an improvement of the MAC-factor. For instance Liewen and Ewins [88.8] introduced the so-called coordinate modal assurance coordinate (COMAC), which has also been used as DI in some papers (see e.g. Alampalli et al.

[92.1], Biswas et al. [90.5]). The COMAC-factor in point i between two sets of mode shapes Φ^A and Φ^B is defined as

$$COMAC(i) = \frac{\left[\sum_{j=1}^{N} |\phi_{i,j}^{A} \; \phi_{i,j}^{B}|\right]^2}{\sum_{j=1}^{N} (\phi_{i,j}^{A})^2 \sum_{j=1}^{N} (\phi_{i,j}^{B})^2} \tag{5.3}$$

where N is the number mode shapes. Thus, the COMAC compares the two sets of mode shapes in a point-wise manner.

The MAC and COMAC have been calculated for mode shape nos. 1 and 2 of beam B5 (see figure 1.1) for different crack lengths (see figure 5.7 and figure 5.8).

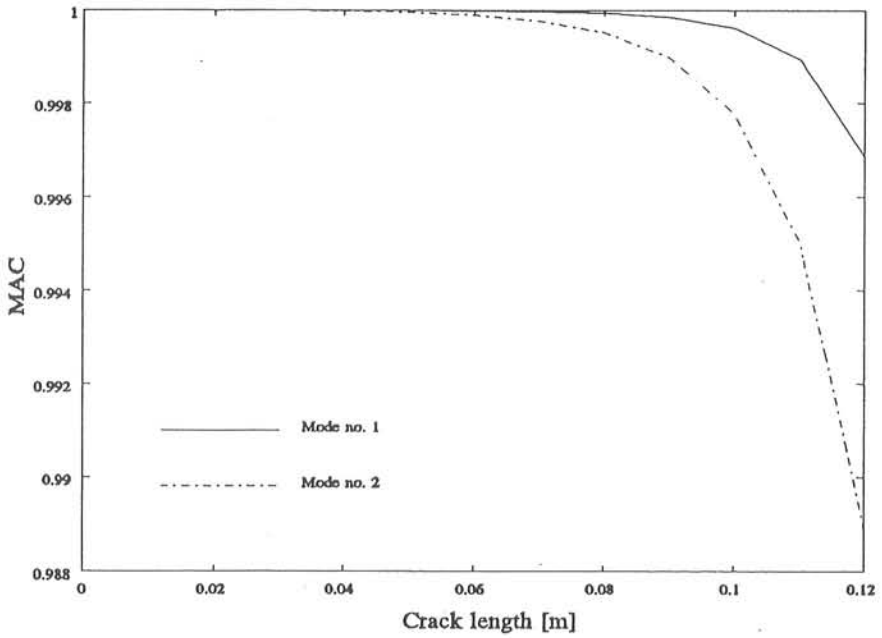

Figure 5.7 MAC(1,1) and MAC(2,2) for beam B5.

A maximum change in the MAC-values of $\approx$ 1 % is observed for the second mode, even though this mode shape has maximum deflection/curvature for z $\approx$ 1.0m. Thus, the MAC-values seem not to be particularly potential as DI. A similar conclusion is reached in Fox [92.4] and Pandey et al. [91.9] from simulation studies on a free-free beam and a cantilever, respectively. However, Alampalli et al. [92.1] find the MAC-values applicable as DIs in their studies on the bridge deck. Alampalli et al. even suggest the use MAC-values to localize the damage.

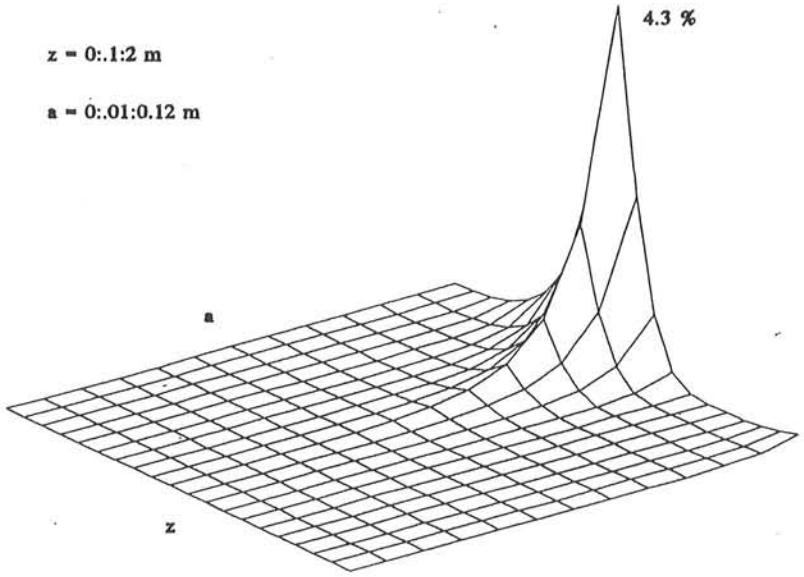

Figure 5.8 COMAC, mode 1 and 2, beam B5.

A maximum change of the COMAC-values for each crack length is observed for z = 1.0 m, which is identical with the position of the crack. Thus immediately the COMAC-values seem to be potential as DI. However, the COMAC-values are almost constant for a < 0.08 m (= width of the flange), which means that the beam should be seriously damaged before the COMAC-values change. Therefore, the applicability of COMAC-values as DIs seems to be limited. Pandey et al. [91.9] draw the same conclusion about the COMAC-values as DIs. However, Alampalli et al. [92.1] report on relatively large changes in COMAC-values for moderate damage in the bridge deck.

The presentation of the COMAC and MAC given above has shown that the applicability of these values as DIs is highly dependent of the geometry of the structure and the location of the damage. The simulations performed on relatively simple structures have shown, that apparently the COMAC and MAC are not sensitive enough to detect damage in the earlier stage.

The mode shapes of a linear beam are generally written as

$$\phi_i(z) = A_1 cosh(\beta_i z) + A_2 sinh(\beta_i z) + A_3 cos(\beta_i z) + A_4 sin(\beta_i z) \qquad (5.4)$$

where A_1, A_2, A_3, A_4 and β_i are constants, which depend on the boundary conditions only. Therefore, a uniformed smeared damage like e.g. corrosion of steel beams will not cause any changes in the mode shape. Thus, the efficiency of the mode shape as a DI decreases as the extent of the damage increases.

The presentation has shown that the use of mode shapes as DI in many cases results in a rough estimate of the location of the damage, which in principle is a simple level 2 method.

5.3 DAMPING

The introduction of damage in a structure will usually cause changes in the damping capacity of the structure. For instance such changes can be observed in the results from experimental case no. 1 (see figure 4.21). These results show, that the modal damping ratios of the cantilevers were extremely sensitive to even small cracks. Thus, increases by a factor of up to 70 were found. Similar results are reported in Hearn and Testa [91.7].

However, as mentioned in section 4.2, the changes in damping are highly dependent on several factors such as e.g. load history and the treatment at the mill. Therefore, an analytical relation between crack length and damping has never been given.

The instability of the damping becomes even more pronounced when VBI is used on real structures. For such structures a lot of time-varying and non-structural sources may contribute to the total damping, as shown in figure 5.9 for an offshore platform.

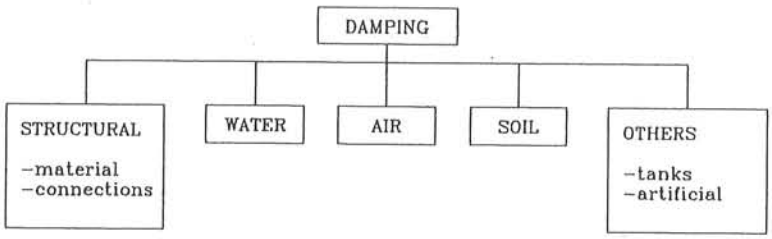

Figure 5.9 Damping source in an offshore platform.

Dealing with real structures separation of the total damping in portions related to the different sources will be impossible with a satisfactory accuracy from a VBI point of view. Further, the damage dependent changes in damping will often only make out a relatively small part of the total damping. Thus, a change in damping due to damage can easily be missed.

The damping is mentioned as a potential DI in many papers (see e.g. Agbabian et al. [88.7] and Tsai et al. [88.17]), but it has only been used in a limited number of papers. This is probably due to the above mentioned facts.

For instance Alampalli et al. [92.1] have investigated the possibility of using modal damping ratios as DIs in connection with the performance of VBI on bridges. However, repetitive tests performed on a model of a composite bridge deck showed that the modal damping ratios are very sensitive to environmental conditions as e.g. temperature. Similar observations have been reported in Turner and Pretlove [84.1] and Askegaard and Mossing [88.2] (see figure 3.4 and table 3.1). Further, the uncertainties were increased due to difficulties in estimating light damping. Therefore, the possibility of using modal damping ratios as DIs was rejected by Alampalli et al. [92.1].

Hochrein and Yeager [78.1] use damping as DI in VBI of some vessels. To overcome the uncertainty problem they define damage as the situation, where the measured damping capacity is more than 3 standard deviations away from the estimated baseline and the subsequent measurements show the same trend.

From the above it can be concluded that damping is applicable and recommendable as DI, but it can/shall never be used as the only DI. Thus a measurement of a change always has to be taken seriously due to the high sensitivity to damage and result in subsequent measurement of other DIs, which may form the basis for a conclusion.

5.4 ANTI-RESONANCE FREQUENCIES

The equation of motion of an undamped structure with N degrees of freedom can be written as

$$\boldsymbol{M}\ddot{\boldsymbol{x}} + \boldsymbol{K}\boldsymbol{x} = \boldsymbol{F} \tag{5.5}$$

where $\boldsymbol{M}$ is the mass matrix, $\boldsymbol{K}$ is the stiffness matrix, $\ddot{\boldsymbol{x}}$ is the acceleration vector, $\boldsymbol{x}$ is the displacement vector and $\boldsymbol{F}$ is the load vector.

The N natural frequencies can be found by solving the following eigenvalue problem

$$\boldsymbol{M}^{-1}\boldsymbol{K}\boldsymbol{x} = \lambda\boldsymbol{x} \tag{5.6}$$

where the square of the cyclic natural frequencies ω are elements in $\boldsymbol{\lambda}$. Equation (5.6) is obtained from equation (5.5) by setting $\boldsymbol{F} = \boldsymbol{0}$ and $\boldsymbol{x(t)} = \boldsymbol{x}e^{-\imath\omega t}$, where $\imath = \sqrt{-1}$.

The frequency response function (abbreviated FRF) $\alpha_{jk}(\omega)$, which expresses the relationsship between the response x_j at point j and a given load F_k at point k, is given by

$$\alpha_{jk}(\omega) = \frac{x_j(\omega)}{F_k(\omega)} \tag{5.7}$$

A plot of a so-called point FRF ($j=k$) will show the N natural frequencies. Further, the plot will reveal *(N-1)* anti-resonance frequencies, which are situated with one in between each consecutive natural frequencies.

At the ith anti-resonance frequency $\omega^A_{j,i}$ of $\alpha_{jj}(\omega)$ the response x_j must become infinitisimally small even if the excitation at the same point is increased without bounds, i.e

$$\omega^A_{j,i} = \omega(x_j \to 0, F_j \to \infty) \; given \; F_k = 0 \; ; \; k \neq j \tag{5.8}$$

The anti-resonance frequencies can be found by solving a reduced version of the eigen value problem in equation (5.6). The jth column and row of $\boldsymbol{M}^{-1}\boldsymbol{K}$ have been removed to fulfil $x_j \to 0$ and $F_j \to \infty$,respectively. Different columns and rows are removed in the calculation of the anti-resonance frequencies of the different $\alpha_{jj}(\omega)$. Therefore, these frequencies may vary from FRF to FRF contrary to the natural frequencies, which remain constant.

On the basis of these facts Afolabi [87.9] suggests the use of anti-resonance frequencies to detect and localize damage. Afolabi performs numerical calculations on a 3 degree of freedom model of a cantilever. He considers both changes in mass and stiffness. In both cases the results from the simulations show: *that as the point of measurement gets closer to the location of the defect, fewer and fewer anti-resonances are shifted from their original values until one gets to the location of the defect, at which all the anti-resonances are exactly as they were in the undamaged state.*

The applicability of the anti-resonance frequencies as DIs in connection with experimental case no. 1 has been investigated in example 5.1.

Example 5.1

The aim of this example is to

- demonstrate the practical use of anti-resonance frequencies as DIs
- evaluate the usefulness of anti-resonance frequencies as DIs

FE-models of the test beams B3 and B5 have been established (see figure 5.10). Each model consists of 7 elements of equal length. A crack of 0.08 m was introduced in elements 1 and 4, respectively. The cracks are assumed to be symmetric with respect to z-axis. 3 lumped masses of 0.1 kg were included to take into account the presence of the accelerometers during the tests.

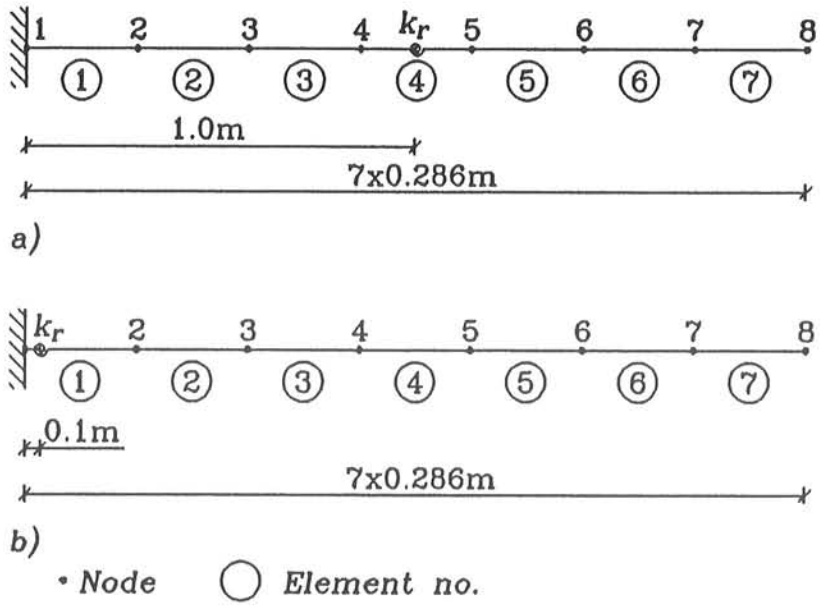

Figure 5.10 FE-models. a) beam B3, b) beam B5

The relative anti-resonance frequencies (ω_d^A/ω_u^A) are shown in table 5.1 and table 5.2.

The results from beam B3 show a certain degree of scatter in the changes in anti-resonance frequencies with respect to node no. According to Afolabi [87.9] the maximum relative anti-resonance frequencies should be found at nodes 4 and 5. These two nodes are situated on each side of the damage. This is certainly not true in this case. However, the results from beam B5 are in accordance with the conclusions made by Afolabi [87.9].

The performed analysis has shown that anti-resonance frequencies are potential as DI, but they should be used with care.

The results from example 5.1 show a certain degree of scatter, which indicates that the conclusions made by Afolabi [87.9] may be are too optimistic.

However, the main disadvantage in using anti-resonance frequencies as DIs is that measurement of response and load at a large number of points on the structure have to

Node	Anti-resonance frequency no.						
	1	2	3	4	5	6	Mean
2	0,980	0,959	0,989	0,982	0,984	1,000	0,982
3	0,965	0,978	0,960	1,000	0,994	0,997	0,982
4	0,935	1,000	0,974	0,998	0,989	0,998	0,982
5	0,937	1,000	0,975	0,996	0,992	0,995	0,983
6	0,959	0,992	0,961	0,999	0,995	0,997	0,984
7	0,956	1,000	0,983	0,983	0,987	0,999	0,985
8	0,967	0,997	0,961	1,000	0,987	1,000	0,985

Table 5.1 Relative anti-resonance frequencies of B3.

Node	Anti-resonance frequency no.						
	1	2	3	4	5	6	Mean
2	1,000	1,000	1,000	1,000	1,000	1,000	1,000
3	0,996	0,997	0,997	0,988	0,990	1,000	0,995
4	0,991	0,993	0,962	0,998	0,993	0,999	0,989
5	0,987	0,952	0,994	0,984	0,999	0,996	0,985
6	0,972	0,960	0,977	0,996	0,994	0,998	0,983
7	0,944	0,974	0,986	0,988	0,994	0,998	0,981
8	0,942	0,965	0,982	0,993	0,996	0,999	0,979

Table 5.2 Relative anti-resonance frequencies of B5.

be performed. This activity will be quite time consuming.

5.5 TRANSMISSIBILITY

Transmissibility is defined as the non-dimensional ratio of the response amplitude of a system in steady-state forced vibration to excitation amplitude (see e.g. Shock and Vibration Handbook [88.12]). The response can be either displacement, velocity or acceleration.

Ju and Akgun [86.1] present a damage diagnostic method in which they utilize the transmissibility T between acceleration and excitation as DI, i.e. as

$$T = \left| \frac{\ddot{X}}{F_m} \right| \tag{5.9}$$

where $\ddot{X}$ is the amplitude of the acceleration at the response station and F_m is the amplitude of the load.

Ju and Akgun [86.1] use a sinusoidal force, i.e.

$$F(t) = F_m \sin(\omega t) \tag{5.10}$$

which gives raise to the following response at the response station

$$x(t) = X_m \sin(\omega t + \phi) \tag{5.11}$$

where X_m is the amplitude of the transverse deflection at the measurement station. X_m varies with the position of the measurement station.

Introduction of equation (5.10) and (5.11) into equation (5.9) gives

$$T = \frac{\omega^2 X_m}{F_m} \tag{5.12}$$

The changes in stiffness due to the introduction of damage as e.g a crack will cause a change in x_m to a certain frequency and amplitude of the load too. The magnitude of this change will depend on the extent of the damage and the relative location of the damage with respect to the measurement station. Therefore, Ju and Akgun [86.1] introduce the relative change in transmissibility R_T as DI, i.e.

$$R_T = \frac{T_d - T_u}{T_u} = \frac{T_d}{T_u} - 1 \tag{5.13}$$

where T_d and T_u are the transmissibility of the damaged and the undamaged structures respectively.

In general, R_T will adopt values in the interval $[-1; \infty[$. The lower and upper limit will be reached in connection with measurements on an undamped structure if the response station is place at a node of the mode shape for the damaged and undamaged undamped structure, respectively. Ju and Akgun introduce a definition called a pseudo-node point (briefly PNP), which is a point on a damped structure with a locally minimum amplitude of transverse deflection in the mode shape. Thus, for a damped structure R_T will adopt

a maximum value at PNPs of the undamaged structure and minimum value at PNPs of the damaged structure.

Sets of R_T are the cornerstones in the damage diagnostic method presented by Ju and Akgun [86.1]. For further information about this method see section 8.3.

5.6 RDD-SIGNATURES

The random decrement was according to Brinker et al. [90.11] developed by H.A. Cole and others at NASA in the late sixties to obtain a quick system identification method and a method for on-line failure detection.

The Random Decrement signature (RDD-signature) $\hat{D}(\tau)$ is extracted from a time series $x(t)$ by averaging N segments of the time series, i.e.

$$\hat{D}(\tau) = \frac{1}{N}\sum_{i=1}^{N} x(\tau - t_i) \qquad (5.14)$$

where the segments of the time series at the times t_i satisfy a so-called trig condition, like e.g. $x(t_i) = a$.

The RDD-signature is closly related to the auto-correlation function and thereby the free decay of a linear structure, when the load is a white-noise. This has made the RDD-technique attractive in connection with e.g. estimation of natural frequencies and damping ratios (see e.g. Brincker et al. [90.11] and [91.2]). However, the raw RDD-signature might be used as a level 1 method i.e. as a DI. Therefore, the RDD-signature is included in the present chapter.

For instance Yang et al. [80.5] present an on-line failure detection scheme based on the use of RDD-signatures. At virgin state a confidence level region for the reference RDD-signature is established (see figure 5.11). The width of this confidence region will increase with τ, since all N segments of time series in equation (5.14) are equal for $\tau = 0$. For inexplicable reasons the figure given by Yang et al. [80.5] does not show this effect.
Yang et al. [80.5] define damage to be present, when a peak of the RDD-signature obtained from a periodical or an on-line measurement is beyond the confidence region,

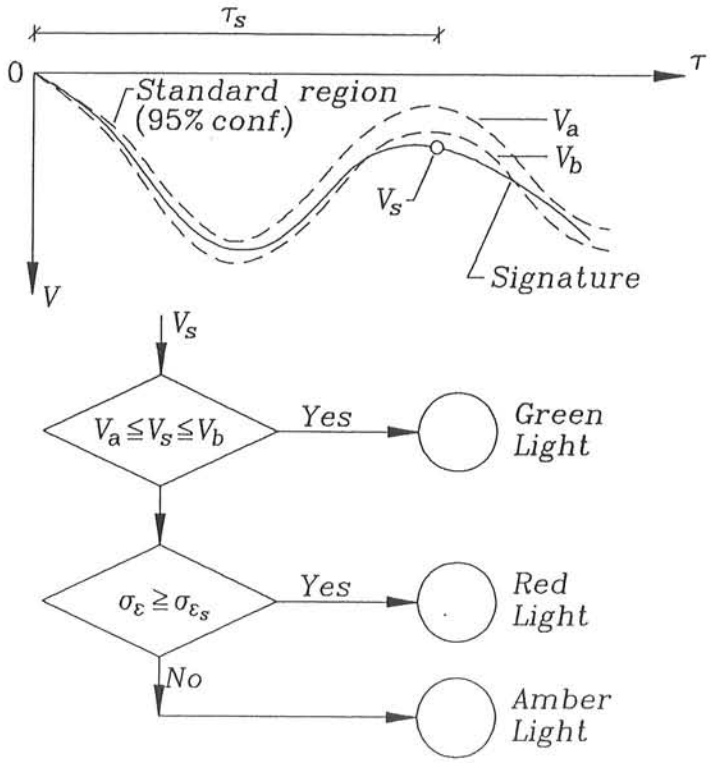

Figure 5.11 On-line failure detection at a single point on a RDD-signature (Yang et al. [80.5]).

and the standard deviation of the periodical RDD-signature at $\tau = \tau_s$ is lower than the corresponding standard deviation obtained at virgin state (see figure 5.11).

An on-line use of the scheme proposed by Yang et al. [80.5] will require that the load is not changed reasonably as time goes by.

The raw time series should pass through a bandpass filter before the averaging in equation (5.14) is commenced. The bandpass filter should be centered around one of the natural frequencies of the structure. The optimal choice of natural frequency, which depends on several factors like e.g. the damage type and location and the spectral density of the load, should be found through sensitivity studies (see section 6.2).

5.7 UNEXPECTED RESONANCE FREQUENCIES

Unexpected resonance frequencies (denoted $f_{i,y}$) appeared in between the expected resonance frequencies (denoted $f_{i,x}$) in the auto spectra of the acceleration processes during the test on beam B1 in experimental case no. 1 (see figure 5.12). A closer study

of the test beam revealed a fatigue crack in the weld at the fixture of the beam. The crack was situated at a corner of the profile. The unsymmetrical placing of this crack caused a rotation of the primary axes of the cross-section. The unexpected resonance frequencies were identical to the natural frequencies for vibrations in a direction perpendicular to the measurement direction of the accelerometers.

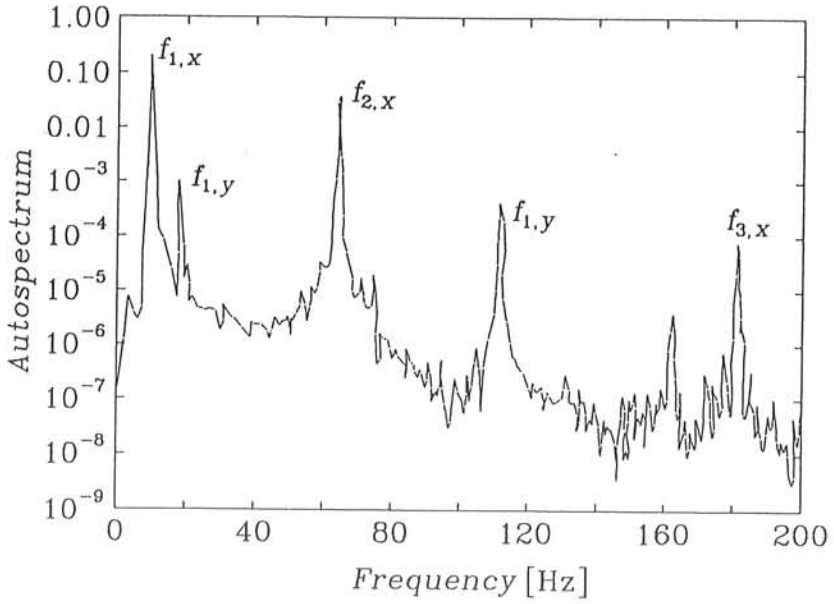

Figure 5.12 Auto spectral density function of the acceleration process during free decay test G on beam B1 (Rytter et al [92.7]).

This means that the appearance of unexpected resonance frequencies in the spectra can be used as an indication of damage somewhere in the structure.

5.8 SUB-/SUPERHARMONIC PEAKS IN THE SPECTRA

The introduction of a crack in a beam can often imply that the stiffness of the beam becomes non-linear.

This non-linearity is often included (see section 4.1.5) by means of a rotational spring with a piece-wise linear relationship between the bending moment and the rotation.

The fracture mechanical model (see section 4.1.3) can be used to calculate the stiffness in different cases. For instance the local flexibility at a crack, which is open for positive

moments at the crack position and closed for negative moments at the crack position, is given by :

$$\frac{1}{k_r} = \frac{2\beta}{E}\int_0^{A_c}\left(\frac{K_I}{M}\right)^2 dA \quad for\ M<0$$
$$\frac{1}{k_r} = 0 \qquad\qquad for\ M\geq 0 \tag{5.15}$$

where k_r is the stiffness of the rotational spring (see section 4.1.3).

It can be shown (see e.g. Friswell and Penny [92.3]) that this kind of non-linearity will cause subharmonic and superharmonic peaks in the autospectral density function for the response of the structure. This effect is studied for the beams B4-B6 used in experimental case no. 1 for 3 different types of load.

Example 5.2

The aim of this example is to present the results from a simulation study of the effect of local flexibility given by equation (5.15) on the autospectral density function of the displacement $S_{xx}(f)$ at the top of beams B4-B6 from the experimental case no. 1. The FE-models shown in figure 5.13 have been used in the performed study.

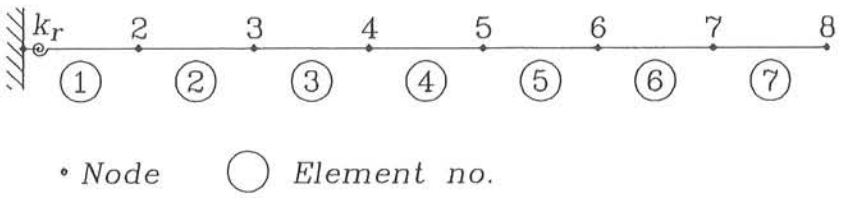

Figure 5.13 FE-model used in time simulation tests.

The response of the beam has been calculated by means of the Newmark time integration scheme (see e.g. Barltrop and Adams [91.14]) for the following three load situations :

a) Free decay similar to the free decay test used in the laboratory (see Rytter et al. [92.7]).

b) A sinusoidally-varying load applied at node 8. The frequency of the sinus was 8 Hz.

c) A Gaussian white noise load applied at node 8.

The response was sampled per T_{samp}, but the time step used in the time integration T_{cal} was taken as $T_{samp}/7$ to obtain stability and accuracy.

The natural frequencies of the beam are shown in table 5.3.

Frequency no.	f_c Hz	f_o Hz	$(f_o+f_c)/2$ Hz
1	11,89	9,89	10,89
2	74,76	68,00	71,38
3	205,71	195,06	200,39
4	408,87	397,99	403,43
5	688,39	679,64	684,02

f_c the natural frequency for closed crack
f_o the natural frequency for open crack

Table 5.3 Natural frequencies

The autospectral density functions are shown in figure 5.14-figure 5.16 for damaged and undamaged beam in the three load situations. It can be seen from these plots, that the introduction of opening and closing crack causes additional peaks in the autospectral density function in all three situations. However, the number of additional peaks depends on the load type. The effect is most pronounced in the case of the sinusoidal-varying load, where several additional peaks are introduced, whereas only one superharmonic peak appears in the autospectral density function in the case of white noise excitation.

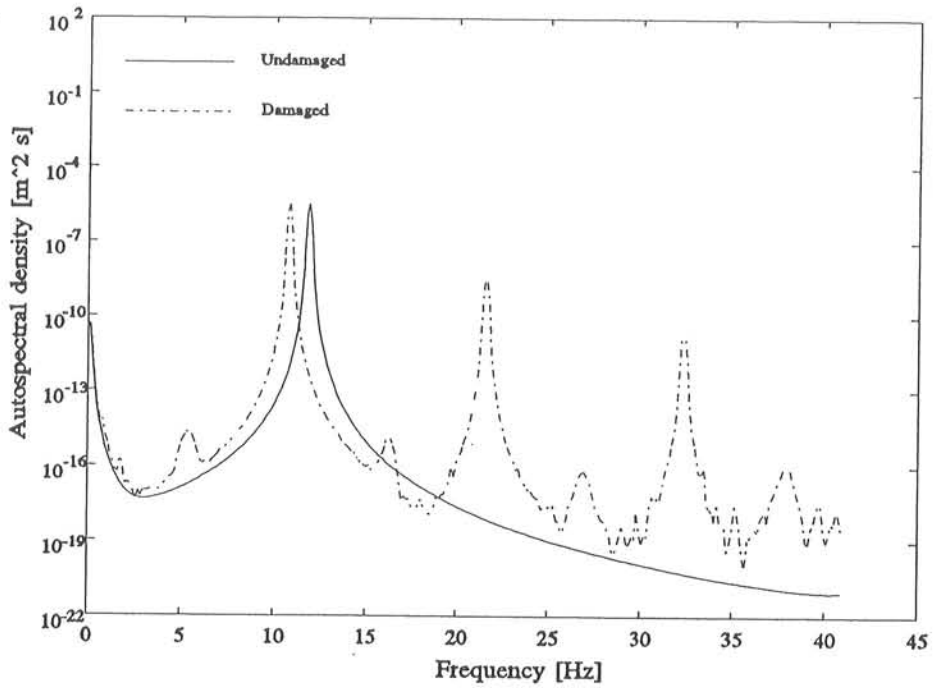

Figure 5.14 Autospectral density function, free decay.

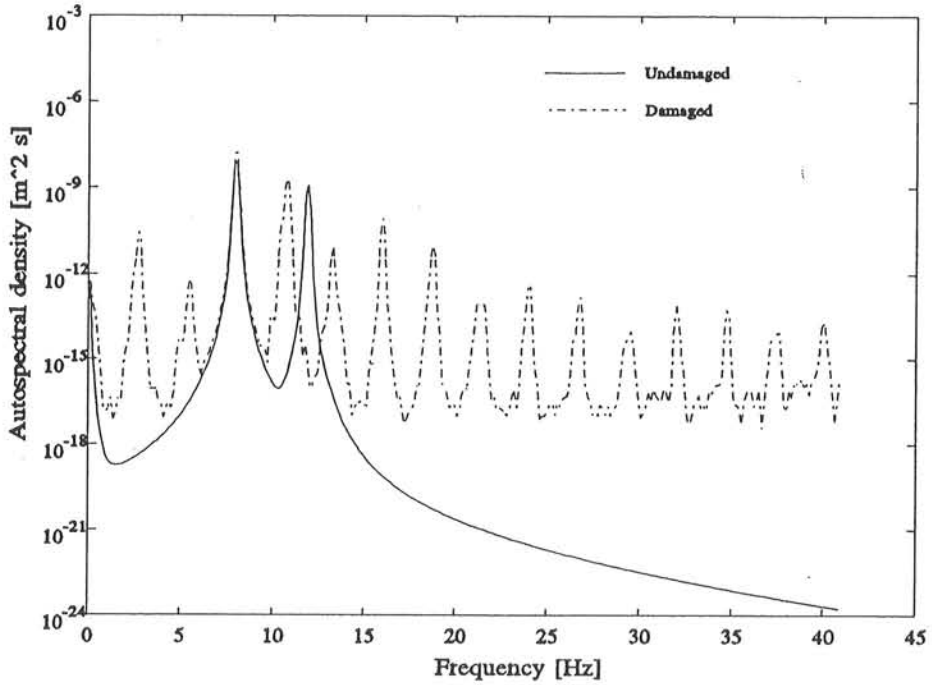

Figure 5.15 Autospectral density function, sinusoidally-varying load.

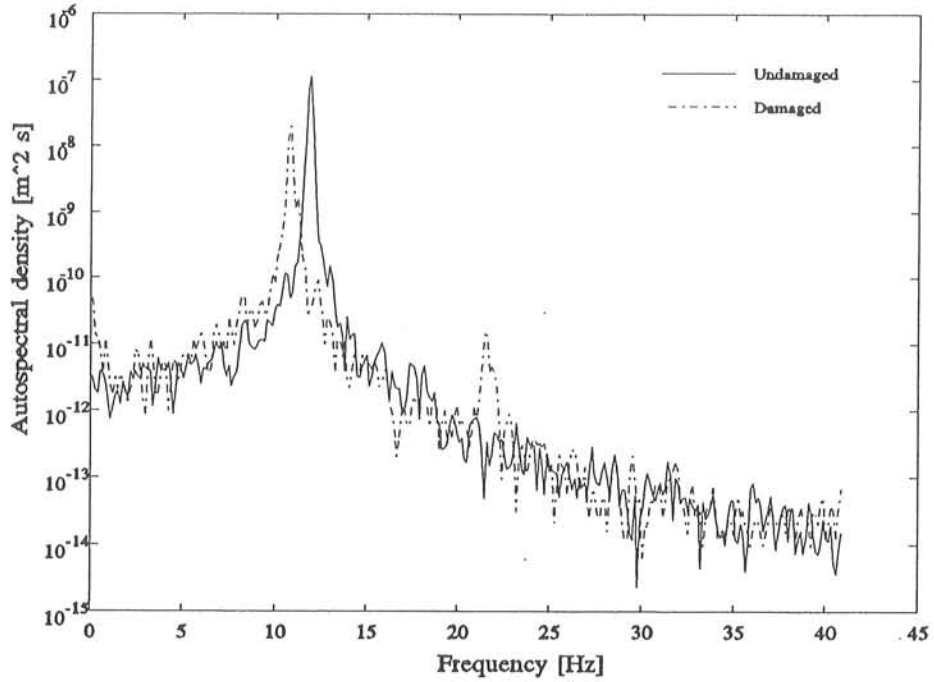

Figure 5.16 Autospectral density function, white noise.

The results from example 5.2 show that the existence of this certain kind of damage might be revealed through periodical checks of the autospectral density function for the response due to e.g. environmental dynamic loads.

The most simple and still efficient way to perform such checks is to calculate the ratio between the spectral value at load frequencies and/or natural frequencies and their sub-/superharmonic frequencies after each periodical measurement. This approach was suggested by Tsyfanskii et al. [85.4]. The optimal choice of load type and frequencies will vary from structure to structure and should be found through sensitivity studies.

5.9 PHASE PLANE PLOT

The equation of motion for an undamped linear system with one degree of freedom during a free vibration is given by

$$m\ddot{x} + kx = 0 \tag{5.16}$$

where m is the mass, k is the stiffness, x is the displacement and $\ddot{x}$ is the acceleration.

Equation (5.16) can be rewritten to

$$(\dot{x})^2 + \left(\frac{k}{m}\right)^2 x^2 = C \tag{5.17}$$

where $\dot{x}$ is the velocity and C is a constant. From equation (5.17) it can be seen that a phase plane plot for the system during a free vibration will be an ellipsis, whose size is determined by C.

The equation of motion for the piecewise-linear undamped system shown in figure 5.17 is given by

$$\begin{aligned} m\ddot{x} + k_1 x &= 0 \quad \textit{for } x \geq a \\ m\ddot{x} + k_2 x &= 0 \quad \textit{for } x < a \end{aligned} \tag{5.18}$$

As for the linear system these equations can be rewritten as

$$\begin{aligned} (\dot{x})^2 + \left(\frac{k_1}{m}\right)^2 x^2 &= C_1 \,, \quad \textit{for } x \geq a \\ (\dot{x})^2 + \left(\frac{k_2}{m}\right)^2 x^2 &= C_2 \,, \quad \textit{for } x < a \end{aligned} \tag{5.19}$$

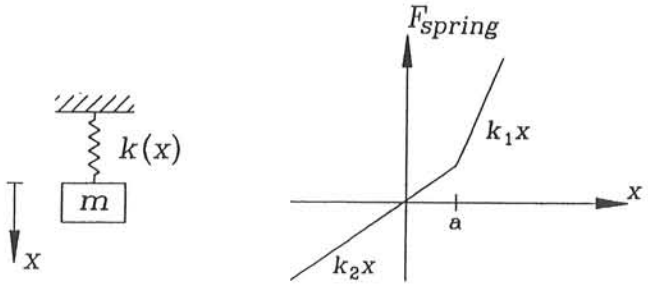

Figure 5.17 Two-slope system.

From equation (5.19) it can be seen that a phase plane plot for a piecewise-linear system will consist of fragments of different ellipses.

The introduction of a crack will typically make a structure piecewise-linear. This means that phase plane plots can be used to reveal the existence of cracks.

Phase plane plots for the upper measurement point of beam B4 (see figure 1.1) for two different crack lengths are shown in figure 5.18. The plot for test B4_B1 exhibits a linear behaviour for the beam, whereas the plot for test B4_O1 clearly reveals a non-linear behaviour of the beam. Thus, phase plane plots are potential as DIs for damped structures with more than one degree of freedom.

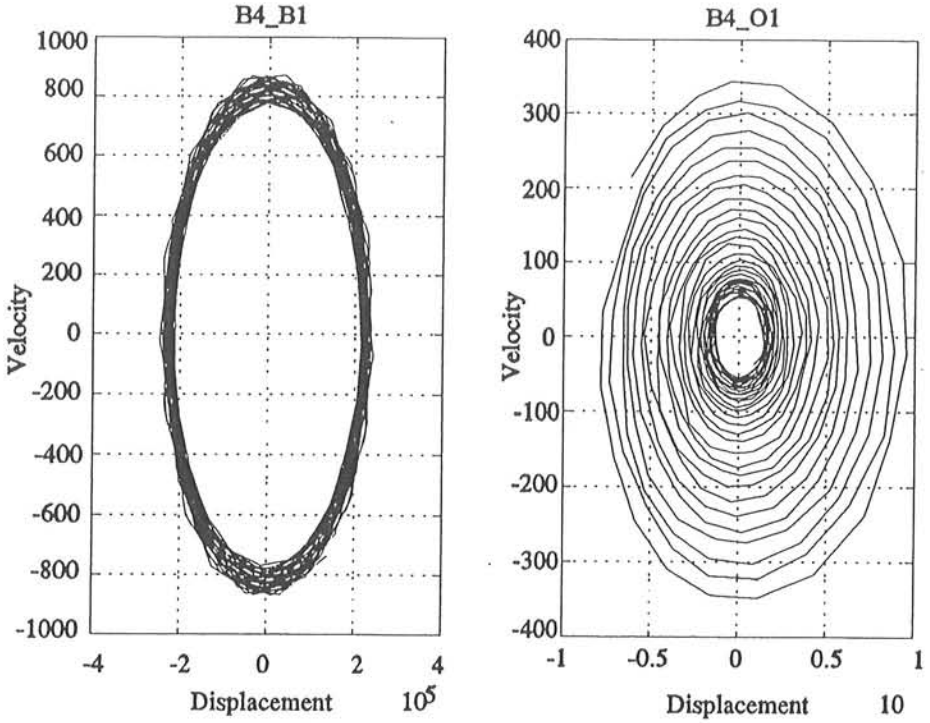

Figure 5.18 Phase-plan plots. Beam no. 4 case B4_B1 and B4_O1.

5.10 PROBABILITY DENSITY FUNCTIONS

The existence of non-linarities in a structure can in some cases be revealed and identified by the probability density function (PDF) of the output. For instance it can be shown (see Bendat [90.22]) that the PDF of the output from two-slope systems (see figure 5.19) loaded by a zero mean value Gaussian input will have a discontinuity and either a shorter or longer tail (see figure 5.20).

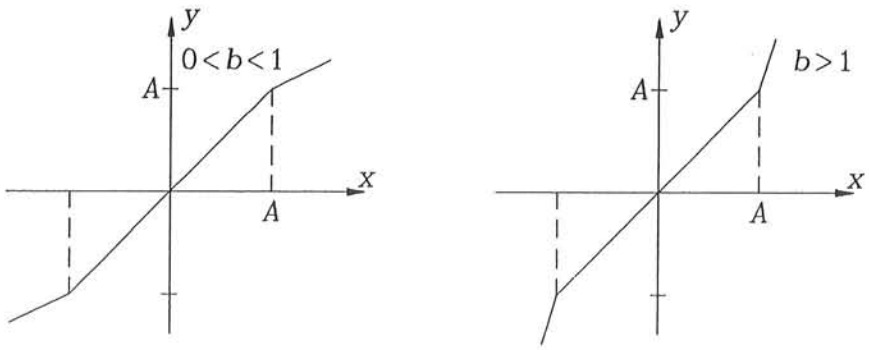

Figure 5.19 Two-slope systems (Bendat [90.22]).

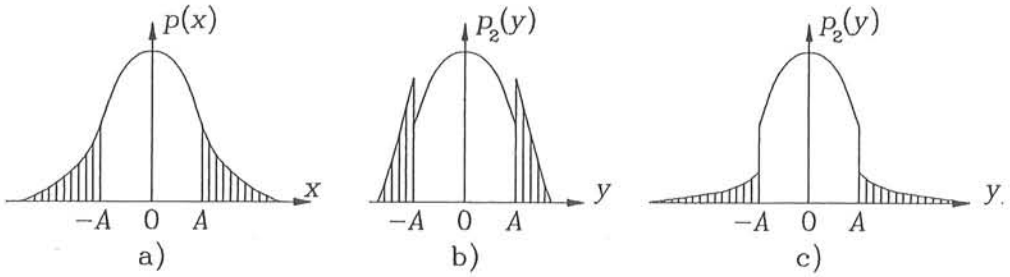

Figure 5.20 PDF of the output from two-slope systems loaded by a zero mean value Gaussian input. a) input, b) output when $0 < b < 1$, c) output when $b > 1$ (Bendat [90.22]).

Similar characteristics can be found in the PDF of the output from other types of zero-memory non-linear systems (see Bendat [90.22]).

5.11 CONCLUSION

More than 16 more or less different DIs have been presented in this chapter. The beam from experimental case no. 1 and some simple 1 DOF systems have been used to demonstrate the use of these DIs.

The performed tests of the DI have shown, that some of the DIs are more efficient than others in the particular cases considered. However, a generally fixed order of priority for the applicability of the presented DIs has not been made, because such a list will vary from structure to structure. This is because the applicability of a DI depends on several different factors, which will be briefly summarized and explained in the following.

The type of damage can be a significant factor for the applicability of a certain DI. For instance, the mode shape related DIs are very applicable with respect to detection of local damage and almost unusable for detection of global damage.

The location of the damage is of great importance, because some of the DIs will hardly be affected by the introduction of damage at certain positions. For instance, the third natural frequency of beam B3 (see figure 5.1) is almost constant for all crack lengths. However, such a DI will be valuable if it used together with damage depending DI in a level 2 or 3 method (see e.g. section 8.10). A constant DI will be obtained, if either the sensor or the location of the damage coincides with a node of the particular mode shape to which the DI is related.

The performed tests have shown that the deflection mode shape and its derivative of the test beams will be efficient as DIs. However, the use of these will require an extensive measurement. Thereby the mode shape related DI becomes more expensive in use than for instance the natural frequencies, which in principle can be found from measurements at only one point.

The different non-linear effects may cause trouble when using the traditional DIs as for instance natural frequencies. Crack closure combined with weak loading during testing may in the worst case have the effect that a crack will never be open. Therefore, great attention should be given to those DI, which can reveal non-linearities.

The acceptable level of the damage with respect to the safety must be determined. These can then be used as input to sensitivity studies (see section 6.2) to get estimates for

changes in the different DIs and thereby establish the requirement for the accuracy of the estimates for DIs found through measurement.

The estimated values for the DIs will allways be encumbered with errors, no matter how they have been found. The introduction of the errors are primarily due to noise on the signals, the load used during the measurements, the location of the measurement points and the SI method in use. Therefore, the magnitude of these errors of the different DIs will vary from structure to structure. However, the errors can be minimized through a careful design of the measuring programme (see section 6.4).

Primarily the choice of the DIs to be applied to a given structure should be based on the results from sensitivity studies. In other words all the potential DIs are "equal" at the start of the sensitivity analysis, which will give a fixed order of priority for the applicability of the different DIs in connection with VBI on a given structure.

However, all DIs, which are measureable from a given instrumentation, should be estimated and incorporated in the subsequent diagnostic analysis. The inclusion of all available information will cause an increased accuracy of the results from the diagnostic analysis. For instance, an example of such a sensitivity analysis is given in Alampalli et al. [92.1], who test the usability of natural frequencies, damping, mode shapes, MAC and COMAC as DI on a model of a bridge.

Therefore, it is very misleading, when one particular DI is presented in a paper to be much better than others (see e.g. Fox [92.4], Sunder and Ting [85.1] and Afolabi [87.9]). A common feature of these papers is that the presented results are based on simulation studies with one or two types of structures.

CHAPTER 6
INTRODUCTORY ANALYSIS

As mentioned earlier, VBI can in principle be used on all types of structures. However, a series of practical questions have to be answered before the decision whether VBI should be used on a certain structure or not can be made. For instance, a question which must be dealt with is whether or to what extent, the experimentally obtained data can be processed to pick out the systematic changes which occur due to the presence of defects from the random uncertainties due to experimental errors and time-varying effects.

These questions should be answered in the introductory analysis, which are described in this chapter. The introductory analysis includes sensitivity analysis (see section 6.2), choice of system identification method(-s) (briefly SI-method) (see section 6.3) and design of a measurement programme (see section 6.4). These three topics are presented separately and in a certain order in this chapter although they typically will be performed parallel.

Further, the methods to be used in connection with diagnostic sessions should be chosen during the introductory analysis to reveal whether the damage(-s) can be detected before the acceptable level of damage is reached. A comprehensive review of diagnostic methods is given in chapter 8.

The dynamic characteristics of a structure will vary with time due to time dependent variations in both non-structural and structural parameters which do not depend on damage. It is of great importance to include the variations of all the factors of relevance in the sensitivity analysis and the diagnostic session (see chapter 8) to avoid misinterpretations. A short review of typical time-varying effects is given in section 6.1.

6.1 TIME-VARYING EFFECTS

The dynamic characteristics of a structure depend on several factors such as e.g. mass and stiffness properties. These factors may vary during the lifetime of the structure. The aim of the present section is to give a short review of the most common time-varying effects to be taken into account for civil engineering structures. The review is supplemented with examples reported in papers etc.

Ageing will in many cases cause changes in the properties of building materials. For instance, the modulus of elasticity and strength of concrete will increase with time. Further, the density of the concrete will change due to evaporation of surplus water. These effects have e.g. been reported in König et al. [87.5], who measured changes of 2.4-5.0 % in the three lower natural frequencies of a concrete bridge. A common feature of the ageing dependences is that their variation decreases with time.

A high degree of correlation between the dynamic characteristics of civil engineering structures and the ambient temperature and humidity has been reported in several papers dealing with in-field measurements (see e.g. Turner and Pretlove [84.1], Askegaard and Mossing [88.2] and Flesch and Kernbichler [88.4]). The results reported by Turner and Pretlove [84.1] (see table 3.1) and Askegaard and Mossing [88.2] (see figure 3.4) show that the damping of concrete bridges is very susceptible and unstable to environmentally-induced changes. Further, Askegaard and Mossing found correlation between the natural frequency and the temperature.

The effect of these variations in the ambient climate is more pronounced in some mode shapes than others. Therefore, Flesch [90.2] suggested that the most sensitive of the modes should be dropped in connection with VBI. However, it will be better to make use of these in the subsequent analysis either by giving them a low weight or by including the variations in temperature in the mathematical models. The latter is to be preferred and the first is the easiest way to include such sensitive modes.

Spidsoe and Skjaastad [87.8] report on measured storm induced variations of the soil-structure interaction properties of a gravity platform. Similar results have been reported by Olagnon and Prevosto [84.6]. The natural frequencies and damping ratios vary up to 50 % during a storm. Therefore, when one is dealing with a VBI-programme for an offshore platform a proper modelling of the foundation is required. Further, the changes in foundation have to be included as "damage types" during the diagnostic sessions.

Rubin [80.8] reports from an ambient vibration survey of an offshore platform that the frequencies for these in rough seas are 1%-2% lower than those measured in calm seas.

Non-structural masses placed on a structure will have influence on the dynamic characteristics of the structure. The influence depends on both the size and the location of these masses. Therefore, time dependent variations in such non-structural masses should be given much attention when VBI is to be applied to real civil engineering structures. In fact, changes in the non-structural masses will often occur during the lifetime of civil engineering structures.

For offshore platforms time dependent variations in the dynamic characteristics will always occur due to variation in the deck mass (see e.g. Idichandy et al. [87.6]), marine growth, flooding (see e.g. Kenley and Dodds [80.1] and Crohas and Lepert [82.2]) and iced-up structures.

Some people have claimed (see e.g. Mazurek and DeWolf [90.13] and Flesch [90.2]) that it would be most reasonable to use traffic-induced vibrations (see table 6.4) in connection with the performance of VBI on bridges. However, this kind of excitation should be used with great care because the size and location of the non-structural masses (cars or trains) will vary throughout a measurement session and from one measurement session to another.

Repair and relocation of the roadbed on bridges are other factors which may cause changes in the non-structural masses and thereby in the dynamic characteristics of the bridge.

Sometimes the mass of the measurement equipment can have a significant influence on the measured dynamic characteristics of a structure. The effect is most pronounced for relatively small structures. For instance, the first natural frequencies of the test beams used in experimental case no. 1 were reduced by 5-10 % when the three accelerometers were mounted.

Secondary structure elements such as e.g. exterior cladding and partition walls in high-rise blocks can in some cases have a significant influence on the dynamic characteristics of the building (see e.g. Torkamani and Ahmadi [88.5]). Therefore, time dependent variations in such secondary structural elements have to be taken into account during the introductory analysis and recorded at each periodical measurement.

The main part of the damping capacity in civil engineering structures often comes from non-structural sources which may vary with time. This effect is very pronounced for

offshore platforms where the damping due to water and air (see figure 5.9) will depend on the sea conditions and the wind conditions during the measurement session. Further, the damping originated by the liquid in storage tanks placed on the deck is highly dependent on the amount of liquid in the tank (see e.g. Vandiver and Mitome [82.6]).

Cars and trains consist, roughly speaking, of a mass placed on a number of dampers and springs which are the same components included in a tuned mass damper. Therefore, large variations in the damping should be expected if traffic-induced vibrations are used in connection with VBI on bridges.

The review given above has shown that a great number of time-varying effects exist. If it is possible these effects have to be considered and recorded in connection with application of VBI to civil engineering structures. If this is not performed, wrong results may be obtained during the diagnostic sessions. Therefore, it is of great importance to obtain reliable estimates for the time-varying effects of importance at each measurement session. The time-varying effects of importance should be revealed through the sensitivity studies (see section 6.2). Further, it would be a good idea to perform a superior visual inspection in connection with each measurement session.

6.2 SENSITIVITY ANALYSIS

The aim of the sensitivity analysis is to determine the sensitivity of all the potential DIs to the development of the expected damage scenarios to an acceptable level and to set up a fixed order of priority for the DIs. Secondly, the sensitivity analysis should reveal whether these damage depending changes in the dynamic characteristics are significantly different from the changes due to time-varying effects. Thirdly, the non-deterministic model parameters which have a significant influence on the dynamic characteristics should be determined in preparation for the virgin state calibration.

The design of civil engineering structures is based on more or less sophisticated mathematical models, like e.g. FEMs. A common feature of the models is that they are always chosen conservative. Further, the models are adjusted to the actual loads, whether they are dynamic or not. If the the loads are dynamic then the model will typically cover a certain frequency span with a good accuracy.

The dynamic effect of the loads on structures such as e.g. chimneys and bridges with a limited span is typical encountered in the design by multiplication of the expected load

by a dynamic amplification factor. Typically, a rough estimate for the fundamental bending natural frequency is the solely information of the dynamic behaviour needed for the calculation of these dynamic amplification factors.

Therefore, in most cases an adjustment of the design model has to be performed before the model can be used in connection with VBI.

Better estimates for the modal parameter of the higher order modes can be obtained by increasing the number of elements in the FEM in a proper manner until convergence is reached for the natural frequencies which are potential as DIs. However, the increased number of elements may cause an unwanted increase in the duration of e.g. the solution of the eigenvalue problem (see figure 4.13). Therefore, in some cases it might be profitable to include the number of elements and the configuration of the nodes in the virgin state calibration (see chapter 7). Modelling a truss structure like e.g. the one in experimental case no. 2 as either a continuous Bernoulli or Timoshenko beam has frequently been used to reduce the number DOF in FEMs (see e.g. Sun and Kim [85.10], Stubbs and Osegueda [85.3] and Hajela and Soero [90.18]). Finally, it should be mentioned that standard method for reducing the number of DOF exist where the Guyan reduction scheme (see Guyan [65.1]) is probably the most used.

The enlargement of the FEM should be terminated when the changes in the potential DIs are lower than the expected uncertainties of their estimates found through SI and the uncertainties in the calculated estimates due to assumptions of e.g. the distribution of masses and stiffness. For instance, due to this Flesch and Kernbichler [88.4] only make use of spring and beam elements in their model of the Lavant Bridge (see figure 6.1).

The locations where the calculations during the design have shown a utilization ratio (the ratio between the actual stress and the permissible stress) higher than a certain level due to overloading and/or fatigue should be taken as possible damage locations during the sensitivity studies. In some cases it may be reasonable to group the possible damages into damage scenarios including more than one of the possible damages. This grouping can for instance be done with respect to loads which cause the different types of damage. However, in all cases each single possible damage location should always be included as a damage scenario.

The acceptable level of damage for each damage scenario should be calculated by means of the updated analytical model. This calculation may be made more or less sophisticated depending on the types of damage included in the damage scenario. Next, the changes in all potential DIs due to the introduction of these allowable damage scenarios should be calculated (see example 6.1). Which DIs should be considered in this calculation

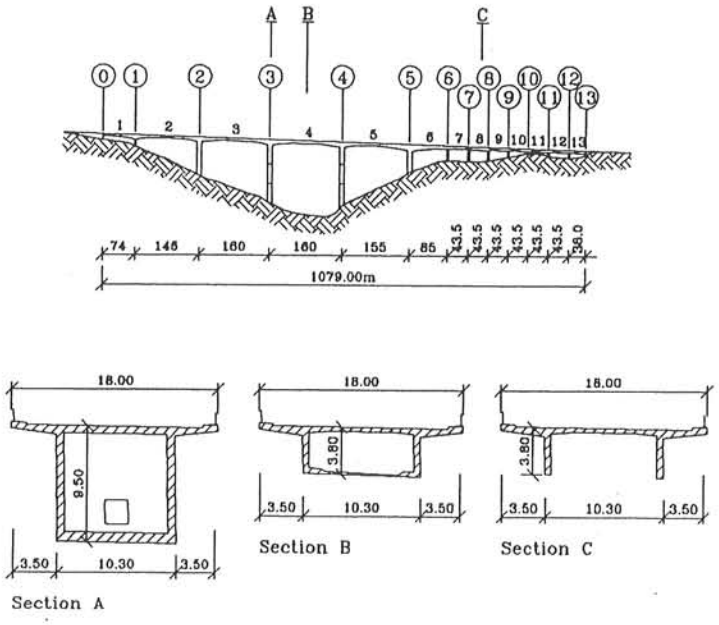

Figure 6.1 Dimensions of the Lavant Bridge (Flesch and Kernbichler [88.4]).

depends on several factors, such as e.g. the SI-method and the instrumentation in use.

Errors made during the construction work may lead to damage in other locations than the ones with high utilization ratios. As mentioned in section 3.1, such an error led to the failure of the offshore platform Alexander Kielland (see Moan [85.2]). Therefore, it is very important that other damage scenarios than those established for the performance of the sensitivity analysis are considered during the diagnostic sessions (see chapter 8).

Example 6.1

The aim of this example is to show a simple example of a sensibility analysis for the mast used in experimental case no. 2.

Eight different damage scenarios are considered. In these damage scenarios damage is assumed in one of the eight lower diagonals, which are denoted AB101, AB102, BC101, BC102, CD101, CD102, DA101 and DA102, respectively (see figure 6.2).

The six lower natural frequencies of the mast are chosen as potential DIs in this example. These natural frequencies have been found by means of the FE-programme ROSA from the computer package ROSAP (see ROSAP [92.9]) for the intact structure and total damage in the 8 elements inherent in the damage scenarios (see table 6.1). Frequencies no. 1 and 4 correspond to bending parallel to the x-axis, no. 2 and 5 correspond to bending parallel to the y-axis and frequency no. 3 and 6 correspond to rotation around the vertical centre line of the mast.

Nat. Freq. no.	DAMAGE STATE								
	0	1	2	3	4	5	6	7	8
1	2.012	1.943	2.012	1.937	2.012	1.921	2.012	1.913	2.012
2	2.018	2.018	1.944	2.018	1.949	2.018	1.920	2.018	1.926
3	8.184	6.011	6.163	6.123	6.081	5.559	5.714	5.674	5.613
4	11.528	10.389	11.528	10.165	11.530	10.345	11.530	10.111	11.531
5	11.622	11.622	10.179	11.621	10.422	11.623	10.121	11.622	10.372
6	26.982	19.851	20.076	20.095	19.647	20.153	20.392	20.415	19.925

Damage state no. 0 : Intact structure
Damage state no. 1 : Elem. AB101 removed
Damage state no. 2 : Elem. BC101 removed
Damage state no. 3 : Elem. CD101 removed
Damage state no. 4 : Elem. DA101 removed
Damage state no. 5 : Elem. AB102 removed
Damage state no. 6 : Elem. BC102 removed
Damage state no. 7 : Elem. CD102 removed
Damage state no. 8 : Elem. DA102 removed

Table 6.1 The six lower natural frequencies (Hz) of the mast for the intact and the damaged structure.

The results in table 6.1 show that significant changes in the natural frequencies should be expected when one of the eight lower diagonals is removed. The rotational frequencies (frequency no. 3 and 6) are the most sensible. Further, it can be seen that the natural frequencies of the bending modes parallel to the x-axis and y-axis, respectively, do not change when the damage is introduced in a diagonal perpendicular to the actual axis. Thus, the natural frequencies no. 1 and 4 which correspond to deflections parallel to the x-axis are affected in damage states no. 1, 3, 5 and 7 only, whereas the natural frequencies no. 2 and 5, which correspond to deflections parallel to the y-axis, are affected in the damage states no. 2, 4, 6 and 8.

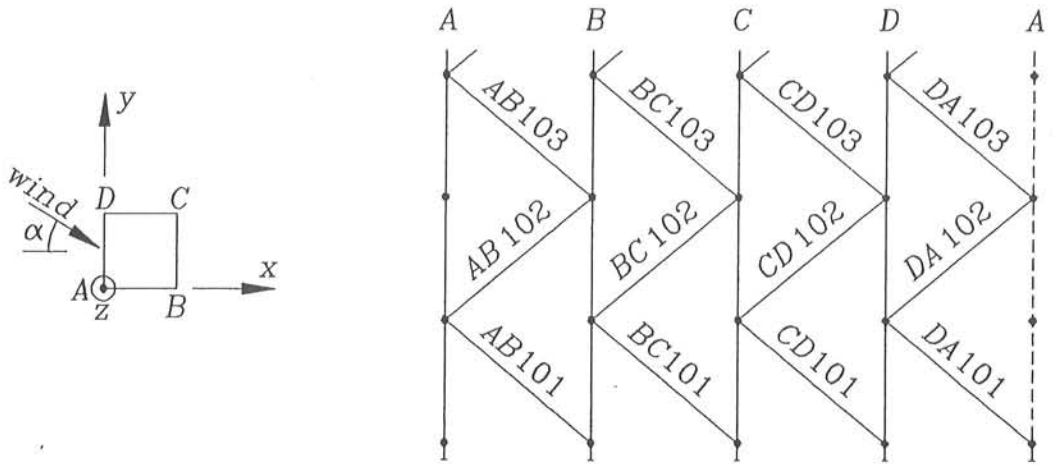

Figure 6.2 FEM of the lower two sections of the mast

Further, the utility ratios (abbreviated URs) of the different elements of the mast have been calculated by means of the post-processor programme STRECH (see ROSAP [92.9]) in accordance with the Danish codes for safety and loads (DS409 and DS410 [82.3]) and steel structures (DS412 [83.8]). The URs are defined as the ratio between the actual stress and the allowable stress in a member. Thus, the safety is in order when the URs are less than or equal to 1. Dead loads and wind loads are the sole basic loads, which have been included in the performed analysis. 8 different combined load cases corresponding to $\alpha = i*45$, i=0,7 (see figure 6.2) have been included. The maximum URs for each of the 8 damage states defined in table 6.1 are shown in table 6.2.

Damage state	Maximum UR	Comments
0	0.52	
1	0.89	
2	0.89	
3	0.89	
4	0.89	
5	1.10	The high URs occurs due to global buckling of element AB101, BC101, CD101 and DA101, respectively. The maximum URs will decrease to about 0.92, if these element are removed from the FEM
6	1.12	
7	1.10	
8	1.12	

Table 6.2 Maximum utility ratios.

The performed analysis has shown that a total collapse of one of the 8 lower diagonals is an acceptable level of damage in the mast. Further, the analysis has shown that these damage scenarios cause a decrease of about 0.06 Hz in one of the two fundamental bending frequencies depending on the location of the damage. A decrease of 2.0-2.6 Hz and 6.6-7.3 Hz has been estimated for the first and second rotational natural frequencies. The natural frequencies of the second bending mode parallel to the x-axis and y-axis, respectively, either decrease about 1.5 Hz or remain unchanged depending on the location of the damage.

Thus, from the results of the performed analysis it may be reasonable to demand that the standard deviation of the estimates for the six lower natural frequencies obtained by means of the SI-method should be of the order 0.025 Hz. If this demand is not fulfilled, then the two fundamental natural frequencies should either be included with a lower weight or excluded in the diagnostic session. Further, it should be requested that the level two or three method(-s) to be used in the diagnostic session should manage to reveal a total collapse in one of the eight lower diagonals.

The adjusted analytical model has to be calibrated to the results obtained in the virgin state measurements. Several factors are potential to be adjusted in this calibration. However, the factors of importance can relatively easy be found trough simple sensibility studies, as shown in example 6.2 for the beams used in the experimental case no. 1.

Example 6.2

The aim of this example is to present a sensibility analysis for the beams used in experimental case no. 1 to find those non-deterministic model parameters which have a significant influence on the dynamic characteristics of the beams. These parameters should be used as design variables in connection with the virgin state calibration (see example 7.1). The analysis is limited to concern the variations of the three lower natural frequencies with respect to the parameters presented in table 6.3 together with their deterministic values and upper and lower boundaries. The values given by the contractor or measured in the laboratory have been used as the determinitic

values of all the design variables except for k_f. The deterministic value of k_f has been found through a rough calculation. Engineering judgement has been used to establish the upper and lower bounds. An FEM consisting of 21 elements of equal length was used in the calculations (see figure 6.3).

Variables	Lower bound	Deterministic	Upper bound
I [m^4]	$0.120*10^{-6}$	$0.126*10^{-6}$	$0.130*10^{-6}$
E [N/m^2]	$2.05*10^{11}$	$2.1*10^{11}$	$2.15*10^{11}$
k_f [Nm/rad]	$0.1*10^{6}$	$1.0*10^{6}$	inf
μ [kg/m]	3.30	3.37	3.70
z_1 [m]	0.48	0.50	0.52
z_2 [m]	1.38	1.40	1.42
z_3 [m]	1.97	2.00	2.00
M_1 [kg]	0.09	0.10	0.11
M_2 [kg]	0.09	0.10	0.11
M_3 [kg]	0.09	0.10	0.11

Table 6.3 Boundaries for design variables.

The results from the performed analysis are shown in figure 6.4. It can be seen that the modulus of elasticity E, the flexural moment of inertia I, the density and the stiffness of the rational spring at the fixture are the most governing parameters for the value of the three natural frequencies. Therefore, these four parameters will be used as design variables in connection with the virgin state calibration.

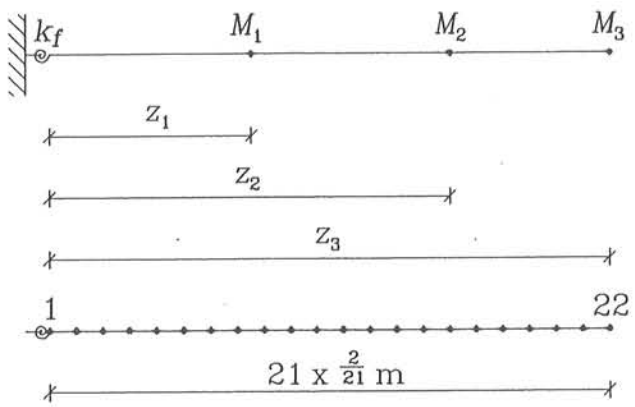

Figure 6.3 FE-model used for sensitivity study for the beam in experimental case no. 1.

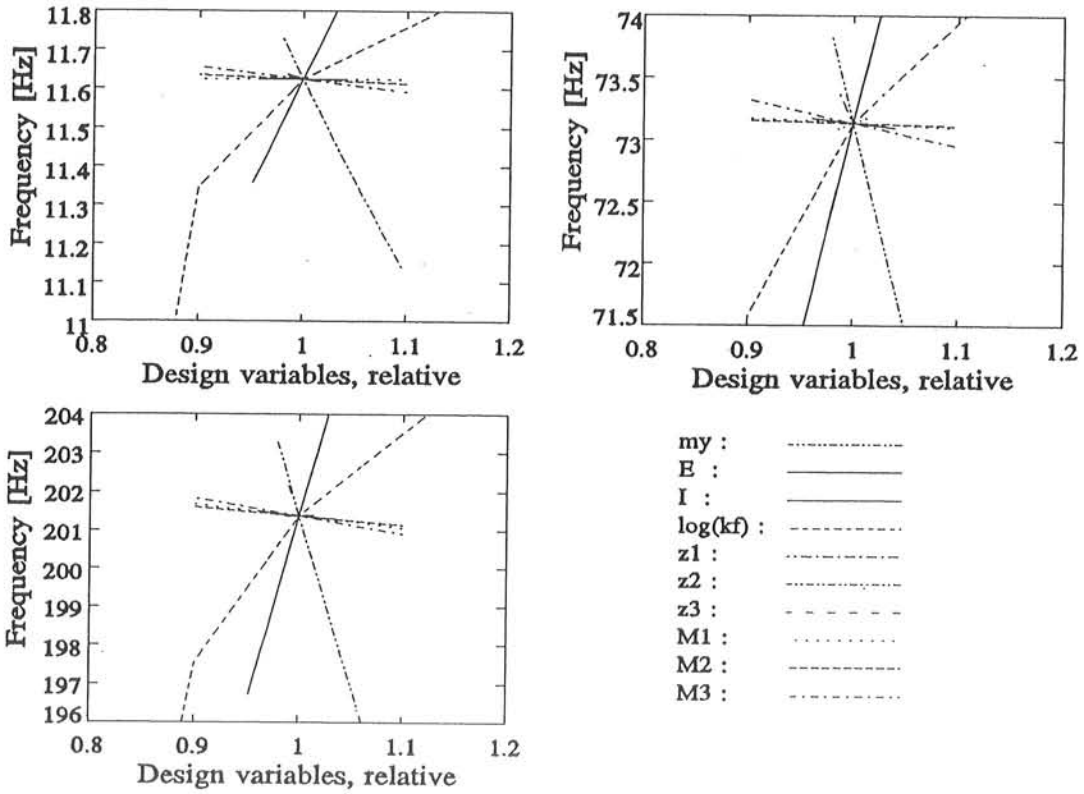

Figure 6.4 Results from the sensitivity study for the beams in experimental case no. 1.

One of the aims of the sensitivity analysis is, as mentioned earlier in this section, to set up a more or less fixed order of priority for the potential DIs. However, such lists should only be used in connection with the other activities in the introductory analysis, such as choice of SI-methods (see section 6.3) and choice of sensor locations (see section 6.4), since they are based on expected damage scenarios. In fact, the use of such lists in connection with the periodical measurement may in the worst case might cause non-expected damages to be missed. Therefore, all DIs which can be estimated from the measurement should be estimated during each periodical measurement. These topics are illustrated in example 6.3.

Example 6.3

The aim of this example is to present a sensibility analysis for the beam used in experimental case no. 1 with respect to the possible damage scenarios. For simplicity the latter has been taken as one crack of a length $a_c \in [0;0.12]$m located at $z_c \in [0;2.0]$m.

An FEM consisting of 21 elements has been used in the performed analysis (see figure 6.3).

The four lower natural frequencies and the ratio of the coordinate at M_3 of the first mode shape to the coordinate at M_1 and M_2 of the first mode shape (mode shape ratios) have been taken as potential DIs. The results from the performed analysis are shown in figure 6.5.

The first natural frequency and the two mode shape ratios should be given a high priority during the introductory analysis because they change with the crack growth in all locations. Opposite the second to fourth natural frequencies remain unchanged during crack growth when the crack is located in one of the nodes of the corresponding mode shapes. On the other hand the potential crack location(-s) will be reduced considerably if one of these natural frequencies remains unchanged when changes in the estimates for other DIs are observed. Therefore, a diagnostic session would in many cases be more efficient if these three natural frequencies are estimated after each periodical and included in the solution of the diagnostic problem. Thus, the fixed order of the potential DIs should be put in the background when the introductory analysis is over.

Further, it should be noticed that any change in the possible damage scenarios will lead to a change in the list of priority for the potential DIs as well. For instance, if the interval of possible location is restricted to [0.8;1.2]m then it obvious that the second natural frequencies should be given the highest priority during the introductory analysis.

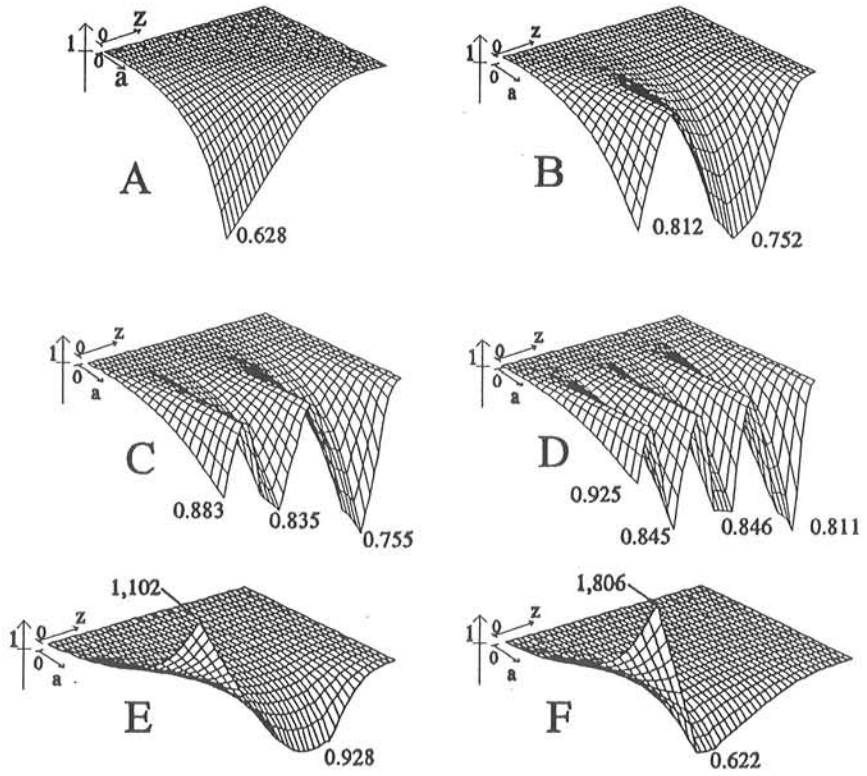

Figure 6.5 Expm. case no. 1 , $0 \leq a \leq 0.12$m, $0 \leq z \leq 2.0$m . A-D : First to fourth natural frequencies, relative, E-F : Mode shape ratio between the upper and mid and lower measurement points, respectively.

6.3 SYSTEM IDENTIFICATION

The SI-methods should, according to figure 3.1, first be used after each measurement session. However, the expected level of accuracy in the obtained estimates has to be compared with the changes due to the damages below the acceptable levels (see section

6.2) when the decision on whether or not VBI should be applied to a certain structure or not has to be made. Further, the planning of the measurement programme cannot be performed without knowing the SI-method(-s) to be used. Therefore, they should always be chosen in connection with the introductory analysis.

In general the goal of a system identification process is to obtain a set of estimates for the system parameters in a proper model of the structure from measurements performed on the structure. The system parameters could be dynamic characteristics (e.g. modal parameters), model parameters (e.g. stiffness matrix) and/or physical parameters (e.g. bending stiffness of a beam). The goal depends on the subsequent use of the results.

Many of the SI-methods work in two steps where the dynamic characteristics are estimated first. These estimates are then subsequently used to estimate model and/or physical parameters. Therefore, in principle some of the methods used for updating at the virgin state and in the diagnosing sessions are some sort of SI-methods.

The SI-methods work either in the frequency domain or the time domain. The choice of domain/method is highly dependent on the nature of the problem and especially on the dynamic characteristics which have to be identified. For instance, usually the identification of natural frequencies can be made with required accuracy in both domains, whereas the identification of damping ratios of lightly damped structures normally gives much more reliable estimates, when the identification is performed in the time domain than in the frequency domain. The latter is due to the fact that the information about the damping is spread over a long time interval in the time domain and concentrated in small areas around the resonance peaks in the frequency domain. Civil engineering structures are usually lightly damped. This means, as a rule of thumb, that the time domain system identification should be used for these structures.

Numerous of SI-methods have been developed for use in either the time domain or the frequency domain. The basis of the traditional system identification methods is that both the system input (e.g. loads) and output (e.g. accelerations) are known. However, it is often quite difficult or impossible to measure the natural loads, etc. on large civil engineering structures (as e.g. offshore platforms) with the required accuracy. Furthermore, it can be difficult to persuade the owner of the structures to allow the use of artificial loading systems like for instance rotating unbalance. This means that the traditional methods of system identification are not suitable for vibration based inspection of civil engineering structures. This means that the choice of SI-methods will depend highly on the possible loading process.

A list of examples of types of excitation applied to civil engineering structures is given in table 6.4. The choice of excitation type to be used in the different cases depends on several factors such as the system parameters to be estimated, the purpose of the measurement, the required accuracy and the demands for serviceability of the structure during the measurement.

Excitation	Structure	References
Synchron pulling	Chimney	Andersen & Heiden [84.4]
Man swaying	Offshore platform High-rise building	Vandiver & Mitome [82.6] Czarnecki [74.2]
Eccentric masses	Bridges	Kernbichler & Flesch [84.3]
Wind	Mast	Rytter and Kirkegaard [93.1]
Ambient sea	Offshore structures	Vanmarcke [71.1] Rubin [80.8] Nataraja [83.2]
Traffic	Bridges	Mazurek and DeWolf [90.13]
IMPULSE EXCITATION		
Lorry	Bridges	Kernbichler & Flesch [84.3] Casas & Aparicio [90.15]
Falling weight	Bridges	Ågårdh [90.6] + [91.4] Askegaard & Mossing [88.2]
'Bolt gun'	Bridges	Wood et al. [92.8]
Boat pulls/impact	Offshore structures	Ruhl [76.3]
Hammer	Bridges	Maguire [90.14]

Table 6.4 Examples of types of excitation and their field of application.

Mazurek and DeWolf [90.13] point out that ambient vibration is the only type of excitation, which is applicable in an automated monitoring system.

Several authors have found (see e.g. Rubin [80.8], Nataraja [83.2]) that vibrations of offshore platforms due to ambient sea are a sufficient base for identification of natural frequencies and mode shapes. However, Crohas and Lepert [82.2] recommend the use of controlled and measured excitation, because the damage sensitive higher order modes are not identified through ambient vibration monitoring. The latter is because the natural frequencies of the higher order modes are outside the energy rich part of the wave spectrum.

Similar problems are reported by Flesch and Kernbichler [88.4] and Flesch [90.2] in connection with application of VBI to concrete bridges. They recommend the use of

sinus sweep induced by means of an eccentric mass instead of impulse, ambient and white noise loading.

In some situations it will be necessary to perform the measurement, while the structure is in service due to e.g economy. For instance, it will be impossible to close down the machinery on an offshore platform for even a short period. Similarly, the closing of a bridge could lead to traffic problems and/or unreasonable diversions. Flesch [90.2] reports on measurements performed on partly closed bridges and suggests the noise in measurements and the additional mass introduced by the cars to be averaged away. However, the latter will always lead to estimates for natural frequencies lower than the actual and should therefore be used with great care.

The traditional SI-methods were developed for use in the electronic industry and the machine industry where it has been possible to use a well-defined loading process. These SI-methods were adopted for use in connection with civil engineering structures in the early seventies. However, the above-mentioned problems with unknown loading process were soon realized. Therefore, much effort has been given to the development and the implementation of system identification methods, which provide reliable estimates of the dynamic characteristics of a civil engineering structure when only the system output due to natural dynamic and random environmental loads is known.

The most commonly used frequency and time domain SI-method will be mentioned in the following. A more comprehensive presentation is given in e.g. Jensen [90.8].

The basic idea in most of the SI-methods working in the frequency domain is to estimate the modal parameters from either measured frequency response function or measured auto spectral density function for the response. The first-mentioned methods can be used when the input is measured and the last-mentioned methods should be used when only the response of the structure is known.

Experimental modal analysis (see e.g. Ewins [86.2]) which belongs to the first group is probably the most widely used SI-methods in connection with measurement on structures in general and has also been used in connection with measurement on real civil engineering structures (see Flesch and Kernbichler [88.4] and [90.2], Biswas et al. [90.5] and Ågårdh [90.6] og [91.4]). However, the above-mentioned problems with unknown input makes the method less attractive in connection with large civil engineering structures. The method has also been applied to beam B5 from experimental case no. 1 where the modal parameters were estimated by means of the STAR*Struct*-software from SMS (see SMS [89.1]).

A number of more or less advanced frequency domain methods based on measured output may only be found in the literature (see e.g. Rytter et al. [90.9], Mazurek and DeWolf [90.13] and Casas and Aparicio [90.15]). A common feature of most of the methods is that they are based on assumptions about the auto spectral density function for the loading process, typically a white noise assumption. Further, some methods make use of the fact that the ratio between the auto spectral density functions for the response in two different locations is equal to the square of the gain factor between these two locations (see e.g. Herlufsen [85.6]).

The basic idea in most of the SI-methods working in the time domain is to obtain estimates of the dynamic characteristics by fitting a model to either the raw signal, a filtered signal or a time-domain function as e.g. an auto correlation function obtained from the measured signals. Curve fitting on free decays (see e.g Jensen et al. [90.10]), ARMA-models (see e.g Ljung [87.4], Pandit and Wu [83.3], Pandit [91.18] and Pandit and Mehta [88.14]), the Ibrahim Time Domain method (see e.g. Ibrahim [86.3]) and the Random Decrement Technique (see e.g. Yang et al. [80.5] and Brincker et al. [90.11] and [91.2]) are some of the time domain methods, which are suitable for system identification of civil engineering structures. Curve fitting on free decays has been used in connection with experimental case no. 1 (see Rytter et al. [92.7]) and ARMA-models have been used in connection with experimental case no. 2 (see Rytter and Kirkegaard [93.1]).

The estimates obtained by means of SI-methods will allways be encumbered with bias and random errors (see e.g. Bendat and Piersol [86.4]). The magnitude of these errors varies from method to method. However, the main emphasis in papers on SI-methods has been laid on comparing the exactness of estimates obtained by means of the different SI-methods. Thus, there has only be given a little attention to investigate and compare the effectiveness of the different SI-methods with respect to these two kinds of errors and to minimize them. An example of such study may be found in Brincker et al. [91.16] and [91.17].

A common feature of all the above-mentioned SI-methods is that the structure is linear. However, all structures are non-linear to a certain degree which normally depends on the level of vibration during the measurements. Thus, in such cases the assumption about linearity can be fulfilled by using a limited level of vibration during the measurement. However, the introduction of damage as e.g. cracks may cause non-linear behaviour for even a low level of excitation (see section 4.1.5). Neglecting such non-linearity may lead to a very poor diagnosis, where damage of importance is not revealed. The existence of such damage depending non-linearities can be revealed by means of some of the DIs presented in chapter 5. Therefore, these DIs should be used if there is any suspicion

about non-linearity. The use of non-linear SI-methods is the most obvious way to be aware non-linearities. However, it is only during the last five years that emphasis has been given to development of such SI-methods and their number is still very limited.

6.4 PLANNING OF MEASUREMENT PROGRAMMES

The accuracy and thereby the applicability of the dynamic parameters of a structure found by means of a certain SI-method will be highly dependent on the experimental conditions, such as e.g. sensor locations, number of sensors, excitation, duration of the measurement and sampling strategy. Therefore, it is very important to choose these conditions so that the information provided from the experiment is maximized.

According to Kirkegaard [91.15] the problem of experiment design has been given much attention in the literature since the early thirties. However, the models considered in this literature are generally static and their applicability to dynamic problems has apparently become clear only recently. Therefore, the design of SI-experiments in relation to structural problems seems to be a subject, which has received only little attention during the last decade. However, the problem has been adopted as a subject of research by more and more people during the last two years.

For economic and sometimes practical problems the number of sensors will be limited in connection with all kinds of dynamic experiments. Traditionally, this limited number of sensors has been placed from intuition and sound engineering judgement (see e.g. Nataraja [83.2] and König et al. [87.5]). Typically, the sensors have been placed at locations with large deflection in one or more of the mode shapes of interest, This rule of thumb also forms the basis in two numerical methods for choosing the optimal sensor locations presented by Flanigan and Botos [92.11] and Penny et al. [92.10].

Flanigan and Botos [92.11] suggest the use of a so-called Test-Analysis-Model (TAM) for selecting good accelerometer locations in connection with modal survey tests. A TAM is a mathematically reduced version of the FEM in which master degrees of freedom are retained at potential accelerometer locations in the modal survey test. Flanigan and Botos recommend the use of Guyan reduction to obtain the TAM. The best master DOF, i.e. the best accelerometer locations, are taken as those for which a linear combination of the static flexibility shapes matches with the FEM mode shapes within a user-specified tolerance. The static flexibility shapes are calculated by applying unit forces and moments at potential DOF.

Guyan reduction is also the corner stone in a method for automatic choice of sensor locations for dynamic testing presented by Penny et al. [92.10]. The algorithm given by Guyan [65.1] is used to reduce the number of master DOF in the FEM by one DOF at a time to the number required for sensor location. The choice of the eliminated coordinates is automated and designed to give an accurate, reduced model at low frequencies. Penny et al. use either the maximum and RMS of the off-diagonal elements in the MAC-matrix (see equation (5.2)) or the ratio of the largest to smallest singular value of the eigenvector matrix to judge the applicability of the chosen sensor locations.

Further, Penny et al. [92.10] evaluate their method by comparing the obtained results from a method based on average driving point residues (*ADPR*). If N modes have to be measured, then the *ADPR* of point j is given as

$$ADPR_j = \sum_{i=1}^{N} \frac{\phi_{ji}^2}{\omega_i} \qquad (6.1)$$

where ϕ_{ji} is the jth element of the ith mode shape vector weigthed with respect to the generalized massess and ω_i is the cyclic natural frequency of the ith mode. The coordinates with the highest *ADPR*-values should be taken as sensor locations.

Penny et al. [92.10] conclude that their method based on Guyan reduction gives the best results when the structure is grounded with no rigid body modes. On the other hand the method based on *ADPR* gives the best results when the structure has one or more rigid body modes.

The more advanced methods for design of an SI-experiment are based on minimization of a scalar measure of the covariance matrix of the system parameters (see e.g. Shah and Udwadia [78.2]) or the inverse of the Fischer information matrix (see Kirkegaard [91.15]). In this way the expected accuracy of the system parameter estimates is included in the design. However, such a qualitative measure can only be used to compare different designs. They cannot tell how much one design is better than another. Kirkegaard [91.15] has solved this problem by including the additional costs due to the measurement and using a preposterior analysis as a basis for the design of SI-experiments.

Accelerometers are the most commonly used sensors in connection with vibrational measurements. However, other sensor types can be more applicable in some cases. For instance, it would preferable to use strain gauges if mode shapes and especially the curvature of the mode shape are used as DI (see e.g. Pandey et al. [91.9] and Yao et al.

[92.13]). From a practical point of view the accelerometer is to prefer in most cases because they have relatively good stability.

In fact the stability and lifetime of a sensor can be of great importance in connection with instrumentation for continuous measurement and for measurements on structures with poor accessibility like e.g. control systems for large space structures (see Velde and Carignan [84.5]).

6.5 CONCLUSION

From an economic point of view the introductory analysis is probably the most important in connection with VBI, because its results form the basis for making the decision about starting the VBI-programme or not.

The going through of the different topics to be treated during the introductory analysis has been performed in four different sections. These sections have been placed in the order in which it is recommendable to start them. However, the going through has shown that there is a high degree of correlation between the results from the different analyses. Therefore, completion of the different analyses has to be performed parallel. For instance, one cannot choose the SI-method(s) without having an idea about e.g. the sensor locations, and on the other hand the sensor locations cannot be chosen without having knowledge about e.g. the loading process and SI-method(-s).

The review of time-varying parameters given in section 6.1 showed that damages are not the sole cause of changes in the dynamic characteristics of a structure. In fact such changes due to variation with time of both non-structural and structural parameters have been reported in the literature to be comparable with damage induced changes. This means in the worst case that damages may be overlooked in connection with a periodical measurement due to changes in the time-varying parameters. Therefore, a list of all potential time-varying effects and their expected variations should be written at the start of the introductory analysis. The time-varying effects of importance should then be found from the sensitivity analysis and recorded in connection with periodical measurement. The optimal situation would be to incorporate these time-varying effects on equal terms with the potential damages in the diagnostic session.

The performance of the introductory analysis is highly dependent on that one have a good analytical model of the structure. In most cases some kind of adjustment of the

model used in connection with the design will be required (see section 6.2). A rule of thumb is that the number of DOF in an FEM should be kept as low as possible to limit the duration of calculation because the model has to be used after almost each periodical measurement. The optimal would be that the introductory analysis is performed parallel or at least started before the design has been finished.

However, the adjusted model will be established from assumptions about e.g. the distribution of stiffness and mass. Therefore, there will always be differences between the calculated and the true dynamic characteristics. These differences are reduced through a calibration of the model after the virgin state measurements. The model parameters which have a significant influence on the dynamic characteristics should be found from the sensitivity analysis and used as design variables in connection with the virgin state calibration (see chapter 7).

The results from the design should be used to arrange sets of damage scenarios including the expected combinations of damage in the different hot spots in the structure. The acceptable level of damage for each damage scenario and the corresponding changes in the potential DIs should be calculated. The result should be used to specify the requirement for the accuracy of the SI-methods and the diagnostic methods.

A lot of different types of excitation have been used in connection with the performance of SI-experiments on civil engineering structures (see table 6.4). However, the number of possible types of excitation which can be applied to a certain structure will often be very limited. Therefore, in many cases the excitation to be used in connection with the performance of the periodical measurements will be governing for the choice of SI-method(-s) and the instrumentation to be used. A short surwey of SI-methods is given in section 6.3.

The experimental conditions, such as e.g. sensor locations, number of sensors, excitation, duration of the measurement and sampling strategy are governing for the accuracy and thereby the applicability of the dynamic parameters of a structure found by means of a certain SI-method. Therefore, it is very important to chose these conditions so that the information provided from the experiment is maximized. The review of this topic given in section 6.4 shows that optimal choice of location for a limit number of sensors typically has been a governing factor in connection with many field measurements. A number of different methods for solving such problem have been presented in section 6.4.

Further to the topics described in the present chapter the choice of diagnostic method(-s) should also be included in the introductory analysis. A comprehensive review of diagnostic methods is given in chapter 8.

CHAPTER 7
VIRGIN STATE CALIBRATION

The first dynamic measurements made on a civil engineering structure in connection with a VBI-programme are the most important measurements in the whole programme. Firstly, the results from these measurements will be used as reference values in the remaining part of the VBI-programme. Secondly, in most cases the results should be used as a basis for a calibration of an analytical model for the structure. This calibrated version of the mathematical model is then used in connection with the diagnostic sessions. Thus, poor estimates for the dynamic characteristics and/or a badly calibrated mathematical model may lead to problems during the diagnostic session later on in the VBI-programme.

The aim of this chapter is to present and discuss some of the problems which occur in connection with the performance of the virgin state measurements and to give a review of some of the methods applicable for updating a mathematical model to correlate with measured dynamic characteristics.

Optimally the first measurements should be performed immediately after the end of construction, i.e. at the virgin state. Therefore, in the remaining part of this thesis the first measurements will be referred to as *Virgin State Measurements* (in brief VS-measurements). The structure should be free of damage at the virgin state. However, in some cases this may not be true. Therefore, an alarm should be given if the mathematical model cannot be calibrated with the required level of accuracy because this could be a warning about damages etc. somewhere in the structure.

It is never too late to start up a VBI-programme for a structure if the results from other kinds of inspection methods have shown that the structure is sound. Therefore, if the structure has been in use for more than 1-3 years then it is recommendable to supplement the VS-measurements with another kind of inspection. The extent of this inspection should be at least as in the "Special inspections" mentioned in section 2.2.1. Thereby, the risk of overlooking damage at the virgin state should be reduced to an acceptable

level and the actual value of the time-varying parameters could be used in the VS-calibration.

Further, the risk of overlooking a damage could be reduced by including damage parameters such as e.g. crack size and length as design parameters during the updating of the mathematical model (hereafter denoted as the VS-calibration). Subsequently, the obtained estimates for the design parameters should be verified through inspection by other methods. The VS-calibration should be repeated until a user defined acceptable degree of correlation between the dynamic characteristics of the mathematical model and the estimates found through measurements is obtained.

A structure will in many cases become non-linear due to the introduction of damage. Therefore, Flesch and Kernbichler [88.4] suggest : *Test phases carried out with different levels of excitation force could result in different non-linear reactions in areas of damage. If the bridge behaves mainly linear in non damaged condition maybe only some dynamic parameters, especially damping, could change. Hence, an identification could be possible.*

The extent of the VS-measurement and the subsequent SI-session should often be much larger than the extent of the periodical measurements due to the great importance of the VS-measurements. For instance, it may be a good idea to test if there is any correlation between the estimated dynamic characteristics and the direction and/or average speed of the wind during the measurements, if wind is planned to be the sole loading process.

Normally, the design of civil engineering structures is based upon results from analysis of an FEM. This FEM has been adjusted during the sensitivity analysis (see section 6.2) to give more exact estimates for the potential DIs. However, this adjustment is solely based on expected values for the distribution of stiffness, mass and damping. The effect of several factors of importance as e.g. stiffness in non-structural components, damping and mass distribution cannot be modelled exactly. Therefore, a calibration of the FEM should be performed, when the first measurements of the dynamic parameters are made.

The FEMs have become more and more advanced during the last ten years, for instance non-linearities and stability effects can now be included. The use of these advanced FEM has led to more exact estimates for the dynamic behaviour of the structures. However, still the modelling will be conservative since it is based on approximation of boundary conditions; lumping of distributed parameter systems; lack of damping representation and inadequate modelling of joints and couplings.

The importance of a proper updating of the design model at the virgin state has also been illustrated by Torkamani and Ahmadi [88.5] through experimental tests on models of a storey building. Torkamani and Ahmadi investigates the changes in the natural frequencies when non-bearing components like e.g. exterior cladding and partition walls were added to the model. The stiffness of these non-bearing elements is not included in the models used in the design phase. Another example of VS-calibration is given by Coppolino and Rubin [80.6] who report on changes in the model of the deck structure and the foundation in connection with a VS-calibration on an offshore platform.

The significant development in the area of computer technology in the sixties led to an extended use of FEA in connection with the design of structures. However, often the FEA were very time consuming and costly which resulted in a limitation of the number of trial designs which could be analyzed. These conditions caused the start of the development of numerous methods for performing calibration of numerical models as e.g. FEMs to either requirements given at the design state or to measured values.

Roughly the methods can be grouped in two main groups depending on whether they give answer to the question "*What happens if ?*" or the question "*What should be done to ?*".

The methods in the first group are designed for the performance of eigen solution reanalysis or modal synthesis for predicting the effects of changes in the design variables without solving the complete eigen-value problem again (see e.g. Wittrick [62.1], Fox and Kapoor [68.1], Wang et al. [83.9] and Stetson and Palma [76.4]). However, the methods may be used in connection with e.g. an iterative VS-calibration.

The methods in the second group are designed to give estimates for the changes in the design variables for obtaining a set of specified values of the dynamic characteristics of the structure. These specified values can be either design requirements or estimates obtained through measurements. The methods in the second group have been given a lot of different names such as updating method, improvement method, linking analysis although they are often very similar.

The set of design variables used in the different methods varies. Some methods are based on corrections of physical parameters, as e.g. the density, other methods are based on corrections of model parameters as e.g. the elements in a stiffness matrix. The latter can lead to a correction without any physical meaning which is quite unfortunate. Further, uncertainties in the measured values and numerical errors may cause changes in the elements of e.g. a stiffness matrix which should not have been changed. For instance, coefficients with values of zero in the original matrix may be given a small non-zero

value even though they should remain zero. However, it is often the only way of performing a correction of the damping because the modelling of damping is quite poor.

Further, the set of input variables varies from method to method. Traditionally, the modal parameters (natural frequencies and mode shapes) have been used as input variables. However, methods using other kinds of input have been developed lately.

The development of updating methods was started in the early seventies when both the analysis and test techniques began to formulate a well-defined trend. The emphasis was laid on developing methods where the elements of the model matrices were used as design variables.

An FEM of a continuous system will have as many modes as DOF. Further, it should often contain a considerable number of DOF to give reliable estimates for the dynamic characteristics of interest. On the other hand, the estimates for dynamic characteristics obtained through measurement will be restricted to cover only a finite frequency range and a limit number of points (the sensor locations). Therefore, in most cases the number of design variables will be larger than the number of measured dynamic characteristics or, in other words, the number of unknown parameters exceeds the number of known parameters.

In 1971 Berman and Flannelly [71.2] presented the first generally accepted method to solve this basic problem in connection with updating of FEMs. The basic idea in the method is to obtain a so-called incomplete FEM which gives good estimates for the natural frequency in the frequency range of interest and the coordinates of the corresponding mode shapes at the points of interest. The elements in the stiffness matrix are used as design variables. A reasonable analytical mass matrix, measured estimates for the natural frequency in the frequency range of interest and the coordinates of the corresponding mode shapes at the points of interest are used as input.

A lot of work has been performed subsequent to the presentation of the method in Berman and Flannelly [71.2]. The goal of this work has been to improve the method or develop similar methods for solving the problem of incomplete test data by using model reduction like e.g Guyan reduction, analytical methods for completing the modal vectors and sensitivity based optimization techniques (see e.g. Baruch and Itzhack [78.3], Berman et al. [80.9], Berman and Nagy [83.10], Kabe [85.11], Ibrahim [88.6] and Kammer [88.15]).

Minas and Inmam [90.23] propose a technique in which the desired perturbations in stiffness and damping matrices are considered as gain matrices in a feed-back control

algorithm designed to perform eigen structure assignment. Minas and Inmam use two examples concerning relatively simple structures to demonstrate the usefulness of the method. Apparently the method is applicable to undamped, proportionally damped and non-proportionally damped structures which makes the method attractive in many cases.

The development of faster and faster computers up through the eighties has among other things caused an increased activity of formulating fast and reliable optimization schemes. These methods have been given more and more attention in the area of model updating during the last five years.

The least square fit shown in equation (7.1) has been the most commonly used method in connection with correlation of a numerical model to measure data (see e.g. Jensen et al. [90.10], Ting et al. [91.10], Rytter et al. [91.12] and Hemami and Abdelhamid [92.11]). In most cases the objective function should be supplemented with inequality, equality or side constraints.

$$F_V(X) = \sum_{i=1}^{N_m} \varepsilon^2 = \sum_{i=1}^{N_m} \left(\Theta_i^M - \Theta_i^C(X)\right)^2 W_i \tag{7.1}$$

where N_M is the number of measured dynamic characteristics, $\boldsymbol{\Theta}^M$ are the measured dynamic characteristics, $\boldsymbol{\Theta}^C(X)$ are the calculated dynamic characteristics, W are the weighting parameters and X are the design variables.

The weighting vector W was introduced in Rytter et al. [91.12] for two purposes. The first purpose was to favour the potential DIs in accordance with the fixed order of priority which was established in the sensitivity analysis. The second purpose was to ensure that the parameters in $\boldsymbol{\Theta}^M$ are weighted with respect to how well they have been identified.

Both elements of model matrices and physical parameters have been used as design variables. Further, there is a certain difference in the sets of input parameters used in the above-mentioned papers. For instance, Jensen et al. [90.10] use measured free decays as input variables for updating the matrices in a FEM of a structure containing non-linear damping mechanisms. Ting et al. [91.10] use the response in a grid of points on the structure to constant-amplitude harmonic force as input variables, and physical parameters as e.g. masses and modulus of elasticity as design variables. Rytter et al. [91.12] use natural frequencies and mode shape ratios as input variables and the mesh in an FEM as design variables. The latter can be of great importance because the number of elements can be held at a minimum. Thereby the duration of the computer runs is reduced.

The use of the least square fit method from Rytter et al. [91.12] is demonstrated in example 7.1 for the beams in experimental case no. 1.

Example 7.1

The aim of this example is

- to demonstrate the practical use of equation (7.1) in connection with the VS-calibration of FEMs for the six beams from experimental case no. 1
- to study the differences in the calibrated models for the six beams

The performed analysis will concern a VS-calibration of the FEM used in example 6.2 in connection with sensitivity analysis (see figure 6.3).

The following vector of design variables has been chosen in the light of the results from the sensitivity analysis in example 6.2

$$X = [I_1, I_{2\text{-}21}, k_f, \mu] \tag{7.2}$$

where I_1 is the flexural moment of inertia of element no. 1, $I_{2\text{-}21}$ is the flexural moment of inertia of elements no. 2-21, k_f is the stiffness of the rotational spring at the fixture and μ is the mass per unit length.

The beams are welded to a relatively thick base plate at the fixture which could have influence on the stiffness of the beams in this area. Therefore, I_1 was introduced as a separate design variable.

The upper and lower bounds for the design variables are shown in table 7.1. The bounds for the flexural moment of inertia were set to 0.95 and 1.05 times the value given by the steel contractor, respectively. A $\pm$ 2 % variation around of the modulus of elasticity has been included in the bounds for the flexural moments of inertia. The mass per unit length was measured in the laboratory to 3.38 kg/m and given as 3.58 kg/m by the contractor which gave the bounds shown. Due to this discrepancy the mass per unit length was included a design variable. The upper and lower bound were established with respect to the fact, that the measured value is the most reliable of the two estimates. A rough calculation of k_f gave $1*10^6$ Nm/rad which was used as the deterministic value in example 6.2. The bounds for k_f were chosen in the light of the results from the sensitivity analysis.

Design variables	Lower bound	Upper bound
I_1 [m^4]	$0.118*10^{-6}$	$0.127*10^{-6}$
I_2-I_{21} [m^4]	$0.120*10^{-6}$	$0.130*10^{-6}$
k_f [Nm/rad]	$0.5*10^6$	$10*10^6$
μ [kg/m]	3.35	3.45

Table 7.1 Boundaries for design variables.

The three lower natural frequencies of beam B1-B3 and B5-B6 were used as input variables for these beams. Only the first natural frequency was use as input variable for beam B4.

The objective function used in the VS-calibration was taken as

$$\min_{X} \left[\sum_{i=1}^{N_f} \left(\frac{f_i^M - f_i^C(X)}{f_i^M} \right)^2 W_i \right] \tag{7.3}$$

subject to

$$\left| \frac{f_1^M}{f_1^C(X)} - 1 \right| \leq 0.005 \tag{7.4}$$

$$\left| \frac{f_2^M}{f_2^C(X)} - 1 \right| \leq 0.01 \tag{7.5}$$

where N_f is the number of natural frequencies, f_i^M and $f_i^C(X)$ are the measured and calculated estimate for the ith natural frequency. The weighting vector W was taken as [1,0.5,0.05] to reflect the degree of accuracy in the measured values for the three natural frequencies.

The test beams were removed from their fixture between test A (a = 0 m) and test B (a = 0.02 m) for practical reasons. However, this has caused an increase in the natural frequencies from test A to B even though damage was introduced. Therefore, the test B series have been taken as virgin state measurements in the analysis performed in this example. Thus a crack of 0.02 is included in the FEMs during the calibration. This crack will be removed from the models when these are used as a virgin state model in the diagnostic methods.

The final values of the four design variables for the six beams are shown in table 7.2. The corresponding natural frequencies are shown in table 7.3.

	BEAM NO.					
	1	2	3	4	5	6
$I_1 * 10^6$ [m^4]	0.1357	0.1371	0.1371	0.1206	0.1371	0.1369
$I_{2\text{-}21} * 10^6$ [m^4]	0.1192	0.1192	0.1192	0.1192	0.1192	0.1192
$k_f * 10^{-6}$ [Nm/rad]	1.384	1.732	1.456	1.540	2.159	2.058
μ [kg/m]	3.45	3.43	3.43	3.45	3.42	3.45

Table 7.2 Final values of design variables.

BEAM	f^M_1	f^C_1	f^M_1/f^C_1	f^M_2	f^C_2	f^M_2/f^C_2	f^M_3	f^C_3	f^M_3/f^C_3
1	11,361	11,348	1,00	71,832	71,191	1,01	191,0	195,9	0,98
2	11,447	11,426	1,00	71,139	71,666	0,99	191,7	197,2	0,97
3	11,418	11,401	1,00	71,123	71,515	0,99	191,6	196,7	0,97
4	11,227	11,227	1,00	-	-	-	-	-	-
5	11,460	11,435	1,00	71,333	71,922	0,99	191,2	197,7	0,97
6	11,409	11,387	1,00	71,054	71,618	0,99	191,1	196,8	0,97

Table 7.3 Measured and calculated natural frequencies in Hz.

The final values for the design variables showed a certain scatter in the values for I_1 and k_f which are related to the stiffness in the fixture. The scatter is probably due to different stress levels in the 6 bolts connecting the beams to the ground.

The results in table 7.3 show that the least square fit method has given good estimates for the design variables for all six beams.

Flesch [90.2] recommend the use of a so-called structural dynamic modification model (in brief SDM-model) as VS-model. An SDM-model may be generated by using the STAR*Struct* Modal Analysis Software Package from Structural Measurement System (in brief SMS) [89.1] in the analysis of the VS-measurements. Thus, the troublesome updating of numerical models as e.g. FEMs can be avoided by using such an SDM-model.

For completeness, it should be mentioned that the VS-calibration of the mast in experimental case no. 2 for practical reasons was performed through a trial and error session. The FEM was manually adjusted until a reasonable agreement between the calculated and measured values of the six lower natural frequencies was obtained. The results from sensitivity studies combined with experience and engineering judgement are the corner stones in this method. The method can only be used for relatively small and simple structures or structures with only a limit number of uncertainties. The stiffness of the fixture, the density, the modulus of elasticity and the lumped masses were used as design variables. The analysis revealed that the modelling of the fixtures was the most important factor. A reasonably good agreement between the two sets of natural frequencies was obtained (see table 7.4).

Frequency no.	Description[1)]	Frequency [Hz]	
		Measured	Calculated
1	x-axis	2.029	2.011
2	y-axis	2.025	2.018
3	rotation	8.135	8.184
4	x-axis	11.483	11.523
5	y-axis	11.486	11.622
6	rotation	26.660	26.981

1) x-axis : deflection parallel to the x-axis
y-axis : deflection parallel to the y-axis
rotation : rotation about the z-axis

Table 7.4 Measured and calculated natural frequencies at virgin state.

In principle the diagnosis schemes presented in chapter 8 can be used for updating the analytical model (and vice versa). However, these methods are often focused on the location of a limit number of local changes, while all elements have to be included in the updating at the virgin state.

The survey of methods should not be considered as a complete state-art-of-the-art review. Such review may be found in e.g. Natke [88.16].

The numerical model should not be changed at any time during the remaining part of the VBI-programme since such changes will introduce changes in the dynamic parameters as well. These changes could lead to mistake in connection with a later diagnostic session.

A revision of the sensitivity analysis (see section 6.2) can be necessary in some situations, when the VS-calibration has been finished (see e.g Flesch and Kernbichler [88.4]).

The VS-calibrated model should be used for reanalysis of the safety of the structure if the model has been changed significantly. Further, as a by-product the results from the VS-calibration can be used in the design of subsequent structures of similar type. For

instance, this may be of great importance in connection with offshore platforms where the safety is very dependent on e.g. the damping (see figure 7.1).

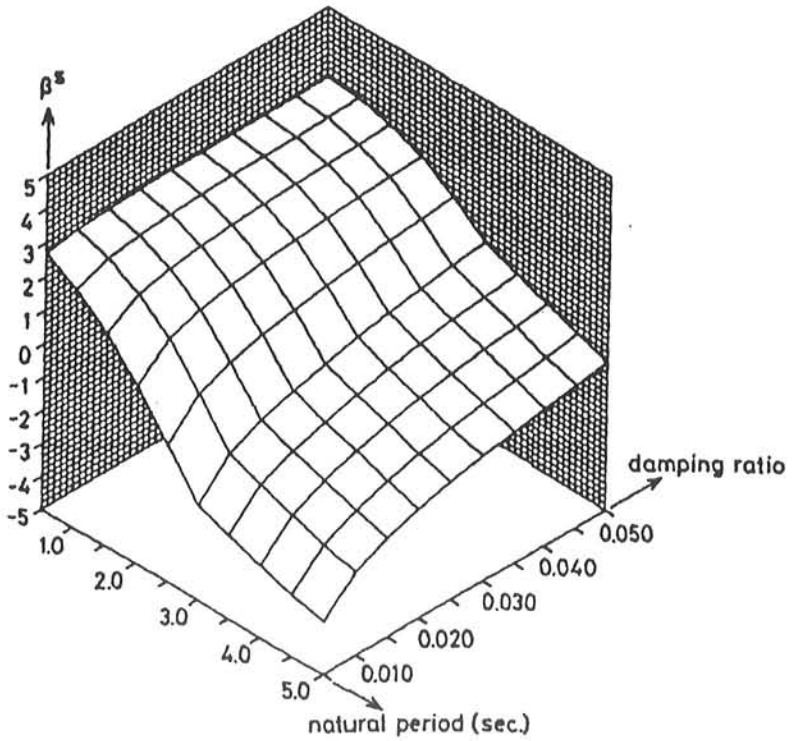

Figure 7.1. Sensitivity of the reliability index of a Mono-tower platform to variations of the natural period and modal damping ratio (Kirkegaard et al. [91.19]).

CHAPTER 8
LEVEL 2 AND 3 VBI-METHODS

A diagnosis of the state of damage has to be given if any significant changes in the dynamic characteristics are revealed during a periodic measurement in a VBI-programme. This diagnostic problem can in general be written as shown in equation (3.1)

$$\boldsymbol{D}=F(\boldsymbol{R}) \tag{3.1}$$

$\boldsymbol{D}$ is a damage vector, which for instance contains information about the size and location of a crack. The vector $\boldsymbol{R}$ contains information about the actual damage indicators (see chapter 5). Thus, the main task in the development of a damage diagnostic scheme based upon results from vibration measurements is to develop an expression for the function $F(\boldsymbol{R})$, which gives an unambiguous $\boldsymbol{D}$ for a given $\boldsymbol{R}$.

The size of the vector $\boldsymbol{D}$ is of course unknown in a practical problem and can in principle be infinite, whereas the number of elements in the vector $\boldsymbol{R}$ will normally be limited by the measurement system in use. Furthermore, the elements in $\boldsymbol{R}$ will be defective due to different factors such as the signal-to-noise ratio and the length of the records. These problems imply that a given $\boldsymbol{R}$ might lead to multiple solutions of equation (3.1). For instance, a crack in a structure is defined by its size and location, thus $\boldsymbol{D}$ contains two elements for each crack. Therefore, it is obvious that $\boldsymbol{R}$ should contain at least two elements for each crack to be revealed. However, the required number of elements in $\boldsymbol{R}$ will in many cases be increased for symmetry reasons.

The problem becomes even more complicated, when the dynamic characteristics are influenced by non-damage depending time-varying factors such as for instance changes in the mass. One way to tackle this problem is to incorporate these factors in $\boldsymbol{D}$.

In a number of studies (see e.g. Wendtland [72.1], Gudmundson [82.4], Stubbs and Osegueda [85.3], Shen and Pierre [90.17] and Joshi and Madhusudhan [91.5]) dynamic characteristics like natural frequencies and mode shapes are used as the basis for damage detection. However, a common feature of these studies is that they mostly concern

analysis and determination of the behaviour of damaged structures given $\boldsymbol{D}$. Thus, in the developed methods the function $F(\boldsymbol{R})$ has been found by solving equation (3.2).

$$\boldsymbol{R}=F^{-1}(\boldsymbol{D}) \tag{3.2}$$

A great number of damage detection methods based on the solution of equation (3.2) has been proposed in the literature while only a limited number of methods based on equation (3.1) has been proposed. The aim of this chapter is to present and evaluate a number of both kinds of methods. Some of the methods presented in this chapter have been used subsequently to their presentation with or without a reference to the originator(s). Reference to these papers is only given if they include improvements or test of applicability to real structures.

Some simple level 2 methods have already been presented in chapter 5 *Damage Indicators* since the use of some DIs gives a rough estimate of the location of the damage. These methods are not included in the present chapter.

Only non-propagating cracks are considered since crack growth during the measuring will indicate a collapse soon. Therefore, such cracks should have been detected at an earlier stage.

8.1 FOX'S METHODS

Fox [92.4] suggests two relatively simple level 2 methods which are based solely on measured natural frequencies and mode shapes.

In the first method the possible damage positions are located by looking for points on the structure where the nodes of relatively unaffected modes ($\sim$ relatively small changes in the natural frequency) are close to antinodes of relatively heavily affected modes. The changes in natural frequencies are used to graduate the level of affection for the different modes.

Plots of the absolute and the relative changes in mode shapes of heavily affected modes are used to locate damage in the second method presented in Fox [92.4]. The relative change in mode shapes $RD(z)$ is defined as

$$RD_i(z) = \frac{\phi_i^u(z) - \phi_i^d(z)}{\phi_i^u(z)} \tag{8.1}$$

where $\phi_i^u(z)$ and $\phi_i^d(z)$ are the ith mode shape functions in the undamaged and the damaged case, respectively. The locations with relatively big differences and/or relatively large $RD(z)$ are taken as potential damage locations. Further, the affection of the corresponding natural frequencies should be used to make a list of priority in cases with more than one potential damage locations. The results from the test series B (a = 0.02 m) and C (a = 0.03 m) for beam B5 have been used to test the applicability of the method (see figure 8.1).

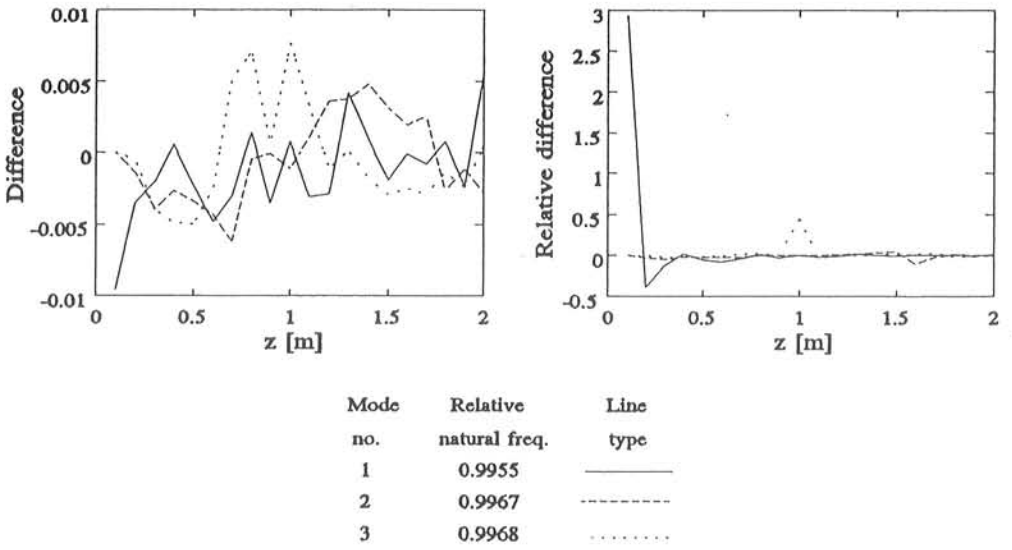

Mode no.	Relative natural freq.	Line type
1	0.9955	———
2	0.9967	- - - - -
3	0.9968	.....

Figure 8.1 Results from a test of Fox's second method.

The plots of the absolute differences between the mode shapes do not point out any locations as more potential as damage location than other locations. However, the plots of the $RD(z)$ give the real damage location z = 0.1 as the most potential damage location. It very interesting to notice that the method gives the correct location even though the corresponding relative changes in natural frequencies are below 0.5 ‰.

Fox [92.4] points out that the method works well in the cases of simple structures, but it might be less straightforward to apply the method to a more complex structure.

8.2 NOMOGRAMS

The results from sensitivity analysis (see section 6.2) or similar data for relatively simple structures, such as beams and frames, can in some cases be used to establish different kinds of nomograms. For instance, such nomograms have been used in connection with VBI of offshore structures (see e.g. Chondros and Dimarogonas [80.4] and Coppolino and Rubin [80.6]), bridges (see e.g. Flesch and Kernbichler [88.4]) and vessels (see Hochrein and Yeager [78.1]). The nomograms may be used to make rough estimates of the damage location and size or to give an alarm.

Normally, FEAs will be used to establish the graphs because analytical solutions will be too troublesome to use. For instance, the inclusion of the three accelerometer masses and a crack will increase the size of the matrix in the frequency equation for the beams in experimental case no. 1 from 4x4 to 16x16. Further, three different frequency equations must be established to take the position of the crack with respect to the accelerometer locations into account.

However, analytically solutions have been presented and used. For instance, Gudmundson [82.4] presents an analytical obtained expression for a function relating the size and location of a crack in a cantilever with a constant rectangular cross-section to the natural frequencies of the beam.

Ju et al. [82.5] use the fracture mechanical model (see section 4.1.3) to include the effect of a crack in the frequency equation of beams and frames. The solutions to the frequency equation for different crack sizes and locations are used to establish nomograms for the structure. The applicability of the method was demonstrated in Ju and Mimovich [87.11] where the method was used for experimental diagnosis of fracture damage in some aluminum cantilevers containing saw cuts. However, the method fails when there is more than one crack in the structure (see Ju and Akgun [86.1]).

A common feature in the above-mentioned references is that the used graphs only include information about natural frequencies. However, only a limited number of natural frequencies will normally be estimated in connection with a periodical measurement. Therefore, there may be more than one admissible solution. In such cases Ju et al. [82.5] suggest that the moment distribution of the mode showing the greatest variation in natural frequency should be used as a guide for the probability of the different solutions. Further, it should be noticed that nomograms will normally only be reliable for detection of one damage as e.g. a crack in a steel structure.

Figure 8.2 shows an example of a nomogram for the beam in experimental case no. 1, established from the variations of the three lower natural frequencies, which were found in example 6.3.

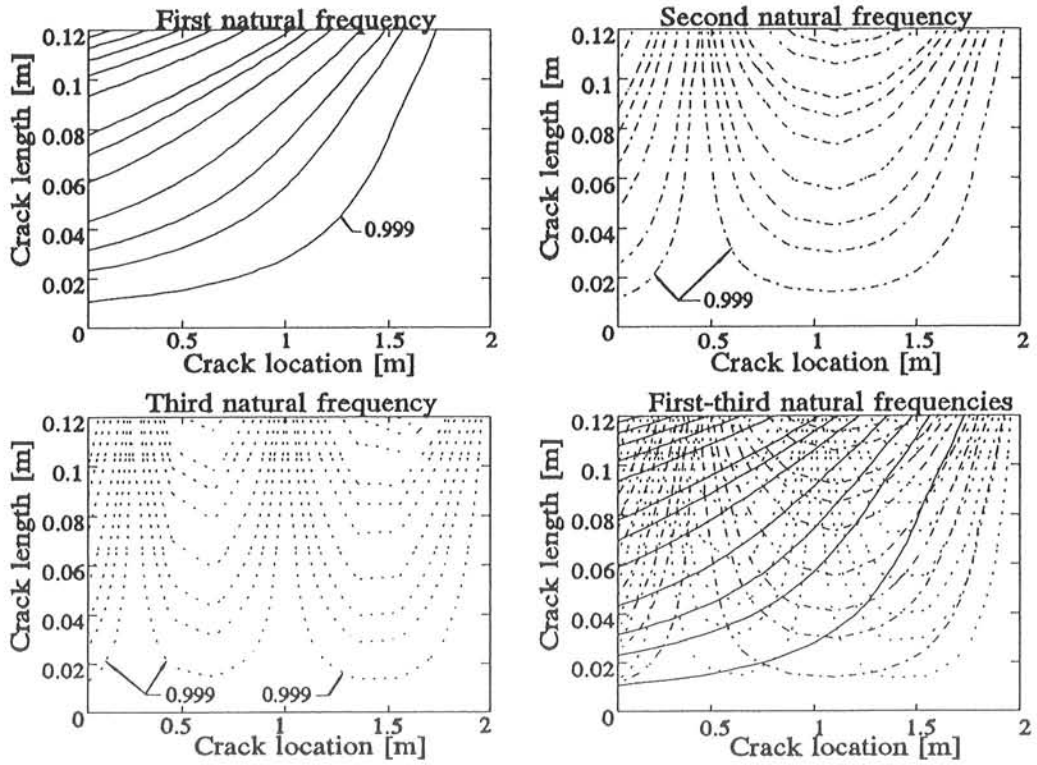

Figure 8.2 Nomogram for the beam of experimental case no. 1. The lines represent the following relative changes in natural frequencies f_d/f_u ϵ (0.71,0.76,0.81, 0.86,0.92,0.96 0.98 0.99 0.995,0.999).

8.3 THE DYNAMIC RESPONSE METHOD

Akgun and Ju [86.1] presented a diagnosis method which utilizes the dynamic response changes at several locations, called the response stations, on the structure. The method is based on the relative transmissibility R_T, which was defined in equation (5.13), in section 5.5.

R_T is a function of the excitation location and frequency, the location of the response station, the crack location and severity and the structural parameters. Further, an increase in the number of response stations will cause an increase in the efficiency of the damage diagnosis method with respect to determination of the exact location and the

extent of the damage. However, from a practical point of view it is desirable to use a minimum number of response stations. Thus, an optimal choice of these parameters will increase the possibility of a successfull damage detection.

Ju and Akgun [86.1] have performed extensive sensitivity studies on a frame structure to obtain rules of thumbs for the optimal choice of the parameter values. These sensitivity analyses showed: a) the excitation frequency should be close to one of the natural frequencies, b) the probability of detection increases if R_T from more than one natural frequencies are used, c) the best results are obtained when the excitation is attached to the structure on a column in the vicinity of a joint, d) response stations should be placed close to PNPs on the girders, e) the probability of detection is highest for cracks near joints and f) the most significant R_T-values are usually observed at response stations in the neighbourhood.

Ju and Akgun point out that conclusion e) is especially encouraging in the light of the fact that structures such as offshore platforms usually fail at the foundation or develop cracks in the welded joints.

Based on their experiences from the sensitivity studies Ju and Akgun set up a procedure for the introductory analysis of a VBI-programme based on the use of R_T. Firstly, R_T at each temporary measurement stations should be found through a numerical analysis, as e.g. an FEA, for varying location of a well-defined damage. The results from the first analysis should then be used to choose optimal values of the above-mentioned variables. Finally, the numerical analysis should be repeated and maps of influence regions for each measurement station should be established. The latter is defined as the region in which the presence of damage affects the R_T of the respective station the most.

8.4 FLEXIBILITY MONITORING

In 1983 Rubin and Coppolino [83.4] presented the flexibility monitoring method (in brief the FM-method) to detect potential damage in offshore jacket platforms. The method is a level 2 method which utilizes changes in the deflection shapes of the three fundamental vibration modes (two sway and one torsional).

A typical steel jacket acts as a shear beam in the lower modes. Therefore, a damage in a diagonal member will cause a discontinuity in the deflection shapes of the mode shapes. However, it might be difficult to see these discontinuities from measured mode

shapes. Rubin and Coppolino avoid this problem by using a relative flexibility parameter for each jacket framing bay for diagnosis of the potential damage. The relative flexibility parameters are taken as the average horizontal deflection across each bay normalized to the corresponding deflection of the top bay. Thus, the flexibility parameter Δ_i of bay i is given as

$$\Delta_i = \frac{\bar{x}_i - \bar{x}_{i+1}}{\bar{x}_0 - \bar{x}_1} \tag{8.2}$$

where $\bar{x}_0$, $\bar{x}_1$, $\bar{x}_i$ and $\bar{x}_{i+1}$ are the average deflection at level *0*, *1*, *i* and *i+1*, respectively (see figure 8.3).

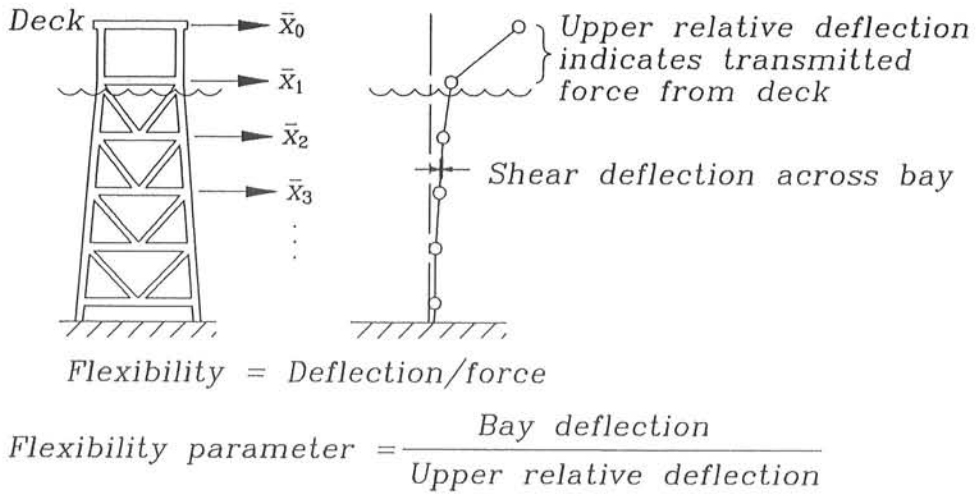

Figure 8.3 Conceptual basis for Flexibility Monitoring (Rubin and Coppolino [83.4]).

The change in Δ for a damaged bay will be significantly bigger than the corresponding changes of Δ for other bays.

The main part of the mass will be concentrated at the deck. This mass will, as mentioned in section 6.1, often vary with time. However, the fundamental mode shapes are approximately equivalent to the static deflection shapes due to the actual deck mass. Therefore, a change in the deck mass will approximately correspond to multiplication of the mode shapes by a proportionality factor. Thus, variations in deck mass should only cause very small variations in the flexibility parameters.

Sunder and Ting [85.4] have verified this non-mass dependence through sensitivity studies on a four-leg, X-braced production platform with a height of 45 m divided into four bays. For this platform a 10 % increase of the deck mass causes changes in the

flexibility factors on the order of 1 %. Further, Sunder and Ting found that the FM-method is able to distinguish structural damage from changes in the foundation stiffness.

As can be seen from the above-mentioned features the FM-method has several advantages. However, the sensitivity studies performed by Sunder and Ting revealed that the flexibility ratios are quite sensitive to random and bias errors in the estimated mode shapes ordinates. Further, often measuring of mode shapes will , as mentioned in section 5.2, be troublesome and time-consuming. These two facts are the main disadvantages of the FM-method.

8.5 STRUCTURAL DYNAMIC MODIFICATION (SDM)

The standard programme packages for experimental modal analysis, as e.g. STAR*Struct* Modal Analysis Programme Package from SMS [89.1], have a structural dynamic modification (in brief SDM) post processor programme. In the SDM-part the user can perform structural modifications, as e.g. adding of stiffness and mass to the structure, on an SDM-model and study their effects in the modal parameters. This facility has been used by many people in connection with VBI (see e.g. Flesch [90.2], Aagaardh [90.6] and Richardson and Mannan [92.5]).

The equation of motion of a modified linear and viscous damped structure in free vibrations can be written as

$$(M+\Delta M)\ddot{x}+(C+\Delta C)\dot{x}+(K+\Delta K)x = 0 \qquad (8.3)$$

where M is the mass matrix of the original system, C is the damping matrix of the original system, K is the stiffness matrix of the original system, ΔM is the additional mass matrix, ΔC is the additional damping matrix and ΔK is the additional stiffness matrix.

In the SDM-routine equation (8.3) is transformed into modal coordinates (see equation (8.4)) by using the measured mode shape matrix Φ .

$$M_m \ddot{q} + C_m \dot{q} + K_m q = 0$$

where

$$\begin{aligned} M_m &= I + \Phi^T \Delta M \Phi \\ C_m &= \lceil 2\zeta_{i,u}\omega_{i,u} \rfloor + \Phi^T \Delta C \Phi \\ K_m &= \lceil \omega_{i,u}^2 \rfloor + \Phi^T \Delta K \Phi \end{aligned} \tag{8.4}$$

where I is a unit matrix, $\lceil\ \rfloor$ denotes a diagonal matrix, $\zeta_{i,u}$ is the modal damping ratio of the ith mode of the original structure and $\omega_{i,u}$ is the ith cyclic natural frequency for the original structure.

Equation (8.4) shows that M_m, C_m and K_m only depend on the user-defined modifications and measured modal parameters of the original structure. The modal parameters of the modified structure can simply be calculated by solving the eigenvalue problem of equation (8.4). Thus, a VS-calibration of M, C and K is not necessary. This is one of the major advantages of using SDM-models in connection with the performance of a VBI-programme. The high degree of user-friendliness is another factor which makes the SDM-model attractive.

Calibration of SDM-models might be used as either a level 2 or level 3 method depending on the model for the actual damage how well it is defined and how easily it can be implemented in the standard programmes. The VS-measurements are used to create an SDM-model which is subsequently modified until a satisfactory agreement between the modal parameter of the modified structure and the modal parameters from the periodical measurement is obtained. Thus, the diagnostic session should be performed more or less manually. This may lead to a troublesome and time-consuming diagnostic session if the potential damage scenarios are in large numbers or if they are not defined well.

The structure is assumed to be linear and viscous damped when one is using an SDM-model. However, often these requests will not be fulfilled completely for a damaged structure (see e.g. section 4.1.5). Therefore, when SDM-models are used in connection with VBI great attention should be given to those DIs (see e.g. section 5.7-5.10) which can reveal such non-linearities.

8.6 CHANGES IN MODEL MATRIX METHODS

The introduction of damage in a structure will be reflected as changes in some of the elements in the model matrices, as e.g. the stiffness matrix. Therefore, comparison of the matrices estimated at the VS-measurements and the corresponding estimates obtained after a periodical measurement could lead to the localization of the damage(s), i.e. as a level 2 method.

Proper estimates for the model matrices are essential for obtaining reliable estimates for damage locations. These estimates might be obtained by means of the methods applicable to VS-calibration of model matrices which were mentioned in chapter 7. Thus, the problems caused by a limited number of sensors, noise on measurements etc., which were mentioned in chapter 7, are also present when one of these methods is used in connection with a diagnostic session.

Different approaches for the performance of such comparisons of model matrices have been suggested in the literature. A short review of the basic ideas in a number of different approaches will be given in the following.

An evaluation of the elements in the error matrix E defined in equation (8.5) is the most straightforward way of comparing two stiffness matrices. However, the method may cause problems because the comparison is based on absolute values. Therefore, a damage which causes relatively large changes in small elements in K^u might be overlooked (see Park et al. [88.9]).

$$E = K^d - K^u \tag{8.5}$$

where K^u and K^d are the stiffness matrices for the undamaged and the damaged structure, respectively.

He and Ewins [86.5] have developed the formula for E given in equation (8.6), which could be advantageous to use if E is to locate damage.

$$E = K^u\left(\tilde{\Phi}^u \left\lceil(\tilde{\lambda}_i^u M_i)^{-1}\right\rfloor \tilde{\Phi}^{u\,T} - \tilde{\Phi}^d \left\lceil(\tilde{\lambda}_i^d M_i)^{-1}\right\rfloor \tilde{\Phi}^{d\,T}\right)K^u \tag{8.6}$$

where $\tilde{\Phi}^u$ and $\tilde{\Phi}^d$ are the measured modal matrices, $\tilde{\lambda}_i^u$ and $\tilde{\lambda}_i^d$ are the measured ith eigenvalues for the undamaged and the damaged structure, respectively, and M_i is the ith modal mass of the undamaged structure.

Park et al. [88.9] use an FEM to assemble $\boldsymbol{K}^u$ in their test of the applicability of $\boldsymbol{E}$ given by equation (8.6) for detection of damage in a beam structure and a plate structure. Park et al. found it was difficult to distinguish damage induced changes from changes due to the inevitable measurement errors by looking on the elements in $\boldsymbol{E}$. To avoid this problem they suggested a weighting technique which magnified the amount of stiffness error only in certain nodal points related to the damaged element. Park et al. make use of the following ratio in their weighting technique

$$a_{ij} = \frac{\Delta f_i^m}{\Delta f_{i,j}^c} \quad ; \quad i = 1, N_f \; ; \; j = 1, N_E \tag{8.7}$$

where $\Delta \tilde{f}_i^m$ is the measured change in the ith natural frequency, $\Delta f_{i,j}^c$ is the calculated change in ith natural frequency given damage in element j, N_f is the number of measured natural frequencies and N_E is the number of elements in the FEM. Park et al. use the algorithm presented by Fox and Kapoor [68.1] to calculate Δf_i^c. The weighted error matrix $\boldsymbol{W}$ is obtained from $\boldsymbol{E}$ by multiplying the inverse of the variance $(1/\sigma_j^2)$ to the related rows and columns of $\boldsymbol{E}$. Park et al. obtained more distinct indication of potential damage locations in their two test structures by using $\boldsymbol{W}$ instead of $\boldsymbol{E}$.

Agbabian et al. [88.7] proposed the ratios r_{ij} and d_{ij} given by equation (8.8) and (8.9) for estimating the location of damages in a structure form measured changes in the stiffness matrix.

$$r_{ij} = \frac{\tilde{k}_{ij}^d - \tilde{k}_{ij}^u}{\tilde{k}_{ij}^u} \tag{8.8}$$

$$d_{ij} = \frac{\tilde{k}_{ij}^d - \tilde{k}_{ij}^u}{\tilde{\sigma}_{ij}^u} \tag{8.9}$$

where $\tilde{k}_{ij}$ is a measured estimate for the (i,j) element of the stiffness matrix and $\tilde{\sigma}_{ij}$ is the standard deviation of $\tilde{k}_{ij}$. Agbabian et al. use a time domain SI-method giving an ensemble for $\boldsymbol{K}$ after each measurement which makes it possible to calculate $\tilde{\sigma}_{ij}$. The applicability of r_{ij} and d_{ij} for detection damages was tested by Agbabian et al. on a relatively simple 3 DOF system for three different damage cases only. Apparently the best results are obtained when the damage is located in an element which is connected to one of the DOFs only. However, the introduction of statistical uncertainties on $\tilde{k}_{ij}$ make the methods attractive for further development.

Tsai and Yang [85.8] use plots of the following flexibility ratios α_{ij} and mass ratios μ_{ij} to locate damage in a cantilever :

$$\alpha_{ij} = \frac{a_{ij}^{d}}{a_{ij}^{u}} \quad ; \quad \mu_{ij} = \frac{m_{ij}^{d}}{m_{ij}^{u}} \tag{8.10}$$

where a_{ij} and m_{ij} are the (i,j) elements of the flexibility matrix and the mass matrix, respectively. The test with the damaged cantilever showed that plots of both ratios were applicable to identification of the location of damage. Further, it was seen that μ_{ij} is more sensitive than α_{ij}. Similar conclusions were made by Tsai et al. [88.17] in their tests of the applicability of the method in connection with detection of damage in a model of an offshore platform.

Smith and Hendricks [87.12] use the flexibility ratios α_{ij} given in equation (8.10) to locate damage in space trusses. They obtain their estimates K by using the procedure presented by Kabe [85.11] for optimal adjustment of deficient stiffness matrices. Smith and Hendricks [87.12] found that the applicability of α_{ij} for identifying the location of damages decreases as the number of DOF increases.

The introduction of cracks in a linear structure, as e.g. a steel structure, might cause a certain degree of local non-linearity in the structure (see section 4.1.5). Tanrikulu and Özgüven [91.3] presented an SI-method for identification of such localized non-linearities. The locations of the non-linearities can be estimated by means of equation (8.11) if the response of the structure to a harmonic external force has been measured.

$$G = F_o - \alpha^{-1} X \tag{8.11}$$

where G is the complex amplitude vector of the internal non-linear forces at the excitation frequency, F_o is the amplitude vector of the harmonic external forcing, α is the receptance matrix of the linear part of the structure and X is the complex amplitude vector of the steady-state displacement. Tanrikulu and Özgüven suggest that α should be found through a low level sine-wave testing of the structure.

A common feature of the methods presented in this section is that they are level 2 methods.

8.7 STUBBS AND OSEGUEDA

In 1985 Stubbs and Osegueda [85.3] (see also Stubbs [85.12]) presented a method (in brief the SO-method) for location and quantification of damages in such structural elements as beams, plates and shells. Thus, at first sight the SO-method might be considered as a level 3 method. However, the output is given as fractional changes in a typical stiffness parameter, typically the moment of inertia for the elements or groups of elements. This kind of model corresponds to the smeared model described in section 4.1.2 which gives a poor description of a cracked beam (see e.g. figure 4.7). Therefore, the application of the method on structures containing fatigue cracks would rather be at level 2 than 3.

The SO-method was developed for linear proportionally damped structures. The basic formulas and ideas in the method will be summarized in the following.

By using the perturbation of the original equation of motion given in equation (8.3) and negligence of small terms it can be shown that (see e.g. Stubbs and Osegueda [85.3])

$$\frac{\Delta \omega_{id}}{\omega_{id}} = \frac{\Delta K_i}{K_i} - \frac{\Delta M_i}{M_i} + \frac{\Delta \zeta_i^2}{1-\zeta_i^2} \tag{8.12}$$

where ω_{id} is the ith damped cyclic natural frequency, K_i is the ith modal stiffness, M_i is the ith modal mass, ζ_i is the ith modal damping ratio and Δ denotes change in the respective parameters due to the introduction of the damage. Equation (8.12) is the basis of the SO-method.

The sensitivities for the entire structure might then be assembled in the following equation

$$\begin{bmatrix} \frac{\Delta\omega_{1d}}{\omega_{1d}} \\ \cdot \\ \cdot \\ \frac{\Delta\omega_{id}}{\omega_{id}} \\ \cdot \\ \cdot \\ \frac{\Delta\omega_{Nd}}{\omega_{Nd}} \end{bmatrix} = \begin{bmatrix} \frac{\Delta K_1}{K_1} \\ \cdot \\ \cdot \\ \frac{\Delta K_i}{K_i} \\ \cdot \\ \cdot \\ \frac{\Delta K_N}{K_N} \end{bmatrix} - \begin{bmatrix} \frac{\Delta M_1}{M_1} \\ \cdot \\ \cdot \\ \frac{\Delta M_i}{M_i} \\ \cdot \\ \cdot \\ \frac{\Delta M_N}{M_N} \end{bmatrix} + \begin{bmatrix} \frac{\Delta\zeta_1^2}{1-\zeta_1^2} \\ \cdot \\ \cdot \\ \frac{\Delta\zeta_i^2}{1-\zeta_i^2} \\ \cdot \\ \cdot \\ \frac{\Delta\zeta_N^2}{1-\zeta_N^2} \end{bmatrix} \tag{8.13}$$

$$\Leftrightarrow \mathbf{Z}_d = \mathbf{Z}_{stiff} - \mathbf{Z}_{mass} + \mathbf{Z}_{damp}$$

where N is the number of degrees of freedom in the model of the structure, $\mathbf{Z}_d, \mathbf{Z}_{stiff}, \mathbf{Z}_{mass}$ and $\mathbf{Z}_{damp}$ are $Nx1$ vectors containing the measured changes in the natural frequencies, contributions from changes in stiffness, mass and damping, respectively.

Next, let the original stiffness of the jth element be given by k_j and the change in stiffness of this element due to damage be given by Δk_j. A non-dimensional measure of stiffness change of the jth element is defined as $\alpha_j = \Delta k_j / k_j$. Using this notation it can be shown (see e.g. Stubbs and Osegueda [87.14]), that a first-order approximation $\mathbf{Z}_{stiff}$ of a structure consisting of N_E elements can be calculated from

$$\mathbf{Z}_{stiff} = \boldsymbol{F}\boldsymbol{A} \tag{8.14}$$

where $\boldsymbol{F}$ is an NxN_E sensitivity matrix and $\boldsymbol{A}$ is an $N_E x1$ including all the α_j-values. The matrix $\boldsymbol{F}$ depends on the topology of the structure, the stiffness of the elements and the modal matrix of the undamaged structure.

The coefficients of $\boldsymbol{F}$ may be determined numerically in four steps (see Stubbs and Osegueda [90.24]) : *1)* determine the natural frequencies of the undamaged structure; *2)* introduce a known magnitude of damage α_j in the jth element and calculate the natural

frequencies of the damaged structure; *3)* calculate the corresponding fractional changes in the modal stiffness $\mathbf{Z}_{stiff}$; *4)* finally, compute the elements of the *j*th column of $\boldsymbol{F}$ as $\mathbf{Z}_{stiff}/\alpha_j$.

Introducing equation (8.14) into the lower part of equation (8.13) and rearranging gives

$$\boldsymbol{FA} = \mathbf{Z}_d + \mathbf{Z}_{mass} - \mathbf{Z}_{damp} \tag{8.15}$$

Thus, the location and magnitude of damages might be found by solving equation (8.15) with respect to $\boldsymbol{A}$ if the parameters on the right-hand side are known. Stubbs and Osegueda (see e.g. Stubbs and Osegueda [90.25]) point out that these parameters can be estimated either through measurements or through numerical analysis.

Typically, the sensitivity matrix $\boldsymbol{F}$ will not be a square matrix because the number of degree of freedom N is not equal to the number of element N_E. Therefore, some kind of generalized inverse technique should be applied to solve (8.15). Stubbs and Osegueda suggest the following equation to obtain least squares estimates for $\boldsymbol{A}$

$$\hat{\boldsymbol{A}} = \left(\boldsymbol{F}^T\boldsymbol{F}\right)^{-1}\boldsymbol{F}^T\left(\mathbf{Z}_d + \mathbf{Z}_{mass} - \mathbf{Z}_{damp}\right) \tag{8.16}$$

Normally, the number of measured natural frequencies N_f will be considerably lower than N_E. This can imply numerical instability during the inversion of the $(\boldsymbol{F}^T\boldsymbol{F})$-matrix. Therefore, Stubbs and Osegueda [90.24] propose that an iterative procedure should be used to evaluate the damage. In each iteration the number of potential damage locations is restricted to be around N_f and the area of the potential damage location is very wide during the first iterations and then subsequently reduced. Areas having positive α-values are neglected and the remaining areas are subdivided into the next iteration.

The SO-method was successfully tested on different types of structures, as e.g. an offshore platform (see Stubbs and Osegueda [87.14]), composite structures (see Sanders et al. [89.2]) and space structures (see Stubbs et al. [90.26]), in the last part of the eighties. All the tests showed that the applicability decreases when the number of damages increases.

Further, the influence of the uncertainties in material properties and dynamic measurements of the predicted damage were addressed in Stubbs [85.12]. Stubbs et al. [91.11] study the effect of model uncertainties.

However, all these tests and analyses were all based on simulated data. Not until 1990 an experimental verification of the method was performed through tests on a cantilever

(see Stubbs and Osegueda [90.24]). All damage cases were correctly predicted during the tests. Further, the correct order of magnitude was always predicted. Thus, Stubbs and Osegueda [90.25] concluded that the performed experiment strongly supports the SO-method. However, the latter was expectable when considering the kind of damage used in the tests (see figure 8.4).

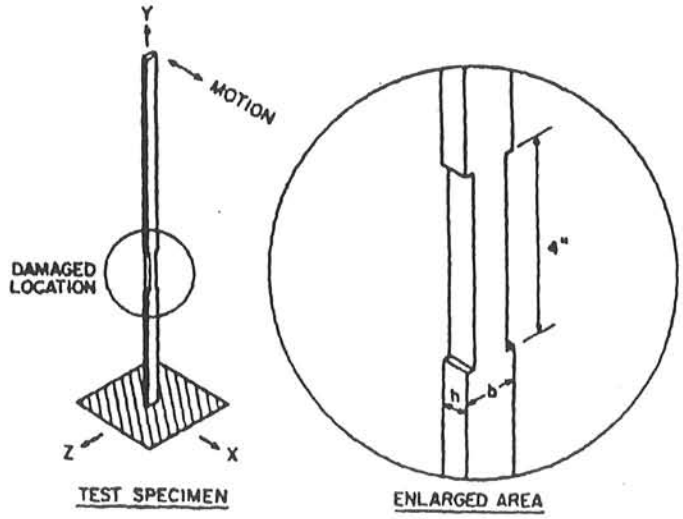

Figure 8.4 Configuration of damage used in the experimental tests performed by Stubbs and Osegueda (Stubbs and Osegueda [90.26]).

The applicability of the method in connection with the beams used in the experimental case no. 1 is tested in example 8.1.

Example 8.1

The aim of this example is to test the applicability of the SO-method in connection with detection of fatigue cracks. The experimentally obtained estimates for the three lower natural frequencies of beam B3 in experimental case no. 1 for the uncracked case and for a crack length of $a = 0.06$ m are used. The corresponding decrease in the bending moment of inertia is $\alpha \approx 0.37$ according to figure 4.4.

The VS-calibrated versions of the FEM shown in figure 6.3 were used in the FEA. The crack was located at $z = 1$m corresponding to the midspan of element 11. During the calculations of F α_j was set to 0.25 in the jth potential area of damage by reducing the bending moment of inertia of the beams in this area.

The iterative procedure proposed by Stubbs and Osegueda [90.24] has been used. Two different approaches for the subdivision of the potential damage areas in the third and fourth iterations have been used. The beams was equally divided at the start of the two approaches. The results are shown in figure 8.5 and figure 8.6.

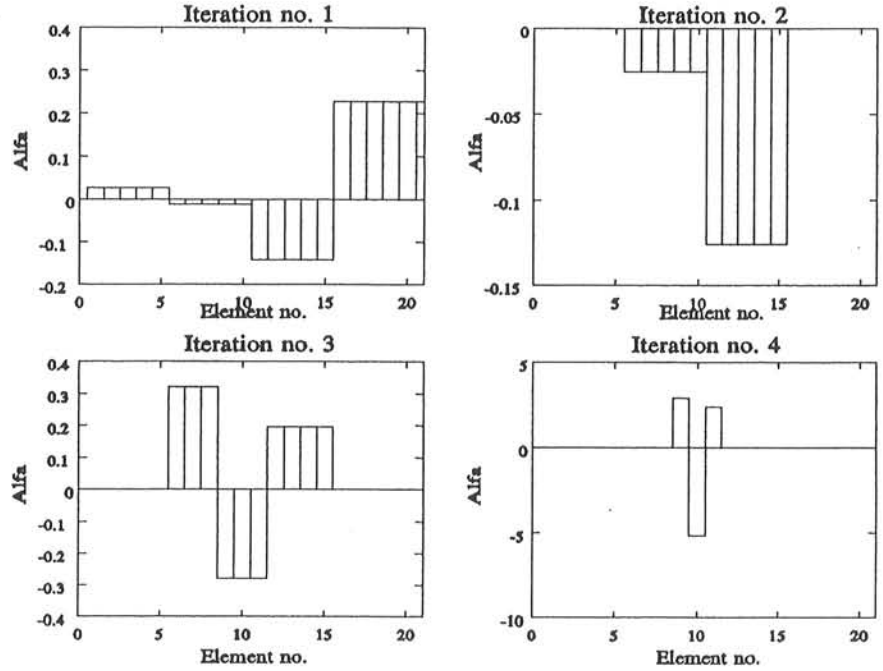

Figure 8.5 Results from test of the SO-method, iteration approach no. 1.

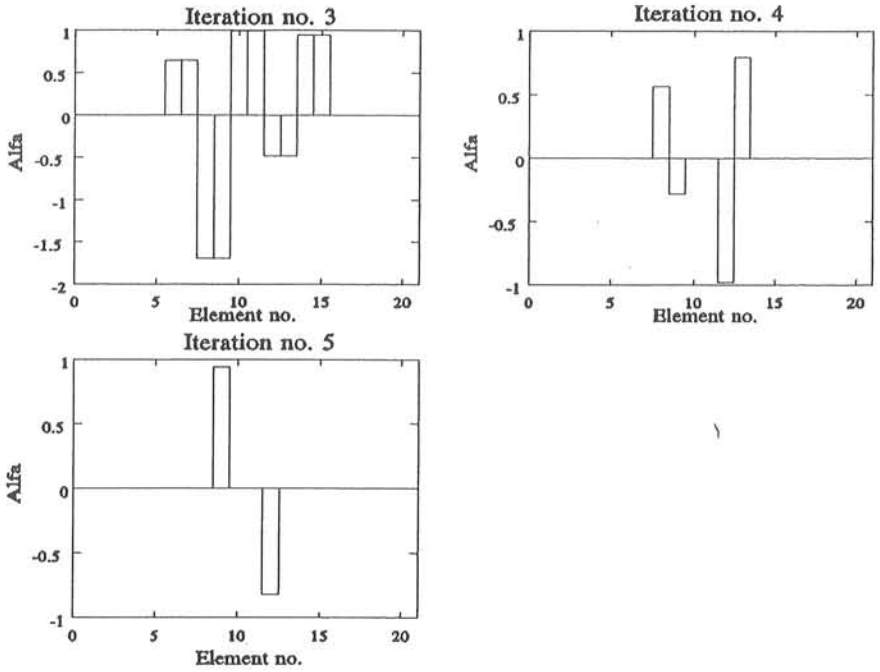

Figure 8.6 Results from test of the SO-method, iteration approach no. 2.

The two approaches gave element no. 10 and element no. 12 as potential damage location instead of the correct element no. 11. Further, the estimates for α of the potential damage location differs considerably from the actual value. Thus, it might be concluded that the application of the SO-method in connection with the beams should be restricted to a level 2 method.

The results from example 8.1 showed that apparently the SO-method might be used as a level 2 method only when dealing with structures containing fatigue cracks. Further,

the example revealed that the outcome of the iterative procedure is highly dependent on the subdivision of the potential areas of damage.

8.8 THE CAWLEY AND ADAMS METHOD (THE CA-METHOD)

Cawley and Adams [79.1] present a level 2 method (abbreviated the CA-method) for estimating the location of defects in structures from measurements of changes in the natural frequencies. The basic formulas and ideas in the CA-method will be summarized in the following.

The change Δf_i in f_i due to a localized damage is a function of the position vector r of the damage and the reduction in stiffness ΔK caused by the damage. Thus

$$\Delta f_i = g_i(\Delta K, r) \tag{8.17}$$

A first order expansion of the function g_i about the undamaged state gives

$$\Delta f_i = \Delta K \frac{\partial g_i}{\partial(\Delta K)}(0, r) \tag{8.18}$$

since $g_i(0,r) \equiv 0$ for all r. A similar expression is valid for Δf_j. Thus, provided that the changes in stiffness ΔK are independent of frequency, then

$$\frac{\Delta f_i}{\Delta f_j} = \frac{\Delta K \dfrac{\partial g_i}{\partial(\Delta K)}(0, r)}{\Delta K \dfrac{\partial g_j}{\partial(\Delta K)}(0, r)} = h_{ij}(r) \tag{8.19}$$

This means that the ratio of frequency changes in two modes is a function of the location of the damage only. Equation (8.19) is the cornerstone in the CA-method.

The first step in the CA-method is to perform an FE-calculation of the changes in the natural frequencies due to damage at a series of points successively. The change of f_i to a certain damage state at position r is denoted Δf_{ri}^{C}.

Cawley and Adams [79.1] define the error of assuming the damage to be located at position r, given measured changes Δf_i^M and Δf_j^M in mode i and j, respectively, as

$$\left.\begin{aligned} e_{rij} &= \frac{\Delta f_{ri}^C / \Delta f_{rj}^C}{\Delta f_i^M / \Delta f_j^M} - 1, \qquad \frac{\Delta f_{ri}^C}{\Delta f_{rj}^C} \geq \frac{\Delta f_i^M}{\Delta f_j^M} \\ e_{rij} &= \frac{\Delta f_i^M / \Delta f_j^M}{\Delta f_{ri}^C / \Delta f_{rj}^C} - 1, \qquad \frac{\Delta f_{ri}^C}{\Delta f_{rj}^C} < \frac{\Delta f_i^M}{\Delta f_j^M} \end{aligned}\right\} \tag{8.20}$$

Thus the total error e_r in assuming the damage to be positioned at r may then be calculated as

$$e_r = \sum_{i=1}^{N_f} \sum_{j=1}^{N_f} e_{rij} W_{rij} \tag{8.21}$$

where N_f is the number of measured natural frequencies and W_{rij} is a weighting factor. Cawley and Adams recommend W_{rij} to be used in cases where the change in stiffness at the damage position is anisotropic as e.g. at a crack in a plate (see figure 8.7).

In general high significance should be attached to modes in which the direction of the stress vectors at the point of interest are similar and less significance to modes in which there are low similarity at the point of interest. Thus W_{rij} may be taken as

$$W_{rij} = \left| \frac{\sigma_{ri} \cdot \sigma_{rj}}{|\sigma_{ri}| \; |\sigma_{rj}|} \right| \tag{8.22}$$

where σ_{ri} and σ_{rj} are the stress vectors at position r of mode i and j, respectively.

The total errors calculated by means of equation (8.21) are normalized with respect to the minimum of the total errors e_{min}, i.e.

$$E_r = \frac{100\, e_{min}}{e_r} \tag{8.23}$$

The most probable damage position(-s) is/are that/those where $E_r = 100$.

The necessary number of points, where damage has to be assumed in the FEA will vary from structure to structure. Optimally, the series of points should be a mixture of an overall grid and hot spots known from the sensitivity analysis.

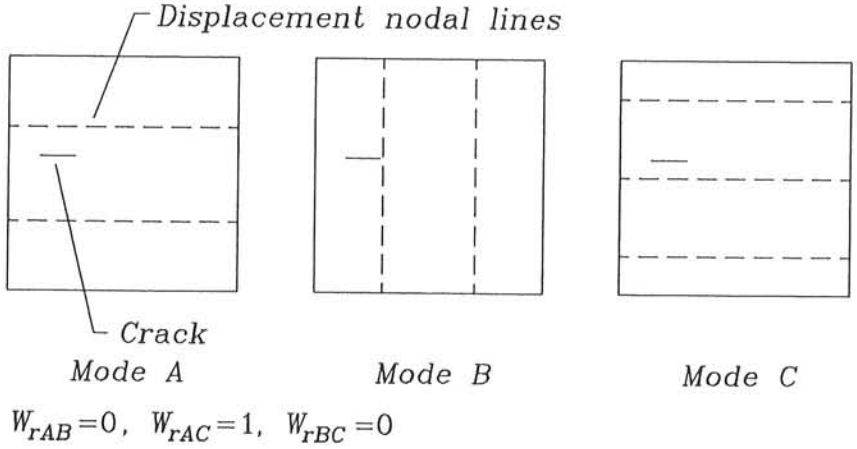

Figure 8.7 Weighting factors for a free-free plate (Cawley and Adams [79.1]).

In principle the CA-method gives information about the location of the damage only. However, Cawley and Adams [79.1] point out that a comparison of the changes in natural frequencies obtained from measurements and FEA , respectively, can be used to give a rough indication of the magnitude of the damage.

The number of probable damage positions will exceed 1 when dealing with symmetric structures like e.g. a simply supported beam (see figure 8.8). In the case of a simply supported beam a certain state of damage will give rise to the same changes in the natural frequencies whether it is placed at $x = \alpha L$ or at $x = (1-\alpha)L$. However, this situation with multiple solutions might be avoided by disturbing the symmetry. For instance, this can be done by placing a lumped mass on the structures during the measurements (see figure 8.8).

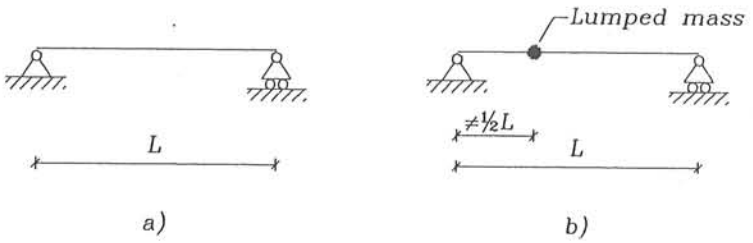

Figure 8.8 Simply supported beam. a) Normal situation, b) Measurement situation.

The CA-method was developed for detection of local damage in structures. However, the CA-method may also be used to detect a local change in mass δM since

$$\Delta f_i = g_i^M(\Delta M, r) \qquad (8.24)$$

Equation (8.24) is similar to equation (8.17) which confirms that the CA-method is applicable to detection of local changes in mass.

The applicability of the CA-method in connection with the two experimental cases is tested in the following two examples.

Example 8.2

The aim of this example is to test the usefulness of the CA-method in connection with experimental case no. 1.

The test is based on

- calculated changes in the three lower natural frequencies due to a crack of 0.06m placed at z_c = i*0,025m, i =1,80 , respectively
- measured changes in the three lower frequencies of beam B1-B3 and B5-B6

The VS-calibrated versions of the FEM shown in figure 6.3 were used in the FEA.

The errors given by equation (8.23) have been calculated for each of the test series with a crack in the five beams (see Rytter et al. [92.7]). The estimated crack locations z_c are shown in figure 8.9 as a function of the measured crack lengths.

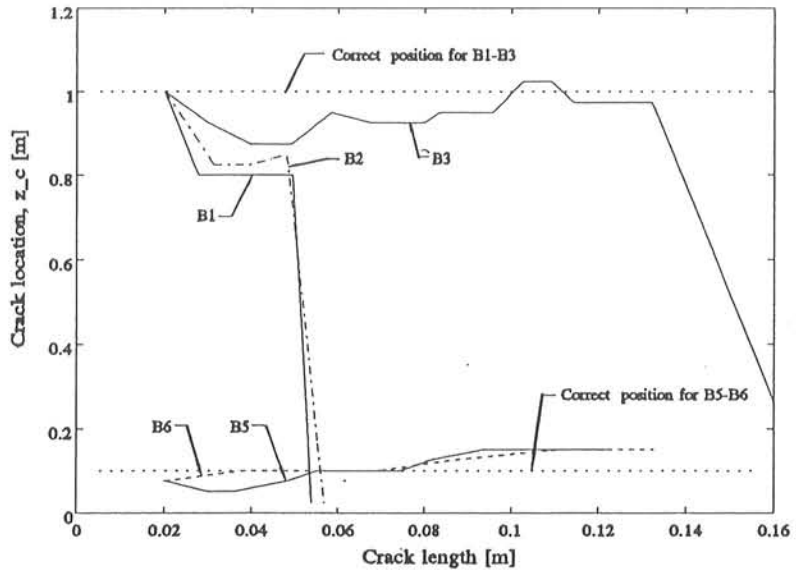

Figure 8.9 Estimated crack locations, experimental case no. 1.

Unwanted fatigue cracks were, as mentioned in section 1.3.1, developed in the weld at the fixture of beam B1 and B2 during the tests. These cracks were much bigger than the cracks at z = 1.0 m and therefore became governing for the changes in the natural frequencies. This fact is clearly demonstrated by the graphs for B1 and B2 in figure 8.9 where the z = 0.025 m is pointed out as the most possible crack location in the end of the test series for the two beams.

The estimates for the location of the cracks in beam B3, B5 and B6, respectively, are reasonably correct for all crack lengths. Especially for B5 and B6 where the maximum difference is 0.05 m which corresponds to 2.5 % of the beam length.

Example 8.3

The aim of this example is to test the applicability of the CA-method in connection with detection of damage in the mast from experimental case no. 2.

The test is based on the results for damage state 0-8 (see table 6.1 and figure 6.2) which were considered in the sensitivity analysis and from field measurements with damage state 0 (intact structure), 1, 2, 5, 6 and 9. The latter corresponds to a 50 % reduction of the cross-sectional area of element AB101.

The six lower natural frequencies are used to calculate the errors given by equation (8.23). The results are shown in table 8.1 where the cells corresponding to the correct damage locations are shadded.

Possible damage location	Damage state				
	1	2	5	6	9
AB101	1.02	0.10	0.10	0.02	100
BC101	100	6.13	0.01	1.38	0.89
CD101	0.99	2.82	9.87	0.25	1.13
DA101	1.02	100	0.19	6.02	1.02
AB102	0.99	2.59	100	0.27	1.15
BC102	1.03	90.56	0.20	100	1.02
CD102	1.12	0.09	0.03	0.02	42.42
DA102	1.02	92.04	0.25	22.05	1.03

Table 8.1 Test of the CA-method, experimental case no. 2.

The results show that the damage in damages state 5, 6 and 9 was successfully located by the CA-method. However, the method failed to locate the damage in damage states 1 and 2 which corresponds to total collapse in one of the four lower diagonals. A poor modelling of the stiffness at the four support points of the mast is the most probable explanation to the bad results for the damage states 1 and 2. A comparison of the measured and calculated changes in natural frequencies shows that the decrease in especially the torsional natural frequencies is overestimated in the FEA. Apparently, this effect increases with the size of the damage since it has not affected the result for damage state 9.

The CA-method is developed to detect damage at one point only. The results for beams B1 and B2 (see figure 8.9) obtained in example 8.2 showed that the largest damage will be located in cases with damage at more than one point.

The results from example 8.3 revealed that the efficiency of the CA-method is highly dependent on the description of the structure by the analytical model in both the undamaged and the damaged situations. This confirms the statement in chapter 7 about the great importance of a proper VS-calibration.

8.9 PATTERN RECOGNITION

Yin et al. [92.2] present a level 2 method based on pattern recognition to diagnose the location of local damages as e.g. slots and cracks. The basic equations and ideas in this method will be summarized in the following. The basic equations of the method have some feature common with the CA-method presented in section 8.8.

It can be shown (see e.g. Yin et al. [92.2]), that the ratio of the changes $\Delta_{i,r}$ and $\Delta_{i+1,r}$ of *i*th and *(i+1)*th natural frequencies due to a local damage at position r is related to the curvature of the corresponding mode shape at r $\Phi_i''(r)$ in following way

$$\frac{\Delta_{i,r}}{\Delta_{(i+1),r}} = \frac{\Phi_i''(r)^2 f_{i+1}^2}{f_i^2 \Phi_{i+1}''(r)^2} = \frac{Z_i(r)}{Z_{i+1}(r)} \tag{8.25}$$

where f_i and f_{i+1} are the natural frequencies of the two modes.

The basic idea in the method suggested by Yin et al. is to compare the ratio on the left hand side of equation (8.25) obtained from measurements and the ratio on the right hand side of equation (8.25) for all possible damage positions obtained from FE-analysis performed on the intact structure. For simplifying and automation of this comparison Yin et al. introduced a pattern vector $\boldsymbol{\beta}$ given by equation (8.26) and a set of characteristic vectors $\boldsymbol{\alpha}_r$ given by equation (8.27).

$$\beta_i = \begin{cases} +1 & 0 < \dfrac{\Delta_i}{\Delta_{i+1}} < \xi \\ 0 & \xi < \dfrac{\Delta_i}{\Delta_{i+1}} < \eta \\ -1 & \eta < \dfrac{\Delta_i}{\Delta_{i+1}} < \infty \end{cases} \tag{8.26}$$

$$\alpha_i(r) = \begin{cases} +1 & 0 < \dfrac{Z_i(r)}{Z_{i+1}(r)} < \xi \\ 0 & \xi < \dfrac{Z_i(r)}{Z_{i+1}(r)} < \eta \\ -1 & \eta < \dfrac{Z_i(r)}{Z_{i+1}(r)} < \infty \end{cases} \qquad (8.27)$$

In equations (8.26) and (8.27) ξ and η are constants which should chosen by the inspector. Yin et al. don't give any rules for choosing these constants.

The method presented by Yin et al. [92.2] is one of the few pattern recognitions which has been proposed for the performance of VBI of civil engineering structures until about one year ago. However, just recently very promising approaches based on the use of neural networks have been presented for VBI on civil engineering structures (see e.g. Kirkegaard and Rytter [93.2] and Worden et al. [93.3]).

During the last decade, the field of neural networks has been subject to intense studies by many researchers from many different disciplines although neural network has been formally investigated since the early forties.

Neural networks are computational models loosely inspired by the neuron architecture and operation of the human brain. A neural network is an assembly of a large number of highly connected processing units, the so-called neurons. The strength of the connections between the neurons is represented by numerical values which are normally called weights. Knowledge is stored in the form of a collection of weigths. The neural networks are capable of self-organization and knowledge aquisition (i.e. learning).

Many different types of neural networks exist. Among these the multilayered neural networks trained by means of the back-propagation algorithm are currently given the greatest attention by application developers. The formulation of this training algorithm in 1986 by Rumelhart et al. [86.6] resulted in an almost explosive increase in the use of neural networks.

A multilayered neural network is made up of one or more hidden layers placed between the input and output layers as shown in figure 8.10. Each layer consists of a number of neurons. Output units cannot receive signals directly from the input layer.

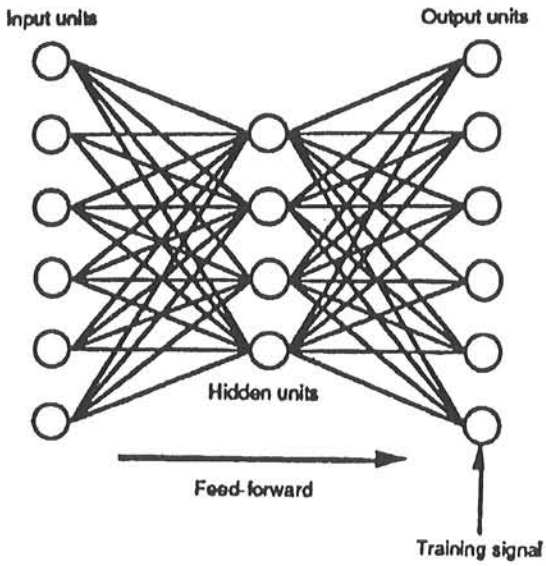

Figure 8.10 Principle of a multilayered neural network (Orchard and Phillips [91.22]).

The first stage of using a neural network to model an input-output model is the so-called training phase in which appropriate values of the weigths are established. The training of a neural network is based on sets of input for which the desired outputs from the neural network are known. During the training activation flows are only allowed in one direction, a feed-forward process, from the input layer to the output layer through the hidden neurons. For a more detailed description of neural networks, see e.g. Hertz et al. [91.21].

The basic strategy for developing a neural network-based approach to be used in connection with VBI on civil engineering structures is to train a neural network to recognize different damage scenarios from the measured response of the structure, strains, modal parameters, etc. For instance, a neural network might be trained with natural frequencies as input and the corresponding damage state as output. Thus optimally, when a neural network trained with such data is given a set of natural frequencies as input it should be able to recognize the corresponding damage state. However, investigation of some issues remains before the neural network approach becomes a true method for the performance of VBI of civil engineering structures. For instance, further research should address problems such as selection of training data and design of network architecture (i.e selection of the number of layers and neurons).

A simple test example of the applicability of artificial neural networks in connection with damage detection in the mast from experimental case no. 2 is presented in example 8.4.

Example 8.4

The aim of this example is to demonstrate the use of neural networks in connection with VBI of civil engineering structures. The mast from experimental case no. 2 is used as test object.

A 3-layered neural network is trained by means of the back propagation algorithm. Measured estimates for the six lower natural frequencies are used as input and the damage state of the eight lower diagonals (see example 6.1, page 96) are used as output during the training. Thus, the neural network has 6 input nodes and 8 output nodes. The hidden layer consists of 5 neurons. The value for the single diagonal adopts the value 1 when not damaged, the value 0 when totally damaged and the value 0.5 when half damaged.

The applicability of the trained neural network has been tested by means of five sets of natural frequencies which were not included during the training session. The results are shown in table 8.2.

Possible damage location	Damage state				
	1	2	5	6	9
AB101	0.2001	1.0114	0.8692	1.3315	0.4782
BC101	1.0051	0.0245	0.9994	0.9992	0.9992
CD101	0.9958	0.9988	1.0005	1.0007	1.007
DA101	0.8110	1.0010	1.0691	0.6558	0.9997
AB102	1.0107	0.9808	0.0162	0.9438	0.9986
BC102	1.0307	0.9954	0.9937	0.1988	1.0153
CD102	1.0046	0.9989	0.9994	0.9994	0.9993
DA102	1.0070	0.9984	0.9992	0.9986	0.9986

Table 8.2 Results from a neural network-based VBI of the mast in experimental case no. 2.

The results in table 8.2 show that the trained neural network is applicable to detection and quantification of damages in the mast or in other words works as a level 3 method.

The results from example 8.4 showed that the trained neural network might be used as a level 3 method. However, in this relatively simple example the training was based on measured data. Before a neural network can be fully accepted as a level 3 method it must be investigated whether or not the training can be based on simulated data.

Results obtained by Wooden et al. [93.3] show that neural networks can be successfully used as a level 2 method when it is trained on strain data from FEA.

8.10 OPTIMIZATION

In 1991 Rytter et al. [91.12] proposed a level 3 method for identifying the location and size of damages in structures. The method was implemented to diagnose fatigue cracks in steel structures. However, in priciple the method is applicable to all kinds of structures and damages. A similar method was almost simultaneously proposed by Shen and Taylor [91.6].

The basic idea is to use a non-linear optimization method to find an estimate for the damage state vector $\hat{\boldsymbol{D}}$. The object function $F(.)$ to be minimized expresses a scalar measure for the differences between the measured estimates for the damage indicator vector $\tilde{\boldsymbol{R}}$ and calculated estimates $\boldsymbol{R}^c(\boldsymbol{D})$ given a certain damage scenario $\boldsymbol{D}$. In most cases the objective function should be supplemented with inequality, equality or side constraints. Thus, in general the method is based on the following equations

$$\hat{\boldsymbol{D}} = \min_{\boldsymbol{D}} [F(\boldsymbol{D},\tilde{\boldsymbol{R}})] \tag{8.28}$$

subject to

$$g_i(\boldsymbol{D},\tilde{\boldsymbol{R}}) \leq 0 \qquad i=1,N_{ic} \tag{8.29}$$

$$h_i(\boldsymbol{D},\tilde{\boldsymbol{R}}) = 0 \qquad i=1,N_{ec} \tag{8.30}$$

$$D_i^l \leq D_i \leq D_i^u \qquad i=1,N_D \tag{8.31}$$

where N_{ic}, N_{ec} and N_{sc} are the number of inequality, equality and side constraints, respectively.

In many cases it might be advantageous to use inequality constraints to perform some kind of weighting with respect to the accuracy of the elements in $\tilde{\boldsymbol{R}}$ (see e.g. equation (8.37)). Vanderplaats [84.8] recommends that an equality constraint should only be used in cases where $h_i(\boldsymbol{d},\tilde{\boldsymbol{R}})$ is either a very complicated explicit function of the variables in $\boldsymbol{d}$ or is implicit in $\boldsymbol{d}$. The side constraints given in equation (8.31) define the upper and lower bounds for the parameters in $\boldsymbol{d}$. In principle these side constraints could be included in the inequality constraints given in equations (8.29). However, according to Vanderplaats it is usually more convenient to treat them separately because they define the region of search for the optimum.

The damage vector $\boldsymbol{D}$ should include the parameters necessary to describe the expected damage scenarios. For instance, in the case of a crack in a beam $\boldsymbol{D}$ should contain the crack position and the crack length. Further, in some cases it might be relevant to include some of the time-varying effects described in section 6.1 in $\boldsymbol{D}$.

In principle, the damage indicator vector $\boldsymbol{R}$ may include all the DIs presented in chapter 5 if a mathematical relation between the expected damage scenarios and the DI can be established. Changes in natural frequencies and mode shapes are the most commonly used parameters included in $\boldsymbol{R}$. Thus, the application of the method requires a reliable mathematical model of the damages. Rytter et al. [91.8] and [91.12] use the fractional model presented in section 4.1.3, whereas Shen and Taylor use the model proposed by Christides and Barr [84.7] and evaluated in Shen and Pierre [90.17]. In the latter model the perturbation in the stresses induced by the crack is incorporated through a local function which assumes an exponential decay with distance from the crack.

The dynamic characteristics included in $\boldsymbol{R}^c(\boldsymbol{d})$ should be calculated in each call of the object function during the optimization process. For simple structures, as e.g. straight uniformed beams, the relationship between damage and e.g. natural frequencies can be given on closed form (see e.g. Gudmundson [82.4]). However, for more complicated structures $\boldsymbol{R}^c(\boldsymbol{d})$ should be found through an FEA. This might result in the optimaztion process getting quite time-consuming. The duration might be reduced by optimal choices of the object function, initial values in $\boldsymbol{D}$ and the constraints. Further, the repetitive use of the object function should be applied to build up a response surface, which will cause a decrease in the duration of a diagnostic session.

The object function might be formulated in many different forms. The optimal choice will depend on which parameters $\tilde{\boldsymbol{R}}$ contains and will probably vary from structure to structure.

Shen and Taylor [91.6] used a least square minimization and a min-max problem formulation in their simulation studies concerning a simply supported beam containing a crack at mid-span. There was no significant differences in the results from the two approaches. Therefore, only the least square formulation will be treated in the present thesis. Shen and Taylor use the object function shown in eqaution (8.32) supplied with two equality constraints concerning the continuity condition on the internal forces and orthogonality between the measure and calculated mode shapes. Further, Shen and Taylor use side constraints for the crack postion z_c and the crack length a.

$$\min_{z_c,a}\left(\sum_{i=1}^{N_M}\left[(\tilde{f}_i-f_i^c)^2+\sum_{j=1}^{N_{MP}}(\tilde{\phi}_{ji}-\phi_{ji}^c)^2\right]\right) \tag{8.32}$$

where N_M is the number of measured modes and N_{MP} is the number sensor locations.

Shen and Taylor use the first and third natural frequency and the corresponding modes shapes in 9 points. The second natural frequncy was not included because this mode of a simply supported beam is not sensitive to a mid-span crack. The method was tested for situations with known z_c and unknown z_c, respectively, for different initial data. Good results were obtained in the cases with z_c known. However, the results in the cases with z_c unknown were quite poor. Therefore, they increased the number of sensor locations from 9 to 45 but this did not help in all cases. Probably, the poor results are caused by a number of local minimum points for the object function. Thus, a new formulation of this function might lead to better results. Further, inclusion of some inequality constraints on the natural frequencies would probably cause better results. Finally, the results could be improved by inclusion of the second natural frequency in the problem since an unchanged value of this frequency would clearly indicate a crack at either the support or the mid span.

Rytter et al [91.12] use the object function shown in equation (8.33) for locating and quantifying a crack in a cantilever from simulated estimates for the five lower natural frequencies. The performed analysis showed that the object function had local minimum points causing multiple solutions to the optimization problem.

$$\min_{a,z_c}\sum_{i=1}^{N_M}\left(\frac{\tilde{f}_i^P-f_i^C(a,z_c)}{\tilde{f}_i^V}\right)^2 \tag{8.33}$$

Rytter et al. state that the problem with local minima might be avoided or reduced by changing the object function and/or including mode shape data.

In Rytter et al. [91.8] a two step solution procedure is used to estimate the position and length of a crack in test beam B4 from experimental case no. 1. Firstly, the CA-method (see section 8.8) was used to estimate the crack location. Finally, the object function shown in equation (8.34) was used to estimate the crack size.

$$\min_{a} \left[\frac{\tilde{\theta}^P - \theta^C(a)}{\tilde{\theta}^V} + \sum_{i=1}^{3} \left(\frac{\tilde{f}_i^P - f_i^C(a)}{\tilde{f}_i^V} \right)^4 \right] \tag{8.34}$$

subject to

$$0 \leq a \leq b \tag{8.35}$$

where θ is the ratio between the coordinates at the upper and the lower measuring positions (see figure 1.1) of the first mode shape and b is the flange width of the box profiles used in experimental case no. 1. The crack location was estimated correctly while the crack length was estimated of 0.06 m versus a measured value of 0.064 m. Thus, the approach might be considered as promising.

Based on the experience from Rytter et al. [91.12] and [91.8] the following formulation of the optimization problem is suggested

$$\min_{\boldsymbol{D}} \log \left[\sum_{i=1}^{N_\Psi} \left(\frac{\tilde{\Psi}_i^P / \tilde{\Psi}_i^V}{\Psi_i^{C,P}(\boldsymbol{D}) / \Psi_i^{C,V}(\mathbf{0})} - 1 \right)^2 w_i \right] \tag{8.36}$$

subject to

$$\left| \tilde{\Psi}_i^P / \tilde{\Psi}_i^V - \Psi_i^{C,P} / \Psi_i^{C,V} \right| \leq \alpha_i \tag{8.37}$$

$$D_i^l \leq D_i \leq D_i^u \qquad i = 1, N_D \tag{8.38}$$

where ψ_i-values are natural frequencies and mode shape ratios and the w_i-values and α_i-values are a kind of weighting parameters which should be established from the accuracy of the $\tilde{\Psi}_i$-values. The applicability of the method is tested in example 8.5.

Example 8.5

The aim of this example is to study the applicability of the optimization problem given in equations (8.36) to (8.38) for estimating the crack size and location in test beams B1-B3 and B5-B6 of experimental case no. 1.

The following version of the optimization problem is used in the present example

$$\min_{a,z_c} \log\left[\sum_{i=1}^{3}\left(\frac{\tilde{f}_i^P/\tilde{f}_i^V}{f_i^{C,P}(D)/f_i^{C,V}(0)} - 1\right)^2 W_i\right] \tag{8.39}$$

subject to

$$|\tilde{f}_1^P/\tilde{f}_1^V - f_1^{C,P}/f_1^{C,V}| \leq 0.001 \tag{8.40}$$

$$|\tilde{f}_2^P/\tilde{f}_2^V - f_2^{C,P}/f_2^{C,V}| \leq 0.005 \tag{8.41}$$

$$|\tilde{f}_3^P/\tilde{f}_3^V - f_3^{C,P}/f_3^{C,V}| \leq 0.01 \tag{8.42}$$

$$0. \leq a \leq 0.160\ m \tag{8.43}$$

$$0. \leq z_c \leq 2.0 \tag{8.44}$$

The vector W was taken as [1 1 1] in all cases.

The estimates for the three lower natural frequencies for the different crack lengths were succesively included in the optimization.

The initial value of a and z_c were taken as 0 m and 1,5 m, respectively, in all the first optimizations for each beam. The results from the previous analysis were used as start values for the remaining optimizations.

The VS-calibrated versions of the FEM shown in figure 6.3 were used in the FEA.

The minimizations were performed by means of the M-file CONSTR from the Matlab Optimization Toolbox (see [90.2]) connected to a group of Finite Element M-files, which have been developedin connection with the preparation of this thesis. The results are shown in figure 8.11 and figure 8.12.

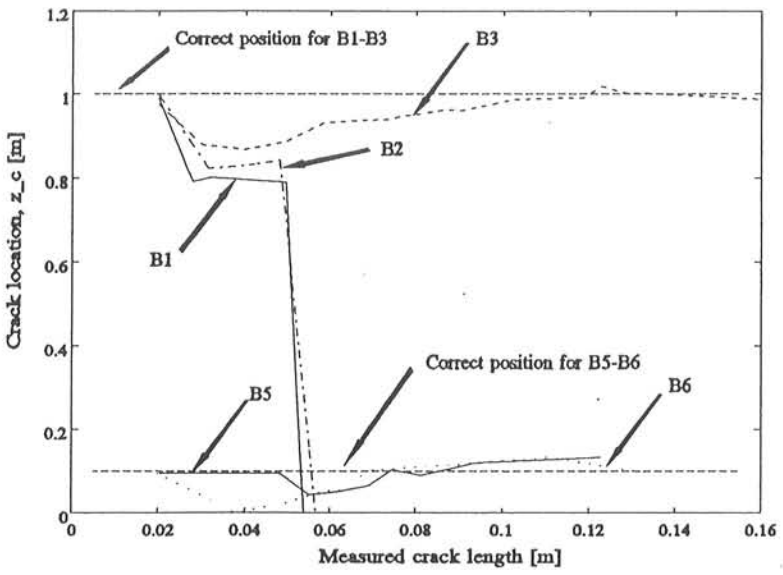

Figure 8.11 Estimated crack locations, experimental case no. 1.

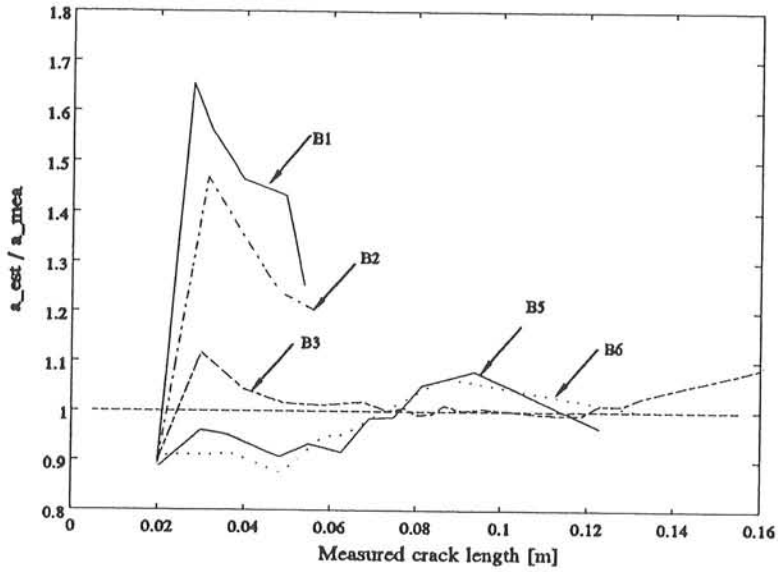

Figure 8.12 Estimated crack lengths (relative) , experimental case no. 1.

The results show that the differences between the estimated values and the measured values for beams B3, B5 and B6 decrease for increases in the measured crack length. The course of these curves reflect that the influence from errors on the measured natural frequencies becomes smaller for increasing crack length.

Unwanted fatigue cracks were, as mentioned in section 1.3.1, developed in the weld at fixture of beams B1 and B2 during the tests. These cracks were much bigger than the cracks at $z = 1.0$ m and therefore became governing for the changes in the natural frequencies. This fact is clearly demonstrated by the graphs for B1 and B2 in figure 8.11 where the $z = 0.0$ m is pointed out as the most possible crack locations in the last test series for the two beams.

The results from example 8.5 show that the optimization problem suggested in equation (8.36) to (8.38) can be used as a level 3 method. However, the results indicate that poor results might be expected for small cracks if the errors (uncertainties) of the estimates in $\tilde{\boldsymbol{R}}$ are too large.

In some case it might be difficult to implement the optimization method in connection with VBI on more complicated structures, as e.g. the mast in experimental case no. 2. For such structures the diagnostic session should be performed in two steps. First, the most possible damage location (on element level) should be found by using one of the methods described in section 8.7 on global measurements. Finally, the results from a local measurement on this element should be used as input to the optimization problem.

Thus, the proposed method might seem to be a powerful tool in connection with VBI of civil engineering structures. However, so far the method has only been tested on a

simple beam containing just one crack. Future research will concern cases with more than one crack and inclusion of lumped masses.

8.11 CONCLUSION

Ten more or less sophisticated and different approaches for solving the diagnostic problem given by equation (3.1) have been presented. Part of the approaches like e.g. the *Changes in Model Matrix Methods* presented in section 8.6 has been used in various ways by different people. The review is not a complete state-of-the-art but a presentation of the most commonly used and most quoted methods.

Roughly, the ten methods can be split up in 6 level 2 methods and 4 level 3 methods if the conclusions made by the originators of the methods are used as a basis. However, the examples given in this chapter have revealed that the level of the method depends on the type of damage (see e.g. example 8.1 concerning a test of the SO-method).

The performed review and the results from the examples have shown that the possibility of a succesful diagnostic session is depending on several factors, as e.g. type of structure, damage size, damage type, damage location, the damage indicators included in $\tilde{R}$, accuracy of the elements in $\tilde{R}$ and the mathematical models of the structures and the damage.

A fixed order of priority for the presented methods cannot be given since the above-mentioned factors together with other important factors as e.g. the acceptable level of damage, the expected damage scenarios and the level of ambition for the VBI will vary from structure to structure.

In many cases it may be rational to use more than one of the methods in multi-step diagnosing session (see e.g. Rytter et al. [91.8]). For instance the CA-method could be used to limit the potential area of damage (global diagnosis) and subsequently the optimization method could be used to give the final estimates for the elements in $\boldsymbol{D}$ (local diagnosis).

CHAPTER 9
DISCUSSION AND CONCLUSION

This chapter is divided into three sections. Section 9.1 contains a summary of chapter 1 to 8 of the thesis. The second section gives an overall discussion and conclusion about the topics treated in the thesis. Finally, the future perspective in using VBI-programmes on civil engineering structures is given in section 9.3.

9.1 SUMMARY

Chapter 1

Chapter 1 contains the introduction to this thesis. The main purpose of the thesis is to establish a basic knowledge to the different activities included in a complete VBI-programme and to describe the interaction between these activities. Thus, the thesis might be used as an introductory handbook for people who want to design a VBI-programme for a certain civil engineering structure. Two experimental cases related to the thesis are presented at end of chapter 1.

Chapter 2

The first section of this chapter contains a presentation of different methods used for the decision making on the extent and the time interval between the periodical inspections. A short survey of the most common used NDI-methods in use for inspection of steel and concrete civil engineering structures is given in section 2.2.

The performed review showed that at the moment there is a high activity in the area of developing of methods for decision-making on the rate and extent of inspection. The

probability-based optimization of fatigue design, inspection and maintenance methods are pointed out as the most promising approaches to solve the problem.

The review of the most commonly used NDI-methods revealed that none of these methods have so far been developed to such an extent yet that they can be used to perform a quick and still reliable inspection of a civil engineering structure. Thus, a complete inspection of a given structure has to be based upon a combination of two or more inspection methods. Vibration monitoring and acoustic emission were found to be the two most promising methods of the nine methods covered by the review.

Chapter 3

A general step by step description of a complete VBI-programme and a review of examples on the field application of VBI on real civil engineering structures are given in this chapter.

A complete VBI-programme includes the use of many different advanced engineering disciplines. These disciplines have been treated in the chapter 4-9 of this thesis.

The performed review shows that the use of VBI on civil engineering structures is an area, which has been given much attention during the last decade. However, it will require a lot of research work before the methods are fully developed. VBI has been most widely used on piles where in fact VBI has become profitable alternative to the other and more traditional NDI-methods for piles.

The results from different tests performed on either models of or real bridges and offshore structures are reported in section 3.2. A common feature of most of the performed tests is that they concern analysis and determination of the dynamic behaviour of structures which contain a well defined state of damage. The inverse problem, i.e., the estimation or determination of the damage state when the dynamic behaviour is known, has not been given much attention.

The results from the performed tests quoted in the review show that choice of DIs and excitation together with the relative size of the damage are topics which are of great importance for the probability of succesfull VBI.

Generally, the performed review has shown that VBI has been used in many cases and it is a serious alternative to other NDI-methods although it is still in its infancy.

Chapter 4

Chapter 4 concerns the modelling of a cracked beam with respect to stiffness and damping.

Five different models for the local changes in flexibility at a crack in a straight linear beam is presented and evaluated. The fracture mechanical model is found to be the optimal model with respect to accuracy and duration of calculation in most cases. This model is used in the remaining part of the thesis.

Further, the evaluation show that great care should be taken with respect to non-linearities and that it is preferable to perform calibration tests.

The review of factors that influence the damping of a cracked beam reveals that the damping is more sensitive to factors like e.g. stress history than the stiffness. Therefore, no mathematical model for the change in damping due to a crack is given.

Chapter 5

Chapter 5 contains a presentation of different dynamic characteristics which might be used as DIs in connection with a VBI-programme.

Measured and simulated data are used to show the properties of the presented DIs.

A generally fixed order of priority for the applicability of the presented DIs is not given since such a list will vary from structure to structure. This is because the applicability of a DI depends on several different factors, such as the type of damage, the location of the damage, etc.

Some of the more rarely used DIs presented in chapter 5 are shown to be effective in cases where the damage causes different non-linear effects, which may cause trouble when using the traditional DIs as for instance natural frequencies.

It is recommended, that the choice of the DIs to be applied to a given structure should be based on the results from sensitivity studies. In other words all the potential DIs are "equal" at the start of the sensitivity analysis, which will give a fixed order of priority for the applicability of the different DIs in connection with VBI on a given structure.

However, all DIs, which are measureable from a given instrumentation, should be estimated and incorporated in the subsequent diagnostic analysis since the inclusion of all available information will cause an increased accuracy of the results from the diagnostic session.

Chapter 6

This chapter gives the outlines of the introductory analysis. These analyses include sensitivity analysis, choice of SI-method(-s) and design of measurement programme. Further, a review of the most common seen time-varying parameters is given in this chapter.

The results from the introductory analysis is the basis for making the decision about starting the VBI-programme or not.

The different topics to be treated during the introductory analysis are presented in four different sections placed in the order in which it is recommendable to start them. However, it is recommended to complete the different analyses in parallel since there is a high degree of correlation between the results from the different analyses.

The review of time-varying parameters shows that they can cause changes in the DIs which are comparable with damage induced changes. Therefore, it is suggested that a list of all potential time-varying effects and their expected variations should be written at the start of the introductory analysis. Subsequently, the time-varying effects of importance should then be found from the sensitivity analysis and recorded in connection with periodical measurement.

The aim of the sensitivity analysis is to determine the sensitivity of all the potential DIs to the development of the expected damage scenarios to an acceptable level and to set up a fixed order of priority for the DIs. Secondly, the sensitivity analysis should reveal whether these damage depending changes in the dynamic characteristics are significantly different from the changes due to time-varying effects. Thirdly, the non-deterministic model parameters which have a significant influence on the dynamic characteristics should be determined in preparation for the virgin state calibration. Examples of the performance of these topics are treated in two examples concerning the beams from experimental case no. 1 and the mast from experimental case no. 2, respectively.

A short survey of SI-methods is given. A list of different types of excitation which have been used in connection with the performance of SI-experiments on civil engineering

structures. The number of possible types of excitation which can be applied to a certain structure will often be very limited. Therefore, in many cases the excitation to be used in connection with the performance of the periodical measurements will be governing for the choice of SI-method(-s) and the instrumentation to be used. Further, topics as e.g. choice of domain, bias and random errors are discussed.

A review of methods proposed for the optimal choice of the experimental conditions so that the information provided from the experiment is maximized is given.

Chapter 7

Chapter 7 contains a presentation of several factors which illustrate the great importance of the VS-calibration.

Further, a general review and discussion of proposed algorithms for the performance of VS-calibrations are given.

An example of optimization based VS-calibrations of the beams from experimental case no. 1 is given.

Chapter 8

This chapter contains a review of ten more or less sophisticated and different approaches for solving the diagnostic problem, i.e. determination of the damage state from measured dynamic characteristics. The review is not a complete state-of-the-art but a presentation of the most common used and most quoted methods.

Roughly, the ten methods can be splitted up as 6 level two methods and 4 level three methods if the conclusions made by the originators of the methods are used as a basis. However, the performed review and the results from the examples have shown that the possibility of a succesfully diagnosing session is depending on several factors such as the damage scenario, the reliability of the damage model, the measured dynamic characteristics and whether calibration tests have been performed or not.

A fixed order of priority for the presented methods is not given since the above-mentioned factors together with other important factors as e.g. the acceptable level of damage, the expected damage scenarios and the level of ambition for the VBI will vary from structure to structure.

easily be done if one is using the neural network approach (see section 8.9) by using the results in a retraining of the neural network.

All the methods proposed for diagnosis of cracks are based on an assumption of linear behaviour in the cracked zone, i.e. a constant open/closed crack. The use of these methods on a structure with cracks which are open and closed in turns will lead to poor results in the diagostic session. In fact, the damage will be underestimated since the changes in the dynamic parameters as e.g. natural frequencies will be estimated too low.

Mathematical Model of the Structure

The use of some of numerical models is a common feature of all the methods except the two methods presented by Fox [92.4] (see section 8.1). The latter methods are based on measured estimates for natural frequencies and mode shapes.

The result from a diagnostic session will be highly dependent on how well the mathematical model describes the dynamic behaviour of both the undamaged (virgin) and the damaged structure. Normally, this correlation is obtained through the VS-calibration (see chapter 7). However, in principle this calibration only secures a reliable description of the undamaged structure. In some cases the calibrated model fails to predict the effect of damages. For instance, the decrease in the rotational frequencies of the mast in experimental case no. 2 was overestimated due to a poor modelling of the stiffness at the four support points. This implied that damage in one of the four lower diagonals could not be located by means of the CA-method (see example 8.3 on page 142). Therefore, great attention should be given to multiple solutions during the VS-calibration and proper modelling of details of great importance.

A priori knowledge of the effect of damage obtained from similar structures will be of great importance. In such cases sensitivity studies should be performed in connection the VS-calibration.

The Damage Indicators

The probability of a successful diagnostic session increases if the amount of information about the structure used during the diagnostic session is increased. Therefore, as a rule of thumb the number of elements in the $\tilde{R}$-vector should be as high as possible.

However, the accuracy of the single parameters in $\tilde{R}$ will be different. Therefore, the elements should be weighted relatively with respect to their accuracy during the diagnostic session. Further, it is obvious that a decrease in the uncertainties of the parameters in $\tilde{R}$ will increase the possibility for a successful diagnostic session unless either the model of the damage or the structure is defective. Normally, the influence of the uncertainties in the elements in $\tilde{R}$ will decrease when the extent/size of the damage is increased (see e.g. example 8.2 on page 141 and example 8.5 on page 150).

Results from examples given in Hemami and Abdelhamid [92.11] and Flanigan [91.23] show that the efficiency of the probability of detection and the exactness of the methods are increased considerably when mode shape data are included. Therefore, the number of sensor locations should be as large as possible from a practical point of view to obtain a good description of the mode shapes. However, the effect of increasing the number of mode shape data in $\tilde{R}$ depends on how they are used in the diagnostic method. For instance, Shen and Taylor [91.6] do not obtain a unique solution even though they increase the number of sensor locations on a simply supported beam from 9 to 45. Generally, the sensors should be kept free of nodes of those mode shapes which are measurable and most sensitive to damage.

The introduction of damage in a structure may cause so-called frequency cross-overs which means that the rank of the natural frequencies with respect to magnitude is changed. An example of such frequency cross-overs can be seen in table 6.1 showing the results from the sensitivity analysis for the mast in experimental case no. 2. The second and fifth natural frequencies are lower than the first and fourth natural frequencies, respectively, for damage states 2, 4, 6 and 8. Negligence of such frequency cross-overs may lead to a totally wrong result of the diagnosis.

Normally, structural damages do not result in loss of material which implies that the mass matrix will be constant. Therefore, the reliability of the results from the diagnostic session might be increased by including the results from statical load tests in $\tilde{R}$ (see e.g. Hajela and Soeiro [90.18] and Sanayei and Onipede [91.20]) since such tests will give information about the stiffness distribution.

A common feature of the reviewed methods except the SO-method is that they are all based on natural frequencies and mode shapes. However, the use of the estimates differs from method to method. Apparently, the best results are obtained when relative changes in the measured values and the calculated are used as input.

Calibration

The reliability of the results from a diagnostic session is highly dependent on the exactness of the function $F(R)$ of the diagnostic method in use. In other words, how well the used analytical models fits with the real structure. Therefore, it will be of major importance if the function $F(R)$ can be calibrated through some tests, where the size and location of the damage are well-defined. An example of such a calibration can be found in Chondros and Dimarogonas [80.4].

9.3 FUTURE PERSPECTIVE

There still exist some unsolved problems in connection with the application of VBI to civil engineering structures. These problems which have to be solved through research and tests are summarized in the following.

The review given in this chapter revealed that only a limited number of the DIs presented in chapter 5 is used as input to the different diagnostic methods. Thus, a lot of research is necessary for inclusion of the more non-traditional DIs.

A common feature of all the methods is that the structure is assumed to behave linearly in the undamaged and the damaged state. The reliability of the results from a diagnostic session concerning cracks would increase if the non-linear models described in section 4.1.5 were included.

Many of the proposed methods have been verified through simulation on rather simple structures in most cases. Obviously there is a need for experimental verification of the methods through experimental tests on both simple and more complex structures.

The elements in $\tilde{R}$ and D should be considered as stochastic variables. Thus, the results from a diagnostic session will consist of a vector D_μ containing mean values and a vector D_σ containing standard deviations. These vectors might subsequently be used in a probabilistic analysis of the safety of the structure, i.e. as a level four method. In this way the uncertainties with respect to damage modelling, uncertainties of the parameters in R, etc. are taken into account in a proper manner. This approach has been partly used by Cho et al. [90.27] for reliability-based capactiy rating of existing bridges. However, they considered the elements in $\tilde{R}$ and thereby the paramaters in D to be deterministic.

CHAPTER 10
RESUME (IN DANISH)

Omfanget af inspektioner på bærende konstruktioner er steget voldsomt gennem de seneste ti år. Stigningen skyldes primært en kombination af to årsager. For det første er det blevet økonomisk fordelagtig at vedligeholde ældre konstruktioner i stedet for at erstatte dem med nye. For det andet har anvendelsen af moderne teknologi medført at de opførte konstruktioner er blevet slankere, hvilket medfører dels en øget risiko for udmattelse i konstruktionen og dels, at konstruktionen i langt højere grad er sårbar overfor svigt i et af dets elementer. Denne stigning i behovet for udførelse af periodisk inspektion på bærende konstruktioner har ført til

- udvikling af nye ikke-destruktive inspektionsmetoder
- forbedringer af de eksisterende ikke-destruktive inspektionsmetoder
- udvikling af metoder til fastlæggelse af optimale inspektionsstrategier

Vibrationsbaseret inspektion (herefter omtalt som VBI) er en af de metoder, der er blevet givet mere og mere opmærksomhed indenfor bærende konstruktioner gennem de sidste tyve år som følge af denne udvikling.

Introduktion og udvikling af en skade vil give anledning til en ændring i konstruktionens dynamiske egenskaber. For eksempel vil en udmattelsesrevne i en stålkonstruktion give anledning til fald i konstruktionens egenfrekvenser. Den grundliggende ide i VBI er at måle en konstruktion dynamiske egenskaber løbende gennem dens levetid og anvende eventuelle målte ændringer i de dynamiske egenskaber til at fastlægge skaders omfang og placering.

Et komplet VBI-program for en bærende konstruktion omfatter en lang række delaktiviteter. Målet med nærværende afhandling har været at få et grundlæggende kendskab til disse aktiviteter samt beskrive sammenspillet i mellem dem. Målet er søgt

nået gennem litteraturstudier og ved udvikling af metoder til løsning af nogle de problemer, der forekommer i forbindelse med et VBI-program. De udviklede metoder samt en del metoder er blevet implementeret og afprøvet på såvel eksperimentelle og simulerede data. Resultater fra disse test og tilsvarende resultater præsenteret i litteraturen anvendes i afhandlingen til at beskrive vigtige faktorer og opstille regler for valg af disse faktorer. Afhandlingen kan således anvendes som en grundlæggende håndbog for personer, som ønsker at designe et VBI-program for en bærende konstruktion.

I kapitel 2 indeholder en kort præsentation af de 9 mest anvendte ikke-destruktive inspektionsmetoder samt en sammenligning af fordele og ulemper ved disse metoder. Resultaterne fra denne sammenligning viser, at VBI og akustisk emission er de to mest lovende af de 9 metoder.

En overordnet gennemgang af de forskellige aktiviteter i et komplet VBI-program gives i første afsnit af kapitel 3. Andet afsnit indeholder et review af artikler, rapporter, etc., der omhandler anvendelse af VBI på modeller af eller virkelige broer, offshore konstruktioner og pæle. Dette udførte review viser, at VBI har været meget anvendt og er et seriøst alternativt til andre ikke-destruktive inspektionsmetoder.

Kapitel 4 indeholder en præsentation af fem forskellige modeller til beskrivelse af de lokale stivhedsforhold omkring en revne i et lineærelastisk materiale. Endvidere gives en redegørelse for de faktorer, der har indflydelse på dæmpningen af en revnet bjælke. En vurdering og sammenligning af de fem metoder med hensyn til nøjagtighed og beregningshastighed viser, at modellen baseret på brudmekanik bør anvendes i de fleste tilfælde.

En konstruktions dynamiske egenskaber kan beskrives ved mange forskellige parametre og grafer. Disse parameter og plot benævnes i afhandlingen som *Skadesindikatorer* (Damage Indicators), når deres følsomhed overfor skader anvendes i forbindelse med VBI. Kapitel 5 indeholder en præsentation og eksempler på anvendelser af mere end 16 forskellige skadesindikatorer. Anvendeligheden af de forskellige skadesindikatorer varierer fra konstruktion til konstruktion og vil endvidere være afhængig af faktorer som skadestype, skadesplacering, de udførte målinger etc. I kapitel 5 gives der derfor ikke nogen prioriteret liste over skadesindikatorene, men det anbefales at man lader alle potentielle skadesindikatorer være lige indtil følsomhedsstudierne (se nedenfor) er afsluttet.

I kapitel 6 beskrives en lang række indledende analyser og aktiviteter hvis resultater skal udgøre grundlaget for beslutningen om hvorvidt et VBI-program skal sættes i gang for

en given konstruktion eller ej. Disse indledende analyser omfatter blandt andet følsomhedsstudier, valg af system identifikationsmetode og design af måleprogram. Formålet med af de forskellige aktiviteter beskrives og illustreres med eksempler.

I de fleste VBI-metoder indgår som regel en finite element model, som anvendes ved udarbejdelsen af diagnoser. Det er derfor vigtigt, at disse modeller beskriver den virkelige konstruktion på bedst mulig måde. Dette kan blandt sikres ved at anvende måledata fra den uskadede konstruktion som grundlag for en kalibrering. Et kort review over de mest anvendte metoder til sådanne kalibreringer gives i kapitel 7.

I kapitel 8 præsenteres ti mere eller mindre sofistikerede og forskellige metoder til at foretage en diagnose ud fra målte ændringer i en konstruktions dynamiske parametre. Det udførte review er ikke nogen komplet state-of-the-art men en præsentation af de mest anvendte og mest citerede metoder. Det viser sig, at sandsynligheden for en succesfuld diagnose afhænger af lang række faktorer såsom skadesbillederne, skadesmodellerne, modellen af konstruktionen og skadesindikatorerne. Anvendeligheden af de forskellige metoder vil således variere fra konstruktion til konstruktion. Derfor er der ikke angivet nogen prioriteret liste over metoderne.

NOMENCLATURE

The lists in this section contain the most frequently used symbols, typically applied in several sections of the thesis. Symbols not included in the lists are explained when used.

Symbols

A_c	: crack area
a, a_c	: crack length
b	: width of beam
$\boldsymbol{C}$	: damping matrix
c	: fictious crack length
$\boldsymbol{D}$	: damage vector
$\hat{D}(\tau)$	: random decrement signature
E	: modulus of elasticity
$\boldsymbol{E}$	: error matrix
E_r	: relative error
e	: error
$\boldsymbol{F}$	: loading vector
F_i	: ith element of $\boldsymbol{F}$
$F(.)$	: damage diagnosing function
F_o	: maximum vertical force applied to head of pile, N
f	: frequency, Hz
f_i	: *i'th* natural frequency, Hz
$f(x)$	: Green function
G	: strain energy release rate
h	: height of beam
I	: bending moment of inertia
$\boldsymbol{I}$	: unit matrix
J	: strain energy release rate
$\boldsymbol{K}$	: stiffness matrix

K_I, K_{II}, K_{III} : stress intensity factor, mode I, II and III
k_{ij} : the *(i,j)* element of $\boldsymbol{K}$
k_i : polynomium coefficients
k : spring stiffness
k_r : stiffness of rotational spring
L : beam length
M : bending moment
lumped mass
$\boldsymbol{M}$: mass matrix
m : mass of a one degree of freedom system
N_E : number of elements
N_f : number of frequencies
N_r : number of released node
P : point load
q : quality of inspection
q : vector of modal coordinates
$\boldsymbol{R}$: damage indicator vector
R_T : relative change in transmissibility
RD : relative change in mode shape
r : damage position vector
T : transmissibility
t : time
u_i : displacement in direction i
V_o : maximum vertical velocity of the pile head, m/s
W : width of slot
$\boldsymbol{W}$: weigthing vector
$\boldsymbol{X}$: vector of design variables
X : amplitude of response
$\boldsymbol{x}$: response vector
$\boldsymbol{Z}$: vector of relative changes in natural frequencies
z_c : crack location
x,y,z : Cartesian coordinates
α : flexibility influence coefficient
$\alpha_{jk}(\omega)$: frequency response function between point j and k
β : constant
Δ : difference
variation
flexibility parameter
ϵ : error

ζ_i : modal damping ratio of mode *i*
$\boldsymbol{\Theta}$: vector of dynamic characteristics
$\boldsymbol{\lambda}$: vector of eigenvalues
μ : mass per unit length
ν : Poisson's ratio
Φ : strain energy
$\boldsymbol{\Phi}$: modal matrix
σ_o : tensile/pressure stress before cracking
$\boldsymbol{\sigma}$: stress vector
τ : time
τ : shear stress
$\boldsymbol{\phi}_i$: mode shape of the *i*th mode
ϕ_{ji} : defelection of mode shape of the *i*th mode in point *j*
ω : cyclic frequency, rad/sec
ω_i : the *i*th cyclic natural frequency

Subscripts

$\hat{}$: estimated value
$\sim$: measured value
$\bar{}$: average
C : calculated
d : damaged
damped
eq : equivalent
F : flange
M : measured
m : modified
P : periodical
tot : total
u : undamaged
V : Virgin state
W : web

Abbreviations

ARMA	: Auto Regressiv Moving Average
B1-B6	: Name of test beams
BW	: Band Width [Hz]
DSB	: Danish State Railways
DI	: Damage Indicator
DOF	: Degree of Freedom
FE	: Finite Element
FEA	: Finite Element Analysis
FEM	: Finite Element Model
FFT	: Fast Fourier transformation
FRF	: Frequency Response Function
IMAC	: The International Modal Analysis Conference
NDI	: Non-Destructive Inspection
NDT	: Non-Destructive Testing
PNP	: Pseudo-Node Point
PTRS	: Percussive Test for Structure Response
SI	: System Identification
SMS	: Structural Measurement Systems
TMM	: Transfer Matrix Method
VBI	: Vibration Based Inspection
VS	: Virgin State

REFERENCES

37.1 Hetényi, M. :"Deflection of Beams of Varying Cross Section", Journal of Applied Mechanics, Vol. 4, no. 2, pp. A49-A52, June 1937.

44.1 Kirmser, P.G. : "The Effect of Discontinuities of the Natural Frequency of Beams", Proceedings of the American Society for Testing and Materials (ASTM), Vol. 44, pp. 897-904, 1944

49.1 Thomson, W.T. :" Vibration of Slender Bars With Discontinuities in Stiffness", Journal of Applied Mechanics, Vol. 16, pp. 203-207, 1949.

60.1 Irwin, G.R. : "Fracture Mechanics ", Structural Mechanics, Proceeding of the 1st Symposium on Naval Structural Mechanics, Eds. J.N. Goodier and N.J. Hoff, p. 564, Pergamon Press, Oxford, 1960.

62.1 Wittrick, W.H. : "Rate of Change of Eigenvalues with Reference to Buckling and Vibration Problems ", Journal of Royal Aeronautic Society, Vol. 66, September, 1962.

64.1 Spain, R.F., N.W. Schubring and M.J. Diamond : "An Electronic Ear for Certifying Reliability", Materials Evaluation, Vol. 22, pp. 113-117, March 1964.

65.1 Guyan, R.J. : "Reduction of Stiffness and Mass Matrices", AIAA Journal, Vol. 3, No. 2, p. 380, February 1965.

67.1 Liebowitz, H., H. Vanderveldt and D.W. Harris : "Carrying Capacity of notched Columns", International Journal of Solids Structure, Vol. 3, pp. 489-500, 1967.

68.1 Fox, R.L. and M.P. Kapoor : " Rates of Change og Eigenvalues and Eigenvectors", AIAA Journal, Vol. 6, No. 12, pp. 2426-2429, December, 1968.

69.1 Okamura, H., H.W. Liu, C.S. Chu and H. Liebowitz : " A Cracked Column under Compression", Engineering Fracture Mechanics, Vol. 1, pp. 547-564, 1969.

71.1 Vanmarcke, E.H. : Estimation of Dynamic Properties of Offshore Structures", OTC 1407, The 3rd Offshore Technology Conference, Houston, Texas, April 1971.

71.2 Berman, A. and W.G. Flannelly : " Theory of Incomplete Models of Dynamics Structures", AIAA Journal, Vol. 9, No. 8, pp. 1481-1487, August, 1971.

72.1 Wendtland, D. : "Änderungen der Biegeeigenfrequenzen einer idealisierten Schaufel durch Risse". Ph.D-Thesis ,University of Karlsruhe, 1972 (in German).

72.2 Okamura, H., K. Watanabe and T. Takano : "Applications of the Compliance Concept in Fracture Mechanics", Progress in Flaw Growth and Fracture Toughness Testing, ASTM, STP 536, 1972.

72.3 R.D. Adams : " The Damping Characteristics of Certain Steels, Cast Irons and other Metals", Journal of Sound and Vibration, Vol. 23, no. 2, pp. 199-216, 1972.

73.1 Tada, H. with cooperation of P.C. Paris and G.R. Irwin : "The Stress Analysis of Cracks Handbook", Del Research Cooperation, 1973.

74.1 Davis, A.G. and C.S. Dunn : "From Theory to Field Experience with the Nondestructive Vibration Testing of Piles", Proceedings of The Institution of Civil Engineers, Part 2, Vol. 57, pp. 571-593, December 1974.

74.2 Czarnecki, R.M. : " Dynamic Testing of Buildings Using Man-Induced Vibration", Sound and Vibration, pp. 18-21, October 1974.

75.1 Vandiver, J.K., "Detection of structural failure on fixed platforms by measurements of dynamic response", OTC 2267, The 7th Offshore Technology Conference, Houston, Texas, May 1975.

76.1 Begg, R.D., A.C. Mackenzie, C. Dodds and O. Loland : "Structural Integrity Monitoring Using Digital Processing of Vibrational Signals", OTC 2549, The Eight Annual Offshore Technology Conference, Houston, Texas, May 1976.

76.2 Loland O. and C.J. Dodds :"Experiences in Developing and Operation Integrity Monitoring Systems in the North Sea", OTC 2551, The 8th Annual Offshore Technology Conference, Houston, Texas, May 1976.

76.3 Ruhl, J.A. : "Offshore Platforms : Observed Behavior and Comparisons with Theory", OTC 2553, The 8th Annual Offshore Technology Conference, Houston, Texas, May 1976.

76.4 Stetson, K.A. and G.E. Palma : " Inversion of First-Order Pertubation Theory and Its Application to Structural Design", AIAA Journal, Vol. 14, No. 4, pp. 454-460, April, 1976.

78.1 Hochrein, A.A. and L.L. Yaeger : "Computer-Assisted Digital Processing System for a Nondestructive Evaluation Technique utilizing the Phenomenon of Internal Friction". Fracture Mechanics Symposium on Naval Structure Mechanics, George Washington University, University Press of Virginia, September 1978.

78.2 Shah, P.C. and F.E. Udwadia : "A Methodology for Optimal Sensor Locations for Identification of Dynamic Systems", Journal of Applied Mechanics, Vol. 45, pp.188-196, March 1978.

78.3 Baruch, M. and I.Y.B. Itzhack : "Optimal Weigthed Orthogonalization of Measured Modes", AIAA Journal, Vol. 16, No. 4, pp. 346-351, April, 1978.

79.1 Cawley, P. and R.D. Adams : " The Location of Defects in Structures from Measurements of Natural Frequencies", Journal of Strain Analysis, Vol. 14, No. 2, pp. 49-57, 1979.

80.1 Kenley, R.M. and C.J. Dodds : "West Sole WE platform: Detection of damage by structural response measurements", OTC 3866, 12th Annual Offshore Technology Conference, Houston, Texas, May 1980.

80.2 Goble, G. and F. Rausche : "Pile drivability predictions by Capwap", Numerical methods in offshore piling, Institution of Civil Engineers, pp. 29-36, London, 1980.

80.3 Curtis, G.F. and P.A. Lloyd : "Schizeophonics, then and now", Chartered Mechanical Engineer, pp. 55-60, October 1980.

80.4 Chondros, T.G. and A.D. Dimarogonas : "Identification of Cracks in welded joints of complex structures." Journal of Sound and Vibration, Vol. 69, No. 4, pp. 531-538, 1980.

80.5 Yang, J.C.S., N Dagalakis and M. Hirt :" Application of the Random Decrement Technique in the Detection of an induced Crack on an Offshore Platform Model", ASME, AMD, Vol. 37, pp. 55-67, 1980.

80.6 Coppolino R.N. and S. Rubin :" Detectability of Structural Failures in Offshore Platforms by Ambient Vibration Monitoring", OTC 3865, 12th Annual Offshore Technology Conference, Houston, Texas, May 1980.

80.7 "Vejbroer, Håndbog i eftersyn af bygværker", 8.20.04 Broteknik, Vejdirektoratet - Vejregeludvalget, Maj 1980. (in Danish)

80.8 Rubin, S.: "Ambient Vibration Survey of Offshore Platform", Journal of Engineering Mechanics, ASCE, Vol. 106, No. EM3, pp. 425-441, June 1980.

80.9 Berman, A., F. Wei and K.V. Rao : " Improvement of Analytical Dynamical Models Using Modal Test Data", AIAA Structures, Structural Dynamics and Material Conference, Paper no. 80-0800, pp. 809-814, 1980.

81.1 Petroski, H.J. :" Simple Static and Dynamic Models for the Cracked Elastic Beams", International Journal of Fracture, Vol. 17, pp. R71-R76, 1981.

81.2 Kummer, E., J.C.S. Yang and N. Dagalakis : " Detection of Fatigue Failure in Structural Members", Proceeedings of Dynamic Response of Structures Conference, 2nd ASCE/EMD specialitynConference, pp. 445-460, Atlanta, Georgia, January 15-16, 1981.

81.3 Thomson, W.T. : "Theory of Vibration with Applications", 2nd Edition, Prentice Hall, 1981.

82.1 Lilley, D.M., R.D. Adams and W.J. Larnach : " Location of Defects within Embedded Model Piles using a Resonant Vibration Technique", Paper 3-4, 10th World Conference on Nondestructive Testing, Moscow, 1982.

82.2 Crohas, H. and P. Lepert : "Damage-detection Monitoring for Offshore Platforms is Field-Tested", Oil and Gas Journal, pp. 94-103, February 22, 1982.

82.3 DS410 : "Loads for the Design of Structures". 3'rd edition ,1982.

82.4 Gudmundson, P. : "Eigenfrequency Changes of Structures due to Cracks, Notches and other Geometrical Changes". Journal of Mech. Phys. Solids, Vol. 30, No. 5, pp. 339-353,1982.

82.5 Ju, F.D., M. Akgun, E.T. Wong and T.L. Lopez : "Modal Method in Diagnosis of Fracture Damage in Simple Structure". Productive Application of Mechanical Vibrations,ASME AMD, Vol. 52, pp. 113-126,1982.

82.6 Vandiver, J.K. and S. Mitome : "Effect of liquid storage tanks on the dynamic repsonse of offshore platforms ", Progress in Engineering Science, Dynamic Analysis of Offshore Structures, Recent Developments, Vol. 1, pp. 25-32, Ed. by C.L. Kirk, CML Publ., Southhampton 1982.

82.7 Allemang, R.J. and D.L. Brown : " A Correlation Coefficient for Modal Vector Analysis", Proceedings of the 1st International Modal Analysis Conference, pp. 110-116, Orlando, Florida, USA, 1982.

82.8 Timoshenko, S.P. and J.N. Goodier : "Theory of Elasticity", 3rd Edition, Mc Graw-Hill, 1982.

83.1 Ishizuka, M., K.S. Fu and J.T.P. Yao : " Rule-Based Damage Assessment System for Existing Structures", Solid Mechanics Archives, Vol. 8, pp. 99-118, 1983.

83.2 Nataraja, R. : "Structural Integrity Monitoring in Real Seas". Proceedings of the 15th Annual Offshore Technology Conference, pp. 221-228, Houston, Texas, USA, May 2-5, 1983.

83.3 Pandit, S.M. and S.M. Wu : "Time Series and System Analysis with Application". John Wiley & Sons, 1983.

83.4 Rubin, S. and R.N. Coppolino : "Flexibility Monitoring of Offshore Jacket Platforms", OTC 4535, 15th Annual Offshore Technology Conference, Houston, Texas, May 1983.

83.5 Sato, H. : "Free Vibration of Beams with Abrupt Changes of Cross-section", Journal of Sound and Vibration, Vol. 89, no. 1, pp. 59-64, 1983.

83.6 Dimarogonas, A.D. and Paipetis, S.A. : "Analytical Methods in Rotor Dynamics", Elsevier Applied Science, London, 1983.

83.7 Gudmundson, P. : "The Dynamic Behaviour of Slender Structures with Cross-Sectional Cracks". Journal of Mech. Phys. Solids, Vol. 31, No. 4, pp. 329-345, 1982.

83.8 DS412 : "Steel Structures". 3'rd edition ,1983.

83.9 Wang, B.P., W.D. Pikey and A.R. Palazzolo : "Reanalysis, Modal Synthesis and Dynamic Design", Chapter 8 in *State-of-the-art surveys on finite element technology*, Edited by K. Ahmed, W Noor and D. Pikey, Sponsored by the Applied Mechanics Division, 1983.

83.10 Berman, A. and E.J. Nagy : " Improvement of Large Analytical Model Using Test Data", AIAA Journal, Vol. 21, No. 8, pp. 1168-1173, August, 1983

84.1 Turner, J.D. and A.J. Pretlove : " A Dynamic Method of Condition Monitoring for Bridges", International Symposium on Long-Term observation on Concrete Structures, Preliminary Reports, pp. 434-444, RILEM & ACI, Budapest, Hungary, September 1984.

84.2 Yang, J.C.S., J.Chen and N.G. Dagalakis : "Damage Detection in Offshore Structures by the Random Decrement Technique ". Journal of Energy Resources Technology, Vol. 106, pp. 38-42, March 1984.

84.3 Kernbichler, K. and R. Flesch : "Static and Dynamic Tests, Their Qualification for Bridge Inspections and Long-term Observations of Bridge Structures", International Symposium on Long-Term observation on Concrete Structures, Preliminary Reports, pp. 71-80, RILEM & ACI, Budapest, Hungary, September 1984.

84.4 Andersen, A. Rytter and J. Heiden : "Svingningsbegrænsning af bærende konstruktioner", M.Sc-thesis, University of Aalborg, Denmark, June 1984 (in Danish)

84.5 Velde, W.E.V and C.R. Carignan :"Number and Placement of Control System Components Considering Possible Failures", Journal of Guidance, Control and Dynamics, Vol. 7 No. 6, Nov.-Dec. 1984.

84.6 Olagnon, M. and M. Prevosto : " The Variations of Damping Ratios With Sea Conditions for Offshore Structure Under Natural Excitation", OTC 4654, pp. 57-66, 16th Annual Offshore Technology Conference, Houston, Texas, May 1984.

84.7 Christides, S. and D.S. Barr : "One-Dimensional Theory of Cracked Bernoulli-Euler Beams", International Journal of Mechanical Science, Vol. 26, No. 11/12, pp. 639-648, 1984.

84.8 Vanderplaats, G.N. : "Numerical Optimization Techniques for Engineering Designs", McGraw-Hill, New York, 1984.

85.1 Sunder, S.S. and S.K. Ting: " Flexibility monitoring of offshore platforms", Applied Ocean Research, Vol. 7, No. 1, 1985.

85.2 Moan, T. : "Case Histories in Offshore Engineering". CISM courses and lectures No. 283, Ed. G. Maier, Int. Center for Mechanical Science, Springer Verlag,1985.

85.3 Stubbs, N. and R. Osegueda : "Damage Detection in Periodic Structures". Damage Mechanics and Continuum Modelling, ASCE, pp. 113-128, 1985.

85.4 Tsyfanskii, S.L., M.A. Magone and V.M. Ozhiganov : "Using Nonlinear Effects to Detect Cracks in the Rod Element of Structures". The Soviet Journal of Nondestructive Testing, Vol. 21, No. 3, pp. 224-229, March 1985.

85.5 Hellan, K.: "Introduction to Fracture Mechanics". McGraw Hill, 1985.

85.6 Herlufsen, H.: "Dual Channel FFT Analysis", DIGITAL SIGNAL ANALYSIS using Digital Filters and FFT Techniques, Selected Reprints from Technical Review, Brüel & Kjær, January 1985.

85.7 Yuen, M.M.F. : "A Numerical Study of the Eigenparameters of a Damaged Cantilever", Journal of Sound and Vibration, Vol. 103, No. 3, pp. 301-310, 1985.

85.8 Tsai, W.H. and J.C.S. Yang : "Damage Detection and Location in Complex Structures", Proceedings of the Failure Prevention and Reliability Confrence, pp. 15-22, ASME, Cincinatti, Ohio, September 10-13, 1985.

85.9 Adams, R.D. and P. Cawley : "Vibration Techniques in Nondestructive Testing", Research Techniques in NDT, Vol. 8, chapter 7, pp. 303-360, ed. R.S. Sharpe, Academic Press, London, 1985.

85.10 Sun, C.T. and B.J. Kim : "Continuum modelling of Periodic Truss Structures". Damage Mechanics and Continuum Modelling, ASCE, pp. 57-71, 1985.

85.11 Kabe, A.M. : "Stiffness Matrix Adjustment Using Mode Data", AIAA Journal, Vol. 23, No. 9, pp. 1431-1436, September 1985.

85.12 Stubbs, N. : " A General Theory of Non-Dstructive Damage Detection in Structures", Proceedings of the 2nd International Symposium on Structural Control, University of Waterloo, 1985.

86.1 Ju, F.D. and M. Akgun : "Structural Dynamic Theories of Fracture Diagnosis", Technical Report ME 135(85) AFOSR-993-2, Mechanical Engineering Department, The University of New Mexico, March, 1986.

86.2 Ewins, D.J. : "Modal Testing: Theory and Practice", Research Studies Press LTD and Brüel & Kjær, 1986.

86.3 Ibrahim, S.R. : " Incipient Failure Detection from Random-Decrement Time Functions", The International Journal of Analytical and Experimental Modal Analysis, Vol. 1, no. 2, pp. 1-8, 1986.

86.4 Bendat, J.S. and A.G. Piersol : "RANDOM DATA Analysis and Measurement Procedures", 2nd Edition, John Wileys & Sons, 1986.

86.5 He, J. and D.J. Ewins : " Analytical Stiffness Matrix Correction Using Measured Vibration Modes", International Journal of Analytical and Experimental Modal Analysis, Vol. 1, No. 3, pp. 1-9, July, 1986.

87.1 Bøving, K.G. et al, "NDE ståbi. Metoder til ikke-destruktiv tilstandskontrol", Teknisk Forlag A/S, Denmark, 1987 (in Danish)

87.2 Thronton, H. and A. Alexander : "Development Of Impact/Resonant Vibration Signature For Inspection Of Concrete Structures", Concrete Durability, Katharine and Bryant Mather International Conference, Ed. John M. Scanlon, American Concrete Institute, 1987.

87.3 Guigné, J.Y., P.G. Williams and V.H. Chin : "A concept for the detection of fatigue cracks in welded steel nodes", Marine Technology, Vol. 18, No. 4, 1987.

87.4 Ljung, L. : "SYSTEM IDENTIFICATION, Theory for the user". Prentice-Hall, 1987.

87.5 König, G., A. Ötes, G. Giegerich and H.J. Miesseler, "Structural Integrity of Bridge Ulenberg-strasse in Düsseldorf", IABSE Report vol 56, Monitoring of Large Structures and Assessment of their Safety, pp. 325-337, 1987.

87.6 Idichandy, V.G., C. Ganapathy and P.S. Rao : "Structural Integrity Monitoring of Fixed Offshore Platforms", IABSE Report vol 56, Monitoring of Large Structures and Assessment of their Safety, pp. 237-261, 1987.

87.7 Clark, R., W.D. Dover and L.J. Bond : "The effect of crack closure on the reliability of NDT predictions of crack size", NDT International, Vol. 20, no. 5, pp. 269-275, October, 1987.

87.8 Spidsoe, N. and O. Skjaastad : "Measured Storm-Induced Variations of the Soil-Structure Interaction Porperties of a Gravity Platform", OTC 5410, pp. 437-445, 19th Annual Offshore Technology Conference, Houston, Texas, April 1987.

87.9 Afolabi, D. : "An Anti-Resonance Technique for Detetcting Structural Damage", Proceedings of the 5th International Modal Analysis Conference, pp. 491-495, London, 1987.

87.10 Papadopoulus, C.A. and A.D. Dimarogonas : "Coupling of Bending and Torsinal Vibration of a Cracked Timoshenko Shaft", Ingenieur-Archiv, Vol. 57, pp. 257-266, 1987.

87.11 Ju, F.D and M. Mimovich : "Experimental Diagnosis of Fracture Damage Using the Modal Frequency Theory", Technical Report ME-141 (87) AFOSR-993-3, Bureau of Engineering Research, The University of New Mexico, April, 1987.

87.12 Smith, S.W. and S.L. Hendricks : "Evaluation of Two Identification Methods for Damage Detection in Large Space Trusses", Dynamics and Control of Large Structures Porceedings of the 6th VPI&SU/AIAA Symposium, pp. 127-141,Blackburg, Virgina, USA, June 29-July 1, 1987.

87.13 Wang, M.-L., T.L. Paez and F. Ju : " System Identification of Nonlinear Damaged Structure", Journal of Modal Analysis, pp. 128-135, July 1987.

87.14 Stubbs, N. and R. Osegueda : " Global Nondestructive Evaluation of Offshore Platforms using Modal Analysis", Proceedings of the 6th International Offshore Mechanic and Arctic Engineering Symposium, Vol. 2, pp. 517-524, 1987.

88.1 Nishimura, A., F. Okumura and S. Tanamura : "Integrity Judgement of Railway Bridges by Percussion Tests for Structure Response", QR of RTRI, Vol. 29, No. 4, November 1988.

88.2 Askegaard, V.and P. Mossing : "Long term observation of RC-bridge using changes in natural frequency", Nordic Concrete, 1988.

88.3 Cawley, P. and R. Ray : "A Comparison of the Natural Frequency Changes Produced by Cracks and Slots". Journal of Vibration, Acoustics, Stress and Reliability in Design, Vol. 110, pp. 366-370, July, 1988.

88.4 Flesch, R.G. and K. Kernbichler, "Bridge Inspection by Dynamic Tests and Calculations Dynamic Investigations of Lavant Bridge", Proceedings of Workshop Structural Safety Evaluation Based on System Identification Approaches, Eds. H.G. Natke and J.T.P. Yao, pp. 433-448, Vieweg, 1988.

88.5 Torkamani, M.A.M and A.K. Ahmadi, "A Two Stage Identification Approach in Updating the Analytical Model of Buildings", Proceedings of Workshop Structural Safety Evaluation Based on System Identification Approaches, Eds. H.G. Natke and J.T.P. Yao, pp. 234-264, Vieweg, 1988.

88.6 Ibrahim, S.R., "Correlation of Analysis and Test in Modelling of Structures: Assessment and Review", Proceedings of Workshop Structural Safety Evaluation Based on System Identification Approaches, Eds. H.G. Natke and J.T.P. Yao, pp. 195-211, Vieweg, 1988.

88.7 Agbabian, M.S., S.F. Masri, R.K. Miller and T.K. Caughey : "A System Identification Approach to the Detection of Changes in Strctural Parameters", Proceedings of Workshop Structural Safety Evaluation Based on System Identification Approaches, Eds. H.G. Natke and J.T.P. Yao, pp. 341-355, Vieweg, 1988.

88.8 Lieven, N.A.J and D.J. Ewins : " Spatial Correlation of Mode Shapes, The Coordinate Modal Assurance Criteria (COMAC)", Proceedings of the 6th International Modal Analysis Conference, pp. 690-695, Las Vegas, USA, 1988.

88.9 Park, Y.-S., H.S. Park and S.S. Lee : " Weighted_Error-Matrix (WEM) Application to Detect Stiffness Damage by Dynamic Characteristic Measurement", The International Journal of Analytical and Experimental Modal Analysis, Vol. 3, No. 3, pp. 101-107, July, 1988.

88.10 Haisty, B. and W.T. Springer : "A General Beam Element for Use in Damage Assessment of Complex Structures", Journal of Vibration, Acoutsics, Stress, and Reliability in Design, Vol. 110, July 1988.

88.11 Gounaris, G. and A. Dimarogonas : " A Finite Element of a Cracked Prismatic Beam for Structural Analysis", Computers and Structures, Vol. 28, No. 3, pp. 309-313, 1988.

88.12 "Shock and Vibration Handbook", 3rd Edition, Edited by C.M. Harris, McGraw-Hill, 1988.

88.13 Ju, F.D. and M.E. Mimovich : "Experimental Diagnosis of Fracture Damage in Structures by the Modal Frequency Method", Journal of Vibration, Acoustics, Stress and Reliability in Design, Vol. 110, pp. 456-463, October, 1988.

88.14 Pandit, S.M. and N.P. Mehta : "Data Dependent Systems Approach to Modal Analysis, Part I : Theory", Journal of Sound and Vibration, Vol. 122, No. 3, pp. 413-422, 1988.

88.15 Kammer, J. : "Optimum Approximation for residual Stiffness in Linear System Identification", AIAA Journal, Vol. 26, No. 1, pp. 104-112, January, 1988.

88.16 Natke, H.G. : "Updating Computational Models in the Frequency Domain based on Measured Data : A Survey", Probalistic Engineering Mechanics, Vol. 3, No. 1, pp. 28-35, 1988.

88.17 Tsai, W.H., D.N. Kung and J.C.S. Yang : "Application of System Identification to Damage Detection and Location in Offshore Platform", Proceedings of the 7th Offshore Mechanics and Arctic Engineering, Houston, Texas, pp. 77-84, February 7-12, 1988.

89.1 STAR*Struct*-software, Manual for version 3.01, Structural Measurement Systems, 1989.

89.2 Sanders, D.R., N. Stubbs and Y.I. Kim : "Global Nondestructive Detection in Composite Structures", Proceedings of the 7th International Modal Analysis Conference, Las Vegas, Nevada, February 13-16, 1989.

90.1 Madsen, H.O. and J.D. Sørensen : "Probability-Based Optimization of Fatigue Design, Inspection and Maintenance". International Symposium on Integrity of Offshore Structures - 4, Eds. D. Faulkner et al, Elsevier(1991), pp.421-438, July 1990.

90.2 Flesch, R. : "A Dynamic Method for the Safety Inspection of Large prestressed Bridges", Paper no. 7, CEEC-Seminar, Dynamic actions on Buildings and Structures, Lehrstuhl für Bautstatik, RWTH Aachen, March 1990.

90.3 Chinn, D.J. : "Dynamic structural integrity measurements", Paper no. 8, CEEC-Seminar, Dynamic actions on Buildings and Structures, Lehrstuhl für Bautstatik, RWTH Aachen, March 1990.

90.4 Sommer, A.M. and P. Thoft-Christensen : "Inspection and maintenance of marine steel structures - State of the art", Structural reliability paper no. 74, Department of Building and Structural Engineering, University of Aalborg, April 1990.

90.5 Biswas, M., A.K. Pandey and M.M. Samman : " Diagnostic experimental spectral/modal analysis of a highway bridge", The International Journal of Analytical and Experimental Modal Analysis, Vol. 5, No. 1, January 1990.

90.6 Ågårdh, L. : "Modal Analysis of a Concrete Prestressed Concrete Bridge at Stora Høga. Nordisk Betong 4, pp. 24-26, 1990.

90.7 Kirkegaard, P.H., J.D. Sørensen and R. Brincker : "Optimization of measurements on dynamically sensitive structures using a reliability approach". Proceedings of the 9th International Conference on Experimental Mechanics, Vol.3, pp. 967-976, Technical University of Denmark, August 20-24, 1990 .

90.8 Jensen, J.L. : "System Identification of Offshore Platforms". Ph.D.-Thesis, Fracture & Dynamics, Paper No. 22, Dept. of Building Technology and Structural Engineering, University of Aalborg, April, 1990.

90.9 Rytter, A., J.L. Jensen and L. Pilegaard Hansen : "System Identification from Output Measurement ". Proceedings of the 8th International Modal Analysis Conference, Vol. 2, pp. 809-813, Kissimmee, Florida, USA, 1990.

90.10 Jensen, J.L., R. Brincker and A. Rytter : "Identification of Light Damping in Structures". Proceedings of the 8th International Modal Analysis Conference, Vol. 2, pp. 1041-1047, Kissimmee, Florida, USA, 1990.

90.11 Brincker, R., J.L. Jensen and S. Krenk : "Spectral Estimation by the Random Dec Technique". Proceedings of the 9th International Conference on Experimental Mechanics, Vol. 5, pp. 2049-2058, Technical University of Denmark, August 20-24, 1990 .

90.12 Gomes, A.J.M.A. and J.M. Montalvao E Silva : "On the use of Modal Analysis for Crack Identification". Proceedings of the 8th International Modal Analysis Conference, Vol. 2, pp. 1108-1115, Kissimmee, Florida, USA, 1990.

90.13 Mazurek, D.F. and J.T. DeWolf : "Experimental Study of Bridge Monitoring Technique", Journal of Structural Engineering, Vol. 116, no. 9, pp. 2532-2549, 9 sep. 1990.

90.14 Maguire, J.R. : "Assessing the Dynamic Properties of Existing Bridge Structures by Hammer Testing", Proceedings of first International Conference on Bridge Management, Inspection, Maintenance Assessment and Repair, pp. 595-605, Elsevier, 28th-30th March 1990.

90.15 Casas, J.R. and A.C. Aparicio : "Dynamic Testing of Bridges using Traffic-induced Vibration", A.S. Nowak (Ed.), Bridge Evaluation, Repair and Rehabilization, pp. 405-420, Kluwer Academic Publishers, 1990.

90.16 Ostachowicz, W.M. and M. Krawczuk : " Vibration Analysis of a Cracked Beam", Computer & Structures, Vol. 36, No. 2, pp. 245-250, 1990.

90.17 Shen, M.-H.H. and C. Pierre : "Natural modes of Bernoulli-Euler Beams with Symmetric Cracks", Journal of Sound and Vibration, Vol. 138, no. 1, pp. 115-134, 1990.

90.18 Hajela, P. and F.J. Soeiro : " Structural Damage Detection Based on Static and Modal Analysis", AIAA Journal, Vol. 28, No. 6, June 1990.

90.19 Abdundur and J.-L. Duchêne : " Structural Assessment of a Bridge with Transversal Cracks", Proceedings of First International Conference on Bridge Management, pp. 489-499, University of Surrey, Guildford, United Kingdom, March 28-30 1990.

90.20 Chou, C.-M. and C.-H. Wu : "System Identification and Damage Localization of Dynamic Structures", A Collection of Technical Papers ,AIAA Dynamic Specialist Conference, Long Beach, California, USA, April 5-6, 1990.

90.21 "OPTIMIZATION TOOLBOX for use with MATLAB"" User's Guide by Andrew Grace, The Math Works Inc., November, 1990

90.22 Bendat, J.S. : "Nonlinear System Analysis & Identification from Random Data", John Wiley & Sons, 1990.

90.23 Minas, C. and D.J. Inman : "Matching Finite Element Models to Modal Data", Journal of Vibration and Acoustics, Vol. 122, pp. 84-92, January, 1990.

90.24 Stubbs, N. and R. Osegueda : "Global Non-Destructive Damage Evaluation in Solids", The International Journal of Analytical and Experimental Analysis, Vol. 5, No. 2, pp. 67-79, April 1990.

90.25 Stubbs, N. and R. Osegueda : "Global Damage Detection in Solids - Experimental Verification", The International Journal of Analytical and Experimental Analysis, Vol. 5, No. 2, pp. 81-97, April 1990.

90.26 Stubbs, N., T.H. Broome and R. Osegueda : "Nondetructive Construction Error Detection in Large Space Structures", AIAA Journal, Vol. 28, No. 1, January, 1990.

90.27 Cho, H-N., C-B. Yun, A.H-S. Ang and M. Shinozuka : "A Reliability-Based Capacity Rating of Existing Bridges by Incorporating System Identification", Developments in Structural Engineering, Proceedings of the Forth Rail Bridge Centenary Conference, pp. 200-209, Edinburgh, Chapman and Hall, August 21-23, 1990.

91.1 Sommer, A.M., A.S. Nowak and P. Thoft-Christensen : "Inspection Strategies for Highway Steel Bridges". Structural Reliability paper no. 80, Department of Building and structural Engineering, University of Aalborg, January, 1991.

91.2 Brincker, R., S. Krenk and J.L. Jensen : "Estimation of Correlation Functions by the Random Dec Technique". Proceedings of the 9th International Modal Analysis Conference , Florence, Italy, April 18-19, 1991.

91.3 Tanrikulu, Ö. and H.N. Özgüven : "A new Method for the Identification of Non-linearities in Vibrating Structures ". Structural Dynamics : Recent advances, Proceedings of the 4th International Conference, Southampton, edited by M. Petyt et al, Elsevier, 1991.

91.4 Ågårdh, L. : "Modal Analyses of Two Concrete Bridges in Sweden", Structural Engineering International, Vol. 1, no. 1, pp. 35-39, 1991.

91.5 Joshi, A. and B.S. Madhusudhan : "A Unified Approach to Free Vibration of Locally Damaged Beams having various homogeneous Boundary Conditions", Journal of Sound and Vibration, Vol. 147, no. 3, pp. 475-488, 1991.

91.6 Shen, M.-H.H. and J.E. Taylor : "An Identification Problem for Vibrating Cracked Beams", Journal of Sound and Vibration, Vol. 150, no. 3, pp. 457-484, 1991.

91.7 Hearn, G. and R.B. Testa : "Modal Analysis for Damage Detection in Structures", Journal of Structural Engineering, Vol. 117, No. 10, pp. 3042-3063, October 1991.

91.8 Rytter, A., R. Brincker and L. Pilegaard Hansen : "Detection of Fatigue Damage in a Steel Member", Proceedings of the Florence Modal Analysis Conference, pp. 373-379, Florence, Italy, September 10-12, 1991.

91.9 Pandey, A.K., M. Biswas and M.M. Samman : " Damage Detection from Changes in Curvature Mode Shapes", Journal of Sound and Vibration, Vol. 145, no. 2, pp. 321-332, 1991.

91.10 Ting, T., W.J. Twomey and T.L.C. Chen : "Determination of Structural Model Parameters From Actual Frequency Response Data", Computational Methods and Experimental Measurement V, pp. 585-597, Eds. : A. Sousa, C.A. Brebbia and G.M. Carlomagno, Elsevier Applied Science, 1991.

91.11 Stubbs, N., J.T. Kim and K.G. Topole : "The Effect of Model Uncertainty on the Accuracy of Global Nondestructive Damage Detection in Structures", Computational Methods and Experimental Measurement V, pp. 157-168, Eds. : A. Sousa, C.A. Brebbia and G.M. Carlomagno, Elsevier Applied Science, 1991.

91.12 Rytter, A., R. Brincker and L. Pilegaard Hansen : "Vibration Based Inspection of Civil Engineering Structures", Bygningsstatiske Meddelelser, Vol. 62, No. 4, pp. 79-110, 1991.

91.13 Ostachowicz, W.M. and M. Krawczuk : "Analysis of the Effect of Cracks on the Natural Frequencies of a Cantilever Beam", Journal of Sound and Vibration, Vol. 150, No. 2, pp. 191-201, 1991.

91.14 Barltrop, N.D.P. and A.J. Adams : " Dynamics of Fixed Marine Structures", 3rd edition, Butterworth-Heinemann, 1991.

91.15 Kirkegaard, P.H. : "Optimal Design of Experiments for Parametric Identification of Civil Engineering Structures", Ph.D. thesis, Department of Building Technology and Strcutural Engineering, University of Aalborg, Denmark, November 1991.

91.16 Brincker, R., P.H. Kirkegaard and A.Rytter: "Identification of System Parameters by the Random Decrement Technique", Proceedings of the Florence Modal Analysis Conference, Florence, Italy, September 10-12, 1991.

91.17 Brincker, R., A.Rytter and S. Krenk : "Non-Parametric Estimation of Correlation Functions", Fracture & Dynamics, Paper no. 31, Department of Building Technology and Strcutural Engineering, University of Aalborg, Denmark (submitted to Experimental Mechanics) , 1991.

91.18 Pandit, S.M. : " Modal Analysis and Spectrum Analysis: Data Dependent Systems in State Space", Wiley Interscience, 1991.

91.19 Kirkegaard, P.H., J.D. Sørensen and R. Brincker : " Fatigue Reliability Analysis of a Mono-Tower Platform", Marine Structures, Vol. 4, pp. 413-434, 1991.

91.20 Sanayei, M. and O. Onipede : "Damage Assessment of Structures Using Static Test Data", AIAA Journal, Vol. 29, No. 7, pp. 1174-1179, July 1991.

91.21 Hertz, J., A. Krogh and R.G. Palmer : "Introduction to the Theory of Neural Computation", Addison-Wesley Publishing Company, 1991.

91.22 Orchard, G.A. and W.A. Phillips : "NEURAL COMPUTATION, A Beginner's Guide", Hove and London, 1991.

91.23 Flanigan, C.C. : "Correlation of Finite Element Models using Mode Shape Design Sensitivity", Proceedings of the 9th International Modal Analysis Conference, pp. 84-88, 1991.

92.1 Alampalli, S., G. Fu and I.A. Aziz : "Modal Analysis as a Bridge Inspection Tool", Proceedings of the 10th International Modal Analysis Conference, Vol. 2, pp. 1359-1366, San Diego, California, USA, 1992.

92.2 Yin, Z.K., G.A. Jun and L.J. Wen : "Diagnosis of a Slot Fault on a Frame Structure", Proceedings of the 10th International Modal Analysis Conference, Vol. 1, pp. 549-553, San Diego, California, USA, 1992.

92.3 Friswell, M.I. and J.E.T. Penny : "A Simple Nonlinear Model of a Cracked Beam", Proceedings of the 10th International Modal Analysis Conference, Vol. 1, pp. 516-521, San Diego, California, USA, 1992.

92.4 Fox, C.H.J. : "The Location of Defects in Structures: A Comparison of the Use of Natural Frequency and Mode Shape Data", Proceedings of the 10th International Modal Analysis Conference, Vol. 1, pp. 522-528, San Diego, California, USA, 1992.

92.5 Richardson, M.H. and M.A. Mannan : "Remote Detection and Location of Structural Faults using Modal Parameters", Proceedings of the 10th International Modal Analysis Conference, Vol. 1, pp. 502-507, San Diego, California, USA, 1992.

92.6 Ostachowicz, W.M. and M. Krawczuk : "Coupled Torsional and Bending Vibrations of a Rotor with an Open Crack", Archive of Applied Mechanics, Vol. 62, pp. 191-201, 1992.

92.7 Rytter, A., R. Brincker and P.H. Kirkegaard : "An Experimental Study of the Modal Parameters of a Damaged Cantilever", Fracture & Dynamics, Paper No. 37, Dept. of Building Technology and Structural Engineering, University of Aalborg, October, 1992.

92.8 Wood, M.G., M.I. Friswell and J.E.T. Penny : "Exciting Large Structures using a 'Bolt-Gun", Proceedings of the 10th International Modal Analysis Conference, vol. 1, pp. 233-238, San Diego, California, USA, 1992.

92.9 Manual for ROSAP, the Rambøll, Hannemann & Højlund Offshore Structural Analysis Package, Version 2.4, 1992.

92.10 Penny, J.E.T, M.I. Friswell and S.D. Garvey : "The Automatic Choice of Measurement Locations for Dynamic Testing", Proceedings of the 10th International Modal Analysis Conference, Vol. 1, pp. 30-36, San Diego, California, USA, 1992.

92.11 Hemami, M.S. and M.K. Abdelhamid : "Finite Element Model Optimization using an Iterative Approach", Proceedings of the 10th International Modal Analysis Conference, pp. 480-486, San Diego, California, USA, 1992.

92.12 Flanigan, C.C. and C.D. Botos : "Automated Selection of Accelerometer Locations for Modal Survey Tests", Proceedings of the 10th International Modal Analysis Conference, Vol. 2, pp. 1205-1208, San Diego, California, USA, 1992.

92.13 Yao, G.C., K.C. Chang and G.C. Lee : "Damage Detection of Steel Frames using Vibrational Signature Analysis", Journal of Engineering Mechanics, Vol. 118, No. 9, September, 1992.

93.1 Rytter, A. and P.H. Kirkegaard : "An Experimental Study of the Modal Parameters of a Steel Mast ", to be published in the Fracture & Dynamics series, Dept. of Building Technology and Structural Engineering, University of Aalborg, 1993.

93.2 Kirkegaard, P.H, and A. Rytter : "Use of Neural Networks for Damage Detection in a Steel Mast", to be published in the Fracture & Dynamics series, Dept. of Building Technology and Structural Engineering, University of Aalborg, 1993.

93.3 Worden, K., A.D. Ball and G.R. Tomlinson : "Neural Networks for Fault Detection and Location", Proceedings of the 11th International Modal Analysis Conference, Vol. 2, pp. 809-813, Kissimmee, Florida, USA, 1993.

APPENDIX A

K_I for a Box Profile

The applicability and accuracy of the fracture mechanical model of a cracked beam (see section 4.1.3) depend on how reliable and accurate the expressions for the stress intensity factors of relevance are. Reliable expressions for the stress intensity factors for a large number of different cross sections can be found in standard handbooks like e.g. Tada et al. [73.1]. However, an expression for K_I for a crack in a rectangular box profile like those used in experimental case no. 1 cannot be found in any of the standard handbooks.

Therefore three different methods have been used to establish such an expression in connection with the preparation of this thesis. The three methods are :

1. Adjustment and piecing together known expression
2. FEM-analysis
3. Calibration based on experimental data

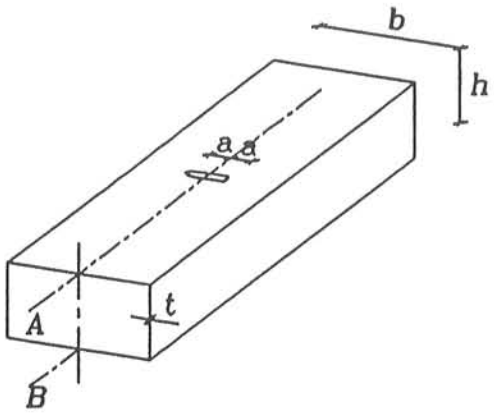

Figure A.1 Geometry of beam and crack.

This aim of this appendix is to present the basic assumptions in and the results from these methods. The geometry of the beam and the crack are shown in figure A.1.

A.1 Adjustment and piecing together Known Expressions

An expression will be establish for the following two distinct situations

situation I $a \leq b/2$

situation II $a > b/2$

A.1.1 Situation I

On the assumption that the crack is symmetrical placed with respect to the centerline of the flange, then there will not be any stresses in line B (see figure A.1). This means that the equilibrium will retained if the profile is cut along line B and folded out (see figure A.2a).

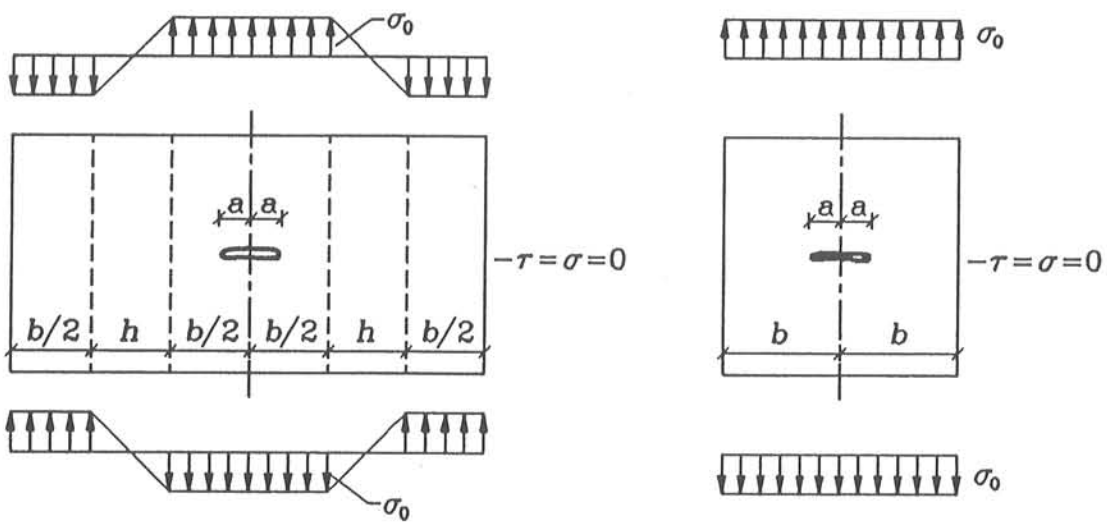

Figure A.2 Folded out beam

The stress intensity factor K_I can be found through superposition by

$$K_I = \int_{-a}^{a} f(x)\,\sigma_o\,dx \quad for\ a \leq b/2 \tag{A.1}$$

where σ_o is the normal stress in the flange of the uncracked beam and $f(x)$ is a Green function, which depends on the geometry only.

This means that the expression for K_I given for the plate shown in figure A.2b can be used for the plate shown in figure A.2a as long as $a \leq b/2$. Thus we have (see e.g. Tada et al. [73.1])

$$K_I^F = \sigma_o\sqrt{\pi a}\,(1+0.128(\frac{a}{b+h})-0.288(\frac{a}{b+h})^2+1.525(\frac{a}{b+h})^3) \qquad \textbf{(A.2)}$$

A.1.2 Situation II

The stress intensity factor for a single sided crack in a prismatic beam in bending is given by (see e.g. Hellan [85.5])

$$K_I = \sigma_o\sqrt{\pi a}\,(1.112-1.4(\frac{a}{h})+7.33(\frac{a}{h})^2-13.08(\frac{a}{h})^3+14.0(\frac{a}{h})^4) \qquad \textbf{(A.3)}$$

The webs of the hollow section will be loaded, as shown i figure A.3a. The distribution and magnitude of the shear stresses τ is unknown. The stress distribution is equalized to the stress distribution shown in figure A.3b. The parameter c is a fictious length, which is introduced to avoid a slip in the curve for K_I at $a = b/2$.

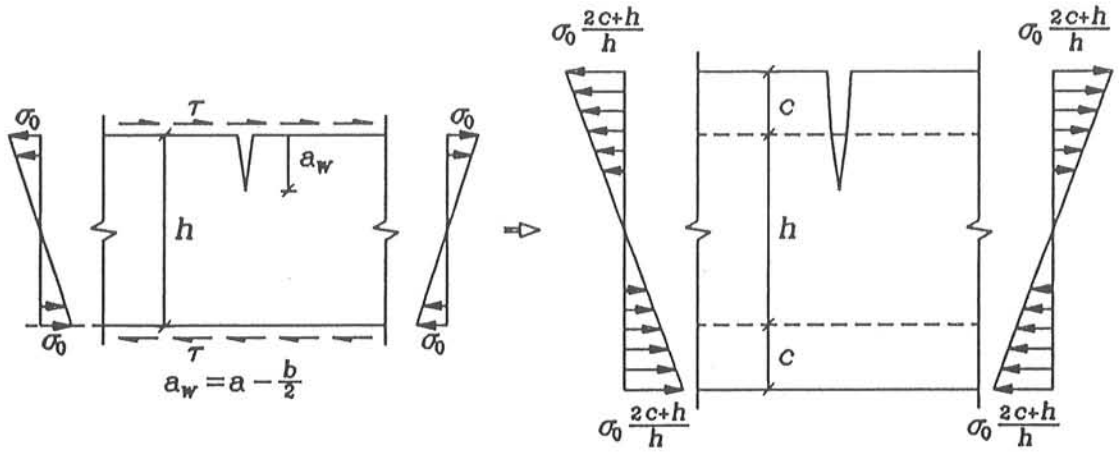

Figure A.3 Stress distribtuions, a) real web b)fictious web.

The following modified version of equation (A.3) can then be used in situation II

$$K_I^W = \sigma_o \frac{2c+h}{h}\sqrt{\pi (a_w+c)}\ (1.112-1.4(\frac{a_w+h}{h+2c})+ 7.33(\frac{a_w+c}{h+2c})^2-13.08(\frac{a_w+c}{h+2c})^3+14(\frac{a_w+c}{h+2c})^4) \quad \text{(A.4)}$$

The fictious length c is found from

$$K_I^F(a=b/2) = K_I^W(a_w=0) \quad \text{(A.5)}$$

A value of 13,4 mm has been calculated been for c for the beams in actual case.

A.2 FEM analysis

The finite element model shown in figure A.4 has been used to establish an expression for K_I. The crack growth was simulated by loosen node no. 1 to 8 successively. Unit points loads in the z-direction were added to point no. 1 to 6 after loosening. Point loads of 3/5 and 1/5 were added in point no. 7 and 8 respectively.
The analysis were performed by means of the IMAGES-3D program.

The strain energy Φ is given by (see e.g. Hellan [85.5])

$$\Phi = \frac{1}{2}\sum_{i=1}^{N_r} P_i u_i \quad \text{(A.6)}$$

where N_r is the number of released nodes, P_i is the load in node no. i and u_i is the displacement of node no. i.

The strain energy release rate G is defined by (see Hellan [85.5])

$$G = \frac{\Delta\Phi}{\Delta a\ t} = \frac{1}{E}K_I^2 \Rightarrow K_I = \sqrt{\frac{E\ \Delta\Phi}{\Delta a\ t}} \quad \text{(A.7)}$$

$\Delta\Phi$ and K_I has been calculated for each step (crack growth of Δa)

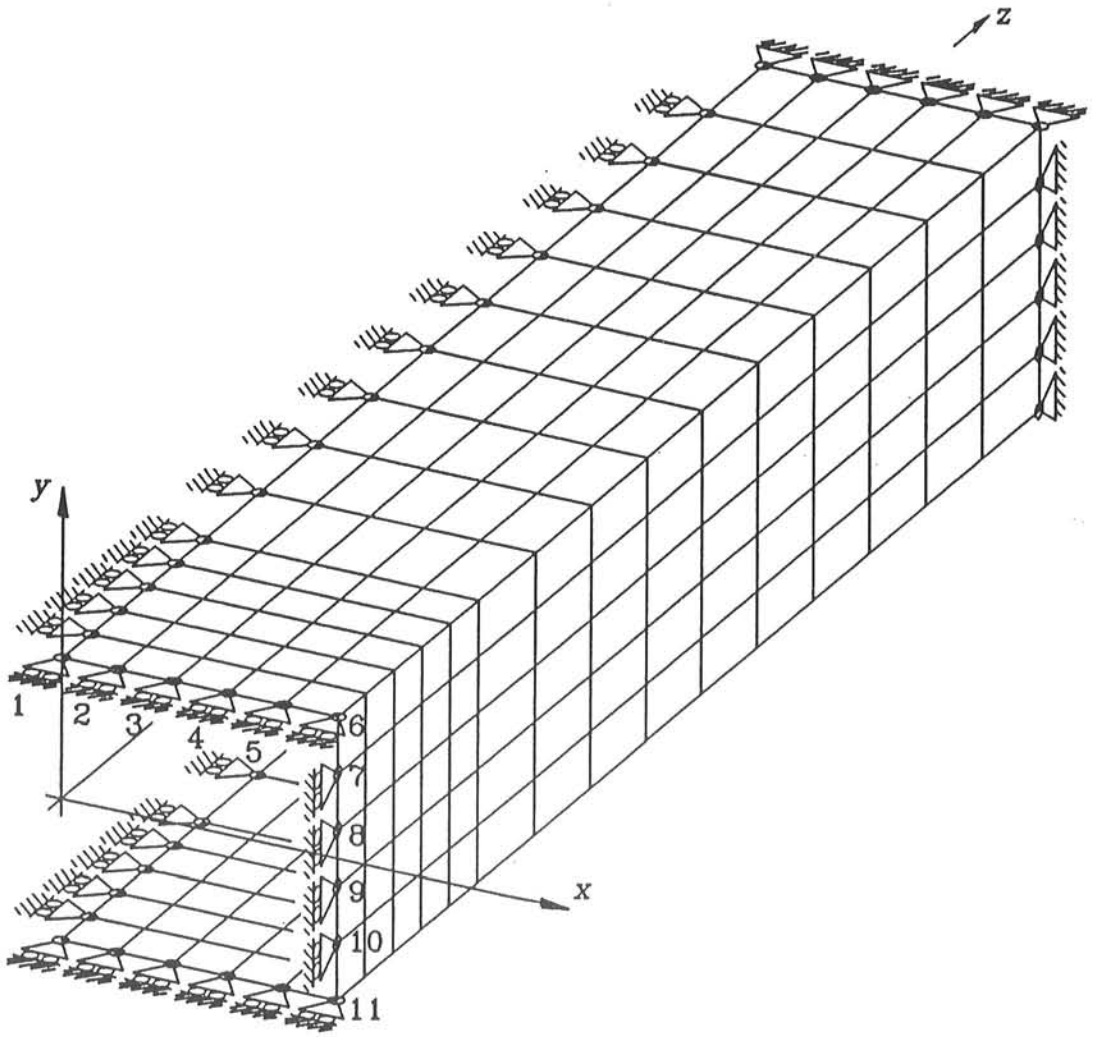

Figure A.4 FEM of box profile

A curve fit of K_I to the calculated discrete values gave the following expression

$$K_I = \sigma_o\sqrt{\pi a}\ (1+0.062(\frac{a}{h})-0.215(\frac{a}{h})^3+0.331(\frac{a}{h})^5) \qquad \text{(A.8)}$$

A.3 Calibration based on Experimental Data

The FEM-analysis in section A.2 showed that the expression for K_I should be of the following form

$$K_I = \sigma_o \sqrt{\pi a}\,(k_o + k_1(\frac{a}{b+h}) + k_2(\frac{a}{b+h})^3 + k_3(\frac{a}{b+h})^5) \qquad \textbf{(A.9)}$$

Estimates for the polynomium coefficients k_o ,k_1 ,k_2 and k_3 have been found through a minimization of the following object function

$$F(k_o,k_1,k_2,k_3) = \sum_{i=1}^{N_{point}} \left(\frac{f_1^*(a_i)}{f_1^*(0.02)} - \frac{f_1^{cal}(a_i)}{f_a^{cal}(0.02)} \right)^2 \qquad \textbf{(A.10)}$$

where $f_1^*(a_i)$ and $f_1^{cal}(a_i)$ are the measured and the calculated values of the first natural frequency for a crack length equal to a_i respectively. N_{point} is the number of measured pairs of a and f_1.

The test results from beam B3 have been used in the performed analysis. N_{point} was taken as 17, which secured that the expression covers $a \in [0;0.120]$. The beam was demounted from its fixture between the measurement for $a = 0.$ and $a = 0.02$. Therefore, $f_1^*(0.02)$ is used as reference value in (A.10).

The FEM of B3 shown in figure A.5 has been used to calculate $f_1^{cal}(a_i)$. The expression for K_I in equation (A.9) was used in the calculations of the rotational spring at the crack position.

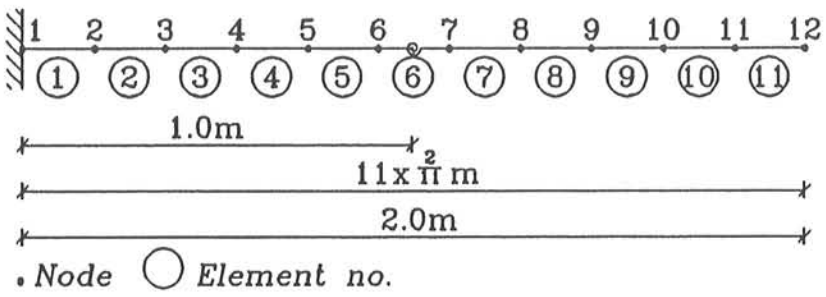

Figure A.5 FEM of beam B3.

The minimization of $F(k_o,k_1,k_2,k_3)$ was performed by means of the M-file CONSTR in the Matlab Optimization Toolbox (see [90.21]).

During the performance of the optimization several local minima of $F(k_o, k_1, k_2, k_3)$ were revealed. Therefore the test results from beam B4 were used to evaluate the different outcome of k_o ,k_1 ,k_2 and k_3. That set of value, which the best fit to the B4-data, was chosen as the final estimates for k_o ,k_1 ,k_2 and k_3.

The performed analysis gave the following results

$$K_I = \sigma_o \sqrt{\pi a}\,(0.90 + 1.72(\frac{a}{b+h}) - 11.42(\frac{a}{b+h})^3 + 140.17(\frac{a}{b+h})^5) \qquad \textbf{(A.11)}$$

$f_1^{cal}(a)$ for B3 and B4 are shown in figure A.6 together with the matching values of $f_1^{*}(a)$.

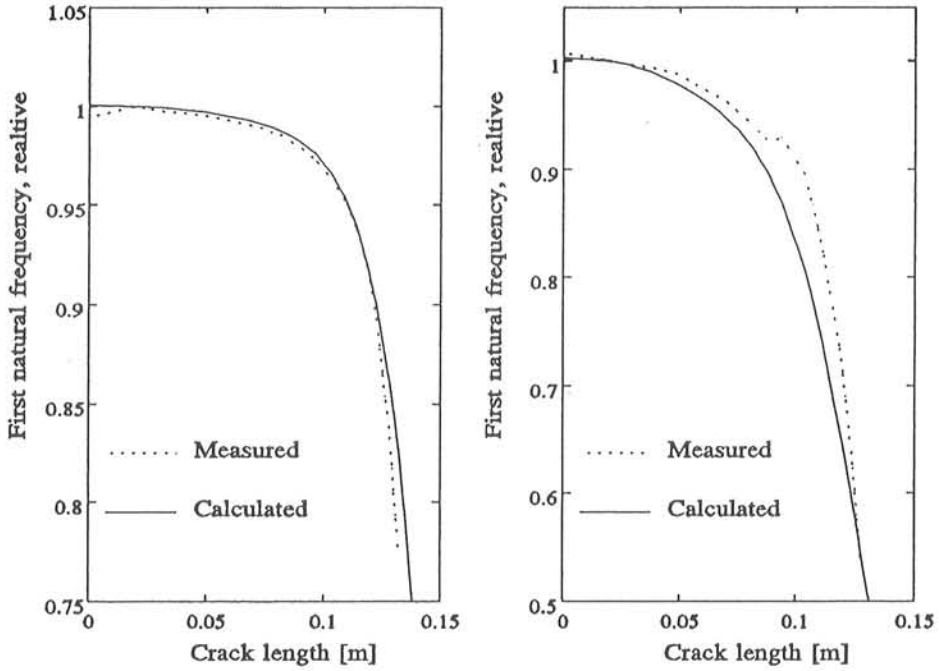

Figure A.6 Variation of the first natural frequency of B3 and B4

The problems with the local minima of $F(k_o, k_1, k_2, k_3)$ could probably be avoided, if test data for different crack positions were included.

A.4 Summary

The performed analysis have given three different expressions for K_I of a hollow sectional beam in bending (see figure A.7).

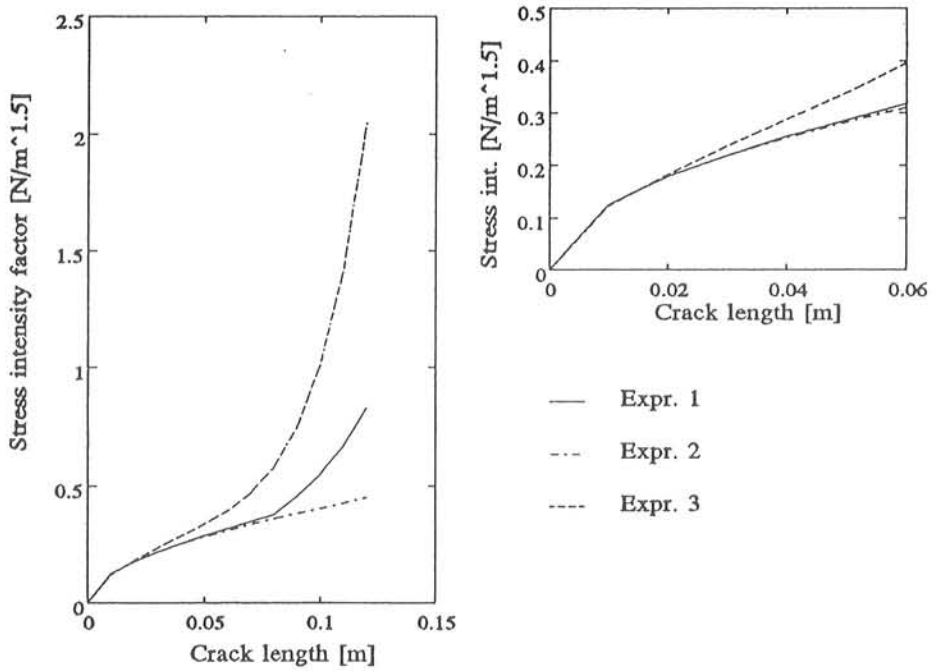

Figure A.7 K_I for a box profile in bending

From the curves in figure A.7 it can be seen that expression 1 (see equation (A.2) and (A.4)) and expression 2 (see equation (A.8)) give almost identical values for $a < 0.08$ m. Expression 3 gives only identical values for $a < 0.02$ m. The method used to determinate c in expression 1 (see figure A.3) give raise to a discontinuity at $a = 0.08$ m. Further it can be seen, that the slope of the curve for expression 2 remain almost unchanged for $a > 0.08$ m whereas the two other curves. This is probably because the mesh in the FEM has been to rough.

The applicability of the 3 expressions has been evaluated by means of the test results for the first natural frequency beam B3 and B4 (see figure A.8)

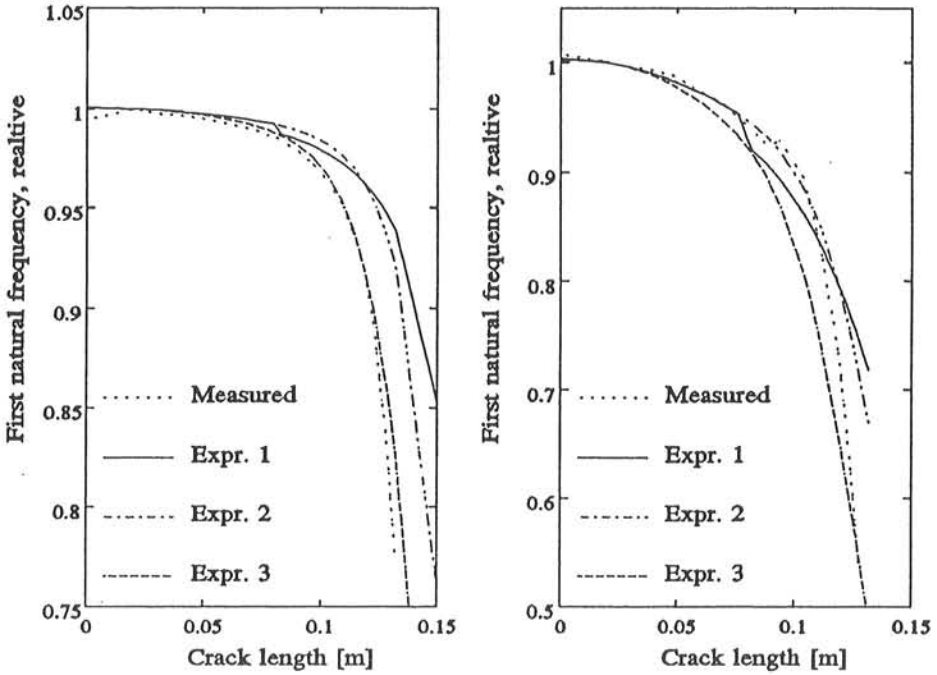

Figure A.8 Variation in the first natural frequency with crack length. Left beam B3 and right beam B4.

Naturally the best fit on the data for f_1 of B3 is obtained by using expression no. 3 (see quation (A.11)). The use of the two other expressions lead to an under estimation of the decrease in f_1 due to crack growth in beam B3.

For B4 the best fits are obtained for $a < 0.08m$ (crack in web only) by using either expression 1 or 2. However, apparently the use of these two expressions for $a > 0.08m$ lead to an under estimation of the effect of a crack. The above mentioned discontinuity in K_I given by expression 1 is clearly reflected in the curve for f_1 of B4. The use of expression 3 lead to an over estimation of the decrease of f_1 due to crack growth in B4.

Symmetric crack growth is a basic assumption in the performed analysis, This assumption was not full filled during the tests (see figure A.9), which probably can explain some the discrepancies between the analytical and experimental esimates for f_1. Furthes is the rounded corners of the profile modelled as sharpe edges, which lead to discrepancies for $a \in [0.7; 0.9]$.

FRACTURE AND DYNAMICS PAPERS

PAPER NO. 13: Lise Gansted: *Fatigue of Steel: Deterministic Loading on CT-Specimens.*

PAPER NO. 14: Jakob Laigaard Jensen, Rune Brincker & Anders Rytter: *Identification of Light Damping in Structures.* ISSN 0902-7513 R8928.

PAPER NO. 15: Anders Rytter, Jakob Laigaard Jensen & Lars Pilegaard Hansen: *System Identification from Output Measurements.* ISSN 0902-7513 R8929.

PAPER NO. 16: Jens Peder Ulfkjær: *Brud i beton - State-of-the-Art. 1. del, brudforløb og brudmodeller.* ISSN 0902-7513 R9001.

PAPER NO. 17: Jakob Laigaard Jensen: *Full-Scale Measurements of Offshore Platforms.* ISSN 0902-7513 R9002.

PAPER NO. 18: Jakob Laigaard Jensen, Rune Brincker & Anders Rytter: *Uncertainty of Modal Parameters Estimated by ARMA Models.* ISSN 0902-7513 R9006.

PAPER NO. 19: Rune Brincker: *Crack Tip Parameters for Growing Cracks in Linear Viscoelastic Materials.* ISSN 0902-7513 R9007.

PAPER NO. 20: Rune Brincker, Jakob L. Jensen & Steen Krenk: *Spectral Estimation by the Random Dec Technique.* ISSN 0902-7513 R9008.

PAPER NO. 21: P. H. Kirkegaard, J. D. Sørensen & Rune Brincker: *Optimization of Measurements on Dynamically Sensitive Structures Using a Reliability Approach.* ISSN 0902-7513 R9009.

PAPER NO. 22: Jakob Laigaard Jensen: *System Identification of Offshore Platforms.* ISSN 0902-7513 R9011.

PAPER NO. 23: Janus Lyngbye & Rune Brincker: *Crack Length Detection by Digital Image Processing.* ISSN 0902-7513 R9018.

PAPER NO 24: Jens Peder Ulfkjær, Rune Brinker & Steen Krenk: *Analytical Model for Complete Moment-Rotation Curves of Concrete Beams in bending.* ISSN 0902-7513 R9021.

PAPER NO 25: Leo Thesbjerg: *Active Vibration Control of Civil Engineering Structures under Earthquake Excitation.* ISSN 0902-7513 R9027.

PAPER NO. 26: Rune Brincker, Steen Krenk & Jakob Laigaard Jensen: *Estimation of correlation Functions by the Random Dec Technique.* ISSN 0902-7513 R9028.

PAPER NO. 27: Jakob Laigaard Jensen, Poul Henning Kirkegaard & Rune Brincker: *Model and Wave Load Identification by ARMA Calibration.* ISSN 0902-7513 R9035.

PAPER NO. 28: Rune Brincker, Steen Krenk & Jakob Laigaard Jensen: *Estimation of Correlation Functions by the Random Decrement Technique.* ISSN 0902-7513 R9041.

FRACTURE AND DYNAMICS PAPERS

PAPER NO. 29: Poul Henning Kirkegaard, John D. Sørensen & Rune Brincker: *Optimal Design of Measurement Programs for the Parameter Identification of Dynamic Systems.* ISSN 0902-7513 R9103.

PAPER NO. 30: L. Gansted & N. B. Sørensen: *Introduction to Fatigue and Fracture Mechanics.* ISSN 0902-7513 R9104.

PAPER NO. 31: R. Brincker, A. Rytter & S. Krenk: *Non-Parametric Estimation of Correlation Functions.* ISSN 0902-7513 R9120.

PAPER NO. 32: R. Brincker, P. H. Kirkegaard & A. Rytter: *Identification of System Parameters by the Random Decrement Technique.* ISSN 0902-7513 R9121.

PAPER NO. 33: A. Rytter, R. Brincker & L. Pilegaard Hansen: *Detection of Fatigue Damage in a Steel Member.* ISSN 0902-7513 R9138.

PAPER NO. 34: J. P. Ulfkjær, S. Krenk & R. Brincker: *Analytical Model for Fictitious Crack Propagation in Concrete Beams.* ISSN 0902-7513 R9206.

PAPER NO. 35: J. Lyngbye: *Applications of Digital Image Analysis in Experimental Mechanics.* Ph.D.-Thesis. ISSN 0902-7513 R9227.

PAPER NO. 36: J. P. Ulfkjær & R. Brincker: *Indirect Determination of the $\sigma - w$ Relation of HSC Through Three-Point Bending.* ISSN 0902-7513 R9229.

PAPER NO. 37: A. Rytter, R. Brincker & P. H. Kirkegaard: *An Experimental Study of the Modal Parameters of a Damaged Cantilever.* ISSN 0902-7513 R9230.

PAPER NO. 38: P. H. Kirkegaard: *Cost Optimal System Identification Experiment Design.* ISSN 0902-7513 R9237.

PAPER NO. 39: P. H. Kirkegaard: *Optimal Selection of the Sampling Interval for Estimation of Modal Parameters by an ARMA-Model.* ISSN 0902-7513 R9238.

PAPER NO. 40: P. H. Kirkegaard & R. Brincker: *On the Optimal Location of Sensors for Parametric Identification of Linear Structural Systems.* ISSN 0902-7513 R9239.

PAPER NO. 41: P. H. Kirkegaard & A. Rytter: *Use of a Neural Network for Damage Detection and Location in a Steel Member.* ISSN 0902-7513 R9245

PAPER NO. 42: L. Gansted: *Analysis and Description of High-Cycle Stochastic Fatigue in Steel.* ISSN 0902-7513 R9135.

PAPER NO. 43: M. Krawczuk: *A New Finite Element for Static and Dynamic Analysis of Cracked Composite Beams.* ISSN 0902-7513 R9305.

PAPER NO. 44: A. Rytter: *Vibrational Based Inspection of Civil Engineering Structures.* Ph.D.-Thesis. ISSN 0902-7513 R9314.

Department of Building Technology and Structural Engineering
The University of Aalborg, Sohngaardsholmsvej 57, DK 9000 Aalborg
Telephone: 45 98 15 85 22 Telefax: 45 98 14 82 43